NASA CONTRACTOR REPORT

NASA CR-923

NASA CR-923

N68-17075
(ACCESSION NUMBER)
227
(PAGES)
1
(NASA CR OR TMX OR AD NUMBER)
(THRU)
1
(CODE)
03
(CATEGORY)
FACILITY FORM 602

TWO-STAGE POTASSIUM TEST TURBINE

Volume II
Mechanical Design and Development

by H. E. Nichols and R. W. Fink

Prepared by
GENERAL ELECTRIC
Cincinnati, Ohio
for Lewis Research Center

GPO PRICE $ _____
CFSTI PRICE(S) $ _____
Hard copy (HC) 3.00
Microfiche (MF) .65
ff 653 July 65

NATIONAL AERONAUTICS AND SPACE ADMINISTRATION • WASHINGTON, D. C. • FEBRUARY 1968

NASA CR-923

TWO-STAGE POTASSIUM TEST TURBINE

Volume II

Mechanical Design and Development

By H. E. Nichols and R. W. Fink

Distribution of this report is provided in the interest of information exchange. Responsibility for the contents resides in the author or organization that prepared it.

Prepared under Contract No. NAS 5-1143 by
GENERAL ELECTRIC
Cincinnati, Ohio

for Lewis Research Center

NATIONAL AERONAUTICS AND SPACE ADMINISTRATION

For sale by the Clearinghouse for Federal Scientific and Technical Information
Springfield, Virginia 22151 – CFSTI price $3.00

PRECEDING PAGE BLANK NOT FILMED.

FOREWORD

The work described in this report is part of the Two-Stage Potassium Test Turbine Program conducted by the Space Power and Propulsion Section of the General Electric Company for the National Aeronautics and Space Administration under Contract NAS 5-1143 for the design, manufacture and testing of a two-stage turbine, using potassium vapor as the working fluid. The contract effort covered the period of May 8, 1961 to January 28, 1966. This work was carried out under the Technical Management of Joseph P. Joyce of NASA-Lewis Research Center, Space Power Systems Division.

PRECEDING PAGE BLANK NOT FILMED.

ABSTRACT

This report is one of a series of reports describing the design and development of a two-stage, Rankine cycle turbine for operation with potassium vapor. This volume presents the turbine mechanical design and describes a three-phase development test program comprising steam and air testing, potassium vapor performance testing, and a 2000-hour endurance test with turbine inlet potassium vapor at 1500° F.

As part of the endurance testing, four each of TZM and TZC molybdenum blades were inserted in the second stage to observe any effects of corrosion and/or erosion.

The average weight changes of the rotor blades during the endurance test were:

Stage 1 (U-700)	-0.304%
Stage 2 (U-700)	-0.019%
Stage 2 (TZM)	-0.105%
Stage 2 (TZC)	-0.102%

The testing demonstrated minimal deterioration of the turbine parts in 2100 hours of vapor operation, and demonstrated the feasibility of long-time operation of a potassium turbine of the design described herein.

PRECEDING PAGE BLANK NOT FILMED.

TABLE OF CONTENTS

		Page No.
	FOREWORD	iii
	ABSTRACT	v
I.	SUMMARY	1
II.	INTRODUCTION	5
III.	TURBINE CONFIGURATION	9
	A. GENERAL ARRANGEMENT	9
	B. TURBINE COMPONENTS	12
IV.	FABRICATION AND TURBINE ASSEMBLY	23
	A. TURBINE MANUFACTURE	23
	B. TURBINE ASSEMBLY	25
	1. Rotor Assembly and Balance	25
	2. Stator Assembly	26
	3. Final Assembly and Installation	28
V.	COMPONENT DESIGN	29
	A. DESIGN CRITERIA	29
	B. STRESS ANALYSIS	31
	1. Rotor	31
	2. Stator	35
	C. VIBRATION	36
	1. Blades	36
	2. Critical Speeds	37
	D. TEMPERATURE DISTRIBUTION	38
VI.	TURBINE TESTING	41
	A. GENERAL	41
	B. TURBINE PRETESTING	41
	1. Instrumentation	42
	2. Bearing Testing	43
	3. Hydrodynamic Seal Test	44
	4. Blade Vibration Testing	47
	5. Steam Pretesting	48

TABLE OF CONTENTS - (Continued)

		Page No.
C.	POTASSIUM VAPOR TESTING	50
	1. Test Preparations & Facility Checkout	50
	2. Potassium Tare Testing	52
	3. Seal Malfunction	52
	4. Initial Potassium Vapor Testing	54
	5. Development Testing and Modifications	57
	6. Metal Removal on Fluid Dynamic Components	63
	7. Test Preparations	65
D.	PERFORMANCE TESTING	66
	1. Test Plan	66
	2. Instrumentation	66
	3. Performance Testing of March 1965	67
	4. Performance Testing of May 1965	68
	5. Post-Test Inspection	69
E.	ENDURANCE TESTING	70
	1. Test Plan	70
	2. Test Preparations	71
	3. 2000-Hour Test	72
VII.	TEST RESULTS	75
	A. PERFORMANCE TESTING	75
	B. ENDURANCE TESTING	76
VIII.	CONCLUSIONS AND RECOMMENDATIONS	81
	A. CONCLUSIONS	81
	B. RECOMMENDATIONS	82
IX.	REFERENCES	85

I. SUMMARY

This report describes the mechanical design and development of a two-stage Rankine cycle turbine for test with potassium vapor. The total design and the development program spanned the time period from May, 1961 to January, 1966.

The turbine assembly is shown in Figure 1, and a photographic exploded view of the turbine components is shown in Figure 2. The test turbine consists of two overhung axial flow stages representing stages three and four of a five stage, 500 KW turbine.

The two test stages are connected to each other and to the main support shaft by curvic coupling teeth and a central tie bolt. The shaft is supported in oil-lubricated bearings, the forward one being a pivoted pad journal bearing, with the rotor thrust being taken by a ball bearing pair. Separation of oil and potassium is effected by a hydrodynamic buffer seal. Brazed nozzle diaphragm assemblies are mounted in the horizontally split casings which are attached to the turbine by means of welded flanges. All instrumentation is welded to prevent contamination of, or leakage from the main loop.

The turbine was fabricated from nickel-based superalloys and other materials common to high temperature gas turbine technology. During potassium testing, it was operated at inlet vapor temperatures of up to 1580^{o}F and at rotative speeds of up to 22,000 rpm. Refractory metal (molybdenum) blades and erosion inserts made from various candidate blade materials were mounted in the second stage to observe the effects of erosion and/or corrosion over a 2000 hour test period at one operating condition. The turbine blades were attached to the wheels by means of dovetail connections to allow interchangeability of blades for testing the refractory materials. During testing, the turbine power was delivered to a water brake through a splined coupling. Startup of the turbine hydrodynamic seal and motoring of the entire system was accomplished by a steam turbine attached to the aft end of the drive train.

A portion of the turbine mechanical design involved the use of available technology within the General Electric Company, including the high-temperature design technology of gas turbines, the vapor and seal technology of gas turbines and the vapor and seal technology of steam and mercury turbines. Available gas turbine turbomachinery design criteria was modified to apply to the long life requirements of this turbine, and for a number of specialized analyses such as critical speeds, blade vibrations, turbine temperature distribution, and wheel blade stress analysis. Available computer programs were employed.

The design was combined with a test program accomplished in three phases:

1. A pretesting phase employing air, water and steam.

2. A potassium test development phase involving checkout testing and a potassium performance test (100 hours on potassium vapor).

3. Potassium vapor endurance testing (2000 hours) at 18,250 rpm, 1500^{o}F inlet vapor temperature and inlet total-to-exit static pressure ratio of 3.47.

The first phase employed easy fluids, to allow visual observation and ease of instrumentation for measurement of turbine system dynamics and flow characteristics. Both the first and the second phases of testing were accompanied by numerous design modifications resulting from the first dynamic testing, and from initial operation of high-temperature potassium vapor. During the early phases of vapor testing, erosion of the turbine inlet region was experienced, due to the injection of insufficiently atomized liquid potassium into the turbine to depress the vapor quality and due to suspected boiler liquid carry over resulting from boiling instabilities.

Following necessary modifications to achieve stable operation and the elimination of large droplet pre-injection, performance testing was successfully completed, proving the validity of the test turbine design. The subsequent 2000-hour endurance test was conducted almost without incident, with a planned shutdown of the turbine facility on December 20, 1965.

A thorough post-testing inspection of the turbine was made. The results showed very minor deterioration of turbine components during the 2000-hour endurance test, thereby demonstrating the feasibility of long-time operation of a turbine having the speed, temperature, vapor quality, and fabrication alloys of the one described herein.

II. INTRODUCTION

The turbine for an alkali metal Rankine cycle space electric power conversion system presents a number of new design tasks. The turbine is thermodynamically similar to steam and mercury turbines, and mechanically similar to high-temperature gas turbines. Therefore, its design required application of both these technologies. In addition, a potassium vapor turbine designed to operate up to 1600°F presents a number of design and development problems not encountered in either of the above fields.

Of major importance are the metallurgical problems, requiring judicious selection of containment and structural materials for maximum corrosion and erosion resistance, and for long operating life. Alkali metal containment and the need for a leak-tight facility are strong considerations in view of the affinity of potassium for oxygen and water, with resulting mechanical damage and/or oxide plugging accompanying any minute leaks or oxygen contamination. Also, potassium represents a new working fluid requiring special fluid design and thermodynamic analysis, in determining flow path and airfoil designs.

The team designing this turbine called upon varied technologies within the General Electric Company, including gas turbine design and development experience within the immediate group, and obtained pertinent knowledge regarding steam and mercury turbines from available reports and direct consultation with other General Electric personnel. Specialized information was obtained with regard to such tasks as design of liquid metal seals, moisture, erosion, and condensate extraction. To minimize the development time and costs, it was attempted to employ present state-of-the-art design and fabrication techniques where possible.

The turbine design was dictated by a number of initial decisions and limits as follows. In advanced space power alkali metal turbogenerator

PRECEDING PAGE BLANK NOT FILMED.

systems, operation will be at turbine inlet temperatures of 1800°F to 2100°F. These temperatures will require refractory metal for both the two-phase test loop and the construction of turbomachinery. The development of such a system will require extensive facilities, involving vacuum equipment and expensive test components (Ref. 25). In consideration of cost and development time, the present program was run in a less complex stainless steel loop and used available gas turbine alloys. The facility loop was made from 316 stainless steel, which limited the turbine inlet vapor temperature to a maximum of 1600°F, which in turn, was chosen as the design point. The testing of candidate refractory turbine alloys for an ultimate space turbine was done by inserting sample blades and stationary inserts in the turbine second stage.

Two stages were tested with the design philosophy that the first stage would act as a "true turbine flow generating" stage to create realistic vapor and atomized liquid flow conditions for the second stage, where actual test evaluations would be made. The stages chosen are stages three and four of a five-stage, 500 KW turbine designed for an 1800°F vapor inlet temperature. Stages three and four were chosen for test, because it is in these stages that the temperature (of the designed five-stage turbine) has dropped sufficiently low to allow the use of existing gas turbine nickel-based super alloys, and they also represent stages where the vapor quality has become sufficiently low to produce possible erosion. The problem of blade erosion becomes of interest, in the light of the long operating time associated with space turbomachinery. For this reason, a major objective of this program was to observe the integrity of the various turbine blade materials (including refractory metals) and to observe their relative erosion resistance. Also, mass transfer and washing erosion on various test turbine and facility loop parts was observed. Assuming saturated vapor at the inlet of a five-stage turbine, stage three would experience a 92 percent quality at inlet. Provisions were made to simulate this quality by injecting liquid metal into the vapor stream ahead of the turbine. It was the intent to use this liquid pre-injection to control vapor quality to values between 85 and 100 percent vapor. In connection with this liquid injection, means were provided for

interstage removal of moisture, as is done on large steam turbines, to improve thermodynamic efficiency.

Another design decision was the selection of an "overhung turbine" arrangement over an alternate "cradled turbine" design. The former was selected to avoid the complexity and aerodynamic compromise of an inlet scroll and the need to locate both a bearing and a second hydrodynamic seal in the hot inlet region of the turbine. This decision was based, to some extent, on available General Electric Company experienc wherein a large seven stage mercury turbine and many production steam turbines have used the overhung arrangement with success.

A three-phase test program was defined, consisting of (1) pretesting, (2) potassium vapor performance testing, and (3) potassium vapor endurance testing. The pretesting involved operation of the turbine in air and in steam to observe its dynamic rotating characteristics, and to allow adequate instrumentation and visual observation of such items as moisture extraction. This was followed by an extensive performance test in potassium vapor and a subsequent two thousand hour endurance test under the conditions defined below.

	Operating Time (Hours)	Turbine Inlet Temp. (°F)	Turbine Pressure Ratio T_T/T_S	Rotational Speed (rpm)
Performance Testing	100	1450 & 1550	1.4 to 4.4	15,400 to 20,000
Endurance Testing	2000	1500	3.47	18,250

This report deals with the mechanical design aspects of the two-stage potassium test turbine. It presents the final design, the functional requirements of the various components, and discusses the detailed design

considerations, stresses, vibration, temperature distributions, and operating life, as well as manufacture and assembly aspects. It covers the test development program in detail, and discusses the experience gained with this turbine from a mechanical design point of view. Conclusions are drawn as to the validity of the design.

III. TURBINE CONFIGURATION

A. GENERAL ARRANGEMENT

The potassium turbine test assembly is an in-line arrangement, comprising three main components. These are the potassium turbine (shown in Figures 1 and 2), water brake, and steam turbine, which are connected by rotor splines as shown in Figure 4. No clutching or reduction gearing is employed, with the result that all three components rotate continuously and at the same speed during testing. The potassium turbine has two axial flow rotor stages which are overhung from the forward bearing. The rotor is supported by two bearings, the forward one being a pivoted pad journal bearing which accommodates only radial loading, and the aft one being a ball thrust bearing pair which takes both a small radial load and all the turbine rotor thrust. Both bearings are oil lubricated, with separation of the oil and potassium vapor being maintained by the hydrodynamic seal immediately forward of the pad bearing. During operation, potassium vapor enters the turbine via the 8-inch diameter pipe from the boiler, which is located about fifteen feet upstream of the turbine. The vapor flows over the inlet bullet nose, and into the two axial-flow stages. After expanding through the turbine, the vapor is collected in a twin-volute exhaust scroll and is directed downward into the condenser which is mounted below the turbine. The installation of the turbine in the test facility is shown schematically in Figure 5. This shows the boiler located upstream of the turbine, and the condenser hanging below the turbine, with associated electromagnetic pump, dump tank, and other major components of the loop. An external view of the test facility, constructed specifically for the testing of this turbine, is shown photographically in Figure 6.

During testing, the power generated by the turbine is delivered through a splined shaft (Koppers Coupling) to the multi-disk water brake*, as shown in Figure 4. The water brake is cantilevered off the face of a Bytrex torque meter*, which registers the torque delivered by the turbine by means of strain gaged flexure plates. The water brake is operated on oil lubricated ball

*See Table V

bearings. During operation, a flow of water is maintained to the brake such that the outlet temperature is held at approximately 200°F. Variation in water brake load is obtained by varying the water level on the disks by adjustment of the back pressure through means of an exhaust valve. The rating of the water brake is 2420 inch-pounds at 20,000 rpm and can operate at rotational speeds up to 30,000 rpm.

The steam turbine,* located aft of the water brake, provides rotation of the test rig during start-up and shutdown, and during tare testing. This is also coupled to the power train by means of a spline shaft which mates with the aft end of the water brake. The steam turbine is a single-stage "Terry" turbine capable of motoring the turbine train at speeds of up to about 18,000 rpm, although it is rated for safe operation to a speed of 30,000 rpm. The steam turbine is also overhung from a Bytrex torque meter,* to allow measurement of its power input during tare testing and during turbine operation. In both the water brake and steam turbine installation, an attempt was made to eliminate any residual torque produced by the flow lines coming to-and-from these components. The steam turbine was provided with a speed pickup on its aft face, and this is used to monitor rotational speed during all testing. An additional speed pickup was provided on the aft coupling to the main potassium turbine, so that duplicate readings were available in case of failure of either of these components during operation. The steam turbine was also operated on conventional oil-lubricated ball bearings, with separation of steam and oil being maintained by an air-purge labyrinth seal, similar to that employed between potassium and oil in the main potassium turbine. The entire power train was supported in a structure consisting of a number of conical and cylindrical members, which were assembled so as to maintain accurate alignment of all components during testing. This structure forms a glove box, which surrounds the test turbine, and maintains an environment of argon gas to prevent in-leakage of air in the event of a casing leak during testing. Although glove parts were provided, they were not used for assembly and disassembly of the turbine during the test program.

---

*See Table V

The entire test assembly was mounted in a cross-spindle trunnion arrangement as shown in Figure 7, which allowed the turbine train to pivot freely to accommodate the vertical thermal expansion of the boiler and the associated movement of the 8-inch inlet pipe. The exit duct from the turbine to the condenser contained a gimballed joint to prevent restraint of the turbine during this adjustment. Axial thermal expansion of the fifteen feet long inlet pipe was accommodated by mounting the entire turbine and condenser assembly fore-and-aft rolling dolly.

Operation of the power train during a potassium vapor test was briefly as follows:

1. The steam turbine was allowed to warm up by supplying a small amount of steam (not great enough to cause rotation of the power train).
2. Argon was turned on to the potassium turbine bearing housing labyrinth seals and then oil to both the pad bearing and the ball bearings.
3. Oil and cooling air was turned on to the water brake and steam turbine.
4. Steam pressure to the steam turbine was increased until rotation occurred.
5. The speed is increased to 8,000 rpm, at which time potassium liquid is introduced into the potassium turbine hydrodynamic seal.
6. The speed is increased to 12,000 rpm and held until potassium vapor starts coming from the boiler which has been heating up in the meantime, at a rate of about $100^{o}F$/hour.
7. At the onset of vapor, the turbine speed reduces slightly, (due to condensate formation in the colder inlet pipe, with subsequent drag on the blades) and then takes on a steady acceleration.

8. At 18,000 rpm, the steam to the steam turbine is slowly reduced, and water is let into the water brake. This speed is held by adjusting the water brake flow and outlet temperature while the amount of vapor to the turbine increases to the design point for the test.

9. Water is added to the water brake as necessary to absorb all the power output of both turbines. The steam turbine power is ultimately reduced to, and held at approximately 3 horsepower throughout testing.

B. TURBINE COMPONENTS

Following is a general description of the important turbine components, and their functions. Some of the basic design considerations mentioned here are discussed in further detail in References 6 and 7. Materials selection for the various components is discussed in Reference 5.

1. Wheels and Rotor Assembly

The turbine rotor comprises two wheels (shown in Figure 8), and a shaft, held together by a central tie bolt, and indexed to each other by a curvic coupling, a method which has been found to give maximum structural stability in high-speed rotors. This attachment, in fact, proved itself extremely well in this turbine during vapor testing where, although, the entire turbine wheels were running at temperatures as high as 1500^{o}F, no loss of balance of the rotor resulted. Both wheels were fabricated from the same superalloy (Astroloy), a material which is very similar in composition and strength to the U-700 used for the turbine blades. The stage two wheel contains a labyrinth interstage seal on the forward torque cylinder, and a screw seal on the aft cylinder to minimize the flow of potassium condensate into the hydrodynamic seal forward entrance.

2. Rotor Blades

The turbine rotor blades for both stages are shown in Figure 9. Both stages employ a dovetail connection between blades and wheel. The same dovetail form is employed for both stages one and two, and allows for complete replacement of blades (found to be a definite advantage during vapor testing), and maximum blade damping in resisting vibratory fatigue. In addition to these advantages, dovetails are a definite requirement in the second stage wheel where insertion of various refractory metal blades along with the superalloy blades (U-700) was required. The dovetail form employed is the same one used as on the J-85 General Electric turbojet engine, thereby allowing the use of existing tooling for wheel broaching and dovetail inspection. The blades were held in the wheels by Rene' 41 fasteners which were inserted under the blades and bent up at each end. The number of blades in the first and second stages are 62 and 60 respectively, with corresponding airfoil heights of 0.735 inches and 0.955 inches along the radial stacking axis. Since the blades are uncooled, no shank is employed, and the dovetail is placed immediately beneath the airfoil platform. The blades were manufactured with straight-sided platforms to allow each blade to be individually replaced without disassembly of the entire blade assemblage. Tip shrouds were not used, and the airfoil contour was continued to the tip of the blade (as opposed to a thin rubbing surface on the blade tip). Instead, a yielding rub surface was provided by the honeycomb tip seal installed directly over each blade row in the turbine casing. The air foils were tangentially offset slightly from the dovetail radial centerline to cancel the effects of gas bending loads. No special preparation was made to prevent fretting or galling of the dovetail connection in the wheel slot (despite similar materials), and in fact, no fretting was observed during the entire turbine test.

3. Hydrodynamic Seal

A schematic of the hydrodynamic seal is shown in Figure 10. Sealing between oil and potassium is accomplished in two steps, (1) by the rotating cup (see Figure 10) filled with liquid potassium, and (2) by the labyrinth seals which are purged by argon gas injected between labyrinths. The purpose of the rotating cup (see Figure 10) is to contain liquid potassium under centrifugal force, which sustains a pressure difference across the liquid leg. This allows the forward region (turbine wheel space) to be evacuated during startup or to allow changes of pressure during operation without affecting the pressure in the seal sump region, (cavity 2) which is kept slightly above atmospheric pressure. The pressure in cavity 2, in turn, is kept nearly the same as that in the oil sump cavity to balance across the labyrinth seals, which actually maintain separation of the potassium and oil by constant purging.

The forward segment of the inboard pivoted pad bearing assembly consists of a screw seal to minimize migration of oil along the shaft into the labyrinth seal region. The argon purge gas flowing into both the potassium seal sump and the oil sump is ultimately extracted from those two fluids and reclaimed for continuous use. The liquid potassium injection into the seal continuously overflows and is withdrawn to remove heat of fluid friction and conduction. A number of physical arrangements for a hydrodynamic seal were originally investigated to minimize the space required, since the seal directly contributes to the rotor overhang. A photograph of the hydrodynamic seal is shown in Figure 11. The four tubes shown are for the injection of potassium liquid into the seal.

4. Pivoted Pad Bearing

The choice of rotor bearings was dictated largely by the choice of an overhung turbine arrangement, since to support the overhanging weight, and to maintain dynamic stability at high operational speeds,

a relatively large diameter rotor shaft is required. For the 3.464-inch diameter journal of this turbine, a peripheral velocity of 290 ft/sec is experienced at the inboard bearing at 19,200 rpm (or a DN value of 1.69×10^6). For conventional ball or roller bearings, DN values of 1 or 1.2 million are fairly common, but a bearing of DN value of 1.69×10^6 would involve considerable risk of failure, especially in the light of the relatively long life requirements of this test turbine. Therefore, instead of a rolling element bearing, a hydrodynamic journal bearing, and specifically, a segmented pivoted pad bearing was selected. The pivoted pad bearing has shown itself to have good damping characteristics, and in addition, provides good dynamic stability at high speeds. It also has extremely good wear characteristics, resulting in long life. For a pivoted pad bearing of almost the exact size required in this turbine, specific design and test data were available within the General Electric Company, and were employed in the design of the bearing for this turbine. The design is discussed further in Reference 20.

A picture of the pivoted pad bearing is shown in Figure 12. It comprises five pads with cylindrical pivots attached to the back of the pads, and is designed for a 0.005-inch diametral clearance, and a L/D of 0.29. It is made of A-286 alloy with a silver-plated surface (0.010 inches thick) for lubricity in the event of momentary journal-pad contact, and for imbeddability of small impurities. The pivot cylinders are silver plated for maximum dry lubrication, but obtain direct oil lubrication from the lube oil injected into the bearing. An "in-lube" design, developed at General Electric is used, wherein oil is injected into the pad and through internal flow ducting, flows to the bearing surface, providing pressurized pad lubrication. The feed slots can be seen in the photograph. The original bearing was manufactured with the pivot center located 51.3 percent of the arc distance from leading-to-trailing edge of the pools. This was later modified to a value of 56 percent, as discussed in Section VII.

5. Stabilizer Bearing

In addition to the rotor support bearings, the original concern that the high rotative speed, in combination with the low rotor weight (approximately 50 pounds), might produce dynamic instabilities in the lightly loaded forward journal bearing, the "stabilizer bearing" was incorporated. This consisted of a single bearing pad actuated by a piston (using argon gas), shown photographically in Figure 13. Although this bearing was tested and found to operate satisfactorily to 23,000 rpm, it was never actually needed because of the inherent damping of the pivoted pad bearing, and therefore, was eliminated from the turbine assemblies during the final performance and endurance potassium vapor testing.

6. Thrust Bearings

The aft thrust bearing consists of a pair of high-precision, ball thrust bearings*, running at a DN value of 0.96 (10^6) at 19,200 rpm. This originally was a single bearing, but because the single bearing allowed a 0.015-inch axial movement, the single bearing design was replaced by the preloaded pair arrangement, which eliminated the axial shifting of the rotor occurring between loop evacuation and vapor testing. The thrust bearings are continuously loaded rearward by a Belleville spring which exerts approximately 400 pounds force in addition to the aft rotor thrust of 622 pounds during vapor operation.

The aft seal of the bearing oil sump is closed by a conventional carbon face seal. Although not vacuum-tight, the seal is adequate, since during operation the oil sump is maintained at above atmospheric argon gas pressure to prevent in-leakage of air.

---

* Fafnir MM-210-VMZ Bearing

7. Inlet Duct

The inlet duct, shown in Figure 14, contains a four strut-supported bullet nose for directing and accelerating the turbine inlet flow. It also contains the stage one nozzle diaphragm assembly during operation.

8. Bearing Housing

The turbine bearing housing, comprising the main support structure for the rotor, and the mounting structure for the turbine is shown in Figure 2. This not only houses the bearings for the rotor, but also supports the turbine exhaust scroll, which in turn attaches to the inlet casing. The bearing housing aft flange is attached to the dished head of the test facility glove box (Figure 4), thereby mounting the turbine in the test facility. The hydrodynamic seal is attached to the forward end of the turbine bearing housing by welding, and its potassium inlet and outlet lines are extended along the outer periphery of the bearing housing to the outside. All other tubes carrying argon and/or oil in and out of the turbine also are conducted through the bearing housing. These lie in a cavity around the outer periphery of the housing, and are enclosed by a sheet metal "heat shield cover" with a bellows for thermal expansion as shown in Figure 15. This comprises an argon purged cavity between the hot exhaust vapors of the scroll and the oil sump of the bearing housing which prevents condensation of potassium vapor around the many flow tubes. The forward end of the bearing housing contains the wear surfaces for the previously discussed labyrinth seals in the hydrodynamic seal assembly. These surfaces were originally nickel-plated because of concern for potassium contamination of the wear material, but were later replaced with copper plating which served well in performance and endurance potassium testing. The tubes extending out of the bearing housing are installed in a helical manner to allow for differential thermal expansion between tubes and main bearing housing. They were originally brazed into the housing, but because of embrittlement of the

tube joints during brazing, they were later attached by welding. The turbine exhaust scroll is attached to the bearing housing by the conical mid-flange which is welded.

9. Casing

Two different turbine casing designs were investigated, involving circumferential and horizontal flanges respectively, as discussed in detail in Reference 7. Although the circumferentially split casing, involving a number of ring segments, offered the possibility of better dimensional stability under the hot turbine running conditions, it did not lend itself to assembly and disassembly, considering the need to weld all nozzle diaphragm pressure and temperature instrumentation to the casing during assembly. With a circumferential flanged casing, the pressure and temperature instrumentation would have had to be "threaded" through the casing wall with each assembly and disassembly with subsequent seal-welding (or cutting) to prevent air-leakage into the loop. As a result, the horizontally split casing shown in Figure 16 has been used wherein nozzle diaphragms, tip seals, etc., are also horizontally split, and become an integral part of the casing after inserting and welding of instrumentation. Both casing-nozzle halves are placed around the rotor as pre-assembled units during final buildup, and the flanges are welded closed. The turbine casing was originally designed for use of bolted flanges in an attempt to avoid weld distortion after assembly resulting from such flange welding and to provide ease of assembly and disassembly. The bolting approach however, was later abandoned due to inability to maintain adequate sealing against potassium and/or oxygen leakage, and weld flanges were incorporated, as discussed later. By special weld-flange design and specifically planned and carefully controlled welding techniques, weld distortion to the casing as final assembly was held within acceptable limits. Also, it was demonstrated that the welded flange could be cut or rewelded a number of times without difficulty. The casing is fabricated from the same material as is used in the rest of the facility loop (316 stainless

steel) for maximum weld compatibility with the major loop ducting and elimination of differential thermal expansion between joining parts.

10. Blade Tip Seals

A turbine tip seal fabricated from 316 stainless steel honeycomb to give maximum protection against blade damage in the event of tip rubs resulting from casing distortion was placed over each rotor blade row. This turned out to be an advantage on a number of occasions where slight tip rubs actually occurred. The tip seals are shown photographically in Figure 17. Also, the similar 321 stainless steel honeycomb interstage rub seal is shown.

11. Nozzle Diaphragm Assemblies

The nozzle diaphragm assemblies are assembled from solid L-605 vanes (except for radial instrumentation tubing holes through selected vanes) brazed to 316 stainless steel outer and inner shroud bands. The nozzle diaphragms are rabbetted and bolted into the casing and their instrumentation tubing is then seal-welded to the casing where it comes through, as indicated above. Stage one nozzle diaphragm assembly is installed in the inlet bullet nose duct, thereby avoiding the necessity of splitting the nozzle diaphragm as is necessary with the stage two nozzle diaphragm, and also, by locating the forward casing flange downstream of the first stage nozzle diaphragm, the pressure stresses on the casing flange are accordingly reduced (from 31 psia to 24 psia at design-point operation). The outlet guide vane assembly, consisting of flow straightening vanes, is horizontally split and rabbetted to the casing in a similar manner as that of the stage two nozzle assembly. Pressure instrumentation is brazed into the nozzle diaphragms during their manufacture, and consists of 1/8-inch diameter tubing in both inner and outer flow path regions. Photographs of the nozzle diaphragm and outlet guide vane assemblies are shown in Figures 18, 19 and 20, respectively.

12. Exhaust Scroll

The turbine exhaust scroll shown in Figure 21, is a 316 stainless steel structure which is welded to the bearing housing and the turbine casing. Any gross distortion of the scroll would allow movement of the casing with resulting turbine tip rubs.

13. Moisture Spray Injection

To simulate conditions of low vapor quality in the incoming potassium vapor, heated-liquid potassium was injected into the essentially dry vapor coming from the boiler at a point just ahead of the turbine. Although the spray valve was designed for maximum atomization of the liquid, it was recognized early in the test program that any spraying technique would be inadequate to simulate submicron droplet formation representative of fog-type condensation that might form in a real turbine stage.

The primary reason for selecting a two-stage turbine was to provide the second stage with moisture having a realistic drop-size distribution. The rotor blades of most interest were mounted in the second stage. The means for injecting liquid consisted of a conical spray valve-nozzle combination which injected up to ten gallons per minute of liquid potassium ahead of the stage one nozzle diaphragm. Figure 22 shows a cross-sectional view of the spray valve and a photograph of its installation into the upstream duct. The valve is gas pressure actuated (using argon).

14. Interstage Condensate Extraction

The turbine in turn, was equipped for interstage removal of the moisture injected into its inlet. This is typically done in the latter stages of steam turbines to improve efficiency and minimize the erosive effects of moist vapor. Shown in Figure 23 is the design employed to extract moisture from this turbine, which consists of drainage slots in

the casing downstream of each rotor blade row. The liquid is collected in a circumferential groove, and feeds out through a tangential drain in the casing. This design differs from that of steam turbines in that in the latter, the casing drainage slots are located directly over the blade tip and comprise a relatively large opening, while tip sealing is done axially by the edges of blade tip shrouds. In this turbine, the blades were not provided with tip shrouds due to the high temperatures and stresses of the rotor. Consequently, the blade tip region was made a smooth flow path contour for sealing purposes, and the drainage slots were located downstream of the rotating blade row with the intention that the liquid would flow axially along the outer wall and into the slots, Reference 6. This approach was only partially effective, as described in Section VII.

IV. FABRICATION AND TURBINE ASSEMBLY

A. TURBINE MANUFACTURE

The potassium turbine was designed with the intent of minimizing the number of components or component groups requiring a development program to effect their manufacture. This was done by using state-of-the-art fabrication techniques and materials which were common to the gas turbine technology of the General Electric Company where possible. This was particularly beneficial during the rotor wheel manufacture for example, since existing broach tooling was available for cutting blade dovetails in the wheels. Also, the curvic coupling on wheels and shaft employed existing design and tooling, and the existence of brazing and welding technology suitable for the potassium turbine allowed manufacture to proceed without extensive proof-testing of the selected techniques.

The superalloys used in the turbine are the same as those in the most advanced gas turbine designs. By using available alloys, extensive material properties data for design purposes were available, and although the forgings had to be procured by special order, they were available from commercial forging sources. Heat treatment cycles for both the U-700 blades and Astroloy wheels are discussed in detail in Reference 5.

An initial concern in fabrication involved the broaching of the turbine wheels. Astroloy, in its fully heat treated condition, exceeds the recommended hardness for available broaching cutters (RC 42). To avoid cutter breakage, an experimental program was run which involved broaching the dovetail in less-than-fully-heat-treated condition, and then measurement of the slot after final heat treat to observe the dimensional stability of the accurate surfaces through final heat treatment. Coupons (shown holding the blades in the test in Figure 56a) were used in this test. They showed excellent dimensional stability, and through heat-treatment, and the technique of broaching before final hardness were successfully incorporated into the turbine wheel manufacture.

PRECEDING PAGE BLANK NOT FILMED.

Turbine blades were machined from bar stock. Manufacturing and inspection of all aerodynamic components was done in General Electric shops and established vendor sources. Some difficulties were encountered initially in machining the hard U-700 blades, but were resolved by use of correct cutting equipment and machining techniques. Machining the refractory metal blades presented particular problems. The low room temperature ductility (discussed in Reference 2), combined with the thin sections of the blade platform resulted in cracking and breakage of the blades during initial machining. This was solved by casting a supporting material (soft metal) around the blades before machining. Special consultation with General Electric development shops was maintained in the machining of refractory metals.

As in any such development program, considerable manufacturing effort consisted of modifications to existing components, done under pressure of a time schedule to prevent testing delays. Close engineering follow-up in manufacturing shops during these modifications were generally successful in providing correctly made parts with maximum speed.

Brazing was accomplished with a cobalt-based braze alloy (discussed in Reference 2 and designated as H-33 alloy) which has shown excellent thermal shock characteristics in gas turbines. This worked well in the present potassium turbine, and despite several thermal shocks during turbine startup, the braze in the nozzle diaphragms never exhibited cracks. Embrittlement of thin-walled tubing during brazing with this alloy was a problem, however, requiring replacement of almost all tubing brazing with welding.

Standard machining techniques were used throughout the program, including electrical discharge machining. Standard plating and/or flame spraying used to apply copper, silver, nickel, and molybdenum to various seal and rabbet surfaces, and a "puddling" process, involving flowing silver onto a surface from a silver weld rod was used in applying silver to the shaft screw seal.

The turbine throughout its testing was assembled on a "selective-fit" basis where necessary. Records were maintained of all dimensional fits in each individual buildup. Individual part-fitting of non-critical components was allowed, in that a single turbine was being built and tested. Since several components were re-used in a number of buildups, thermal distortions required individual remachining and selective fitting of the re-used parts.

During welding of the turbine in final assembly, specific welding sequences, and between-weld cooling schedules were required. In addition, where possible, dimensional measurements were made during the welding, such as with dial indicators which constantly observed the pattern of distortion to indicate where the next weld should be made. These techniques were quite successful in allowing welding to be done on high-precision machined components during final assembly, without excessive distortion.

B. TURBINE ASSEMBLY

Turbine assembly comprises three major phases:

1. Rotor assembly and balance.
2. Subassembly of several sets of stator parts.
3. Final rotor-stator assembly and welding.

An exploded view of the turbine assembly is shown in Figure 2.

1. Rotor Assembly and Balance

The first step in rotor assembly is the buildup of the individual wheels and blades. All blades are preweighed (as are all turbine parts before running) and the blades are installed for the best initial balance of the wheel, as determined on a rotating force balance machine. The blades are tip ground after assembly, and the wheels are rebalanced to a tolerance to 0.5 gram-inches or less residual unbalance. The rotor is then assembled as shown in Figure 24 and is dynamically balanced in a two-plane dynamic balancing machine*, as shown in Figure 25.

*See Table V

In practice, balance levels of better than 0.5 gram-inch for the overall rotor have been typical. Balancing is performed using the standard balance equipment used in the balancing of gas turbine rotors. Balancing is achieved by selective placing of the preweighed buckets and by metal removal from least-stressed areas of the discs and shaft.

Because the hydrodynamic seal contains both static and rotating components which are not separable because of an interlocking of the rotating cup with the stationary discs, and because the rotor cannot be installed as an assembled unit, it was necessary to disassemble the rotor after balance. This was done for every buildup of the turbine without any observed loss of balance during ultimate testing.

2. Stator Assembly

The major subassemblies of static parts are the:

1. Inlet Duct
2. Casings
3. Scroll Assembly

The inlet duct subassembly consists of the inlet duct, first stage nozzle diaphragm, and honeycomb tip seals as shown in Figure 26a. The nozzle diaphragm is held in place by the tip seal, which in turn is bolted to the inlet duct aft flange. Four keys prevent rotation of the nozzle diaphragm in the casing. The complete subassembly is shown in Figure 26b, showing the trailing edges of the first stage nozzle diaphragm.

The casing subassembly (Figure 27) consists of the casing shell forging, second stage nozzle diaphragm, second stage tip seal, interstage seal, and outlet guide vane. All parts are rabbetted and bolted to the casing.

The scroll (Figure 21), when combined with the casings and inlet duct subassemblies makes up the complete stator of the turbine. When completely assembled, the scroll effects the alignment of the bearing housing and rotor with the stator, as indicated previously.

The bearing housing subassemblies comprise the bearing housing hydrodynamic seal weldment, the pad bearing assembly, and the ball bearing housing assembly. This total assembly contains the turbine rotor bearings, the hydrodynamic seal, and all internal piping to provide the argon, potassium, and lube oil flows to and from the internal components. Figure 15 shows the housing with hydrodynamic seal attached, before and after the addition of the heat shield bellows cover.

The pad bearing assembly (Figure 28) comprises the bearing pads, socket ring, forward retainer ring, aft retainer ring and keys. The socket ring contains the five bearing pads by cylinder sockets which have a close fit to the barrels on the pads (0.0005-inch radial clearance). The O.D. of the ring is, in turn, closely fitted to the I.D. of the bearing housing in cold condition. In hot condition - hot casing, cold bearing - six radial keys ensure concentricity of bearing housing and socket ring. At both ends of the socket ring, the pads are contained by the retainer rings, the forward one also comprising the shaft oil screw seal.

The ball thrust bearing housing assembly (Figure 29) consists of the outer housing, two ball bearings, Belleville spring, Belleville loader, and a carbon seal assembly. This assembly established the axial position of the rotor as shown assembled in Figure 1. The two ball bearings fit into the I.D. of the housing with a 0.0007 diametral clearance and are held in a 400-pound axial preload by the Belleville spring.

3. Final Assembly and Installation

The first step in final assembly is welding the bearing housing to the scroll as shown in Figure 30. At this point none of the bearing housing subassemblies are in place. The shaft and pad bearing assemblies are then inserted in the bearing housing, thus effecting the forward mounting of the rotor shaft. Subsequently, installation of the internal instrumentation is done from the aft end, as shown in Figure 31. The casings and rotor are then trial-fitted for verification of clearances as shown in Figure 32. The scroll is placed in a vertical position for this check. The measured clearances are compared to predetermined allowable limits, and are then tabulated as shown in Figure 33, which includes the critical clearances for all major buildups. After verification of clearances, the inlet duct, casings, and scroll are welded together, with the turbine rotor in place to complete the assembly, as shown in Figure 34. The turbine is then mounted in the test facility by welding vapor inlet and outlet ducts to its lead and exit flanges.

V. COMPONENT DESIGN

A. DESIGN CRITERIA

The general design criteria employed in the design of the potassium turbine is similar to that developed for turbojet engines, with some modifications to accommodate the long life and otherwise specific requirements of the present design. Following are the basic failure criteria and general design techniques employed for the potassium test turbine.

1. Life determination: Where stress limitations were set by long-time operating characteristics of creep and stress rupture (which is generally the case of the hot rotating parts), the allowable running conditions were based on a "total life used up" distribution according to the following relationship:

$$\text{Percent of total life used up} = \frac{t_1^1}{t_1} + \frac{t_2^1}{t_2} + \cdots\cdots$$

where t_1^1 = actual operating time under operation condition 1.

t_2^1 = actual operating time under operation condition 2.

t_1 = maximum allowable operating time under operation condition 1.

t_2 = maximum allowable operating time under operation condition 2.

The allowable stress as a function of operating time and temperature was based upon the "Larson-Miller Parameter "M" and the published material strength curve:

$$M = T(C + \log_{10} t) \times 10^{-3}$$

where T = material temperature in ^{o}R

t = required operating time in hours

C = empirical constant depending upon the material and available data.

2. Theory of Failure: It has been found that nearness to failure is most accurately represented by the theory of constant elastic strain energy of distortion (Reference 21), with the resulting "effective stress" being the best measure of nearness to failure, as follows:

$$\sigma_e = \frac{\sqrt{2}}{2} \sqrt{(\sigma_x - \sigma_y)^2 + (\sigma_y - \sigma_z)^2 + (\sigma_z - \sigma_x)^2 + 6\tau_{xy}^2 + 6\tau_{yz}^2 + 6\tau_{zx}^2}$$

where σ_e = effective stress

τ = shear stress

σ = direct stress

x, y, z = the three mutually perpendicular planes

3. Steady-Stage Loads: For steady-stage loads, the stress levels were determined by whichever of the following was lower:

a. 100 percent of 0.2 percent offset yield strength

100 percent of 1 percent plastic creep strength

80 percent of stress rupture strength (except in extremely localized regions of stress, such as dovetail connections, or wheel bore stress, where 90 percent of stress rupture strength was used).

On all published material curves of yield, creep, or stress rupture strength, the allowable strength was determined by the lower band of the spread of material data which, in turn was determined by a 3 sigma statistical distribution or a "material deviation factor", which varies between 75 percent and 90 percent. Shear stresses, when not directly available, were determined as 0.57 of the material's ultimate tensile strength.

4. Alternating Stress: The total stress imposed on a blade comprises a steady component due to centrifugal force, upon which is superimposed an alternating stress resulting primarily from the repeated pulsations of vapor from the passing nozzle vanes. For any steady state level of stress, there is a maximum alternating stress permitted to realize a particular life (for any given material and temperature). This is presented in a "Goodman Diagram" which for U-700 at 1500°F (turbine inlet temperature at endurance testing design point conditions), is shown in Figure 35a.

In this turbine design, the alternating stress level was considered to be that produced by the complete removal and re-application of the total gas bending loads.

Some of the important aspects of specific component design are as follows.

B. STRESS ANALYSIS

1. Rotor

The techniques for analyzing the stresses in turbine blades, dovetails and wheels followed the same as those used for turbojet engine design, and available computer and analytical procedure programs were used where possible. The rotor stress analysis is discussed in Reference 8.

Because the turbine blade airfoils have a rigid cross-section and short length, and because the rotational speed is high (corresponding to low torque for the given turbine horsepower), the gas bending loads in the blades result in bending stresses of only a few hundred psi, so that the primary stresses are due to centrifugal loadings. To compensate for the bending loads, the blade airfoil was offset slightly (0.006 inches) from the dovetail vertical centerline to centrifugally cancel

the bending stresses at the design-point conditions. Because of the relatively short length of the turbine blades, the airfoil stresses were not of primary significance, but rather dovetail stresses in the connection between blade and wheel became the limiting stress. The results of the dovetail stress analysis for both blade and wheel are given for stages one and two in Figure 35c. The stress at the bottom tang of the wheel dovetail comprises the limiting stress in the entire turbine rotor. As seen in Figure 35c, the stress for stage one dovetails is given for the nickel alloy (U-700) blades only, since no refractory materials were used in the first stage. For stage two, stresses in the wheel dovetail for both U-700 (nickel alloy) and TZM and TZC (molybdenum alloy) blades are given, and as can be observed, the stresses in the portion of the turbine wheel carrying the molybdenum blades are higher than for the nickel alloy blades, resulting from the greater density of the molybdenum alloys (0.369 lb/in.^{3} compared with 0.286 lb/in.^{3} for U-700).

For U-700 wrought alloy, the Larson Miller parameter plot for rupture stress is shown in Figure 35b and in Reference 5. This curve represents the lower limit of the band produced by three standard deviations from the "average" material strength resulting from laboratory pull tests. Furthermore, superimposed on this plot is the curve showing the locus of stresses at 90 percent of the above curve, which according to the discussion in the "Design Criteria" section above, represents the maximum allowable level of stresses to be used for blade and wheel design purposes. (The properties of Astroloy used in the wheels are so similar to those of U-700 used in the blades, that the U-700 data are used in the design of both blades and wheels.)

Referring to Figure 35, it can be seen that the maximum stress levels in the wheel dovetails (for the design-point rotative speed of 19,200 rpm) are:

Stage 1 wheel dovetail stress = 32,600 psi
Stage 2 wheel dovetail stress = 50,250 psi

For the stage one and stage two wheel temperatures of 1460°F and 1310°F respectively, (corresponding to a turbine inlet temperature of 1500°F) these stresses allow the following wheel operating life, based upon rupture stress:

Stage 1 allowable life = 2,000 hours
Stage 2 allowable life = 3,000 hours

From this, the turbine continuous operating life is limited by stage one.

Prior to the endurance testing, however, because of anticipated vibrations at the 19,200 rpm condition, (Figure 43b) the operating speed was changed to 18,250 rpm, resulting in a corresponding reduction in all stresses given in Figure 35c (by the square of the initial-to-final speed ratio). This resulted in an increase in the corresponding allowable operating life of stages one and two as follows:

Stage 1 allowable life = 4,000 hours
Stage 2 allowable life = 12,000 hours

From these data, it can be seen that because of its higher temperature, despite its lower stress level, stage one wheel becomes limiting, and fixes the turbine's accumulative operating life at 4,000 hours.

In analyzing turbine wheel web and bore stresses, Reference 8, thermal stresses were ignored, since the wheel is bathed at essentially one temperature during steady-stage operation. Wheel stresses analysis was performed on a digital computer using an available elastic disk analysis program. On stage one, in addition to rotational stresses, the wheel is subjected to an axial load at its bore of 10,000 lbs due to the tension of the tie bolt, this force being counteracted through the curvic coupling torque cylinder, and producing a bending stress around the inner bore of the wheel (about 11,000 psi at initial tie bolt tension). This resulting stress was superimposed upon the centri-

fugal stress calculations to give an overall stress distribution as shown in Figures 36 and 37 for stages one and two wheels respectively. The stresses shown are "effective stresses" according to the previously presented equation (Section V-A-2).

It can be seen that the bore stresses, as usual, are highest and are quite localized. On stage one, the maximum stress values shown represent the bore stress at the aft end of the central hole. Since these are local stresses, their allowable levels were taken as 95 percent of the published stress-rupture data. With time, local creep causes these bore stresses to relax to lower values than those used in the life calculations. Figures 36 and 37 show the average wheel stresses to be 50 to 60 percent of the maximum bore values, and therefore, safe.

The stress and temperature distribution in the tie bolt is shown in Figure 38. A steep temperature gradient exists from the hot end toward the colder end of the bolt. Its axial force pretension (10,000 lbs) is sufficient to hold the rotor together under normal running conditions. The diameter of the bolt was varied according to temperature distribution. It was made relatively large at the hot end to minimize stress, and smaller at the cold end to obtain a higher initial elastic elongation to, in turn, prevent loosening of the bolt under the differential thermal expansion between the bolt and shaft-wheel assembly at operating temperature. The tie bolt stress analysis does not permit direct use of the stress-relaxation design curves which are based on the entire bolt being at a uniform temperature and relaxing with time. Rather, the material property of major concern is the plastic creep rate, because plastic extension of the bolt near its head is the primary factor in reducing the locking stress. The bolt was designed to stay within the 0.2 percent plastic creep range in the short hot section. No torsional stresses were imposed on the bolt, since it was pretensioned axially with a hydraulic ram, and the lock-nut turned finger-tight before releasing the ram load.

2. Stator

(a) Casing and Ducting

The inlet duct, turbine casing and exit scroll have sufficiently heavy wall structures that, under the maximum internal turbine pressure of 21.7 psig, the wall stresses produced were not of significance. The only stresses of concern in these parts were in the welds on the thin sections of the flanges. Figure 39 summarizes these stress levels, which are all within stress-rupture limits for the 316 stainless steel material. The forces considered as stress-producing were:

1. The axial tensile load across the forward and aft diametral flanges resulting from a pulley-weight arrangement which was applied to pull the aft end of the turbine and thereby prevent buckling of the turbine-inlet duct assembly during thermal expansion at startup. This force was approximately 200 lbs, and was treated as a direct tensile stress across the forward and aft flange welds (see Figure 39).

2. The radial forces acting to separate both the radial and horizontal flanges, resulting from the internal pressures within the casing. These are of most significance at the inlet end of the casing, where both the pressure and temperature are highest. The horizontal flange stress was treated in simple tension across the weld.

3. Pressure drop forces across the nozzle diaphragms.

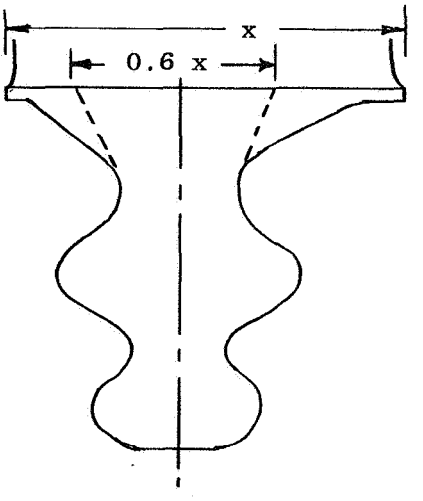
(b) Nozzle Diaphragms

The major nozzle diaphragm stresses were imposed by the pressure differential acting across the nozzle diaphragm. These forces resolve into hoop stresses in the inner and outer bands and bending stresses on the outer diaphragm rabbets, which are quite low, and are summarized in Figure 40.

C. VIBRATION

1. Blades

A vibration analysis was performed on both stages of the rotor blades (Reference 8) to determine their natural frequencies, using an available "twisted blade" program on a digital computer. Because of the high stiffness of the blade airfoil sections, the dovetails could not be considered infinitely stiff by comparison, and the analysis was made with an assumed dovetail spring constant included. Previous experience on small aircraft engine development programs has shown dovetail "spring" to materially reduce blade frequencies below those of the airfoil alone, especially as in this design, where a slender shank is not incorporated. However, although the turbine blades have no long shanks as such, there is a neck section joining the dovetail to the airfoil which for purposes of simulating actual stiffness (based upon available experience within General Electric) was considered to be 60 percent of the true platform width as shown below:



Based upon the above reasoning, a first flexural blade frequency of about 5800 cycles per second was calculated for both stages one and two. Although higher modes were also identified, they become insignificant since the vapor driving forces on the blades were very low. The calculated blade natural frequencies are shown in Figures 41 and 42 for

both stages. Subsequent to this analysis, and as discussed in Section VII in this report, bench tests on actual blades were run with the blades clamped in various manners in a dovetail-slotted coupon. Also, in turbine pretesting, the blades were instrumented for flexural and torsional vibration measurements, and resonant frequencies were observed under actual running conditions in air.

To avoid exciting the blades at even-cycle impulses at blade-passing frequencies from the gas stream (at NASA suggestion), half the nozzle vanes of each diaphragm were rotated through 1/3 vane space as discussed in Reference 4. This appears to have been effective, since in actual testing (Section VII and Figures 65 and 66), the vibratory stresses on the blades were so low as to hardly be measurable. It can be seen that the measured airfoil bending stresses were in the order of 200 to 300 psi. Throughout the entire test program, blade vibrations were not a problem.

2. Critical Speeds

The critical speeds of the entire turbine system were calculated using an available computer program employing the balance of kinetic and potential energies, known as "VAST". In this analysis, the entire system (rotor and stator) is considered to be a series of short segments, linked together, and considered as flexing beams with local stiffness and area properties, and with their mass concentrated at their ends. Bearings are replaced for calculational purposes by springs with assumed spring constants. The critical speed analysis is discussed in Reference 9 and the turbine critical speeds (including the supporting structure and inlet duct) are shown in Figure 43 for the assumed bearing spring constants shown. Of the three critical speeds identified, the only one in the turbine operating range is at 14,792 rpm wherein the rotor is acting as a rigid body in the bearing springs and resonating in the conical mode.

During turbine testing, the presence of any precise potassium turbine critical speed was difficult to identify, and some variations in system vibratory patterns were observed with each buildup. Some slight evidence of increased accelerometer readings in the pivoted pad bearing region was generally observed in the speed range of 14,000 rpm to 16,000 rpm during operation. However, by obtaining a high degree of initial rotor balance with each buildup (residual unbalance of less than 0.5 gram-inches at each turbine bearing) no difficulties were ever encountered in the potassium turbine in passing through critical speeds.

The presence of critical speeds was sensed more acutely in the water brake and steam turbine drive train than in the potassium turbine, as indicated in Figure 43b. This shows measured vibratory amplitudes for all three of these components for one particular buildup (test beginning October, 1964). As can be seen, resonances do occur in the operating range, with the result that during endurance testing, the previously discussed adjustment of operating speed (from 19,200 rpm to 18,250 rpm) was made to obtain a minimum level of vibration. In operation, passing through any of the system critical speeds was not a problem, and in fact, during the numerous changes of rotor speed to accomplish performance testing, the critical speed range was passed through many times.

D. TEMPERATURE DISTRIBUTION

The temperature distribution throughout the turbine was calculated for several inlet temperatures, and is shown in Figure 44 for the 1550°F inlet vapor temperature case. This employed a computer program which uses a thermal-electrical resistance analogy in calculating the temperature distribution. Figure 44 also shows several temperatures actually measured during vapor testing.

Figure 45 shows the calculated opening and closing of various critical radial and axial clearances throughout the turbine (based upon the above temperature distribution). These differential thermal expansions were used

to set the turbine final dimensions prior to manufacture of the components, and were used to determine the hot and cold clearances of each turbine buildup. These clearance changes result both from the existence of temperature differences between parts during operation, and from the significant differences in coefficients of thermal expansion between 316 stainless steel and U-700 superalloy. At 1400°F, for example, 316 stainless steel has a coefficient of 10.4 (10^{-6}) in./in. while U-700 has a coefficient of 8.4 (10^{-6}) in./in. This results in an inherent opening of tip clearances with increasing temperature, for example.

VI. TURBINE TESTING

A. GENERAL

The overall test program for the potassium turbine represents an effort covering three years. The chronology of significant testing events is included in Table VI of this report, and a historic record of accumulated test time on potassium vapor is shown in Figure 3. The turbine testing consisted of both a "pretesting" phase employing water, steam, and air, and ultimately, the "potassium vapor testing" phase in the potassium facility. These testing efforts were accompanied by numerous side-tests of individual components and sub-systems in both the turbine and test facility.

The overall program achieved its objectives of obtaining performance data and accomplishing its endurance test program, and provided valuable test and alkali metal vapor turbomachinery development experience. Typical of development undertakings of this type, the program was also marked, and occasionally directed, by development problems in both the test facility and the turbine. The significant ones are discussed herein. These problems were ultimately solved, to allow accomplishment of the test objectives with a successful completion of a 2000 hour endurance test on December 20, 1965.

B. TURBINE PRETESTING

Prior to committing the two-stage turbine to alkali metal testing, a series of tests were run in easy fluids to identify operation characteristics of individual components (bearings, seals), and to determine the overall system dynamic vibration patterns, (References 10, 11, 12, 13, and 14). This testing was done with dry air, steam and water so that installation, instrumentation, and visual observation of equipment was possible. This involved:

1. Bench testing of individual components and sub-systems.
2. Dynamic testing (wherein the turbine rotor was driven by the steam turbine).

PRECEDING PAGE BLANK NOT FILMED.

3. Pretesting, where the potassium turbine was operated as a power-producing machine using steam and air.

For the dynamic bearing and seal pretesting, the turbine was set up in the test cell as shown schematically in Figure 46a and pictorially in Figure 46b (Reference 12). The potassium turbine rotor (without blades or casing enclosure) was driven by the steam turbine to a speed of 23,000 rpm. The water brake was not installed, since no power was being extracted from the potassium turbine. The purpose of this testing was to:

1. Observe the temperature-flow characteristics of the pad bearing and ball thrust bearing at operating speeds.
2. Observe the sealing capacity and fluid dynamics of the hydrodynamic seal.
3. Observe the general vibratory characteristics of the rotor.

1. Instrumentation

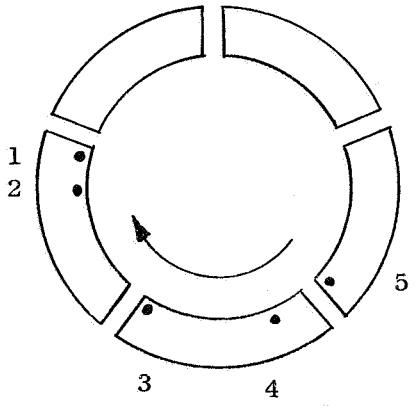
The turbine instrumentation employed during the pretesting phase (see Reference 13) consisted primarily of pressure, temperature, speed and vibration instrumentation. Temperature, speed, and vibration measurements were made with standard thermocouples, inductance pickups, and strain gages, while pressure measurement in the vapor flow stream was made by the "efflux" technique described in References 1 and 22. The technique employed is one of maintaining a small flow of purge gas through the pressure tap line, and measuring the pressure necessary to force this flow inward against the vapor pressure at the tap outlet. This testing provided the first operational checkout of the efflux pressure measuring system which was ultimately successfully employed in potassium vapor testing.

Where both continuous records and visual monitoring of system temperatures were necessary, readout was done both on Sanborn and Multipoint recorders. Bourdon gages and oscilloscopes were used for visual observation of the various cavity pressures and rotor dynamics,

respectively. Blade vibrations and rotor accelerations were recorded on a 14-channel tape recorder (Figure 64b).

2. Bearing Testing

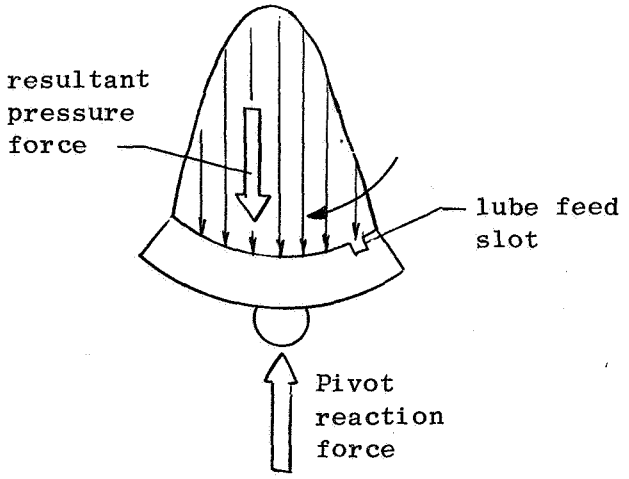
Prior to installing the pivoted pad bearing a series of five thermocouples were installed in the pads, primarily along the trailing edges to read maximum temperatures as shown below.



The bearing was lubricated with Socony Mobil DTE 797 oil, and was tested over the following range of variables:

Running Speed	0 to 23,000 rpm
Lube Inlet Temperature	97°F to 170°F
Lube Flow Rates	2.2 gpm to 4.5 gpm

During the first runs, it was found that an automatic reduction in lube flow occurred with increasing rotative speed for all conditions of flow and temperature. This decrease in oil flow was found to be caused by the pivoted moment produced by the center of hydrodynamic pressure and the pivot roller reaction.



As the speed increased, hydrodynamic forces caused rotation of the pad, thereby pressing the feed slot against the journal with subsequent reduction in the lube flow area. By removing material from the trailing edge of the bearing pads, the flow reduction with speed was essentially eliminated for the flow rate of interest (2.2 gpm) as seen in Figure 47. Also, the curve shows that maximum bearing temperature is essentially independent of lube flow rate for the range of flows tested, indicating that any flow beyond the lower value of 2.2 gpm leaks out around the sides of the bearing pads, and does not add to the cooling capacity of the bearing.

Figure 48 shows the temperature of the outer race of the ball thrust bearing as a function of operation speed for a range of lube inlet temperatures and a flow rate of 0.8 gpm. These were within allowable limits for the bearing material used (52100 steel).

3. Hydrodynamic Seal Test

During the pretesting discussed above, it was observed that the potassium and argon flow exit ducts from the hydrodynamic seal sump (see Figure 10) were too small to carry away the combined seal liquid and purge gas from the seal sump region. Originally, the sealing liquid

was carried from the seal exhaust sump by two tubes of 0.194 inch I.D. which served to scavenge both the seal liquid and seal-side argon. The maximum flow which could be accommodated by this design was not sufficient to carry away the seal fluid friction heat. For this reason, development of the hdyrodynamic seal was pursued in a special test rig, (Reference 11). The test objectives were as follows:

1. To visually observe the operation of the seal, noting any tendency for leakage out the front, or across the gas-purged labyrinth seal.

2. To record pressure-flow-horsepower consumption data to determine the accuracy of previous calculations and to provide a series of operating curves defining the operating limits of the seal.

3. To determine the number of liquid outlets needed in the liquid sump region to adequately pass both the purge gas and the seal liquid flow, and to determine the internal seal pressure distributions during operation.

To observe, visually, the flow through the hydrodynamic seal, and to measure pressures and power consumption of the seal, a test model was set up in a plexiglass housing (as shown in Figure 49a and photographically in Figure 49b) with rotating steel parts of the same geometry and size as those in the actual turbine, but with numerous pressure taps built into them, in the locations shown in Figure 50. The entire test rig was overhung on a bearing-mounted shaft, allowing seal horespower consumption to be determined from torque measurements obtained from a load cell on an arm extending from the main housing. The seal was assembled in an existing high speed air-turbine driven test rig as shown in Figure 51a and schematically installed as in Figure 51b. A total of 11 pressures were measured by a scanning switch which sequentially printed out all pressures on a single strip of Sanborn.

At the beginning of testing a liquid leakage at the forward end of the seal cavity in the vicinity of the forward screw threads was observed (see Figure 49a). The screw threads were incorporated in the seal to pump vapor and condensate away from the liquid in the slinger cup, and had a correspondingly "forward" advance, but it was found that when the threads became fully wetted, they became a "primed pump" which pulled liquid from the slinger cup, and pumped it directly into the forward turbine wheel space.

A number of screw thread configurations were tested, the best solution being the combination right-and-left hand screw thread shown in Figure 52. On the seal's liquid side the liquid would be pumped back into the pump slinger cup, and on the vapor side, the screw thread of opposite hand would pump vapor condensate back into the vapor (wheel space) cavity. In addition to the change in screw thread geometry, the means of injecting liquid to the seal was changed from that shown in Figure 53a to that of Figure 53b, eliminating any direct splashing of incoming liquid into the threads.

Further testing allowed visual confirmation that the fluid and purge gas outlet holes (Figure 53) were too small to pass the required flow. The number and size were increased from a total of two 1/4-inch diameter holes to a total of six 3/8-inch diameter exhaust ports, which provided adequate flow area, and which were subsequently incorporated into the potassium turbine hardware.

The major performance results of this hydrodynamic seal bench testing are shown in Figures 54 and 55.

Figure 54 shows the actual horsepower measurements compared to those of previous calculation, which indicate a good correlation. Figure 55 shows the maximum sealing capabilities across the rotating cup as a function of speed. Included in both these curves are corresponding calculations of seal horsepower consumption and sealing

capacity using potassium as a working fluid. The basic equations for these calculations are included in Reference 11, and a detailed presentation of the seal theory and analysis is presented in Reference 24.

4. Blade Vibration Testing

Prior to installing them in the turbine, both stages one and two turbine blades were subjected to bench tests to determine, and to compare with previous calculations, their various natural frequencies (Reference 15). Also, a plot of nodal patterns and stress distribution throughout the blades was determined. For bench testing, the blades were held in dovetail-broach coupons (such as shown in Figure 56a) which in turn were clamped in vice jaws, and the blades were excited electromagnetically. Provisions were made to exert vertical forces on the blades to somewhat simulate centrifugal force by the screws and push rods extending up through the bottom of the coupon. As the screw was tightened, the natural frequencies were obtained as in Table I. Both the torsional and the second flexural modes were very difficult to identify due to the high stiffness of the blades. Figures 65 and 66, discussed further in this section, show comparison of calculated, bench testing, and rotative testing results of blade resonance for both stages.

To determine the stress distribution in the blades, strain gages were attached as shown in Figure 57. The blades were excited and a plot was made of the strain as shown characteristically in Figures 58 and 59 for stage one and two. This represents the stress pattern within the elastic limit of the material and at the first natural frequency. The strains are represented as percentages of the maximum value measured, thereby also representing a normalized stress distribution. The strain values shown were measured at the points on the airfoil as indicated in the schematic blade drawing directly above the strain plot. The positions of the strain gages attached to the blades for subsequent tests after installation into the turbine are also shown.

Following the bench testing of the blades, they were installed in the turbine wheels and the turbine was prepared for dynamic vibration testing while operating the potassium turbine on steam and air. This involved a complete buildup and assembly of the potassium turbine. The blades were installed in the turbine wheels, as shown typically in Figure 60 where the strain gages are attached to the turbine blades and the wheel web. All the strain gage wires were covered with nichrome ribbon, tack welded to the turbine wheel, and all leads were led axially out through the central hole in the tie bolt. The strain gages were covered with nichrome sheath to prevent gage damage from the erosive qualities of wet steam. In Figure 25 the strain gage wires can be seen coming from the aft end of the turbine rotor. Following installation of the strain gages the turbine was completely assembled with casings and inlet ducting in preparation for operation on steam. Figure 61 shows the turbine partially built up for pretesting, using the bolted casing.

5. Steam Pretesting

For the steam testing, the turbine and drive train were assembled as shown schematically in Figure 62. In this testing, since the turbine produced power, the water brake was installed. Figure 63 is an overall view of the turbine installed and prepared for running. The main steam ducting and inlet throttle valve are shown in the foreground, and in the background is the installed turbine and loading system along with instrumentation and flow lines. These pressure taps were hooked to the efflux pressure measuring system which continuously purges the lines during operation and prevents in-flow of water from steam condensation. Immediately upstream of the turbine can be seen the inlet lines for control and water feed to the spray valve used to control the quality of the vapor entering the turbine. Figures 64a and 64b show the assemblage of control and readout equipment in the control room for vibration testing.

A number of tests were run to rotative speeds of 23,000 rpm. Some problems were encountered in deterioration of the slip ring carbon faces at this speed, and of moisture shorting-out the strain gages, but these were overcome. As indicated previously, the vibration test

results are shown in Figures 65 and 66 for stages one and two respectively, including the results of the first flexural frequency obtained through calculation, and by the previous bench testing. Shown here is the bench test which most closely matches the results obtained in the actual rotating turbine vibration tests. In general, the energy fed into the blades during running is so low that obtaining readings of resonant frequencies was difficult. Indications of the first flexural frequency of the buckets were picked up on both stages, but in no cases were the higher flexural modes or any torsional modes of vibration discernible. It can be seen from Figures 65 and 66 that the blade vibratory stresses are at the very low levels of about 300 psi, which accounts for the difficulty in reading resonant frequencies. The existence of definite resonance points due to jets ejecting from the nozzles was not evident, indicating that the uneven spacing of the nozzle vanes around the turbine flow path was successful in eliminating blade resonance. The graphs show that in both stages, some stiffening of the blades with increasing centrifugal force is evident.

Critical speeds of the turbine were difficult to identify because of the inherent stability and damping characteristics of the pivoted pad bearing, and the high level of rotor balancing obtained (residual unbalance of usually less than 0.3 gram-inch). During operation, however, there was some indication of critical speeds at 15,000 rpm, corresponding to a calculated resonance of 14,792 rpm. The major indication of critical speeds were in the water brake steam turbine load train.

During the operation of the potassium turbine on steam, the techniques of operating the water brake were established. In addition, water was sprayed into the inlet of the turbine with the steam, to simulate low-quality vapor, and operation of the previously discussed condensate extraction system in the turbine was investigated (Reference 14). The results are shown in Figure 67, where it can be seen that irrespective of the absolute level of upstream injection flow, the

condensate extraction effectiveness decreased with increasing speed. At rotative speeds of 3000 to 4000 rpm as much as 30 percent of the injected liquid to stage two could be extracted, but this decreased to about 5 percent for the actual operating speed range of the turbine. The ratio of extracted-to-injected flow had essentially a fixed value for any given speed. The results indicated that at speeds of interest (above 16,000 rpm), the condensate extracted was less than 10 percent of the injected flow, thereby limiting its value as a performance-improving mechanism in the present design. It was concluded that the moisture extraction geometry in the turbine was not optimum, and condensate extraction efforts were eliminated from this test program. Liquid extraction was not incorporated as part of the potassium vapor testing.

During this testing, the hydrodynamic seal which had been modified according to the previously discussed bench testing, operated well, and maintained separation of oil and steam.

C. POTASSIUM VAPOR TESTING

1. Test Preparations and Facility Checkout

Prior to installing and testing the turbine on potassium vapor, a number of preparations and design changes to test equipment were made, and preliminary tests were run to check out both the test turbine and the facility. The checkout of the test facility on potassium vapor was in part accomplished during the converging-diverging flow nozzle test described in Reference 1. The nozzle was installed in place of the test turbine as shown in Figure 68 and served not only to provide the required thermodynamic data, but also provided necessary proof-testing of the bolted flange design which had originally been incorporated to avoid the welding of accurately manufactured turbine casing flanges. The design comprised a metal O-ring and bolted flange arrangement enclosed in an argon-filled sheet metal cover. Testing revealed the bolted

flange to be inadequate, under thermal cycling, for the turbine vapor testing. This testing also revealed some tendency for plugging of the efflux lines during testing, a problem requiring the design and installation of potassium vapor traps described in Reference 3, and shown above the glove box in Figure 71.

The bolted flange testing resulted in the redesign and incorporation of the welded flange (mentioned in Section VI of this report and discussed in References 14 and 16) on all turbine test parts before installation. The general flange design is shown on the casings and scroll in Figure 69. Also shown is the redesign of the attachment of the hydrodynamic seal from bolted to welded construction, as discussed later. The external flange (casing and scroll) is structurally closed by an outer butt weld, and the flange body is designed for minimum heat flow into the structural rabbets during welding. It allows flexibility to prevent weld cracking while providing adequate structural strength. Before incorporating this flange into the test hardware, prototype flanges were machined onto an experimental casing which was welded in a prescribed sequence and then measured. It was found to produce sufficiently low thermal distortions, and these weld flanges were incorporated into all turbine static parts as shown photographically on the inlet duct in Figure 70. Also, shown in this photograph are some of the numerous welded instrumentation lines. The welded flange was used in every subsequent buildup with completely satisfactory results as indicated by the absence of any flange weld cracking or turbine rubs attributable to the welding. In final assembly, the turbine was welded as shown previously in Figure 34, which represents the turbine just prior to its installation in the test facility.

The turbine is shown installed in the glove box of the test facility in Figures 71 and 72, which are forward and aft quarter views after welding it into the facility, and applying thermal insulation. The efflux vapor demister capsules and lines are clearly visible.

Also, in Figure 72 can be seen the various oil, argon, and potassium flow lines which provide these auxiliary flows to and from the turbine. Figures 73 and 74 show forward and aft views after closing the glove box and the addition of all rear drive train equipment preparatory to testing. The trunions which support the entire glove box rear drive train system can be seen.

2. Potassium Tare Testing

Following installation of the turbine, but prior to introduction of potassium vapor, a series of high-speed test runs were made driving the potassium turbine to speeds in excess of 17,000 rpm with the steam turbine, to determine the tare horsepower consumption of rotor windage, hydrodynamic seal friction, and rotor bearing friction. Also, these runs served as a final check of rotor balance, and allowed observations of bearing temperatures, facility flow equipment, and general operation of the test equipment before the commitment to potassium vapor testing. This was adopted as a standard procedure with each new buildup of the turbine throughout the test program. The first tare test was run on April 12, 1964 and revealed the test rig rotor-bearing-vibrational operation to be satisfactory, with the hydrodynamic seal working well, and the test was successfully completed. This represented the first occasion on which potassium was admitted to the hydrodynamic seal. Following the test, the turbine was shut down in preparation for boiler firing and heatup for vapor testing.

3. Seal Malfunction

During the subsequent turbine startup prior to admission of potassium vapor, several attempts to start the hydrodynamic seal loop EM pump were made without success (References 16 and 17). It was discovered that lube oil had entered the seal loop and reacted with it, forming a black residue that blocked the EM pump. Certain amounts of potassium were found in the lube oil system, also rendering these

pumps inoperative. Because of the concern for possible oil leakage into the seal from the turbine bearing sump because of inadequate seal design, the turbine bearing housing was removed from the test facility, and a series of modifications and verification tests were subsequently made and run to prevent a recurrence of fluid mixing.

Analysis of the seal malfunction revealed problems both in operation of the equipment during test and in the design of the seal system. Since the seal volume is small, it has little storage capacity for unbalanced flows, and requires close observation of pressures and flows in all cavities during operation. Such observations have been made in the previously discussed seal pretesting, and while it had been attempted to operate the seal in potassium within these previously established boundaries, no seal pressure instrumentation had been installed in the potassium loop. It was necessary to install pressure instrumentation into all the seal cavities shown in Figure 10 to provide continuous monitoring in the test cell. Also, residual potassium was removed from seal exhaust argon by a freezing process, which if inadequately controlled could plug outlet ducting with subsequent flow backup in the seal. Also, no warning of presence of potassium in the oil system was available. In addition, no means of visual observation of fluids leaving the seal had been provided to check for obvious mixing. Inadequate oil drainage and venting of the turbine oil bearing sump was also suspected as a contributor to fluid mixing, and the concern that oil might leak forward along the shaft, underneath the various sleeves, and thereby bypass the seal, resulted in design modifications. The following system additions were made (Reference 18):

1. Addition of the oil screw seal forward of the pivoted pad bearing (discussed previously and shown in Figure 10) to minimize forward oil flow, and to create an additional seal buffer cavity (cavity 4).

2. Extension of some tubes from cavity 4 out through the turbine to observe exhaust buffer argon during operation for any indications of oil or potassium.

3. Addition of a chevron O-ring combined seal (shown in Figure 10) on the shaft to prevent oil creeping forward underneath the sleeves.

4. Addition of an oil scavenge pump.

5. Installation of "spark plug" warning of potassium-in-oil.

During all subsequent testing, no recurrence of oil entering the hydrodynamic seal loop ever occurred.

4. Initial Potassium Vapor Testing

On July 13, 1964, the turbine was first operated on potassium vapor. The boiler was fired and brought to over 1400°F in about three hours. The hydrodynamic seal was established at 10,000 rpm, and the turbine speed was increased to 16,000 rpm by operating it with the steam turbine. Saturated potassium vapor entered the turbine at about 1100°F, water was admitted to the water brake, the steam driving turbine was slowly shut off, and the speed was controlled with the water brake.

About ten minutes after potassium boiling began, the turbine was self-sustaining, and operating as a power-producing machine. No evidence of malfunctioning of the turbine could be observed, since all flows, temperatures, pressures, and vibrational characteristics were within satisfactory limits. Despite its proximity to the hot turbine wheels, the pivoted pad bearing temperature at no time during the test exceeded 200°F, and the rotor vibrations were never in excess of 1.5 g's. Seal cavities operated with proper pressure differences.

About one-half hour after admission of potassium vapor, the turbine experienced a sharp deceleration from 14,000 rpm to 3,000 rpm in approximately two seconds, and thereafter an automatic recovery of speed to 14,000 rpm (see Figure 75). As testing continued, and the amount of power extracted from the turbine increased, the speed oscillations became more frequent, with each speed drop showing about the same characteristic. It was initially suspected that liquid was being "carried over" with the potassium vapor from the boiler and entering the inlet of the turbine, with a corresponding "braking" effect. For this reason, the inlet throttle valve was partially closed to cause such liquid, if present, to flash into vapor. However, no definite improvement of the speed excursion problem was noted. After about one-half hour of operation during which such speed excursions occurred as often as one every three minutes, the inlet vapor throttle valve was totally closed, and the turbine speed was sustained by the steam turbine. As soon as this was done, the speed smoothed-out with no evidence of oscillation or surges. No other flows, or turbine mechanical characteristics were changed. On attempting to operate with vapor again, the speed excursions returned, and with increasing load, appeared to become more frequent. No "wearing in" was observed, as would be expected in the event of mechanical rubs.

In addition to the speed fluctuations, evidence of leakage in the potassium inlet lines to the hydrodynamic seal was observed by a continuous depletion of the reserve tank supplying potassium to the seal. This potassium was leaking directly into the main loop, at a rate which required the three gallon seal supply tank to be refilled about every fifteen minutes (by transferring potassium from the main dump tank). This seal leakage (which was immediately suspected to be at the junction where the hydrodynamic seal was bolted to the bearing housing, and at which point the potassium inlet flow must bridge, as shown in Figure 69) appeared to become progressively worse with time.

As testing continued, the temperature of the vapor entering the turbine increased to approximately 1500°F. Continuously, during testing a number of data points were taken, providing some performance readings and a checkout of the digital recording system and other vapor and mechanical instrumentation. After about three hours of operation, a small leak occurred in a pressure tap upstream of the turbine which required repair. Also, since no improvements in the speed control or seal leak problems could be achieved it was decided to stop testing and to closely examine the recording charts in an attempt to correlate some facility or turbine flow or mechanical characteristic with the speed excursions.

The boiler was brought to low-fire, and a normal shutdown of the turbine was effected. Its speed was dropped to 2,000 rpm, and was held at this speed for about ten hours with sufficient oil flow to the bearings to keep them cool while the massive facility-turbine system cooled to below 500°F.

It was determined that due to the apparent potassium leak from the hydrodynamic seal, it would be necessary to remove the bearing housing and repair the leak.

Although this initial test resulted in premature shutdown, a number of positive results were achieved. A checkout of the facility and turbine temperature, pressure, flow and mechanical instrumentation operating on potassium vapor was obtained. The digital recording system worked well, and the efflux pressure measurement system proved satisfactory. Also, despite the speed instabilities reported above, the turbine ran at vibration indications of always less than 3 g's on the forward bearing accelerometers, and at rotor temperatures in excess of 1400°F with all bearings operating as predicted in the test plan. The hydrodynamic and labyrinth seals (despite some leakage and rubs) worked satisfactorily, and maintained complete separation of potassium and oil.

All facility subloops (hydrodynamic seal supply, argon reclamation, lube system, and main loop argon extraction) performed as required.

There was some initial concern that speed excursions had been caused by rubs in turbine parts, since it could not yet be concluded from instrumentation measurements that boiler instabilities were the cause of the speed excursions (see Reference 17). This suspicion was reinforced by the observation of a number of seal rubs after removal of the turbine bearing housing from the test facility.

This test represented the first of a number of preliminary potassium vapor tests prior to the ultimate performance testing (as indicated in Section II of this report) and spanning a time period of from July 15 to October 13, 1964 during which a total of 35 hours of testing were accumulated on vapor, but during which a number of intermittent shutdowns were necessary for repair and modification of turbine and facility components. Following is a discussion of the mechanical problems experienced and their associated solution.

5. Development Testing and Modifications

Due to the hydrodynamic seal leakage at its bolted flange as stated above, the joint was modified to a welded connection, thereby eliminating the last bolted seal joint in the turbine (see Reference 18), the welded configuration being shown in Figure 69. It was also found upon disassembly following the first vapor testing that the labyrinth and bearing seals had rubbed (although not the turbine tip seal). This was partly attributed to an opening of the clearance which contains the pivoted pad bearing assembly, caused by the differential thermal expansion between the hot bearing housing and the oil-cooled bearing. This problem was solved by addition of six square keys located circumferentially around the pad bearing retaining ring as shown in Figure 76. To eliminate any radial or axial motion of the

turbine shaft, the single ball thrust bearing was combined with an additional bearing making a spring loaded pair, as discussed in Section V of this report and shown also in Figure 76.

An additional modification was to change the labyrinth seal rub surface material from nickel to copper due to the hardness of the nickel, and the subsequent damage to the seal teeth with any rubbing. Tests performed on copper had shown that it exhibited a good resistance to potassium corrosion to temperatures of about 700°F (Reference 23), and that it would form channels rather than gall when rubbed by a toothed surface. The copper was applied by plating, using established procedures.

The routing of the turbine in the bearing housing had been such that all fluids entering or leaving the turbine passed through the cavity between the bearing housing and the scroll. If leaks were to occur in any two tubes of a different fluid there would be a mixing of these fluids. This would be especially difficult to handle in the case of oil mixing with potassium. A change was therefore made to reroute the oil supply lines directly through the bearing sump leaving only potassium and argon lines in the outer tube cavity. Figure 77 and Figure 1 shows this change where each pad is individually fed with an oil supply tube extending through the oil sump.

Although it was initially suspected that rubs in the turbine could cause the speed excursion problem, calculations indicated that 50 horsepower would be needed to slow the turbine down during each speed excursion, and it was therefore considered unlikely that speed drops consuming this amount of horsepower could be repeated for over 25 times (as was the case during initial testing) without any change of pattern. Evidence of boiler instabilities was increasing, and testing was continued to observe the boiler, and to determine the effect of the above discussed modifications on turbine performance. Resumption of turbine

testing on September 28, 1964 revealed satisfactory turbine operation, but with the same speed excursion problem as indicated previously. The numerous turbomachinery design changes had no effect on changing the characteristic of the speed excursions. Boiler instability was strongly suspected. For further details, see the detailed discussion regarding boiler instability and the corresponding operation of the test facility during this portion of the testing in Section 2.2.2 of Volume III of this report, Reference 3 . It was decided that, since the turbine itself was running well, testing would be continued in an attempt to find more stable operating conditions.

Testing continued through October 13, 1964, while during nine individual runs a total of 35 hours of vapor operation at turbine inlet temperatures exceeding 1450°F (and as high as 1582°F) was accumulated. During this time, 103 of a total of 114 required data points were taken at apeeds of between 16,000 and 20,000 rpm. (Since most of these data were accompanied by inadequate speed control, they were later repeated.)

During this testing, liquid potassium was injected into the inlet of the turbine to control the quality of the incoming vapor, and to bring it to values as low as 85 percent. Liquid was sprayed into the inlet in varying amounts according to the chart shown in Figure 78 for a total of about nine hours. This phase of testing was interrupted by a number of shutdowns, caused by facility and turbomachinery problems as follows (see Reference 18).

On October 2, 1964, a shutdown was required by an electrical failure of the digital data recording system, preventing any data taking. This was repaired within a few hours, and testing was resumed. Problems such as potassium plugging of the hydrodynamic seal loop, EM pump cavitation, and potassium in the argon reclamation system accompanied the testing. On October 2, 1964, a momentary freezing of the potassium-out line from the hydrodynamic seal casued an overflow of

potassium into the oil reservoir, causing a partial plugging and requiring a shutdown for cleaning. Also, during running, some instability of water brake speed control was observed. This was attributed to the low level of power loading on the brake, compared to its capacity. Also, two needle valves were installed for better water flow control. It was also observed during testing that a high pressure (150 psi) was required to force the necessary 2 gpm of potassium liquid into the hydrodynamic seal. This was later solved by installing two additional flow lines into the seal. On October 8, 1964, it was observed that an oxidation scale had formed on some of the boiler tubes and was flaking off. An inspection shutdown revealed that this scale was only 0.002-inch thick, and therefore, of no significance. During testing, on several occasions, shutdowns were necessary because of leaks in efflux pressure measurement lines at weld junctions. On October 4, 1964, one such leak in a pressure tap on the lower portion of the turbine casing resulted in damage to internal turbine parts due to air which was drawn into the loop in this sub-atmospheric pressure region. This damage is discussed later.

During this testing, it was discovered that after reaching a high vapor inlet temperature and then reducing boiler fire to return to a lower temperature, the turbine speed became completely smooth during the temperature reduction period, again indicating that changes in boiler operation had a direct influence on speed control.

On October 13, 1964, testing was progressing with the intention of completing the 1600°F inlet temperature performance testing. Early in the testing, it was observed that a potassium leak from the hydrodynamic seal into the main loop had occurred, presumably due to the thermal cycles imposed on the turbomachinery during the previously discussed shutdowns. Argon was entering the main loop at

a rate exceeding 25 pounds per hour, making it impossible to evacuate the loop below 5 psia. Shortly after reaching 1450°F vapor temperature, smoke was observed coming from one of the boiler exhaust stacks, and subsequently, a small flame was observed coming from the top of the boiler. Emergency shutdown procedures were immediately imposed, and an orderly shutdown ensued. This leak resulted in a down time of five months during which a number of major facility modifications were incorporated as discussed in Reference 3, and during which time some further turbine modifications were made.

Removal of the turbine bearing housing for repair of the leaking hydrodynamic seal revealed two problems. Two of the plugs used to close previous manufacturing holes in the seal had leaked. Also, the sheet metal cover enclosing the numerous tubes on the outer bearing housing had developed a crack, and allowed the leakage of argon into the loop. This was later replaced with the bellows cover, which solved this thermal cracking problem. Observation of the copper on the labyrinth seals showed it to withstand testing quite well.

The above testing, although marked with boiler instability, system leaks, and numereous mechanical problems in both turbomachinery and facility, served a number of purposes.

It proved the ability of the turbine to perform at its design conditions of temperature and speed, with low levels of vibration and freedom from serious problems of excessive stress, or major mechanical failure. It represented the first sustained vapor operation, and

allowed identification of problems and system weaknesses which could not be observed or solved without running on vapor. It provided invaluable operating experience to three crews of testing personnel in the operation of the highly complex turbine-facility system, requiring close coordination of efforts in the test cell. The shakedown of equipment during this development testing afforded much smoother operation during the subsequent performance and endurance testing.

During this downtime, the turbine was opened for inspection. This involved opening the forward flange of the turbine by grinding its weld, and separating the inlet duct from the turbine approximately three inches as shown in Figure 79. This visual inspection of the turbine inlet region revealed the following two problems (discussed in detail in Reference 19):

1. Gross surface metal loss to the inlet region components of the turbine.

2. Damage to the outer band of the second stage nozzle diaphragm as a result of fire caused by a leak on October 4, 1964 as described below.

As a result of the pressure tap leak, air was drawn into the turbine at the bottom-most point of the casing, where it burned through the forward second stage nozzle diaphragm outer band, and then through the nozzle vanes, damaging the trailing edge of three vanes and a segment of the honeycomb seal shown in Figures 80a and 80b after casing disassembly. Figure 80b shows the second stage nozzle diaphragm after further disassembly from the casing, and shows the fire damage on the lower half of the assembly.

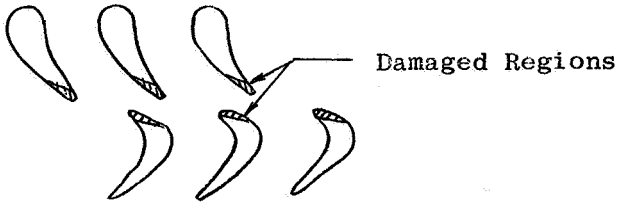
6. Metal Removal on Fluid Dynamic Components

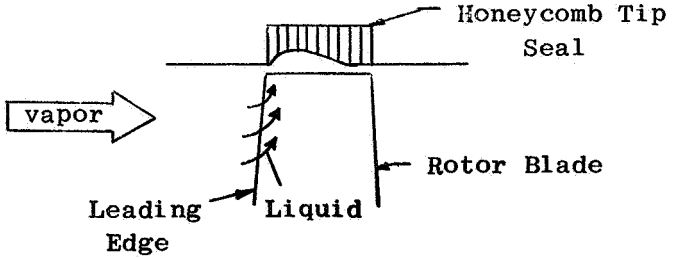
A detailed description of the damage to the inlet region fluid dynamic parts (blades, nozzles, wheels, tip seals) and the metallurgical implications are discussed in Reference 2. Observation of the turbine parts upon disassembly indicated the following.

(a) The liquid droplets hitting the rotor blades had a low axial velocity.

(b) The centrifugal force acting on the liquid hitting the blades was sufficiently high that the liquid thrown off the blade tip hit the honeycomb rub strip at a place only slightly downstream of the rotor blade leading edge.

A velocity diagram of probable droplet motion of liquid entering the first stage rotor blade row is given and is discussed in Reference 2. It is concluded that at a rotor speed of 18,250 rpm, the relative impacting velocity of liquid droplets on the tip of the first stage rotor blades was about 400 fps. The turbine inlet region showed a pattern of metal removal as shown below. It appeared that slow-moving liquid entering through the nozzles was first struck by the fast-moving blades, and was then both thrown back onto the aft edge of the nozzle vanes, and radially outward into the leading region of the honeycomb tip seal, as shown below, and in detail in Figure 81.





A detailed comparison of both new and damaged stage one turbine blades is shown in Figure 82. The leading edge of the airfoil has been sufficiently corroded to change the airfoil shape. On the first stage forward rotor face, the wheel dovetail neck and blade retainer clips were also notched by liquid impact.

It is significant that the second stage showed much less damage on both rotating and stationary parts, even though it experienced about three percent more moisture during testing. A comparison between a new and a damaged stage two rotor blade is given in Figure 82c. Second stage erosion produced only a surface "roughness" and did not affect the basic airfoil contour (Reference 19). The lesser-damaged condition of stage two is attributed in large part to the fine mist generated by the first stage, which is felt to have reduced the overall liquid impact forces on the stage two components, thereby reducing the degree of blade damage from that of stage one. This tends to support the original argument for a two-stage turbine, wherein the first stage generates realistic turbine fluid conditions for testing of the second stage.

Comparison of before-test and after-test blade weights revealed an average weight loss, due to corrosion, of 6.7 percent for stage one and 0.7 percent for stage two. New stage one and two blades weigh about 16.2 grams, and 21.9 grams, respectively.

The component damage was due to liquid carried into the inlet of the turbine with the vapor. One known source of liquid was the injected spray from the upstream valve, intended to control the quality of the incoming vapor. The other was the possible, but unknown, liquid carryover with the vapor from the boiler.

It was concluded that even if boiler carryover were eliminated, the damage to the first stage due to liquid injection may still be

unrealistically great, since no matter how finely the inlet spray is atomized, this pre-injection causes the inlet duct, bullet nose, and nozzle diaphragm upstream of the rotor to be covered with liquid and to act as "collectors" which then discharge liquid into the turbine in large droplets. This mechanism of droplet formation is a function of quality rather than the individual size of the atomized droplets in the injection spray. For this reason, all control of inlet quality by liquid injection upstream of the turbine inlet was eliminated for the remainder of the test program, and second stage moisture was generated only by energy extraction from the flowstream, amounting to vapor quality as low as 96 percent entering stage two.

7. Test Preparations

Prior to continuation of testing, both replacement of damaged turbine parts and repair of the test facility boiler ensued. The turbine rotor blades and eroded honeycomb seals were replaced, and the fire damage to the second stage stator was repaired as shown in Figure 83. Also, pressure instrumentation was replaced with heavier-walled tubing, (probe tube wall thickness increased to 0.030 inch from original 0.015 inch) and the critical instrumentation tubing weld joints were extended outward beyond turbine insulation into a cooler region. See Figure 84 for details of the instrumentation installation and construction. This eliminated any further instrumentation leakage for the remainder of the test program. A bellows was incorporated into the sheet metal tube cavity cover of the bearing housing (as shown in Figure 15) to eliminate thermal cracking.

In addition to repairing the leak in the boiler associated with the previously discussed shutdown, numerous facility changes were made to the boiler and the 8-inch vapor outlet line leading to the turbine as described in detail in Reference 3.

Following these modifications, the turbine was installed for continuation of testing. As discussed in the following, these modifications eliminated speed instability, and allowed successful performance testing.

D. PERFORMANCE TESTING

The performance testing of the turbine was accomplished in two major test runs, accumulating a total of 53 hours of test time.

1. Test Plan

The performance test plan defined testing at two turbine inlet vapor temperatures, 1450°F and 1550°F, with pressure ratio variations of 1.4 to 3.6 at rotational speeds ranging between 15,400 rpm and 22,000 rpm, comprising a total of 77 test points at a constant inlet vapor quality of 99 percent, and reaching a level as low as 96 percent entering the second stage.

2. Instrumentation

The instrumentation for vapor performance testing is shown in Figure 84. This figure shows both the turbine performance instrumentation in the main turbine potassium flow region, and the monitoring instrumentation throughout the turbine drive train. The former is intended primarily for performance data, and the latter for monitoring the mechanical operation of the rotating equipment, and to observe any deterioration of bearings, or couplings as indicated by increased temperatures or vibrations.

In addition to indicating the location of various instruments, Figure 84 also shows the details of construction employed in bringing the pressure and temperature instrumentation out through the casing wall. This comprises a number of tubes, fabricated to allow cutting

and replacement of instrumentation during teardown and assembly of the turbine. The pressure taps consist of 1/8-inch diameter tubing, and the thermocouples are chromel alumel, and are imbedded in 1/8-inch diameter wells. Vibrations were sensed by velocity pickups, except as in Zone E-E of the drawing, wherein accelerometers are used. Numerous thermocouples were located in the vicinity of the hydrodynamic seal and at strategic points in the bearing housing to determine temperature gradients in these components while testing. Two induction gauge proximity probes, mounted at 90°, were employed to observe any whirl or dynamic instabilities in the potassium turbine shaft (see Figure 84, Section G).

3. Performance Testing of March 1965

Potassium vapor operation was started on March 21, 1965, and continued for a period of four days during which time a total of 18.8 hours of vapor operation was obtained. Operation during this period was characterized by elimination of the previously experienced speed control problems induced by boiler instabilities. Operation at low liquid levels in the upper boiler drum was credited with the elimination of the speed instabilities. This testing yielded six data points during which time turbine mechanical operation was characterized by stable running at low vibration levels (less than 2 g's). Two clearly defined resonant points existed at 13,500 rpm and 16,500 rpm, which were sufficiently damped to limit the peak amplitude of the rotor to 0.6 mils. Turbine speed was held within a 400 rpm band. At low levels of turbine power output, some variation in speed was experienced as a result of water brake load control. This was primarily due to the low percentage of its total load absorbing capacity which was being used (20 to 30 percent). During this testing, all bearing temperatures were held below 300°F, and all internal fluid cavity pressures were maintained at within prescribed limits.

A leak in a potassium liquid supply line to the hydrodynamic seal on March 25, 1965 required an unscheduled shutdown. The leak occurred so that the closed tube cavity of the bearing housing filled with potassium, which then provided a heat-conducting path from the scroll to the bearing housing.

The bearing housing was removed from the scroll, the tube was replaced, and testing was continued.

4. Performance Testing of May 1965

Performance testing was resumed on May 19, 1965, and continued without interruption through May 21, 1965 at which time performance testing was successfully completed. During this testing, the turbine speed control continued to be completely satisfactory, namely, within $\pm$ 250 rpm, which in part was accomplished by operating the water brake at outlet temperatures of about 190^{o}F.

Although testing continued without any malfunction of the basic test rig, it was marked by two incidents resulting from malfunctions of support equipment. At 19:25 hours on May 19, with an inlet vapor temperature of 1460^{o}F, a pressure ratio of 3.3, and a speed of 18,300 rpm, an instantaneous interruption of the 120 volt facility electrical control power occurred. All of the items on the control power system were momentarily affected, but recovery of steady-state operation was effected within minutes. On May 20, a momentary loss of oil to the pivoted pad bearing occurred, which was triggered by a malfunction of an interlock in the labyrinth seal argon supply system from an external tank. This resulted in damage to the surface of the pivoted pad bearing, the extent of which was not known until disassembly following performance testing. However, subsequent to this incident during testing, it was observed that the pressure necessary to maintain required lube flow to the bearing had decreased to 20 percent of its initial value, and continued at this lower value for the remainder of

the testing. Although the shaft proximity probe indicated a greater bearing clearance, the turbine continued to operate satisfactorily throughout the testing. On May 21, 1965, at 19:03 hours, turbine performance testing was completed, and shutdown from potassium vapor operation was begun. By 20:27 hours, vapor flow to the turbine had stopped, and the system was continued to motor overnight for a cool-down and for subsequent post-performance tare tests. By May 22, 1965, all after-test tare testing was completed, and the turbine was prepared for disassembly.

5. Post-Test Inspection

Post-test disassembly inspection of the turbine showed negligible mechanical deterioration with exception of the above mentioned pad bearing damage. Measurements showed that the diametral clearance had opened from 0.006 inch to 0.018 inch. All other test bearings were reuseable.

On the stator sections, no deterioration occurred except for the expected out-of-round (0.010 inch) which is inevitable from high temperature operation. On the rotor it was observed that a metallic deposit had formed on the blades of both stages which caused a 0.13 percent weight increase of the first stage blades and a 0.02 percent average increase of the stage two blades. This deposit is shown in Figure 85a on the blades and in 85b on the first stage nozzle inlet. It was attributed to throttling of the inlet valve in the 8-inch upstream line of the test facility. The alloy constituents of this material deposit and further discussion of its source are presented in Reference 2. During the subsequent 2000-hour endurance test, throttling was not done, and this deposit did not occur.

E. ENDURANCE TESTING

The basic objective of the endurance test was to determine the long-time effects of potassium liquid and vapor on blades fabricated from U-700 and the refractory metal alloys, TZM and TZC, which are candidates for the advanced Rankine cycle space power turbines.

The effects were to be measured as follows:

1. Turbine performance change with time.
2. Macroscopic visual inspection of test hardware after testing.
3. Metallurgical analyses (photo micrographs, analysis for interstitials, observation of mass transfer).
4. Creep and/or distortion measurements.

1. Test Plan

The running conditions for the endurance testing were selected as follows:

Rotative Speed	18,250 rpm	± 200
Inlet Vapor Temperature	1500°F	± 10
Inlet Total-To-Exit Static Pressure Ratio	3.47	± 0.25

During testing, data were taken as follows to observe any deterioration of performance, thereby indicating possible corresponding mechanical deterioration.

(a) All the critical test variables, turbine output torque, the test conditions, rotor vibrations, etc., were recorded and observed continuously to identify any trouble areas.

(b) Every two hours, data were recorded on hand log sheets to positively establish proper operation of the test turbine, all subloops, and the test loop.

(c) Every four hours all data were taken with the digital system, to be subsequently used for calculation of performance, and to provide a permanent record of the test.

Provisions were made in the turbine casing for the insertion of borescopes to observe the mechanical integrity of the turbine rotor and stator if it became necessary to shut down during testing for repairs, etc.

2. Test Preparations

The test turbine for the 2000-hour endurance test was built up of components that had previously been used in the performance testing, with some modifications for the endurance test.

One such modification involved elimination of argon efflux pressure measuring instrumentation to a configuration as shown in Figure 86. One efflux pressure measuring device static and one efflux pressure measuring device total pressure tap were retained in the turbine inlet duct to periodically measure inlet vapor flow for comparison with the EM pump. Elimination of these instrumentation lead-outs correspondingly increased the reliability of the turbine against possible leaks. Sufficient instrumentation was left to determine the macroscopic turbine performance. The turbine mechanical design was the same as that used in performance testing. Several new pieces of test hardware were installed to obtain the maximum value from the test.

The turbine wheels were new, in keeping with the 4,000 hour total operating life on stage one, (see Section V). To best observe any effects of erosion, the turbine blades with the least history of previous testing were used. For stage one, new blades were installed, and for stage two, the U-700 blades used during the May, 1965 potassium vapor performance testing were installed. In addition the special refractory blades, viz., four TZC and four TZM, were installed in stage

two. Figure 87 shows the stage one wheel assembly before endurance test, and the corresponding stage two before-test wheel assembly is shown in Figure 88. In stage two, fifty-two of the sixty blades were of U-700, and eight were TZM and TZC molybdenum, position as shown. In addition to the erosion testing of refractory blades, a number of stator material test inserts were installed in the second stage honeycomb tip seal as shown in Figure 89, and the drawing of Figure 1. These were installed to observe erosion resulting from the "slinging" of liquid from the trailing edge of the rotating blades into the leading edge of a subsequent nozzle blade row. A number of other new parts were installed for the endurance test as indicated in the detailed component status list given in Table II.

A number of test facility modifications were made to provide for automatic control of the system, as described in Reference 3.

3. 2000-Hour Test

The 2000-hour test was preceded by the standard rotating calibration and tare tests as was done before the performance testing. All power train mechanical parameters were within prescribed limits, and essentially the same as in previous vapor testing. On September 13 at 13:19 hours, the first vapor entered the turbine, and by 16:35 hours the turbine was "on point" at an inlet temperature of 1500°F. From this point on, the speed was held at 18,250 rpm $\pm$ 250 rpm.

After 254 hours of continuous operation, during a calibration check, the overspeed trip was inadvertently energized by an electronic malfunctioning in the speed-sensing equipment, causing the facility to automatically shut down. No overspeed had actually occurred. The pad bearing was damaged during this emergency condition due to loss of oil lubricant and had to be replaced. The primary oil supply is shut off when an overspeed signal is sensed, as part of an automatic shutdown. An accumulator in the oil system supplies lubricant for a short time.

The primary oil was not resumed until after the accumulator was emptied. Bearing damage resulted. During this shutdown period, the borescope ports in the nozzle diaphragm and wheel sections were opened for a visual inspection of these components. No erosion or damage could be seen.

On October 8, 1965, the turbine was reassembled and started up for continuation of endurance testing. All turbine and facility systems performed normally with no evidence of damage caused by the shutdown. After 1000 hours of accumulated endurance time, the monitored instrumentation showed the turbine to be in excellent condition. Testing was continued without interruption through to the end of 2000 hours. In the last 1000 hours of testing, it was observed that the oil sump pressure varied between 3 psig and 0.5 psig on approximately 48 hour intervals. This caused no problem however, and it was attributed to periodic oil "coking" in the pad bearing forward oil screw seal (see Figure 10), effecting a "tightening" of the seal. Also, during this period it was observed that an increase in oil pressure was accompanied by a slight decrease in turbine vibration.

On December 20, 1965 the 2000-hour test was completed and the turbine was shut down. After 2-1/4 hours of cooling down, vapor had ceased to flow into the turbine and, within five minutes, the turbine suddenly stopped due to a tilting pad bearing seizure. Subsequent analysis of this stoppage has shown the seizure was due to a squeezing of the bearing by the bearing housing from thermal contraction during cool-down, as a result of oil carbon buildup between bearing outer ring and housing.

VII. TEST RESULTS

The turbine testing program resulted in the fulfillment of the objectives discussed in Section III of this report. As discussed previously, the pre-performance testing resulted in some geometric modifications of the turbine, and the testing of October 1964 while injecting liquid spray provided significant, if undesirable, results on turbine flow path materials erosion. The performance testing of May 1965 resulted in measurement of all required performance data points and establishment of characteristic mechanical operation of the turbine at operating temperature. The 2000-hour endurance test of September, October, November and December of 1965 provided information on the long-time effects of high quality vapor on turbine flow-path materials, and in addition, established the mechanical integrity of the turbine for continuous 1500°F operation.

A. PERFORMANCE TESTING

The performance testing of May 1965 completed the test plan of 73 data points. The turbine power output during this test ranged from a maximum of 251.9 horsepower at a total-to-total pressure ratio of 3.57, 1550°F inlet vapor temperature and 19,288 rpm, to a minimum of 18.7 horsepower at a total-to-total pressure ratio of 1.41, 1450°F inlet vapor temperature, and 19,997 rpm. The maximum turbine efficiency (total-to-static) obtained during this testing was 75 percent, as shown in Figure 79 of Volume I of this report, (Reference 1).

In addition to providing the fluid dynamic data discussed in detail in Reference 1, the performance testing established the mechanical characteristics of the hydrodynamic (potassium liquid) seal, labyrinth (argon gas) seals, pad bearing, and ball bearings. The mechanical operation was determined by monitoring temperatures, pressures, flows, horsepower consumption, and vibration.

The hydrodynamic sealing capabilities as shown in Figure 55 were verified. The horsepower consumption (Figure 54) was verified in pre-vapor tare testing. Figure 90 shows the typical temperature rise of

PRECEDING PAGE BLANK NOT FILMED.

potassium in the seal during vapor operation, much of which is due to thermal conduction and condensation of vapor into the seal liquid.

The labyrinth seals, which physically are part of the hydrodynamic seal, and the oil screw seal were effective in preventing potassium from contaminating the oil.

The pad bearing and ball bearing temperatures were 200°F or less during vapor testing as can be seen in Figure 91 . This curve describes expected operation for a 0.006-inch diametral clearance and a 135°F oil supply temperature.

B. ENDURANCE TESTING

The 2000 hour endurance test yielded information regarding long-time, high temperature corrosion and erosion by high quality inlet vapor (99%) on the turbine fluid dynamic components. Turbine mechanical characteristics were observed as shown in the following tabulation. This shows turbine data which were continuously monitored during endurance testing. It can be seen by observing any given parameter at various times that the change throughout the test was slight.

	DATE AND ACCUMULATED HOURS			
POTASSIUM TURBINE	235 hours 9-23-65	536 hours 10-19-65	1014.7 hours 11-19-65	1997.5 hours 12-20-65
Speed, rpm	18,250	18,300	18,100	18,150
Pad Bearing Temp., °F	188	199	198	205
Ball Thrust Bearing, °F	190	194	196	197
Bearing Housing Temp., °F	312	320	315	378
Liquid Potassium into Hydrodynamic Seal, °F	258	280	262	278
Liquid Potassium out of Hydrodynamic Seal, °F	825	862	854	863
Turbine Horizontal Vibration, g's	0.1	0.08	0.01	0.7
Turbine Vertical Vibration, g's	1.1	1.0	0.70	2.0

	DATE AND ACCUMULATED HOURS (Cont'd)			
WATER BRAKE	235 hours 9-23-65	536 hours 10-19-65	1014.7 hours 11-19-65	1997.5 hours 12-20-65
Forward Bearing Temp., °F	274	163	156	152
Aft Bearing Temp., °F	125	117	115	122
Water Inlet Temp., °F	68	68	68	68
Water Outlet Temp., °F	197	193	193	193
STEAM TURBINE				
Forward Bearing Temp., °F	158	154	152	152
Mid Bearing Temp., °F	159	155	153	153
Aft Bearing Temp., °F	168	162	160	158

Figure 92 shows the variation in labyrinth seal pressures for the above tabulated points during the test. Although when disassembled, it was discovered that the bond of the plated copper rubbing surface in the argon labyrinth seals had separated, it did not result in any gas leakage sufficient to affect the seal cavity pressure distribution. Figure 93 shows the oscilloscope traces of the proximity gage outputs which measure the shaft excursions two inches aft of the pad bearing, and indicate the unchanging character of rotor dynamics during the endurance test.

Figure 94 shows the turbine casing assembly upon opening immediately after the 2000 hour test. As can be seen, there was no visible evidence of deterioration of any of its components, and a similar observation was made for all rotor components.

Both stage one and two nozzle diaphragm assemblies withstood the endurance test without visible evidence of deterioration, although both stages exhibited a surface discoloration as shown in Figures 95 and 96 before surface cleaning. The trailing edge wear of stage one resulted from prior testing. Special observation was made of the flow stream exposed fillets of the brazed joints which fasten the nozzle vanes to the inner and outer shroud bands. The fillets were not eroded from any testing even though their location at the hub and tip would make them especially vulnerable to contact with condensed liquid from the duct walls.

The second stage nozzle diaphragm, which had a greater opportunity for potassium liquid particle contact also showed no deterioration, as seen in Figure 97.

As indicated in Figure 97 above, the honeycomb tip seals sustained no visible deterioration from the 2000-hour test. The seals were new at the beginning of the test, and Figure 98 shows enlarged views of the seals immediately after testing. The original sharp edges of the 0.005-inch thick honeycomb stock can be observed.

One of the most significant results of the endurance test is that the turbine blades in both stages endured the testing with almost no deterioration. Figures 99 and 100 show overall views of both of the still-assembled turbine wheels after the test. Figures 101 and 102 show close-up views of representative blades in each stage, first following a superficial steam cleaning before disassembly after the 2000-hour test, and later, after cleaning and re-assembly for continued testing, as requested by Amendment 20 to this contract effort. In the photographs prior to disassembly, it can be seen that, although coated with a residue of potassium oxide, there was no visible evidence of blade deterioration such as gross mass transfer, chemical corrosion, or impingement erosion during testing, and this is further borne out by the "after cleaning" photographs. The metallurgical effects of testing on the blades are discussed in detail in Reference 2, and are indicated partly by the small weight changes discussed below. Figure 103 shows close-up photographs of both stage one and stage two U-700 blades compared before-and-after the 2000-hour endurance test. Figure 104 shows corresponding before-and-after photographic comparison of the refractory metal test blades.

Surface oxide was removed by light vapor blasting* after testing, and blades were weighed. The tabulation of Table III shows an average weight

---

* Vapor blast abrasive: Siliceous Earth #1250 NVB manufactured by "Vapor Blast Manufacturing Company".

decrease of 0.304 percent for all stage one blades. Similarily, a weight decrease of all stage two U-700 blades was 0.019 percent. The refractory blades in stage two experienced some corrosion on the suction surface of the leading edge, giving the appearance of a corrosion trace as shown in Figure 104b. In Table IV it can be seen that both the TZC and TZM blades experienced approximately the same weight loss of 0.10 percent. There was no evidence of fretting or washing erosion of the turbine wheel dovetails as shown in Figure 105. There was also no evidence of blade dovetail fretting. The results of erosion testing on the stator insert (Figure 89) are discussed in Reference

The 2000-hour endurance test also verified the long-time capability of the other turbine components. Table IV shows the physical results of the disassembly inspection following the 2000-hour endurance test. On the hot stator components, resistance to relaxation and creep was demonstrated. During the test there was no indication of mechanical rubs either on startup or during the test. At disassembly, after completion of the test, the measured thermal distortion was essentially comparable to that sustained in the 65-hour performance test with local out-of-roundness of about 0.005 inch on the turbine casing flanges. The turbine rotor balance and bearing damping and stiffness remained constant throughout the entire 2000-hour test. The turbine dynamics were measured by accelerometers, proximity gages, and velocity pickups.

VIII. CONCLUSIONS AND RECOMMENDATIONS

A. CONCLUSIONS

The conclusions regarding the mechanical design and development of the two-stage turbine on this program are as follows:

1. The turbine described herein has demonstrated its design and operational reliability throughout a range of test conditions.

   In a number of test runs, the potassium turbine accumulated over 2100 hours of operation, with the last 1754 hours continuous. Although a number of minor design modifications were made, the basic turbine design was adequate, as evidenced by the absence of any structural failures of fundamental components such as wheels, blades, or nozzle diaphragm assemblies throughout the entire program. Of significance are the following observations:

   a. No critical speed problems were encountered in the potassium turbine.

   b. The pivoted pad bearing operated stably, providing rotor damping in passing through resonances and operated at conservative temperatures ($200^{o}F$) despite its proximity to the hot potassium vapor.

   c. Although the turbine wheels operated at the local vapor temperatures, the rotor balance obtained during buildup was retained through all performance and endurance testing. The curvic coupling - tie bolt arrangement was completely satisfactory with no evidence of relative shifting of parts during running.

   d. Rotor blade vibration, as predicted in analysis and bench testing, was never a problem. Vibratory blade stresses were so low as to make measurement of the

PRECEDING PAGE BLANK NOT FILMED.

exact stresses difficult (approximately 300 psi) and no galling or fretting of dovetail connections was evident.

e. The initial differential thermal expansion analysis of the turbine was verified by testing, in that no axial rubs were ever experienced, and all radial rubs were minor and were in zones where previously anticipated (such as in labyrinth or rotor tip seals).

f. The use of the hydrodynamic seal to separate potassium vapor and bearing lubricating oil worked successfully. Once adequately instrumented to permit control of pressures and pressure differences in the seal, the seal maintained separation of potassium and oil, and performed according to analytical prediction and the results of the initial easy-fluid testing. No rotor unbalance as a result of rotating seal liquid was encountered and, in fact, testing indicated a damping of rotor vibration during periods of seal operation.

2. The 2000-hour test established the feasibility of employing refractory turbine materials for long-time testing in a stainless steel loop.

No evidence of gross deterioration was apparent in the inspection following the 2000-hour test on either refractory metal blades and inserts or non-refractory turbine components, and the rotor blades from both stages are being used in additional testing. Erosion was not a problem at the temperatures, speeds and vapor qualities encountered in this testing. All parts went through the 2000-hour test with almost immeasurable erosion, corrosion or mass transfer.

3. Several design modifications were required to overcome mechanical shortcomings in the original design.

   The original design employed metal O-rings and bolted flanges (with argon cover gas) which revealed themselves to be inadequate in sealing during testing. Bolted connections were eliminated not only from external flanges, but also from the potassium seal joints within the turbine, and all such connections were successfully replaced with welded construction. Also, a number of leaks in instrumentation welds required redesign and heavier construction of instrumentation tubing. Several modifications were required to overcome mechanical problems such as installation of radial keys to center the pivoted pad bearing, and the re-routing of lubrication lines. These minor modifications performed their desired functions, and prevented the need for ever undergoing a major turbine redesign effort.

4. The testing which involves spraying of liquid into the turbine to control inlet quality and the corresponding interstage moisture extraction did not produce the desired results.

   The liquid spraying produced excessive mechanical damage to the inlet stage, and had to be eliminated for final vapor testing. Also, although the means provided for interstage moisture extraction worked in principle, the amount of liquid extracted was inadequate, due to a non-optimum moisture extraction geometry in the turbine.

5. The turbine operating techniques, especially during transient conditions of startup and shutdown worked well.

   The startup with steam turbine, establishment of hydrodynamic seal, and subsequent loading of brake went smoothly in most testing. The turbine power train operated satisfactorily and

reliably during final testing, although marked with minor problems of misalignment during initial testing.

B. RECOMMENDATIONS

In addition to the positive conclusions reached in this program, an area requiring further investigation was revealed, as follows:

1. It was observed that rotor blades of nickel base superalloy and molybdenum metal alloys experience a slight weight loss when tested in wet potassium vapor. This amount of weight loss should increase with a corresponding decrease in the vapor quality, or increase as a result of longer duration test at the same vapor quality in the turbine. Vapor qualities in the testing described herein vary between about 99 percent at the inlet to about 93 percent at exit.

   Further tests of longer duration or testing at lower vapor qualities (more characteristic of multi-stage high power Rankine cycle turbines) is recommended to gain a better understanding of the corrosion and erosion phenomena in potassium vapor turbines. The resulting data should be correlated with available steam turbine data and experience.

IX. REFERENCES

1. "Fluid Dynamic Design and Performance of Two Stage Potassium Test Turbine", R.J. Rossbach, G.C. Wesling, Two Stage Potassium Turbine Topical Report, Contract NAS 5-1143, Space Power & Propulsion Section, General Electric Company, Volume I.

2. "Materials Support of Performance and Endurance Tests", W.F. Zimmerman, J.W. Semmel, D.S. Engleby, R.B. Hand, Two Stage Potassium Turbine Topical Report, Contract NAS 5-1143, Space Power & Propulsion Section, General Electric Company, Volume II.

3. "Potassium Vapor Turbine Test Facility", S.E. Eckard, Two Stage Potassium Turbine Topical Report, Contract NAS 5-1143, Space Power & Propulsion Section, General Electric Company, Volume III.

4. "Theoretical and Experimental Analysis of the Reduction of Rotor Blade Vibration in Turbomachinery Through the Use of Modified Stator Vane Spacing", R.H. Kemp, M.H. Hirschberg and W.C. Morgan, Technical Note 4373, NACA TN 4373, September, 1958.

5. "Two Stage Potassium Test Turbine, Volume I, Materials Support", J.W. Semmel, Jr., H.E. Nichols, R.E. Yount & R.G. Frank, GE63-FPD238, Space Power & Propulsion Section, General Electric Company, NASA Contract NAS 5-1143, May 8, 1963.

6. "Two Stage Potassium Test Turbine", Quarterly Report No. 1, Contract NAS 5-1143, August 8, 1961, SPPS, General Electric Company.

7. "Two Stage Potassium Test Turbine", Quarterly Report No. 2, Contract NAS 5-1143, November 8, 1961, SPPS, General Electric Company.

8. "Two Stage Potassium Test Turbine", Quarterly Report No. 3, Contract NAS 5-1143, February 8, 1962, SPPS, General Electric Company.

9. "Two Stage Potassium Test Turbine", Quarterly Report No. 4, Contract NAS 5-1143, May 8, 1962, SPPS, General Electric Company.

10. "Two Stage Potassium Test Turbine", Quarterly Report No. 7, Contract NAS 5-1143, February 8, 1963, SPPS, General Electric Company.

11. "Two Stage Potassium Test Turbine", Quarterly Report No. 8, Contract NAS 5-1143, May 8, 1963, SPPS, General Electric Company.

12. "Two Stage Potassium Test Turbine", Quarterly Report No. 9, Contract NAS 5-1143, August 8, 1963, SPPS, General Electric Company.

13. "Two Stage Potassium Test Turbine", Quarterly Report No. 10, Contract NAS 5-1143, November 8, 1963, SPPS, General Electric Company.

14. "Two Stage Potassium Test Turbine", Quarterly Report No. 11, Contract NAS 5-1143, February 8, 1964, SPPS, General Electric Company.

15. "Two Stage Potassium Test Turbine", Quarterly Report No. 6, Contract NAS 5-1143, November 8, 1962, SPPS, General Electric Company.

16. "Two Stage Potassium Test Turbine", Quarterly Report No. 12, Contract NAS 5-1143, May 8, 1964, SPPS, General Electric Company, NASACR-54115.

17. "Two Stage Potassium Test Turbine", Quarterly Report No. 13, Contract NAS 5-1143, August 8, 1964, SPPS, General Electric Company, NASACR-54211.

18. "Two Stage Potassium Test Turbine", Quarterly Report No. 14, Contract NAS 5-1143, November 8, 1964, SPPS, General Electric Company, NASCR-54285.

19. "Two Stage Potassium Test Turbine", Quarterly Report No. 15, Contract NAS 5-1143, February 8, 1965, SPPS, General Electric Company, NASCR-54392.

20. "Operating Experience with an Oil-Lubricated High Speed Potassium Turbine Bearing", Hermann Ernst, ASME Paper 65 LUBS-10, Lubrication Symposium, New York, June 6-9, 1965.

21. "Mechanical Design and Systems Handbook", H.A. Rothbart, etal., McGraw Hill Book Company, 1964, pg. 15-16.

22. "Development of an Efflux Measuring Device for Performance Evaluation of a Potassium Vapor Turbine", Wesling, Rossbach, Shaffernocker, Alkali Metal Institute Conference, Argonne National Laboratories, 1965.

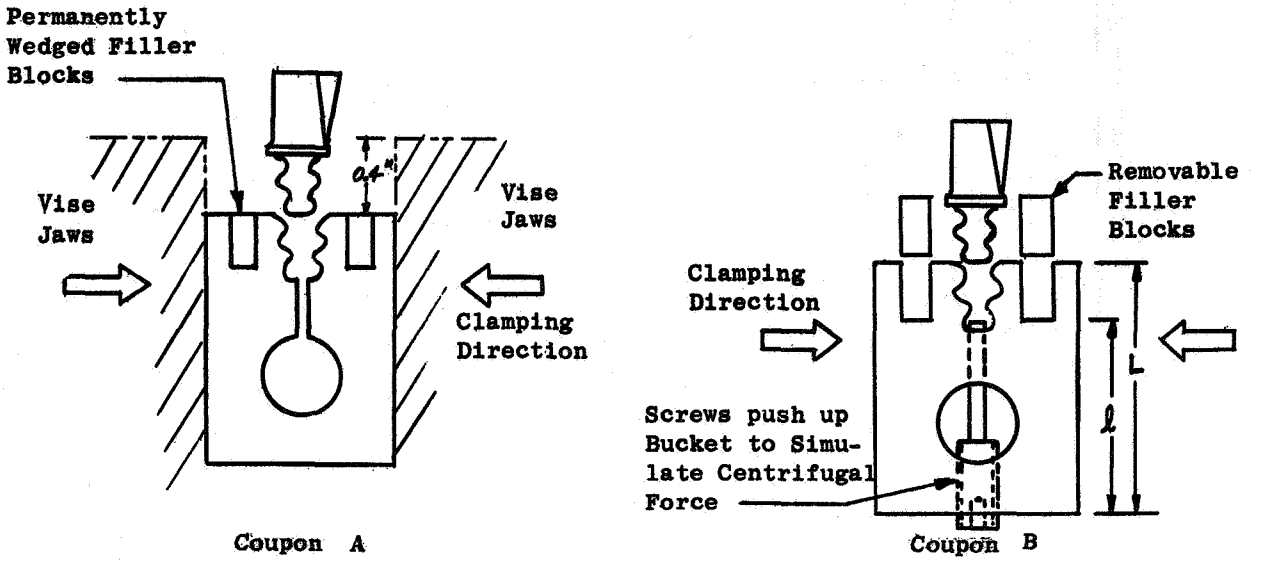
23. "Liquid Metals Handbook", C.B. Jackson, AEC, 1955.

24. "Design Criteria for Rotary Seals for a Space Environment", Schnetzer, Ernst, McGrew, Phillips, Technical Report AFAPL-TR-65-89 Part I, AF Aero Propulsion Laboratory, AF Systems Command, WPAFB, September, 1965.

25. "Rankine Cycle Test Facility Study", Final Report NASA CR 54972, Edited by R.H. Wettach, Contract NAS-943.

TABLE I

BLADE CLAMPING CONDITIONS FOR BENCH VIBRATION TESTING



Clamping Condition Designation	Coupon	Position of Coupon in Vise Jaws	Filler Blocks	Condition of Tightening Screws of Coupon B
1	A	Top of Coupon 0.4 in. Below top of Vise Jaws	in	None Available
2	B	Top of Coupon even with top of Vise Jaws	out	Tight
3	B	Top of Coupon even with top of Vise Jaws	in	Tight
4	B	Top of Coupon even with top of Vise Jaws	in	Snug
5	B	Top of Coupon 0.4 in. Above top of Vise Jaws	in	Tight

TABLE I (Continued)

All frequencies are given in cps.

Stage 3

Blade No. 23

Clamping Condition	1st Flexural (Tangential)	1st Flexural (Axial)	1st Torsional
1	7682	16880	21396
2	6000	11376	18226
3	6476	13948	19864
4	5646	12134	18960
5			

Blade No. 46

Clamping Condition	1st Flexural (Tangential)	1st Flexural (Axial)	1st Torsional
1	7714	16506	21132
2	5818	11236	17464
3	6468	13744	19328
4	5640	11986	18372
5	6198	12526	18318

Stage 4

Blade No. 27

Clamping Condition	1st Flexural (Tangential)	1st Flexural (Axial)	1st Torsional
1	5254	11986	15160
2	3948	8492	12790
3	5230	10288	14876
4	4588	9018	14168
5			

Blade No. 28

Clamping Condition	1st Flexural (Tangential)	1st Flexural (Axial)	1st Torsional
1	5235	11902	15074
2	3952	8448	12866
3	5100	10204	14870
4	4476	9244	13660
5	4116	9054	13410

TABLE II

HISTORY OF TURBINE COMPONENTS AT THE START OF 2000 HR. ENDURANCE TEST

Component	History
First Stage Blades	New
Second Stage Blades (U700)	Same as Used in May 1965 Performance Testing
Second Stage Blades (Refractory)	New
First Stage Honeycomb Tip Seal	New
Second Stage Honeycomb Tip Seal	New
Interstage Honeycomb Seal	New
First Stage Wheel	New
Second Stage Wheel	New
Blade Retainers (First and Second Stage)	New
Casings	Used in Performance Testing of May 1965
Nozzle Diaphragm and OGV	Same as Those Used in All Previous Testing
Exhaust Scroll	Same as the One Used in All Previous Testing
Bearing Housing	Same as the One Used in Potassium Vapor Performance Testing
Pivoted Pad Bearing	New
Ball Thrust Bearings	New
Turbine Shaft	Same as Used in May 1965 Performance Testing
Tie-Bolt	Used in May 1965 Performance Testing
Hydrodynamic Seal	Same as Used in May 1965 Performance Testing
Inlet Duct	Same as Used in All Previous Testing
Koppers Drive Coupling	Same as Used in All Potassium Vapor Testing
Water Brake (Disks, Shaft, Stator)	Same as Used During All Previous Potassium Vapor Testing

TABLE III

TURBINE BUILD-UP FOR 2000 HOUR ENDURANCE TEST: BLADE WEIGHTS BEFORE AND AFTER TEST

STAGE ONE BLADES

Blade No.	Set No.	Weight Before Testing, Grams	Weight After Testing & Brush Cleaning, Grams	Per Cent Change	Weight After Vapor Blast, Grams	Per Cent Change
1	3	16.1574	16.1623	+.030*	16.1176	-.247*
1	2	16.1283	16.1365	+.050	16.0845	-.272
2	3	16.5298	16.5327	+.018	16.4712	-.373
3	2	16.1892	16.2000	+.066	16.1448	-.275
4	3	16.1365	16.1403	+.024	16.0883	-.323
5	3	16.1929	16.1967	+.023	16.1470	-.282
6	3	16.0671	16.0790	+.074	16.0143	-.330
6	2	16.2274	16.2361	+.054	16.1686	-.364
9	3	16.2705	16.2791	+.053	16.2329	-.232
10	3	16.1603	16.1658	+.034	16.1117	-.302
11	3	16.2666	16.2731	+.040	16.2139	-.325
13	2	16.1243	16.1294	+.031	16.0640	-.375
15	3	16.1077	16.1170	+.057	16.0579	-.368
16	3	16.3785	16.3826	+.025	16.3312	-.290
17	3	16.2684	16.2741	+.035	16.2096	-.361
18	2	16.1860	16.1908	+.029	16.1414	-.306
18	3	16.2688	16.2750	+.038	16.2204	-.298
19	3	16.1310	16.1423	+.070	---	---
20	3	16.2629	16.2678	+.030	16.2195	-.268
21	2	16.3705	16.3763	+.035	16.3192	-.314
21	3	16.2390	16.2458	+.042	16.1880	-.315
22	3	16.2579	16.2617	+.023	16.2017	-.347
23	3	16.4296	16.4350	+.033	16.3796	-.305
25	2	16.3460	16.3573	+.069	---	---
26	3	16.1379	16.1425	+.029	16.0948	-.268
27	3	16.2693	16.2740	+.029	16.2278	-.256
28	3	16.0693	16.0760	+.041	16.0178	-.326
30	3	16.2564	16.2614	+.030	16.2041	-.323
33	3	15.9647	15.9720	+.046	15.9239	-.256
36	3	16.3087	16.3150	+.038	---	---
37	3	16.0629	16.0698	+.043	---	---
38	3	16.2312	16.2347	+.022	---	---
39	3	16.3532	16.3593	+.037	16.3037	-.304

Continued On Next Page

* + Weight Gain
- Weight Loss

TABLE III

(Continued)

Blade No.	Set No.	Weight Before Testing, Grams	Weight After Testing & Brush Cleaning, Grams	Per Cent Change	Weight After Vapor Blast, Grams	Per Cent Change
41	3	15.9776	15.9837	+.038	15.9280	-.311
43	3	15.8722	15.8785	+.040	15.8260	-.292
44	3	16.3859	16.3928	+.042	16.3375	-.296
45	3	16.3913	16.3951	+.023	---	---
47	2	16.3410	16.3497	+.053	16.2840	-.350
48	3	16.4137	16.4259	+.037	16.3625	-.350
49	3	16.4360	16.4405	+.027	16.3980	-.231
50	3	16.3400	16.3450	+.031	16.2944	-.280
51	3	16.0629	16.0680	+.031	16.0063	-.354
52	3	16.2578	16.2607	+.017	16.1973	-.374
54	3	16.2711	16.2776	+.040	16.2163	-.338
55	3	16.0941	16.1015	+.046	16.0412	-.330
56	3	16.5699	16.5755	+.033	---	---
57	3	16.3318	16.3379	+.037	16.2749	-.350
58	3	16.1636	16.1673	+.023	---	---
61	3	16.0710	16.0758	+.030	16.0360	-.218
62	3	16.0510	16.0546	+.022	16.0111	-.250
64	3	16.3904	16.3978	+.045	16.3397	-.310
65	3	16.1722	16.1784	+.038	16.1210	-.318
67	3	16.1993	16.2085	+.056	16.1456	-.333
68	3	16.3173	16.3253	+.049	16.2563	-.375
70	3	16.4085	16.4160	+.045	16.3596	-.299
71	3	15.9777	15.9840	+.039	15.9264	-.321
73	3	16.0943	16.1020	+.048	16.0478	-.290
74	2	16.1565	16.1640	+.046	16.1282	-.175
74	3	16.1566	16.2954	Apparently a Misreading was Taken on the Weight Before Testing		
75	3	16.1895	16.1945	+.031	16.1366	-.328
77	3	16.2278	16.2345	+.041	16.1713	-.356
78	2	16.1690	16.1714	+.014	16.1278	-.255
			AVERAGE	+.0380	AVERAGE	-.304

TABLE III

(Continued)

STAGE TWO BLADES

	Blade No.	Set No.	Weight Before Testing, Grams	Weight After Testing & Brush Cleaning, Grams	Per Cent Change	Weight After Vapor Blast, Grams	Per Cent Change
U-700	1	1	21.8200	21.8490	+.133	---	---
	2	1	21.7645	21.8006	+.166	21.7540	-.048
	4	1	21.9408	21.9739	+.151	21.9384	-.011
	5	1	21.8300	21.8608	+.141	21.8246	-.024
	6	1	22.0598	22.0910	+.141	22.0607	+.004
	7	1	22.0718	22.1070	+.159	22.0711	-.003
	8	1	22.3274	22.3644	+.165	22.3228	-.021
	9	1	21.9272	21.9571	+.136	21.9250	-.010
	10	1	22.1263	22.1520	+.116	22.1298	+.016
	12	1	21.9530	21.9836	+.139	21.9662	+.060
	14	1	21.4661	21.5023	+.168	21.4628	-.015
	13	1	22.3506	22.3870	+.163	22.3452	-.024
	16	1	22.0192	22.0517	+.148	22.0152	-.018
	17	1	21.6002	21.6284	+.130	21.5995	-.003
	18	1	21.7043	21.7388	+.159	21.6957	-.040
	19	1	21.7720	21.8040	+.147	21.7650	-.032
	20	1	22.2017	22.2368	+.158	---	---
	21	1	21.6210	21.6578	+.170	21.6179	-.014
	22	1	21.9106	21.9417	+.142	21.9117	+.005
	24	1	22.0456	22.0819	+.164	22.0381	-.034
	25	1	21.5750	21.6054	+.141	21.5687	-.032
	26	1	21.6550	21.6832	+.130	21.6499	-.024
	27	1	21.1207	21.1528	+.152	21.1201	-.003
	29	1	20.9290	20.9595	+.145	20.9238	-.025
	30	1	20.9985	21.0275	+.138	20.9944	-.020
	31	1	21.5878	21.6230	+.163	21.5823	-.026
	32	1	21.4038	21.4367	+.153	21.3976	-.029
	33	1	21.6738	21.7024	+.132	21.6647	-.065
	34	1	21.3474	21.3779	+.143	---	---
	35	1	21.3150	21.3442	+.137	21.3123	-.013
	36A	1	21.2260	21.2580	+.150	21.2243	-.008
	36B	1	21.4488	21.4809	+.149	21.4476	-.006
	37	1	21.7440	21.7747	+.141	21.7460	-.009
	38	1	21.2380	21.2683	+.142	21.2311	-.033

Continued On Next Page

TABLE III

(Continued)

	Bucket No.	Set No.	Weight Before Testing, Grams	Weight After Testing & Brush Cleaning, Grams	Per Cent Change	Weight After Vapor Blast, Grams	Per Cent Change
	39	1	21.4116	21.4441	+.152	21.4032	-.008
	40	1	21.3435	21.3742	+.144	21.3332	-.010
	41	1	21.6153	21.6520	+.170	21.6136	-.002
	42	1	21.1273	21.1571	+.141	21.1218	-.006
	43	1	21.2838	21.3143	+.143	---	---
	44	1	21.2753	21.3068	+.148	21.2690	-.006
	45	1	21.7005	21.7366	+.166	21.6894	-.011
	47	1	21.1148	21.1468	+.151	21.1139	-.001
	49	1	21.4360	21.4677	+.148	21.4300	-.006
	51	1	21.2694	21.2985	+.137	21.2696	+.001
	54	1	21.2065	21.2377	+.147	---	---
	55	1	21.4686	21.5009	+.150	---	---
	58	1	21.2481	21.2782	+.141	---	---
	60	1	21.6222	21.6530	+.142	21.6166	-.026
	61	1	21.3406	21.3713	+.144	21.3351	-.026
	62	1	21.4368	21.4685	+.148	21.4321	-.022
	63	1	21.1203	21.1492	+.137	21.1169	-.016
	64	1	21.5735	21.6080	+.160	21.5584	-.070
				AVERAGE	+.147	AVERAGE	-.019
TZM	17	1	28.0209	28.0090	-.042	---	---
	20	1	26.9403	26.9282	-.045	---	---
	21	1	27.8451	27.8329	-.044	27.8171	-.104
	23	1	27.9722	27.9601	-.043	27.9417	-.109
				AVERAGE	-.044	AVERAGE	-.105
ΓZC	1	1	28.3167	28.3076	-.032	28.2905	-.093
	2	1	28.3958	28.3857	-.035	28.3616	-.121
	11	1	28.5019	28.4908	-.039	28.4738	-.099
	12	1	28.4353	28.4275	-.027	28.4086	-.094
				AVERAGE	-.033	AVERAGE	-.102

TABLE IV

TURBINE DIMENSIONAL INSPECTION* FOLLOWING 2000 HR. ENDURANCE TEST

ROTOR

Tie Bolt

Before - Length	22.229
After - Length	22.231
Measured Relaxation of Bolt Tension at Disassembly	10 per cent

First Stage Wheel

Before - Over Blade Diameter	8.816
After - Over Blade Diameter	8.818

Second Stage Wheel

Before - Over Blade Diameter	9.623 - 9.624
After - Over Blade Diameter	9.625
Before - Interstage Seal Teeth Diameter	4.069
After - Interstage Seal Teeth Diameter	4.069
Before - Screw Seal Diameter	3.870
After - Screw Seal Diameter	3.869

Shaft

Before - Screw Seal Diameter	3.880
After - Screw Seal Diameter	3.844

Hydrodynamic Seal

Before and After - Inner and Outer Labyrinth Teeth Diameters

	Outer	Inner
Before	4.744/4.750	3.745/3.749
After	4.744/4.746	3.745/3.746

STATOR

Inlet Duct

Diameter at 0°	9.483
Diameter at 90°	9.488

Scroll

O.R. of Bearing Housing Flange	
at 0°	8.192
at 90°	8.220

*Unless Specified, Dimensions Given in Inches

TABLE IV
(Continued)

STATOR (Continued)

Bearing Housing and Internal Parts	
Bearing Housing O.R. of Aft Diameter	
at 0°	7.230
at 90°	7.231
O.R. of Pad Bearing Seat Diameter	
at 0°	4.538
at 90°	4.538
Socket Ring O.R.	
at 0°	5.118
at 90°	5.116

TABLE V

COMMERCIALLY OBTAINED TEST RIG COMPONENTS

	Component	Model	Manufacturer
1.	Multi-Disk Water Brake	Hydra-Brake Model C9529-2	Industrial Engineering Co. Philadelphia, Pennsylvania
2.	Steam Drive-Turbine	8-inch Turbine Model 6037 (Modified)	Barbour Stockwell Company Cambridge, Massachusetts
3.	Torque Meter 0 - 200 in.-lb	Model PT 200	Bytrex Corporation Newton, Massachusetts
4.	Torque Meter 0 - 1250 in.-lb	Special Design	Bytrex Corporation Newton, Massachusetts
5.	Dynamic Rotor Balancing Machine	Model 3S USAF No. 296271	Gisholt Machine Corp. Madison, Wisconsin

TABLE VI

TWO-STAGE POTASSIUM TEST TURBINE

OPERATING HISTORY

The history of major milestones and accumulated test time on potassium vapor for the two-stage turbine is given in Figure 3.

Date	Accumulated Operating Time (Hrs.)	Remarks
5-8-61	--	• Contract Signed
5-30-62	--	• Turbine Design Complete
8-31-62	--	• Turbine Components Procurement Complete
12-20-62	--	• First Pre-Test Run of Turbine
11-30-63	--	• Completion of Turbine Pre-Testing (air, water, steam)
12-29-63	--	• Completion of Test Facility Checkout, Flow Nozzle Tests; Convert Turbine to Weld Flanges
4-13-64	--	• Tare Test of Turbine with K is Seal
		• Mixing of Oil and Potassium
		Improve Seal Instrumentation and Oil System, Install Scavenge Pump, Modify Argon Reclamation System and Potassium Loop For Seal
7-13-64	4	• Turbine Operated on K Vapor For Four Hours. Observed Seal Rubs, K Leak in Seal, Instabilities
		Turbine, Improved Bearing Stiffness, Weld Up Seal Housing and Seal Feed Lines
10-13-64	39	• Performance Test For 35 Hours, Taking 102 Data Points
		• Boiler Unstable, Leaks in Instrumentation,
		• Leak in Boiler, Blade Erosion
		Redesign Boiler Feed System Provide Feed Preheat, Improve Instrumentation and Boiler Level Control, Improve Accuracy of Torque and Flow Measurement. Rebuild Turbine.

TABLE VI

TWO-STAGE POTASSIUM TEST TURBINE

OPERATING HISTORY

(Continued)

Date	Accumulated Operating Time (Hrs.)	Remarks
3-23-65	51	• Performance Test for 12 Hours - Six Data Points Improved Method of Data Taking K Leak in Seal Feed Line Repair Bearing Housing Establish Accurate Tare Losses
5-22-65	104	• Successful Completion of Second Performance Test • Good Data, Repeatable Results • 53 Hours Uninterrupted Operation Above 1400°F • No Erosion, No Boiling Instabilities • No Leaks, No Seal Failures • Prepare for Endurance Testing Rebuild Turbine Reduce Instrumentation
9-13-65	104	• Begin Endurance Test 1500°F, 18,250 RPM, p_r = 2.95:1
9-24-65	358	• 254 Hours Completed • Unwanted Shutdown by Triggering Over Speed Trip Borescope Inspection of Turbine, No Erosion, No Observed Mass Transfer
10-8-65	358	• Resume Endurance Testing
12-19-65	2104	• Endurance Test Completed After 2000 Hours • Planned Shutdown
Jan. 1966		• Post Test Inspection of Hardware
Feb. 1966		• Material Evaluation • Evaluation of Test Results • Final Reports

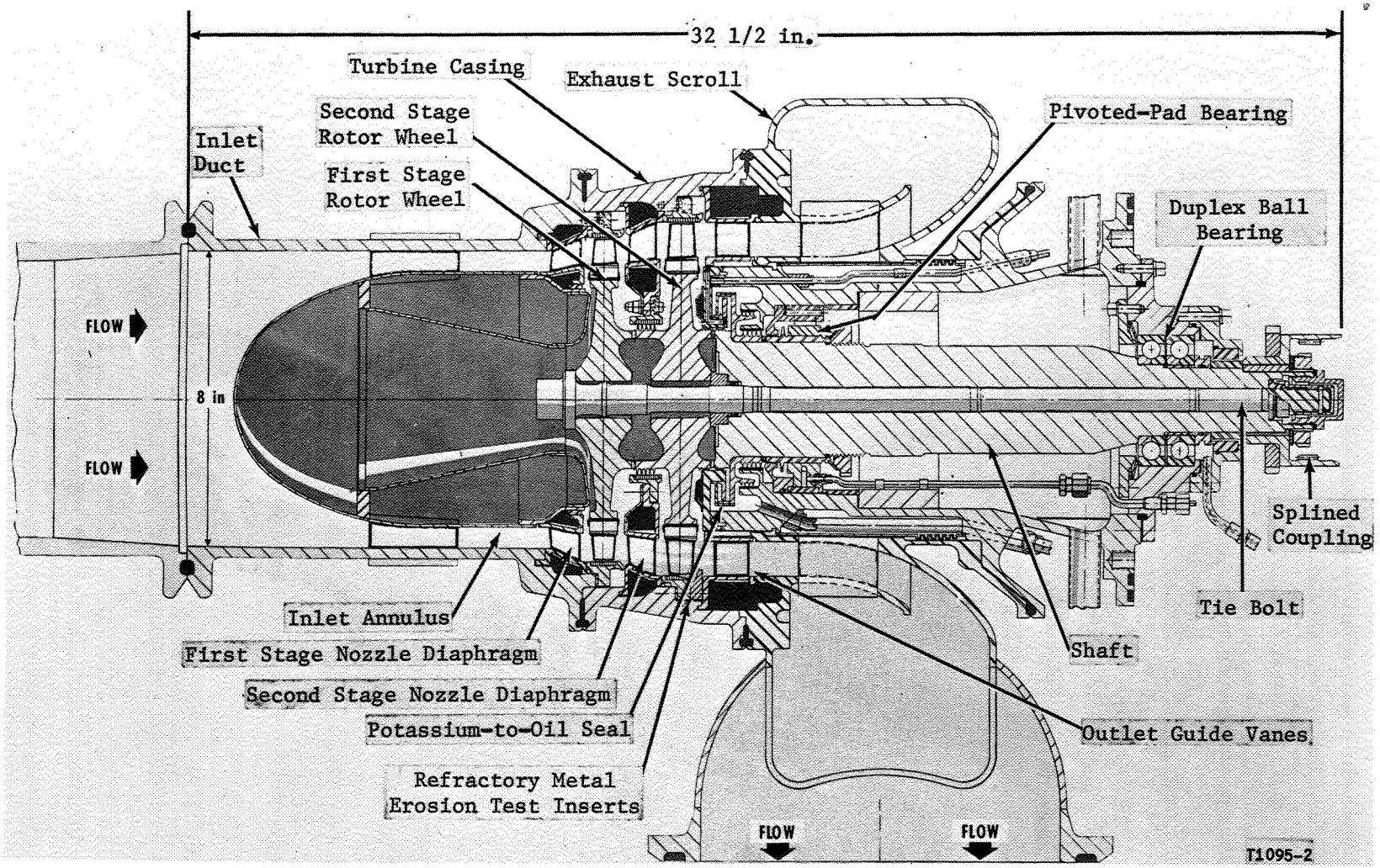


Figure 1a. Section View of Turbine.

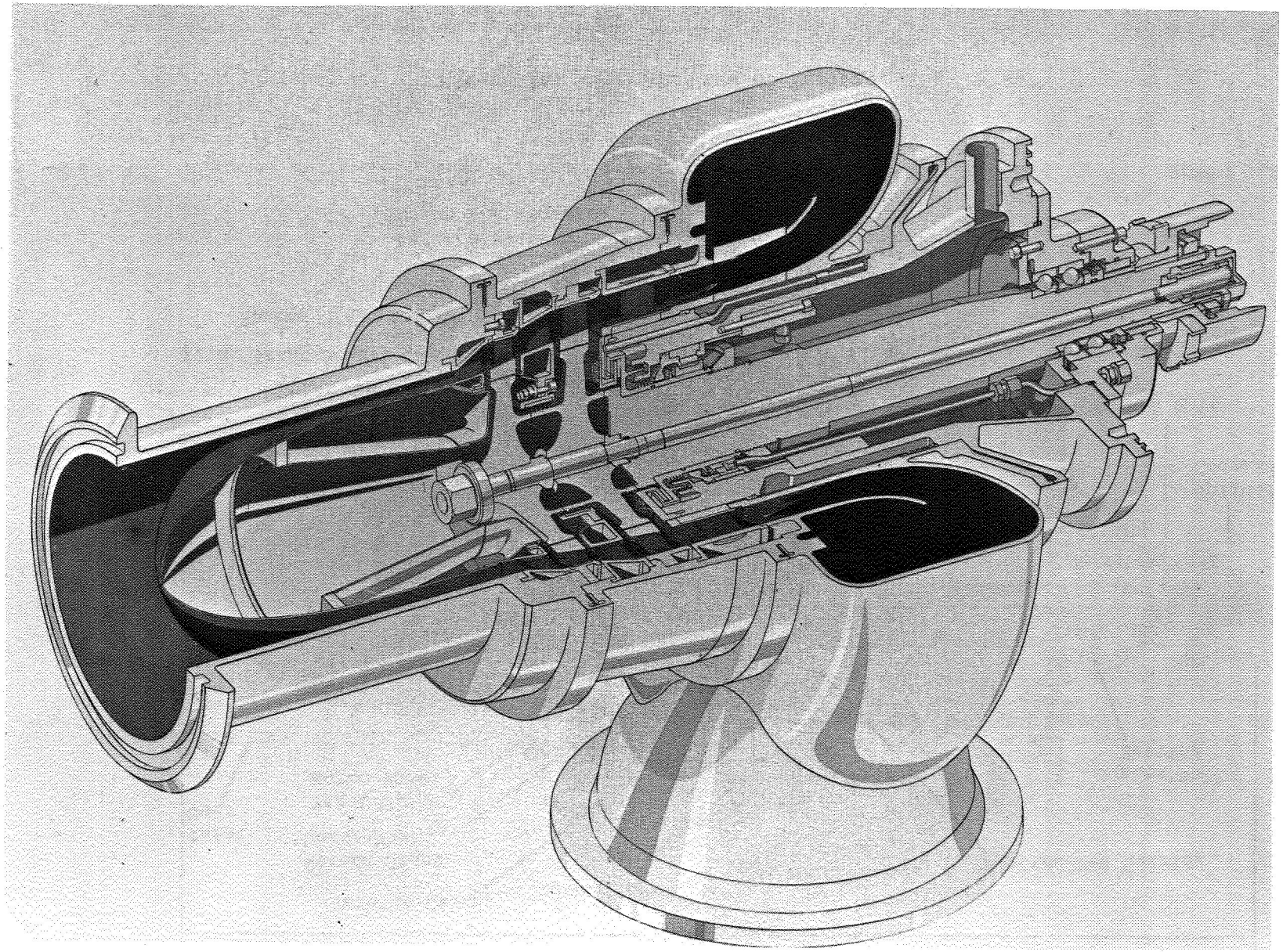


Figure 1b. Isometric Section View of Turbine.

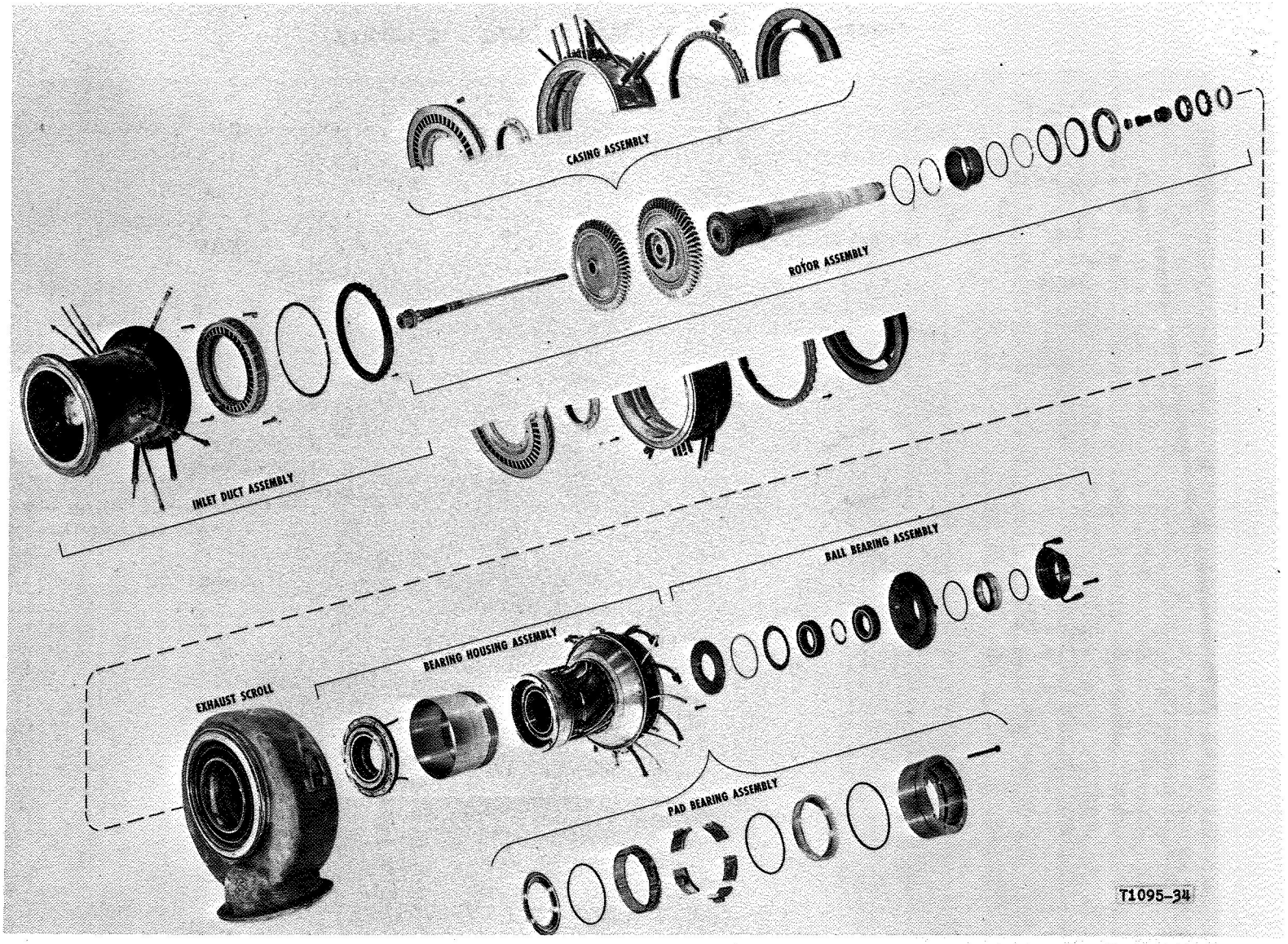


Figure 2. Exploded View of Turbine.

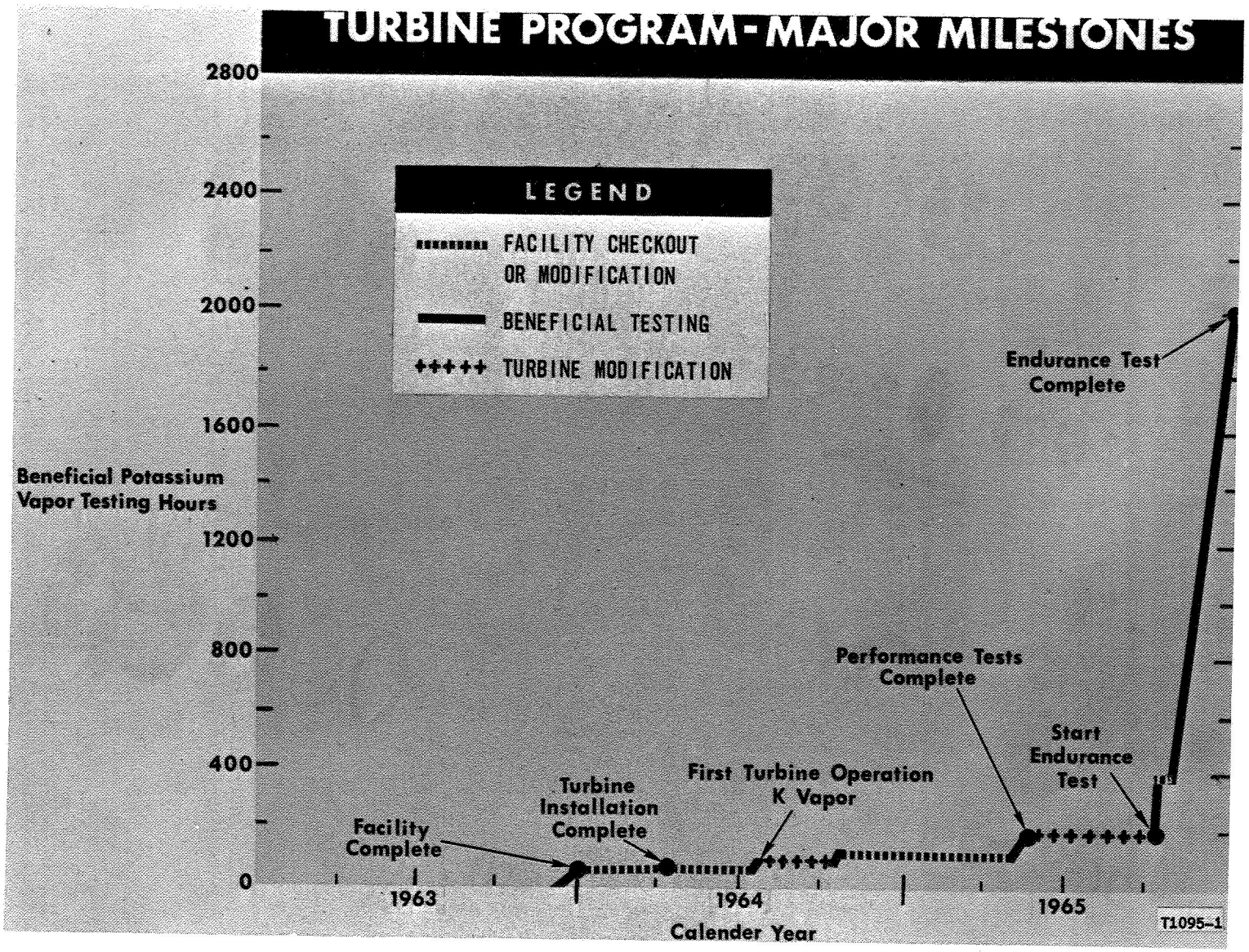


Figure 3. Turbine Program Major Milestones.

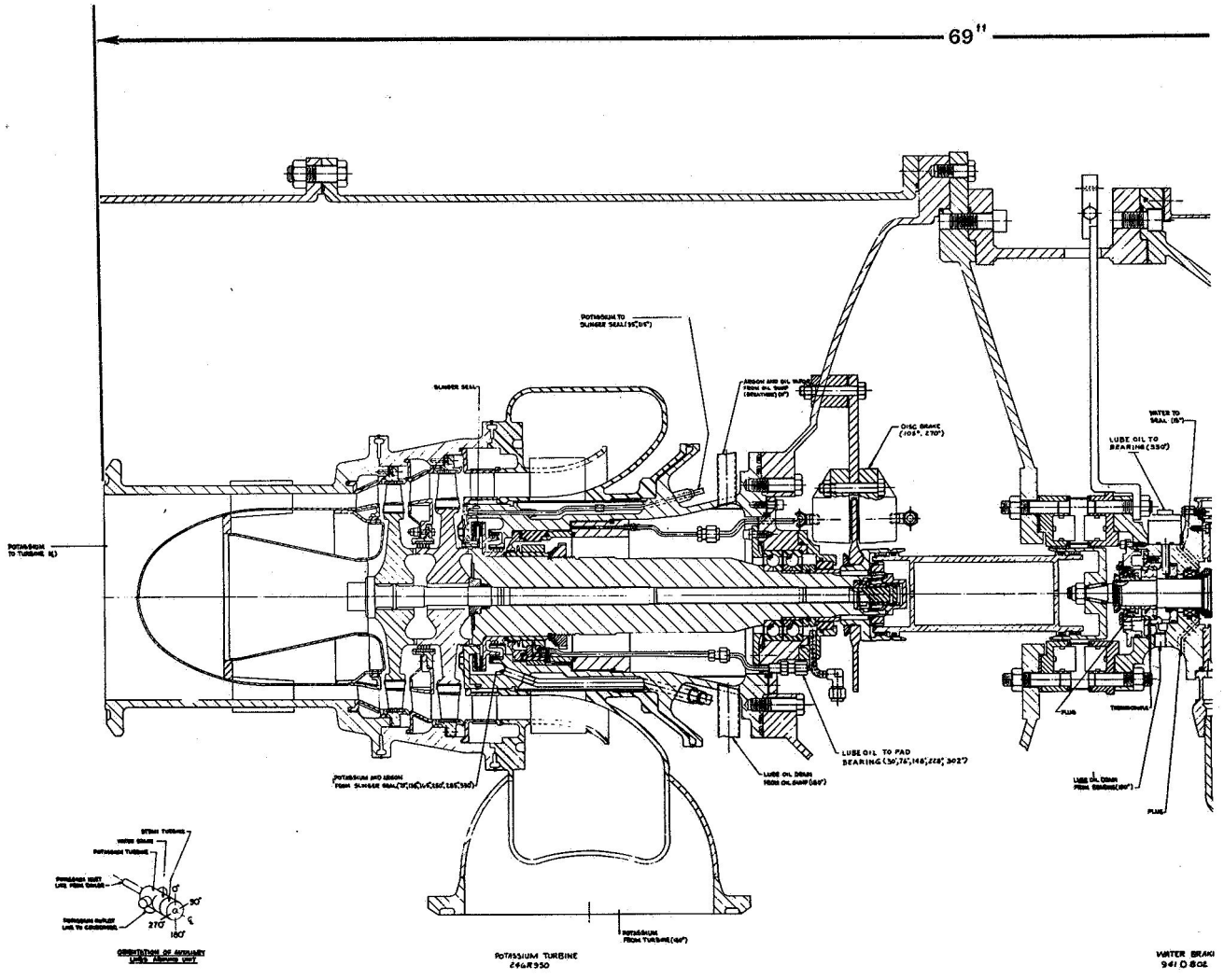
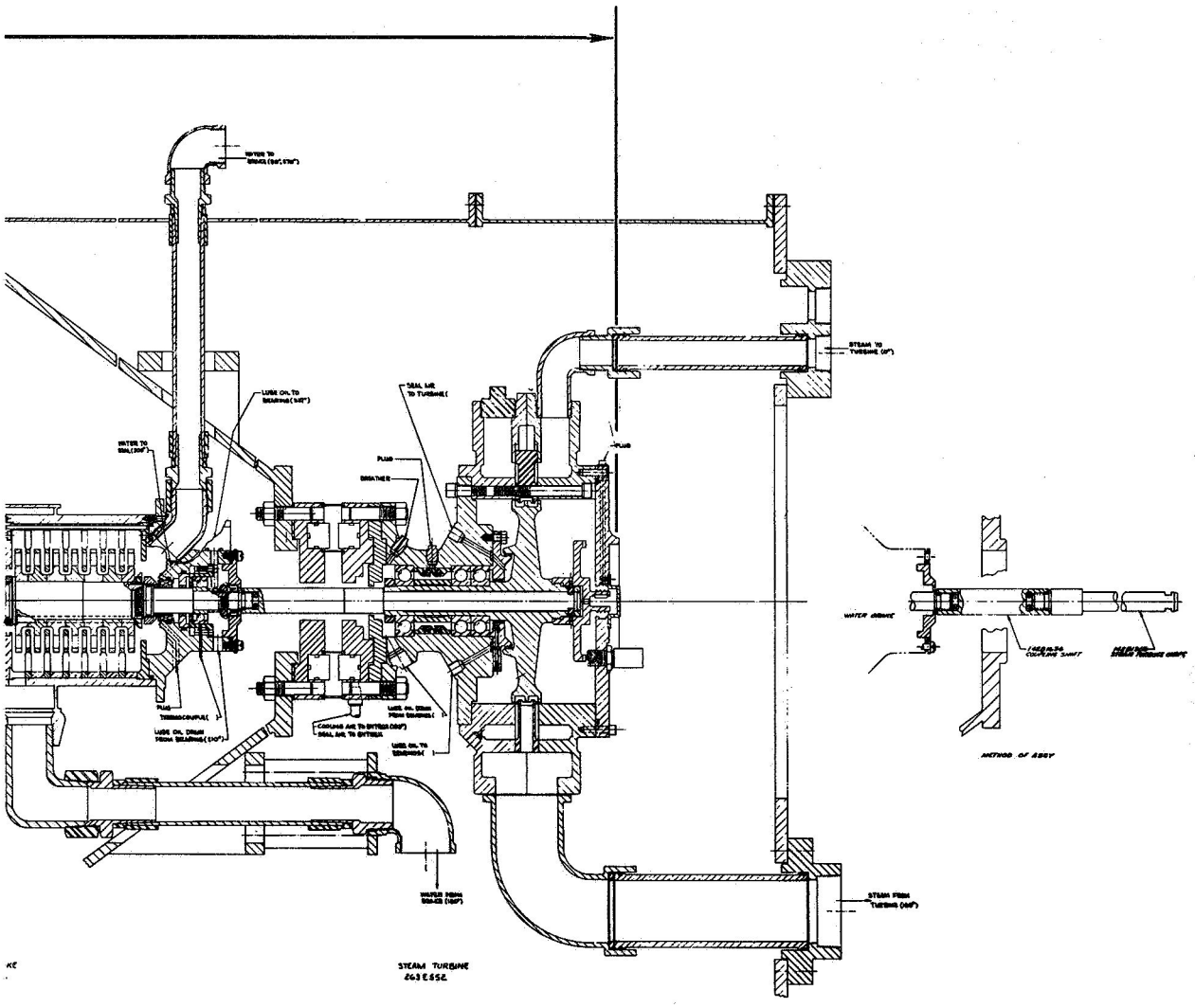


Figure 4. Section View of Potass
System with Load Cell

PRECEDING PAGE BLANK NOT FILMED.



sium Turbine Attached to Loading and Starting
Supported Water Brake and Steam Turbine.

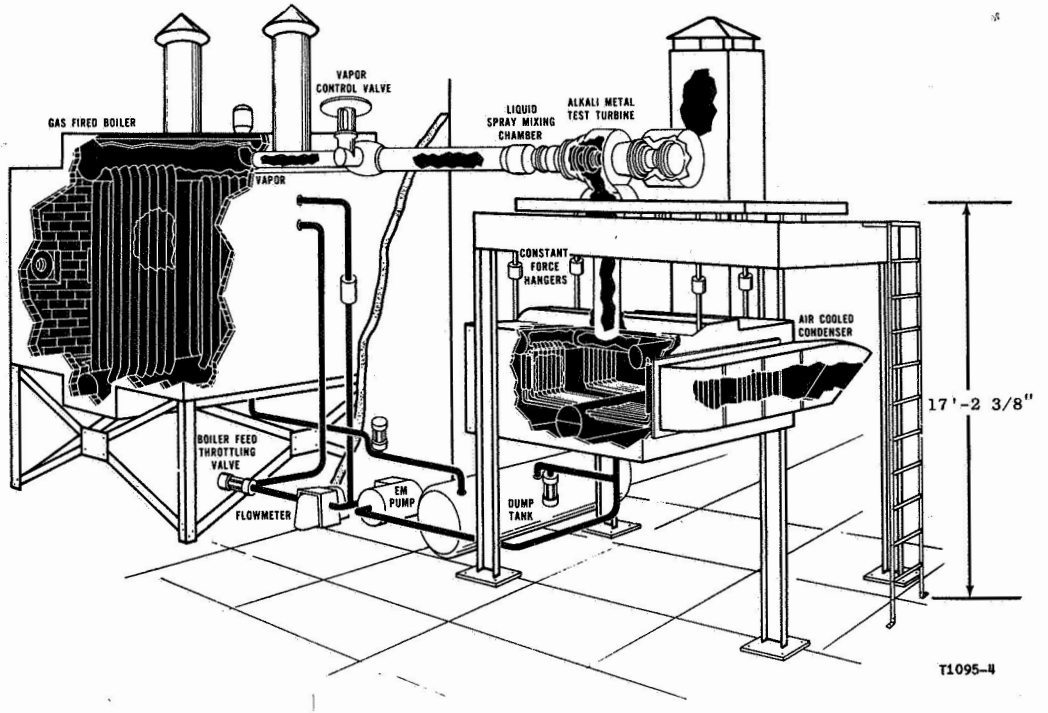


Figure 5. 3000 KW Component Test Facility.

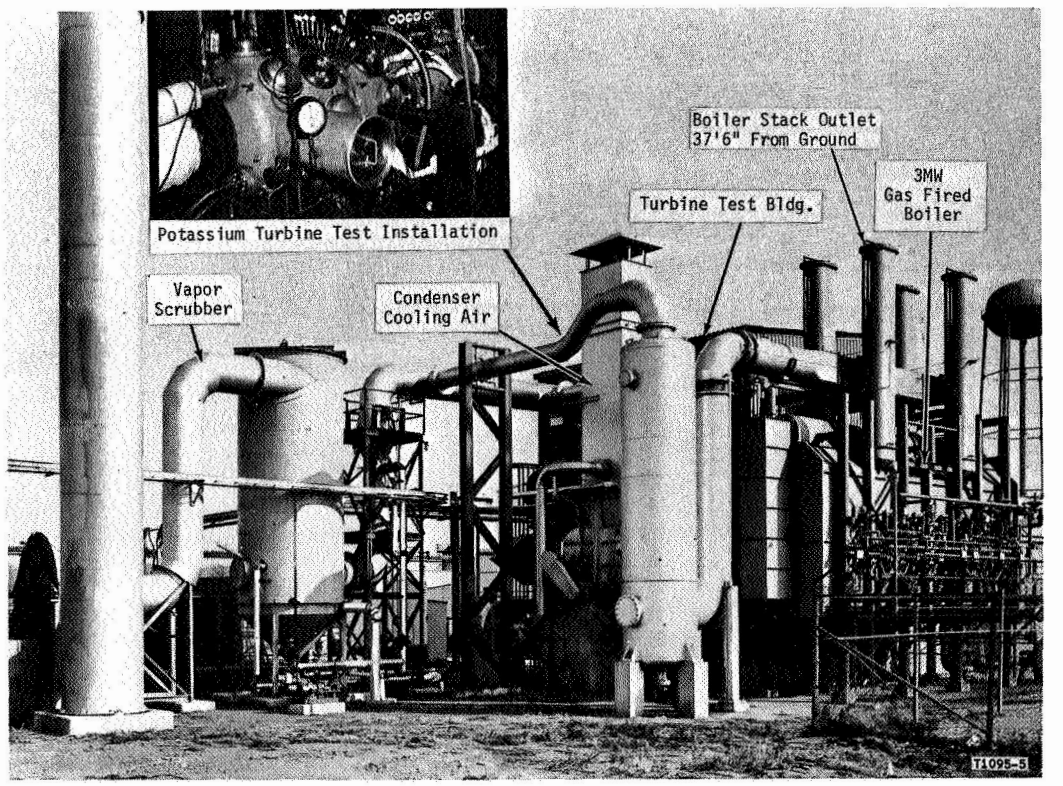


Figure 6. External View of Test Turbine Facility.

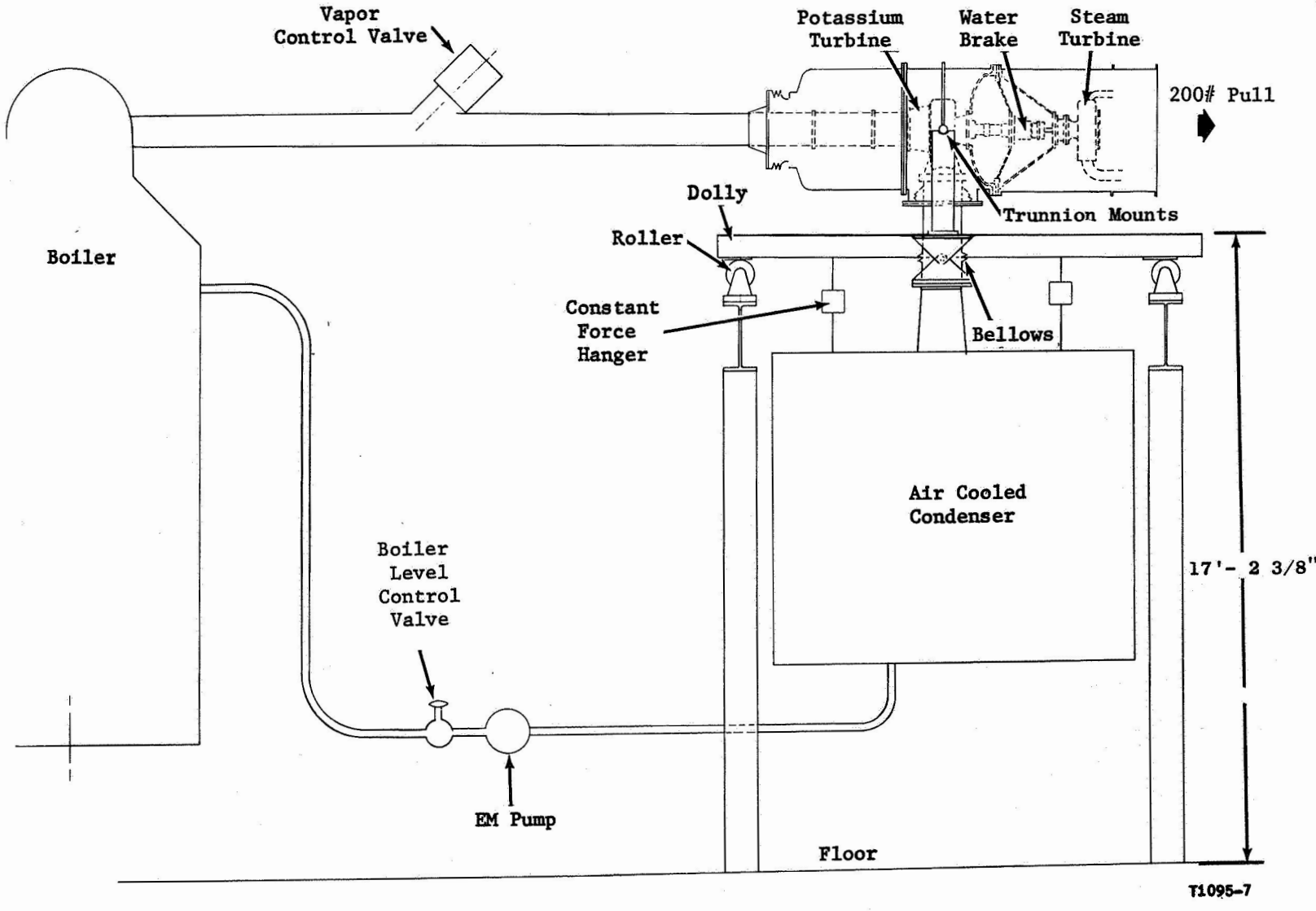


Figure 7. Schematic Diagram of Test Facility.

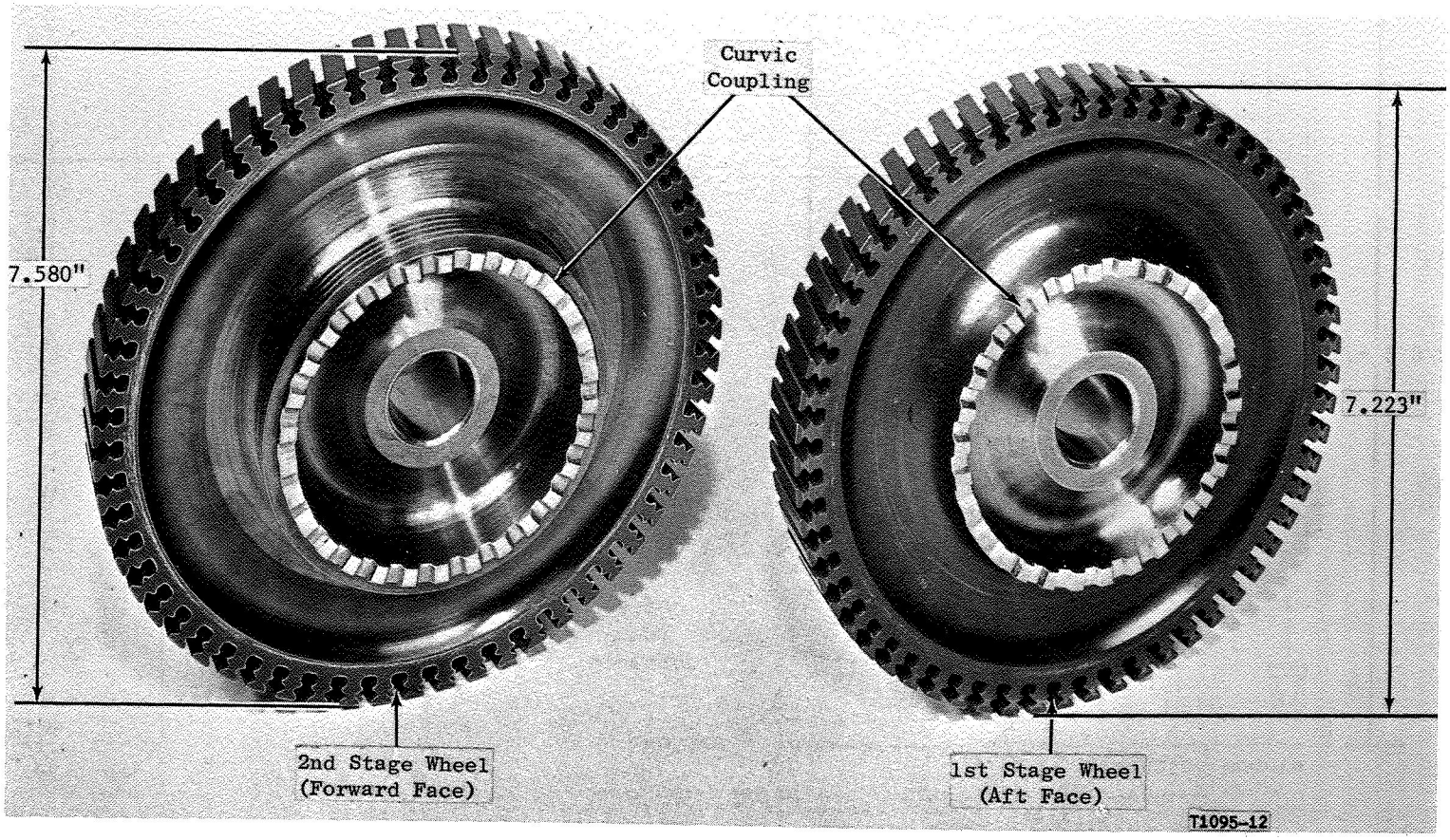


Figure 8. Stage 1 and 2 Turbine Wheels.

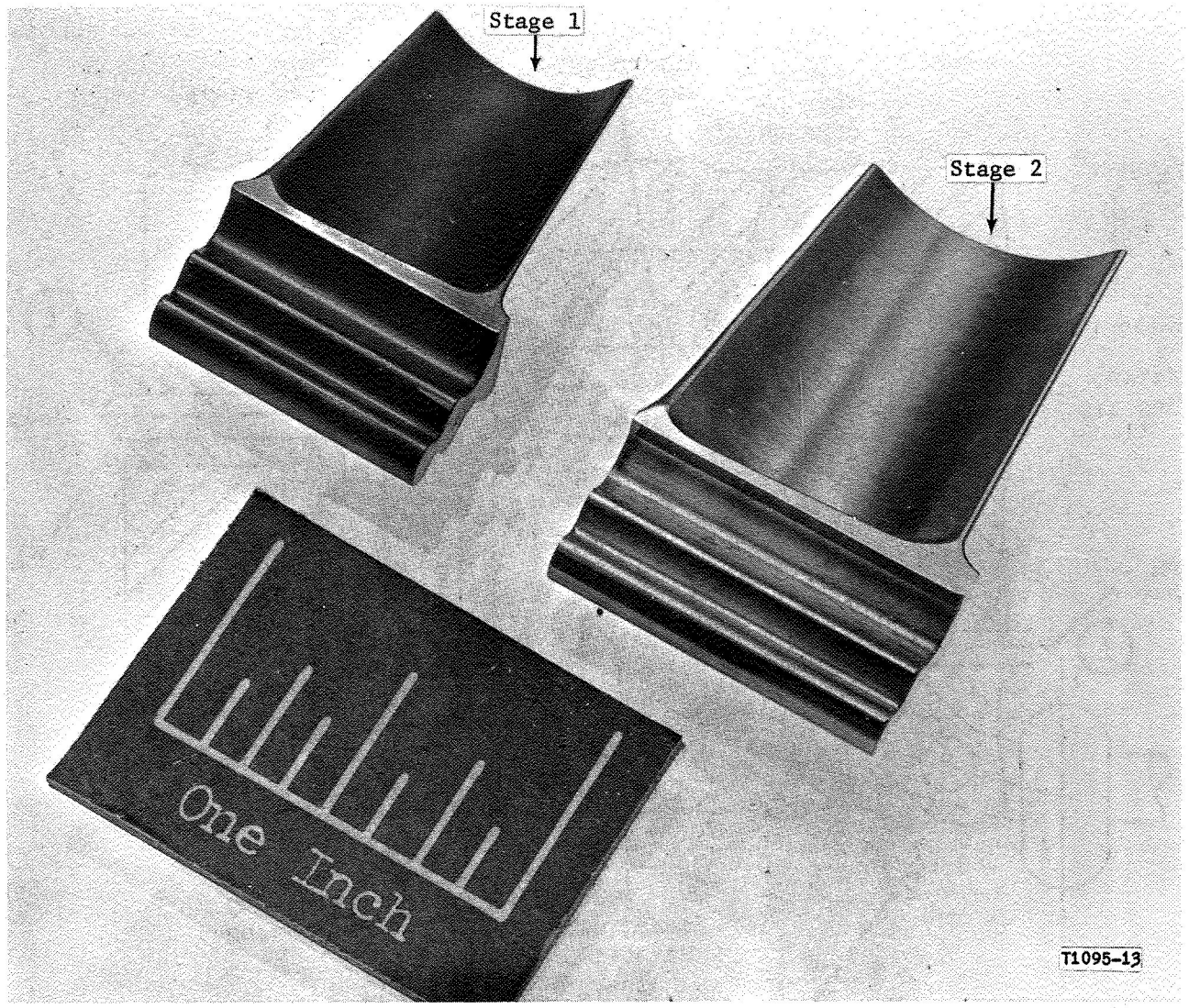


Figure 9. Stage 1 and 2 Turbine Blades Showing Pressure Surfaces.

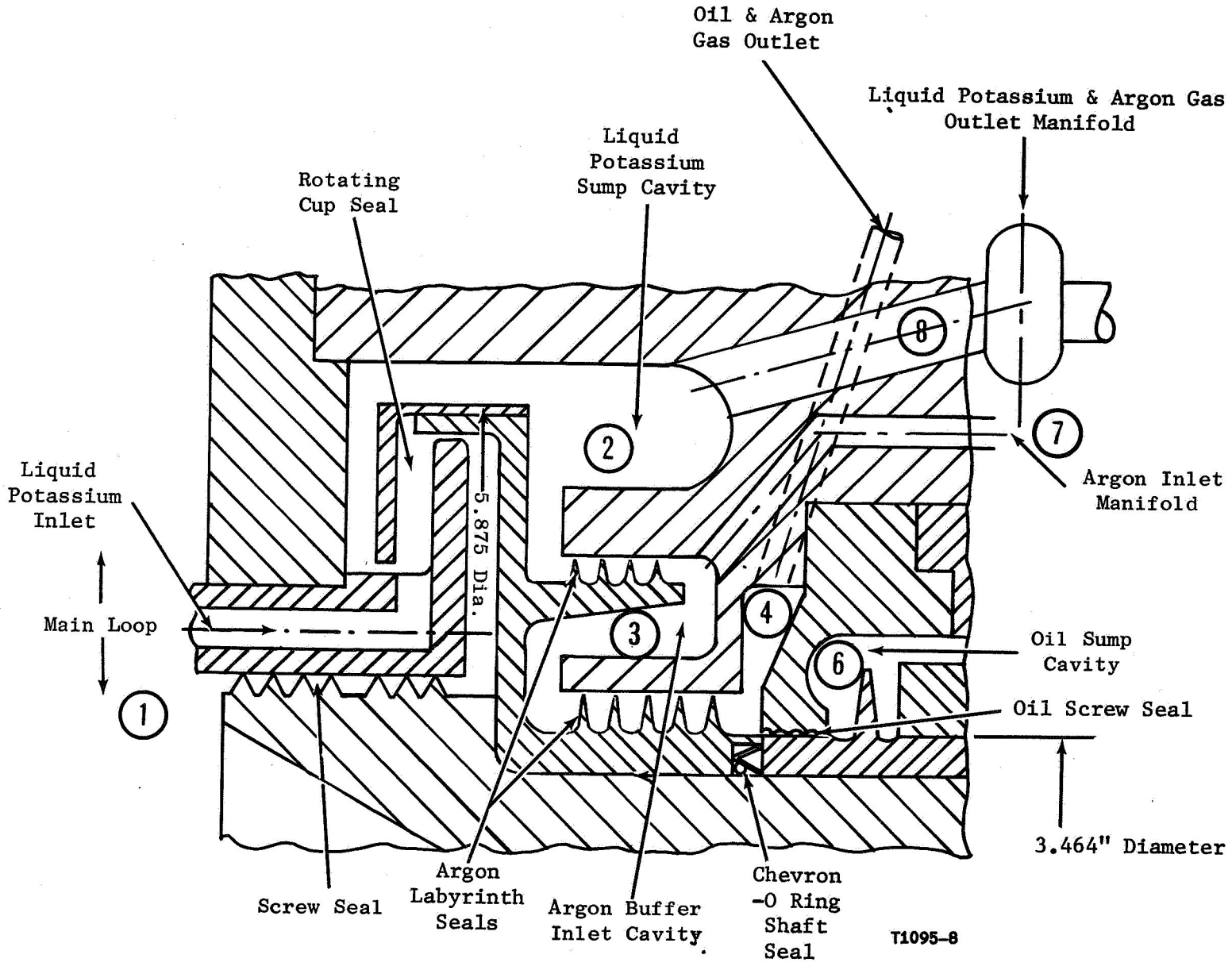


Figure 10. Section View of Turbine Hydrodynamic Seal Assembly.

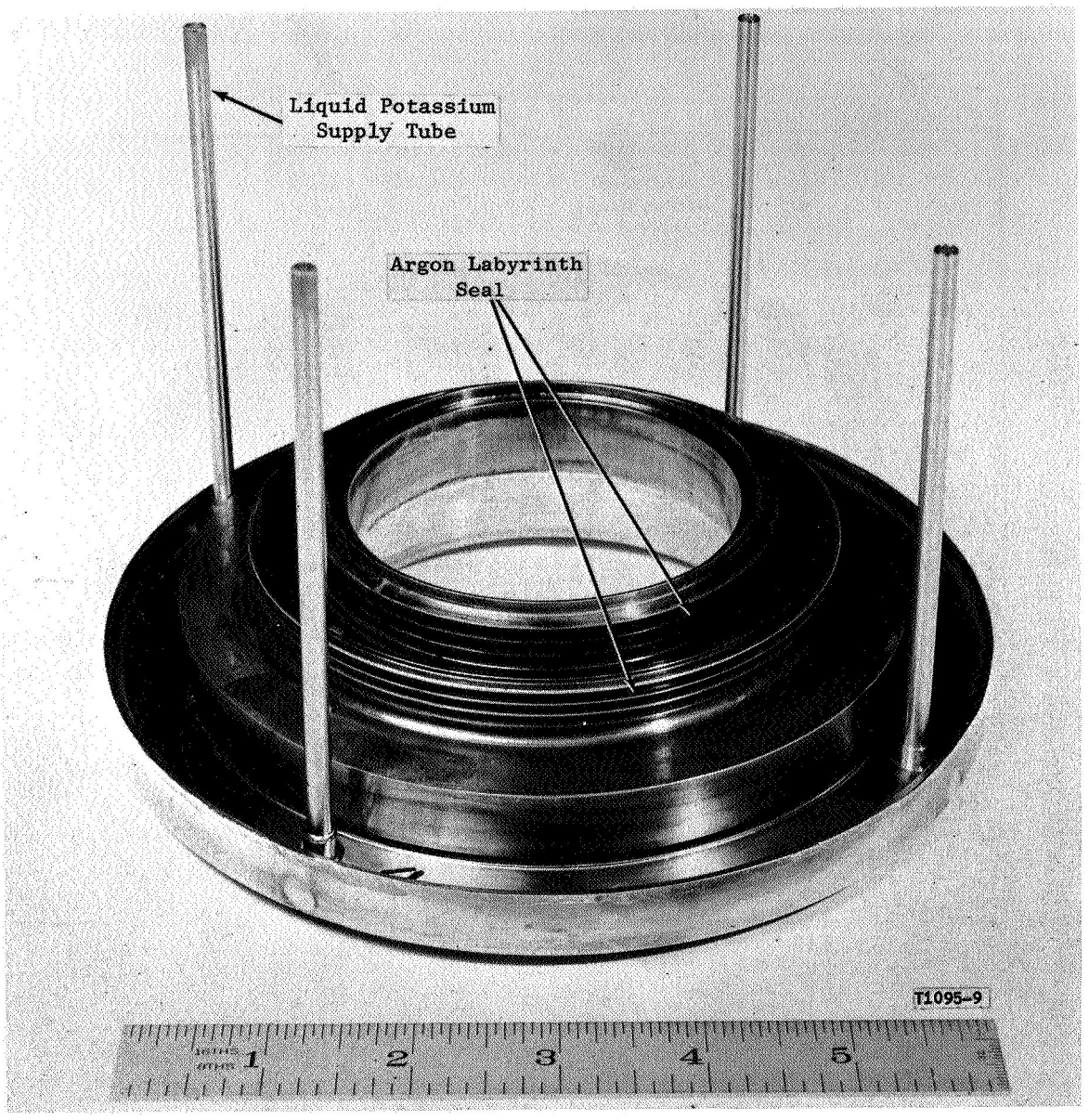


Figure 11. Turbine Hydrodynamic Seal with Potassium Liquid Supply Tubes and Argon Labyrinth Seals Shown.

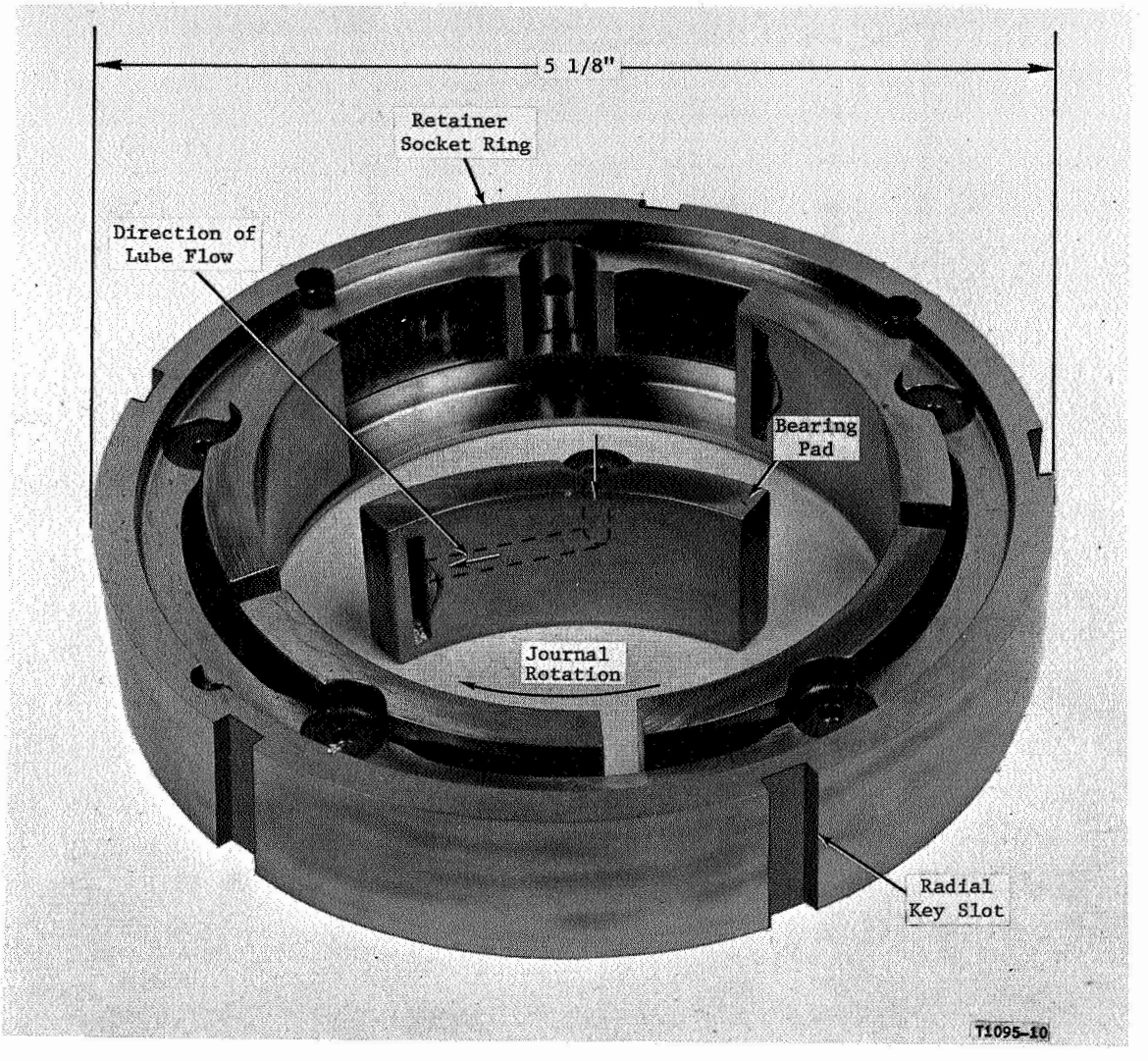


Figure 12. Pivoted Pad Hydrodynamic Bearing.

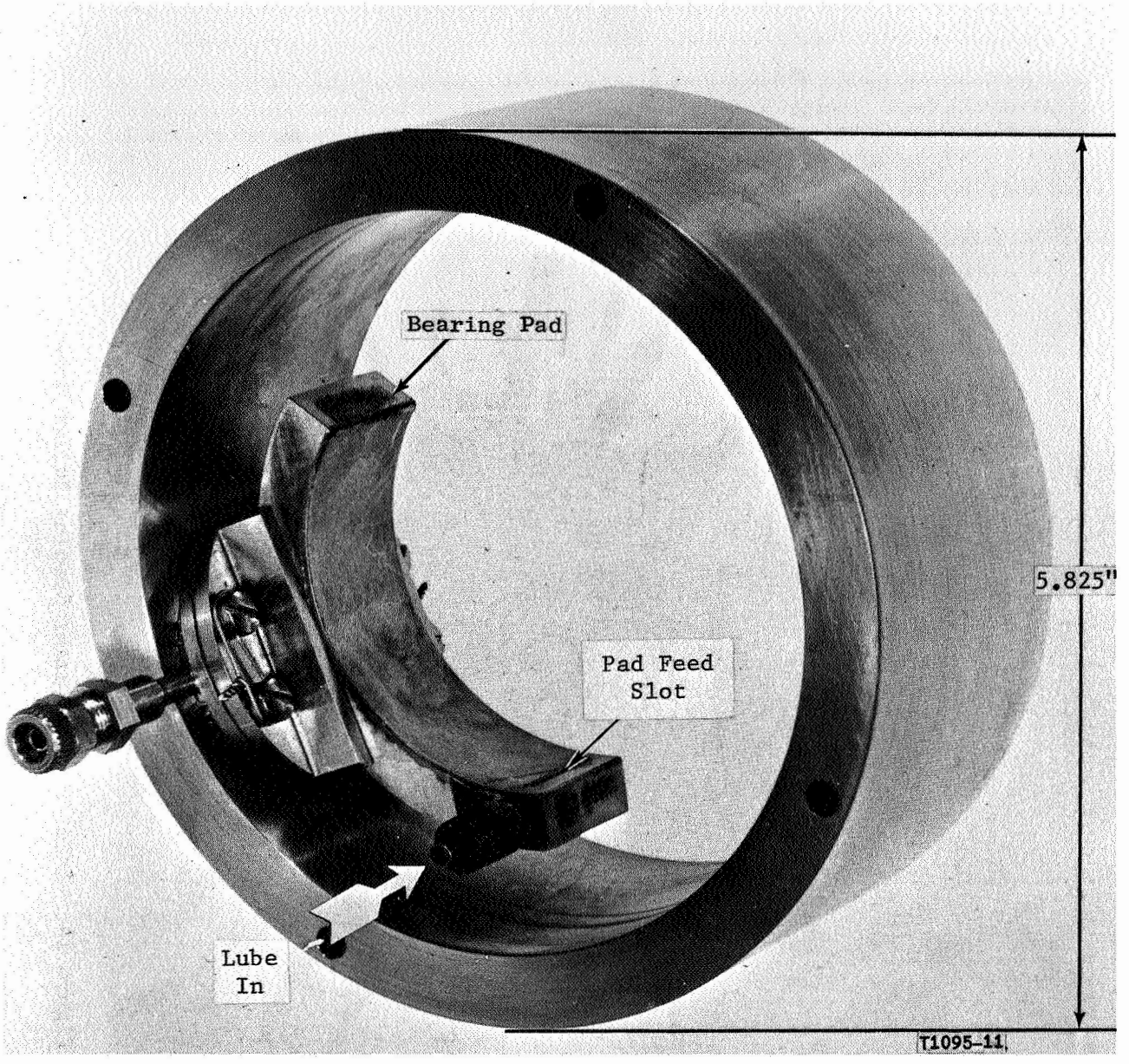


Figure 13. Stabilizer Bearing Assembly.

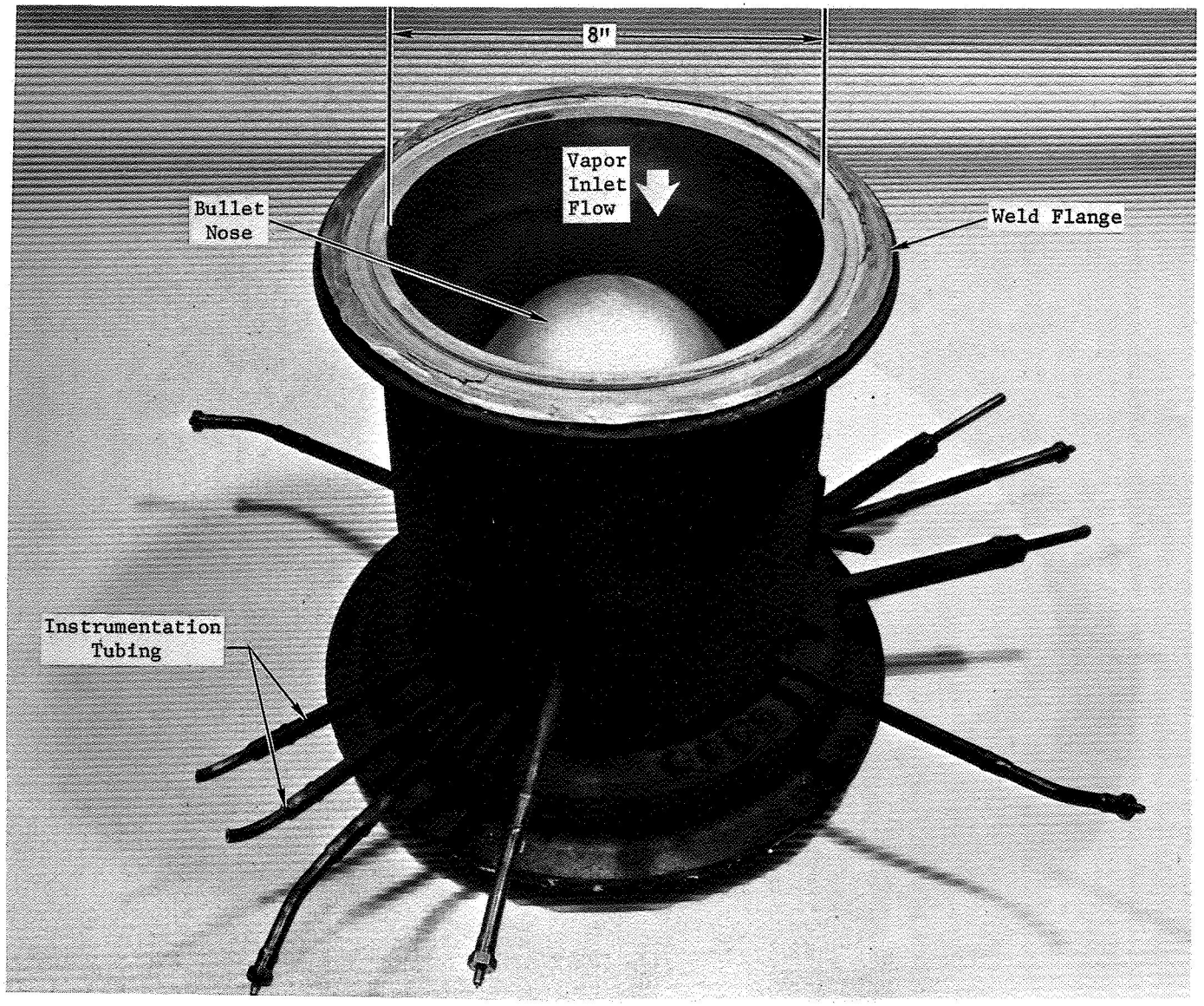


Figure 14. Inlet Duct Weldment Showing Bullet Nose.

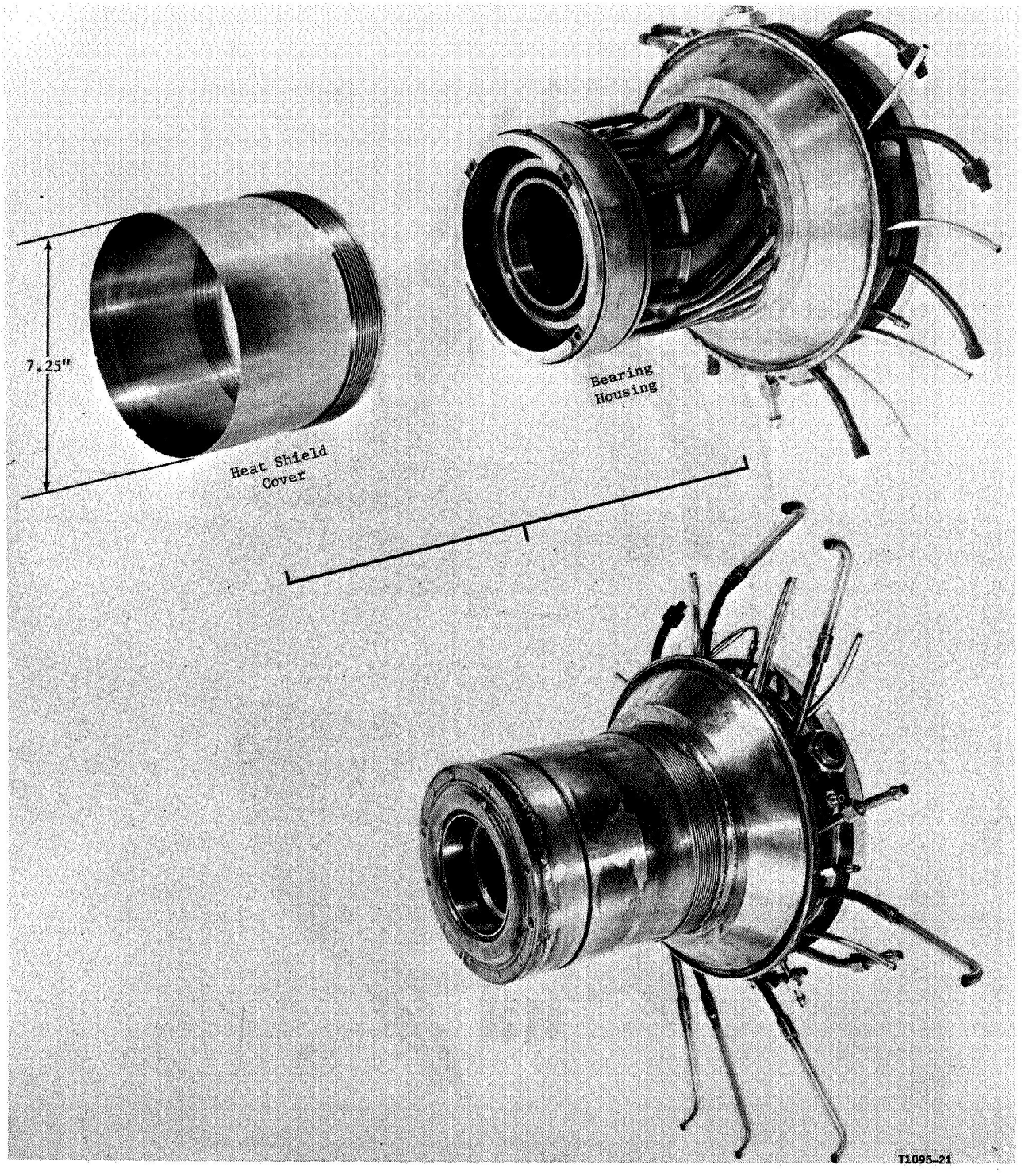


Figure 15. Bearing Housing Showing Assembly of Heat Shield Cover.

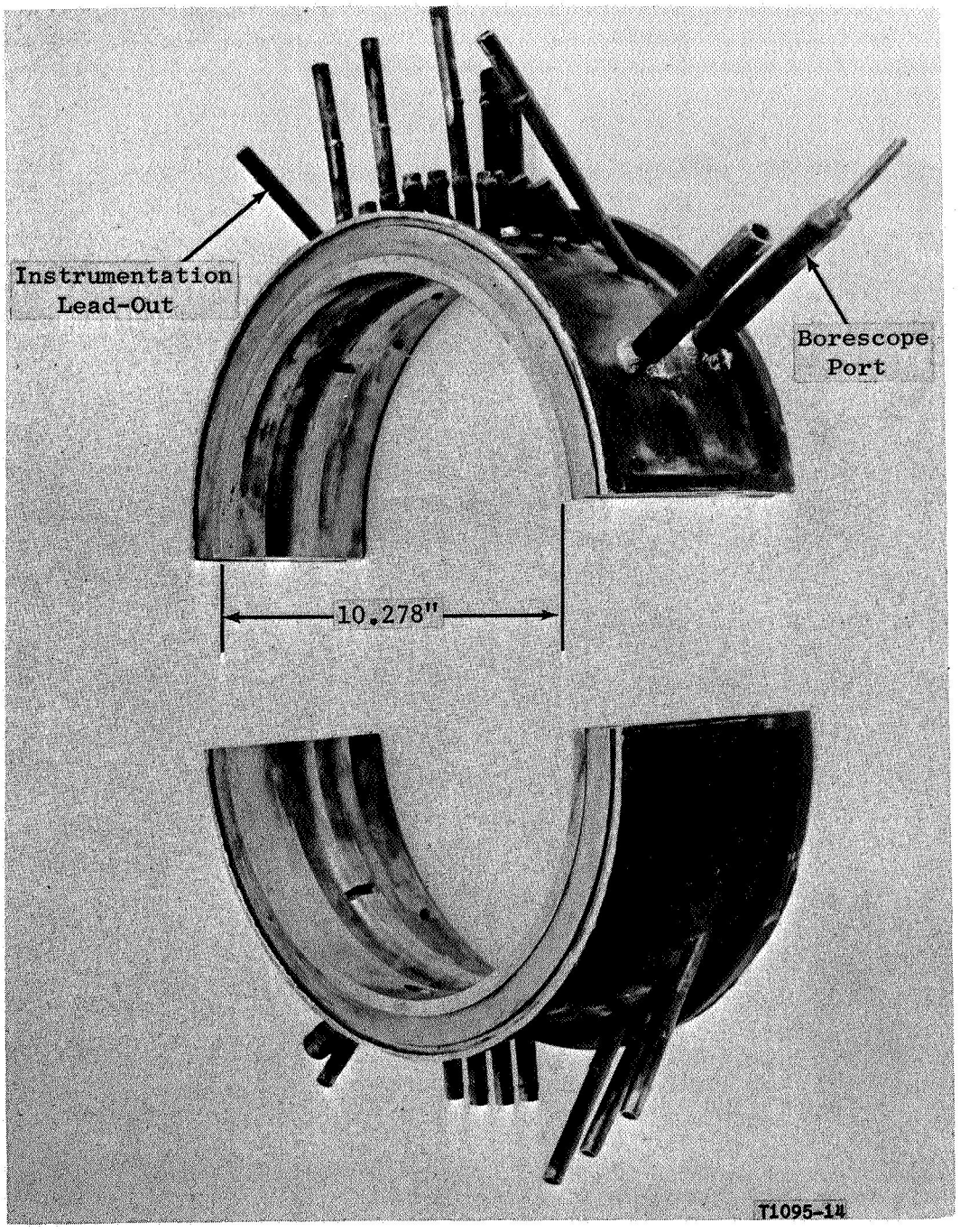


Figure 16. Turbine Casing Top and Bottom Halves Showing Instrumentation Lead Outs and Borescope Ports.

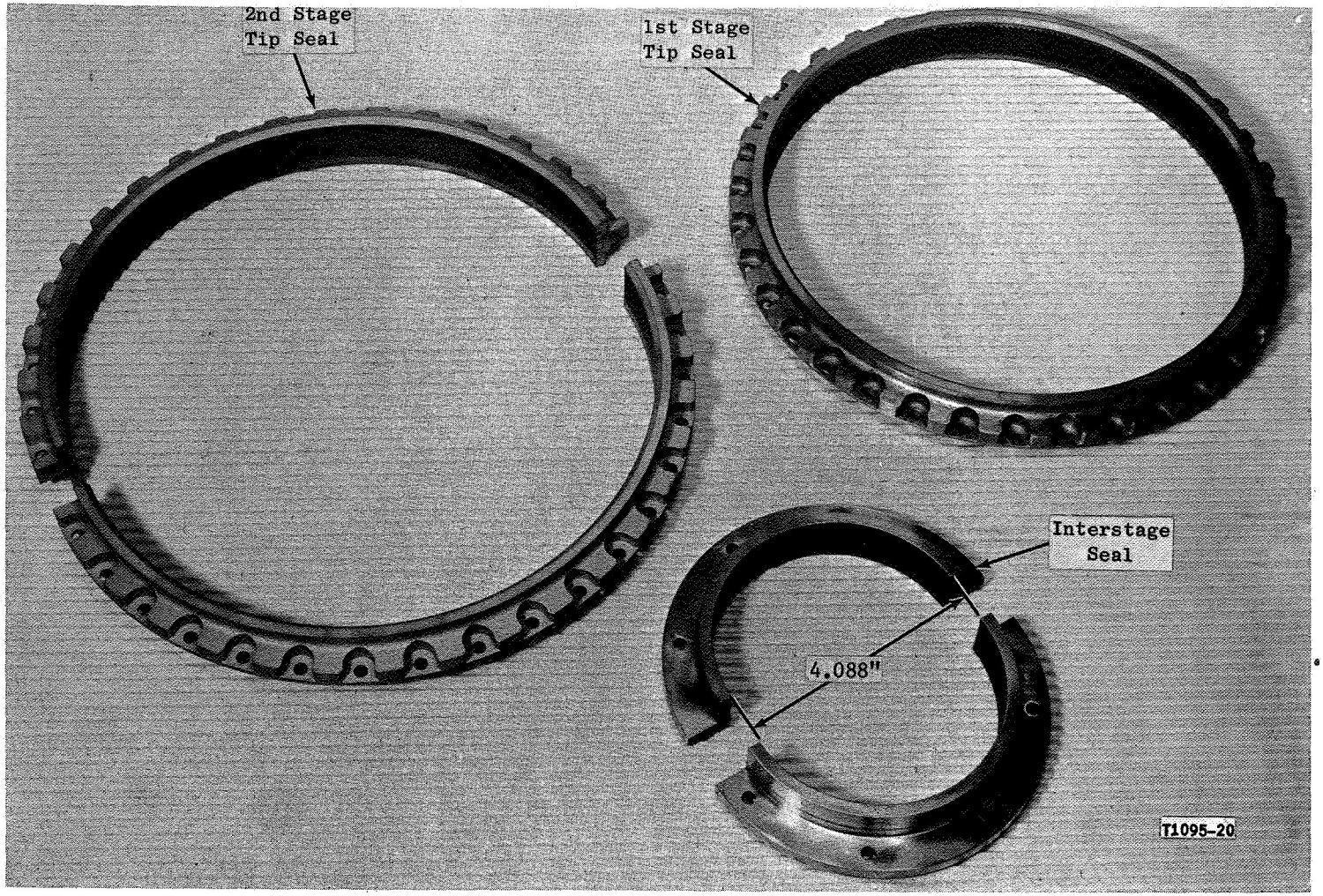


Figure 17. Turbine Rotor Honeycomb Tip Seals.

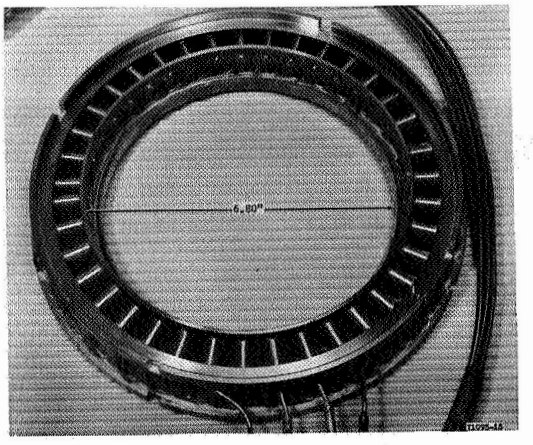


Figure 18. 1st Stage Nozzle Diaphragm (Leading Edge Face).

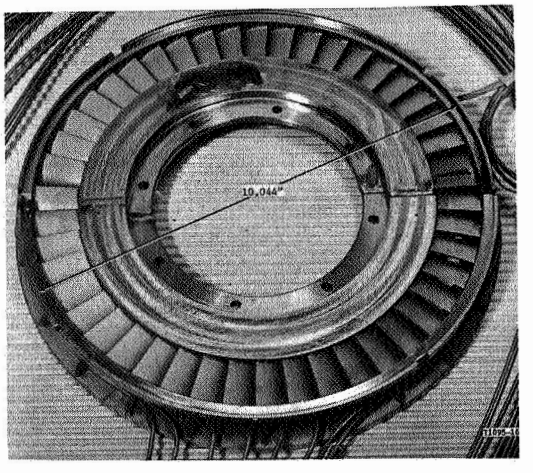


Figure 19. 2nd Stage Nozzle Diaphragm (Trailing Edge Face).

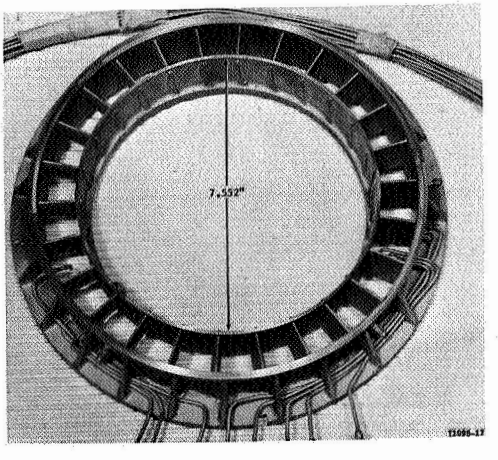
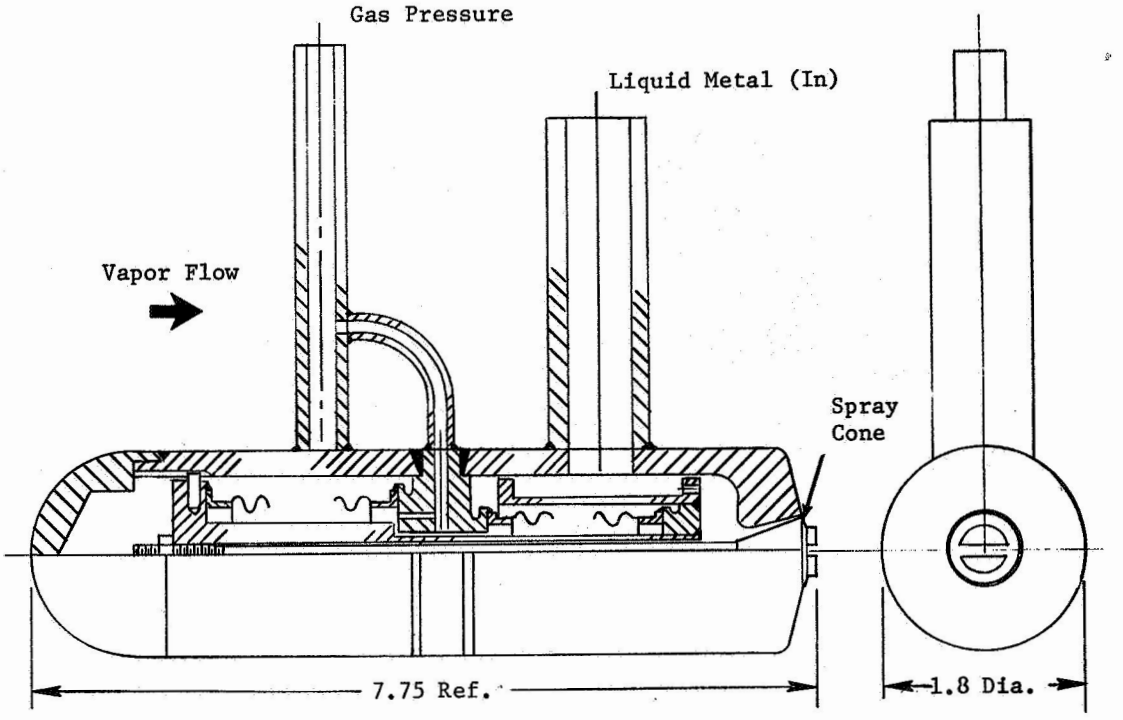


Figure 20. Outlet Guide Vane (Trailing Edge Face).



Figure 21. Turbine Exhaust Scroll.



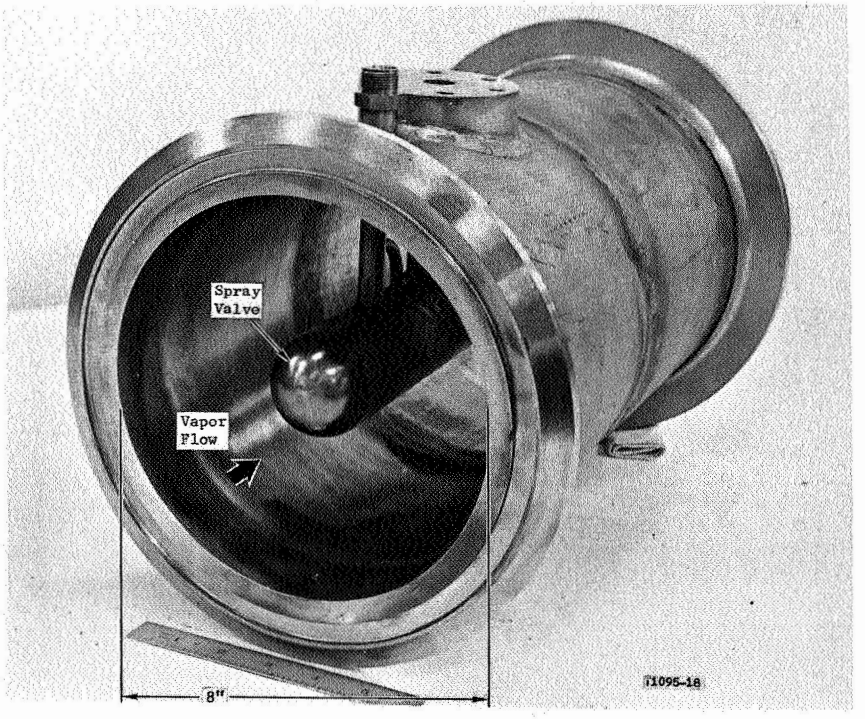


Figure 22. Inlet Duct Showing Installed Spray Valve.

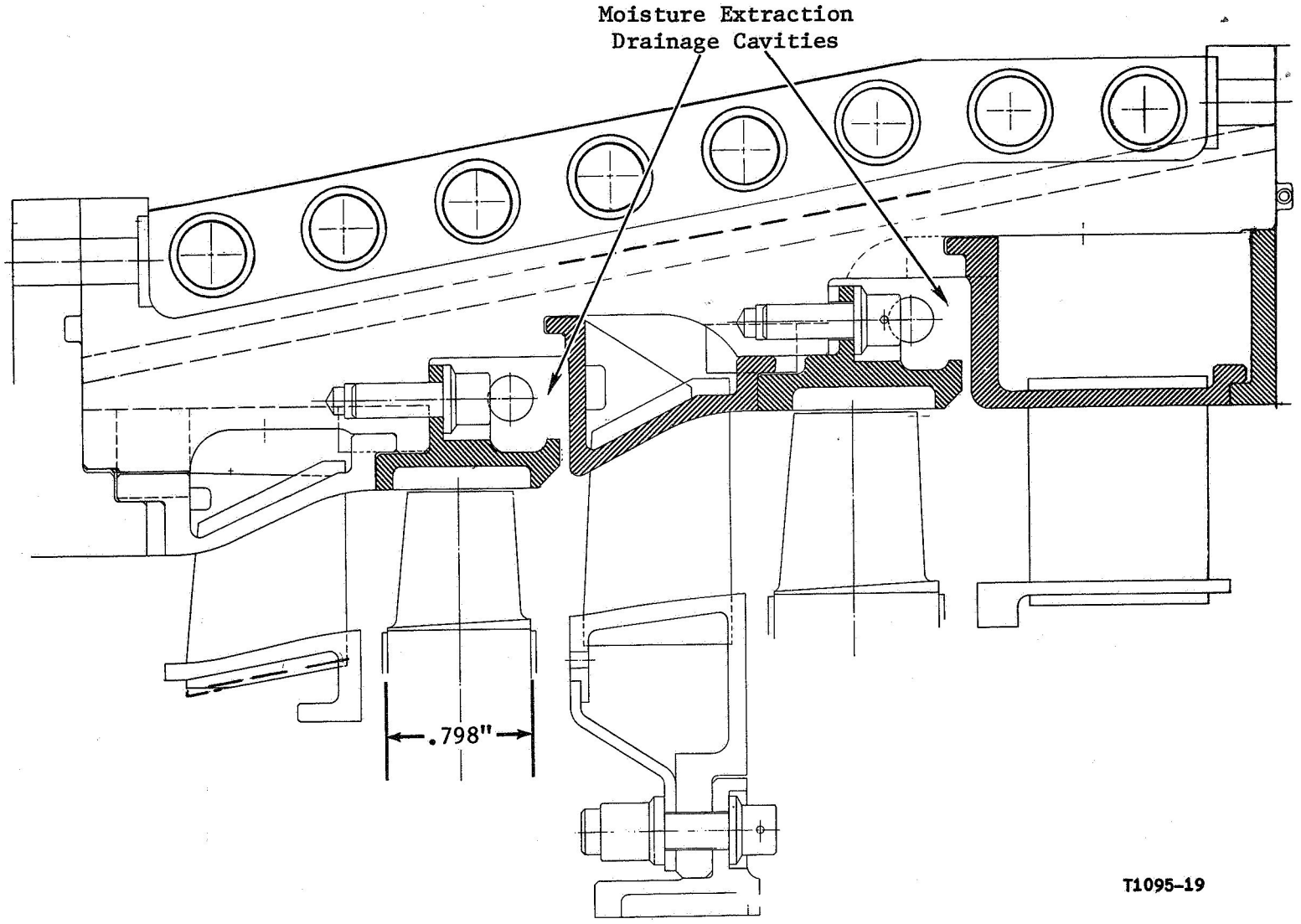


Figure 23. Turbine Casing Assembly Showing Moisture Extraction Geometry.

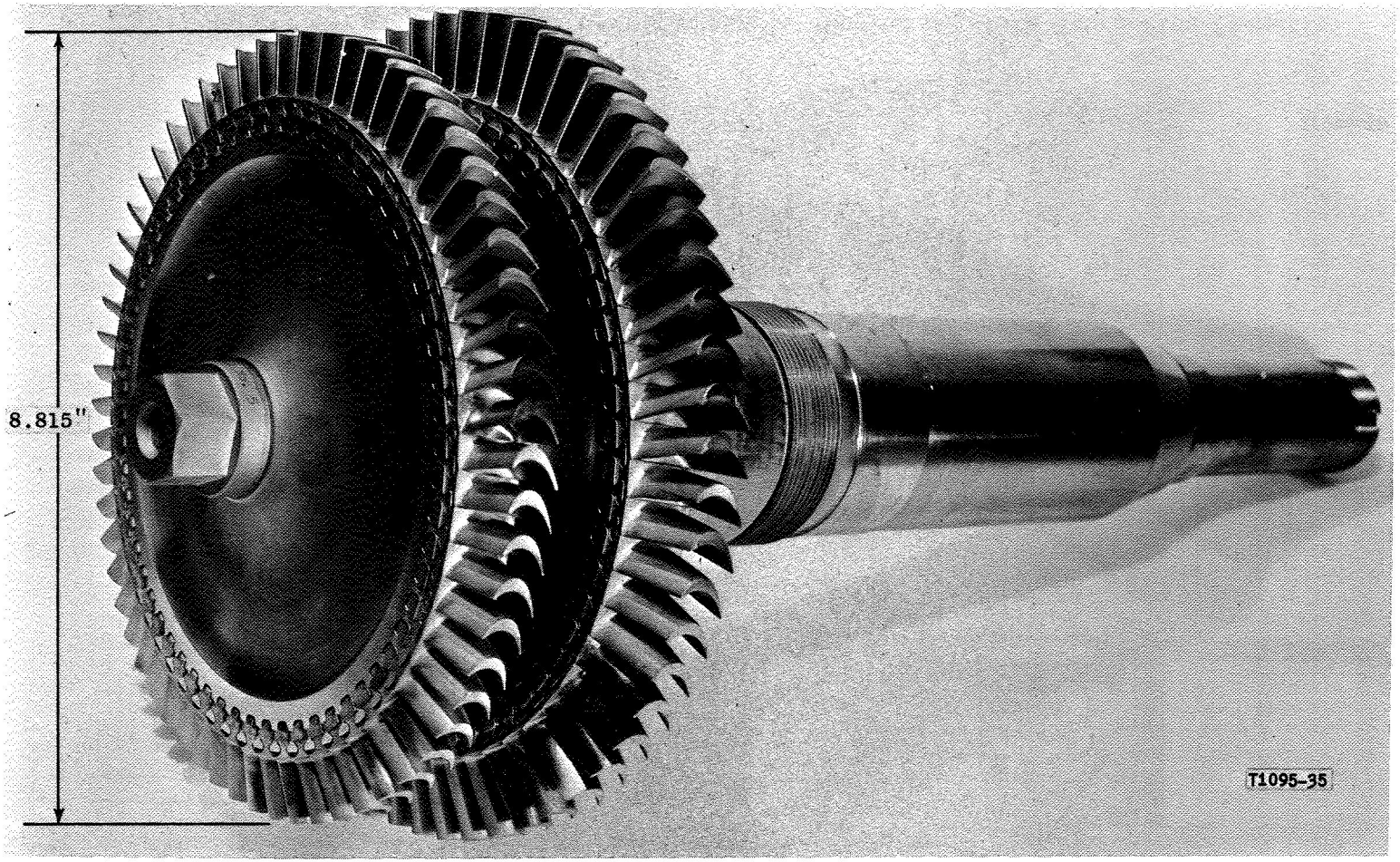


Figure 24. Turbine Rotor.

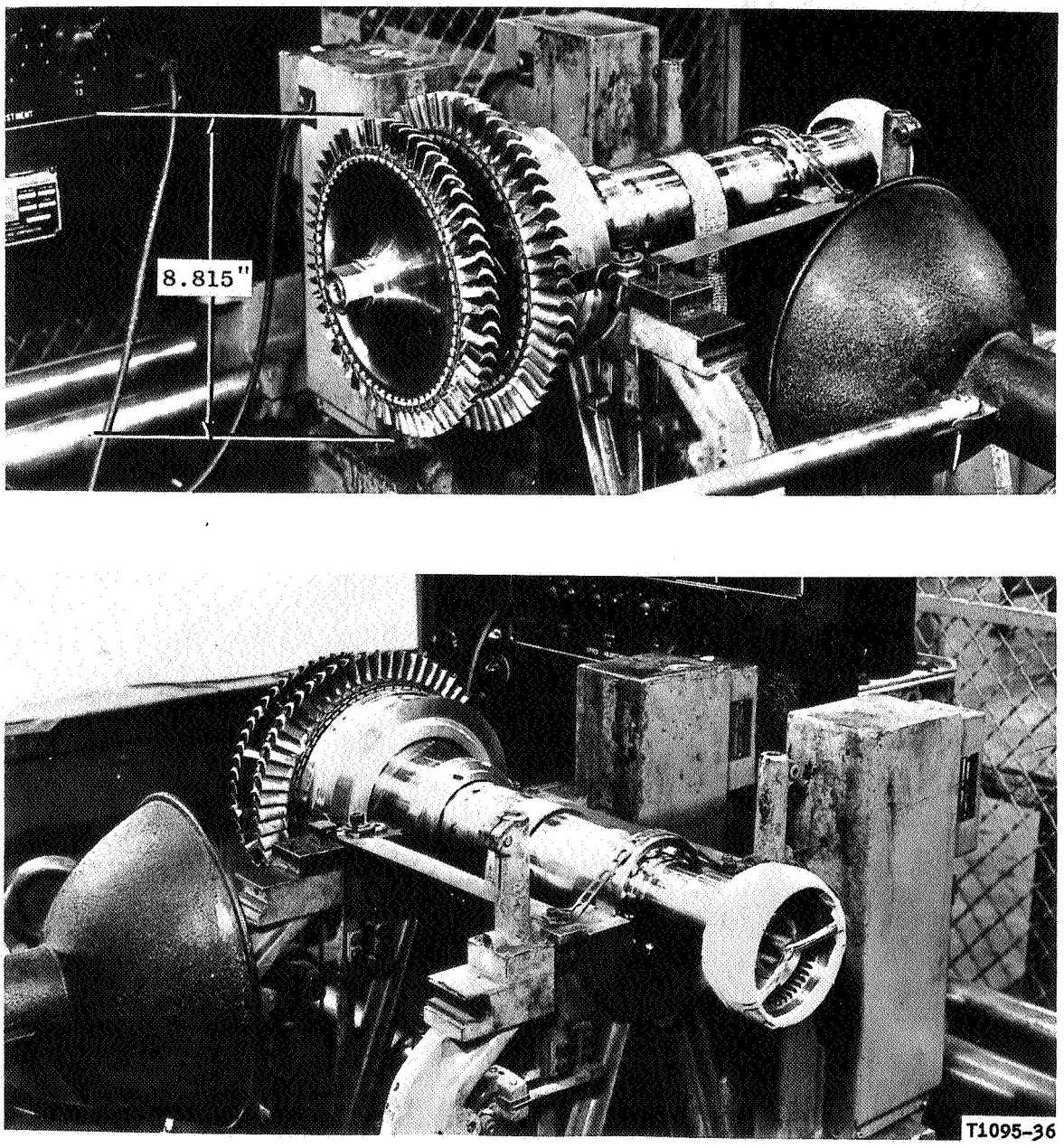


Figure 25. Turbine Rotor Shown In Balance Machine.

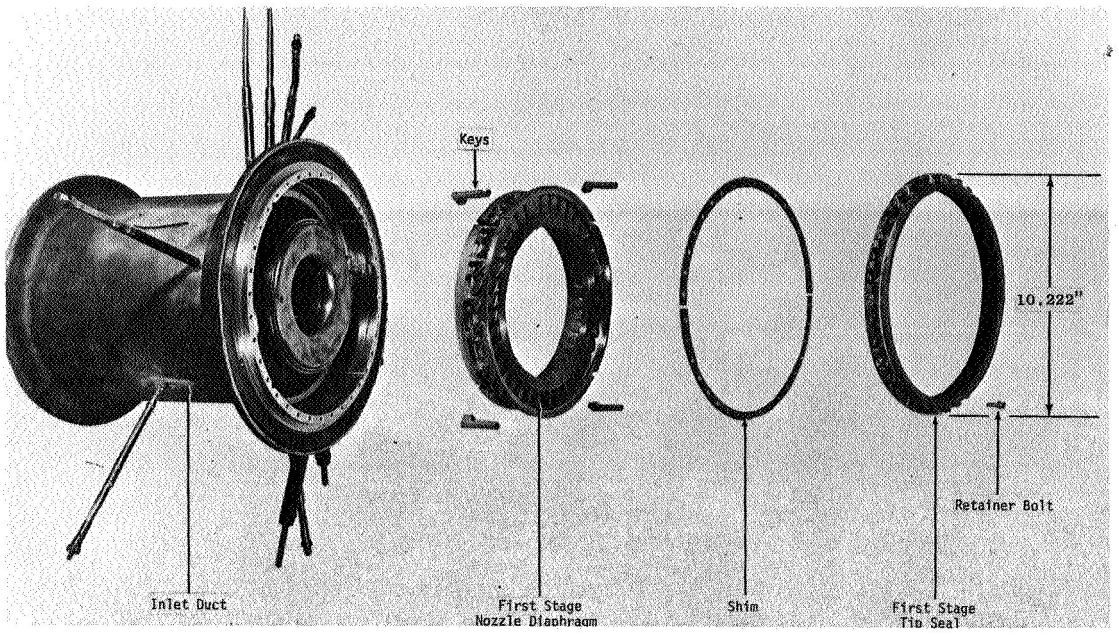


Figure 26a. Exploded View of Inlet Duct Assembly.

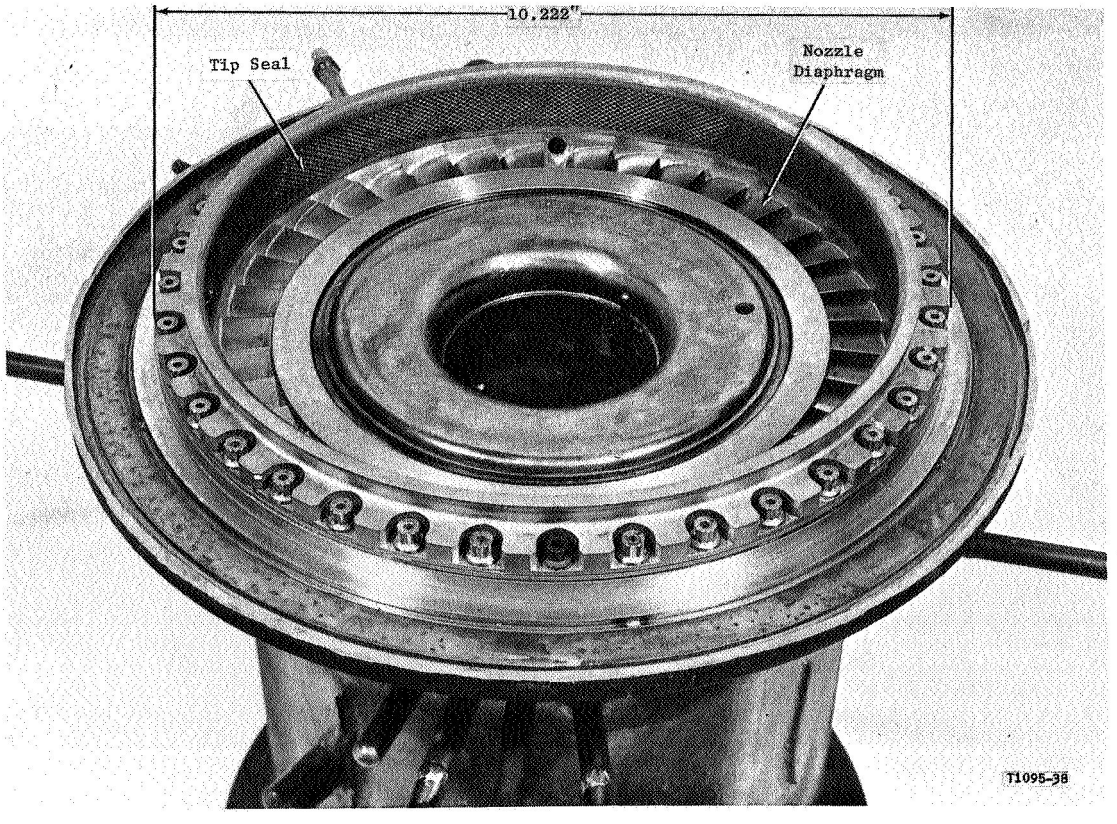


Figure 26b. Inlet Duct Showing Installed 1st Stage Nozzle Diaphragm and 1st Stage Tip Seal.

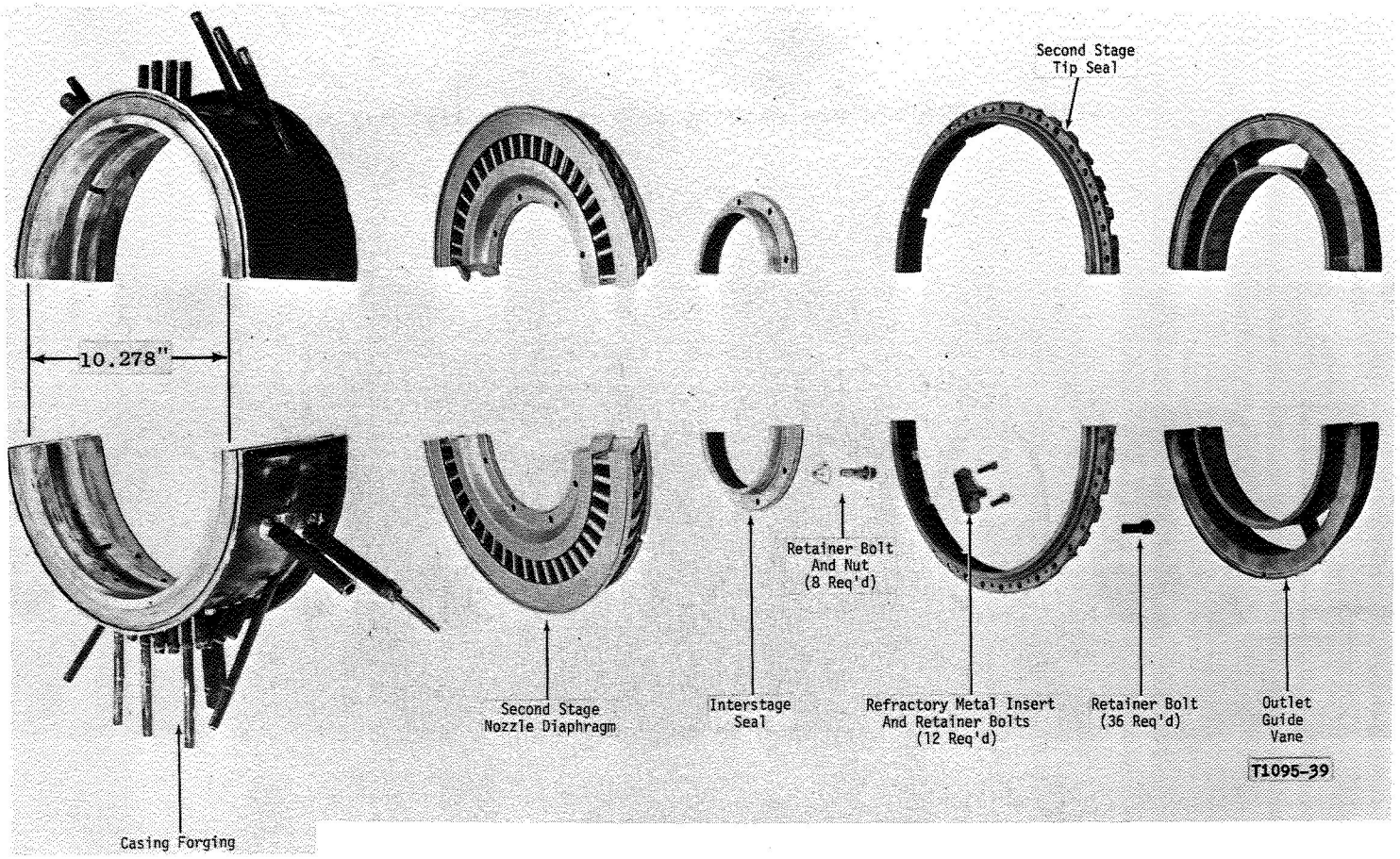


Figure 27. Exploded View of Turbine Casing Assembly.

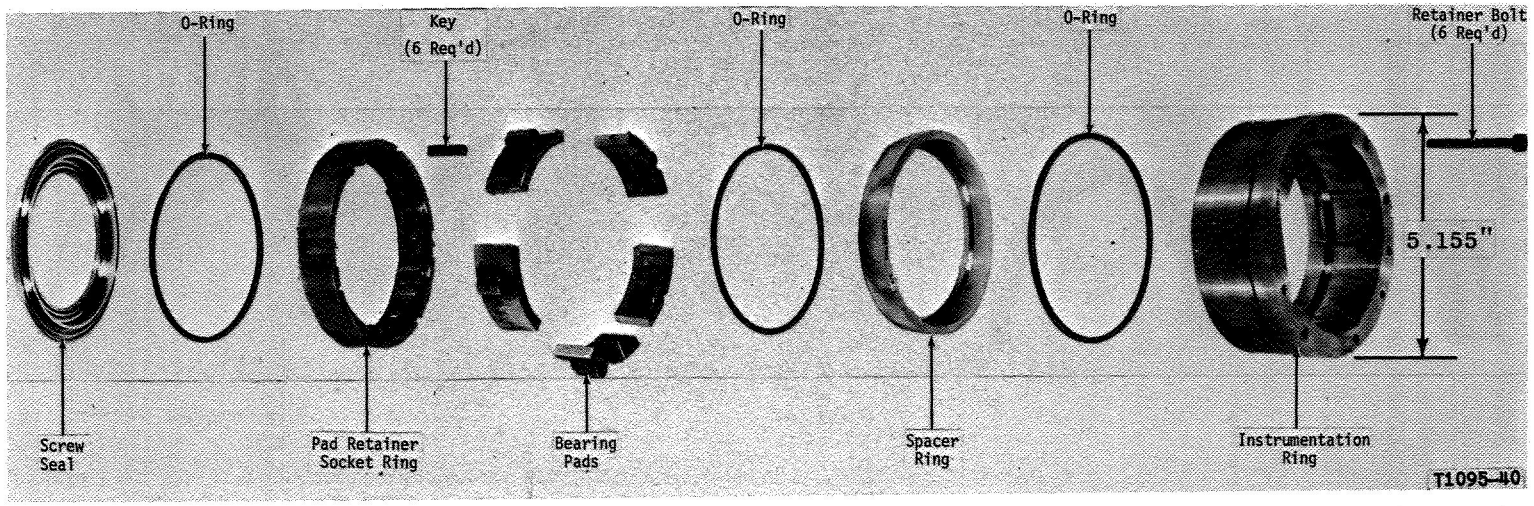


Figure 28. Exploded View of Turbine Pad Bearing Assembly.

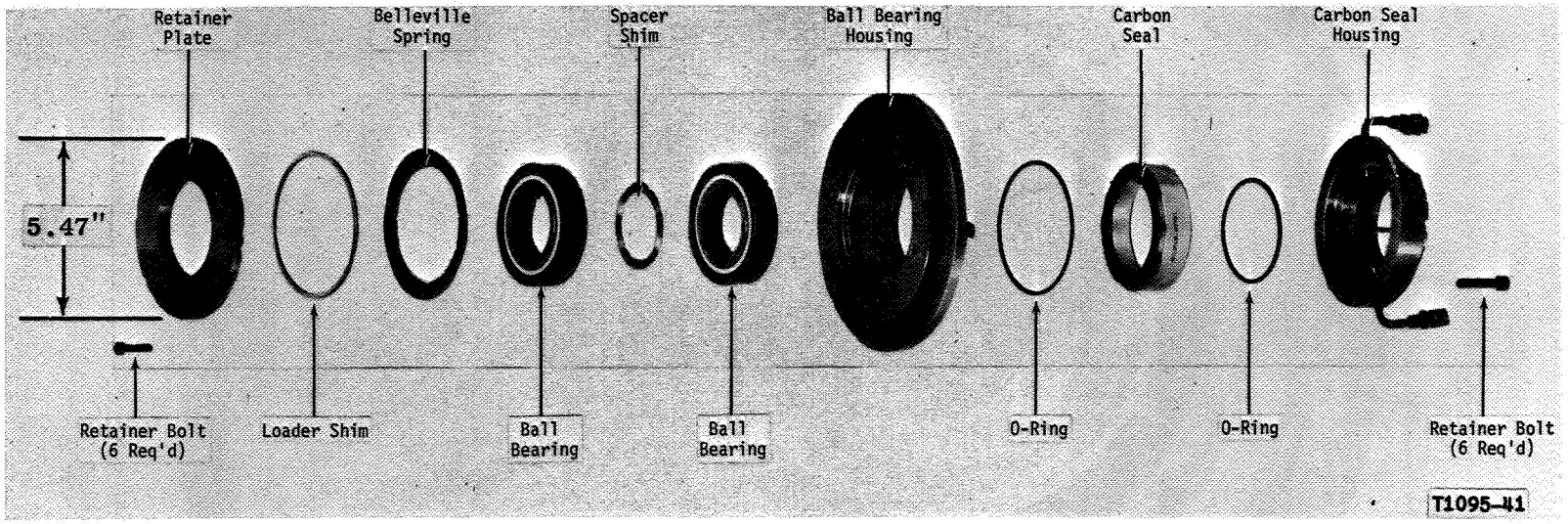


Figure 29. Exploded View of Turbine Ball Thrust Bearing Assembly.

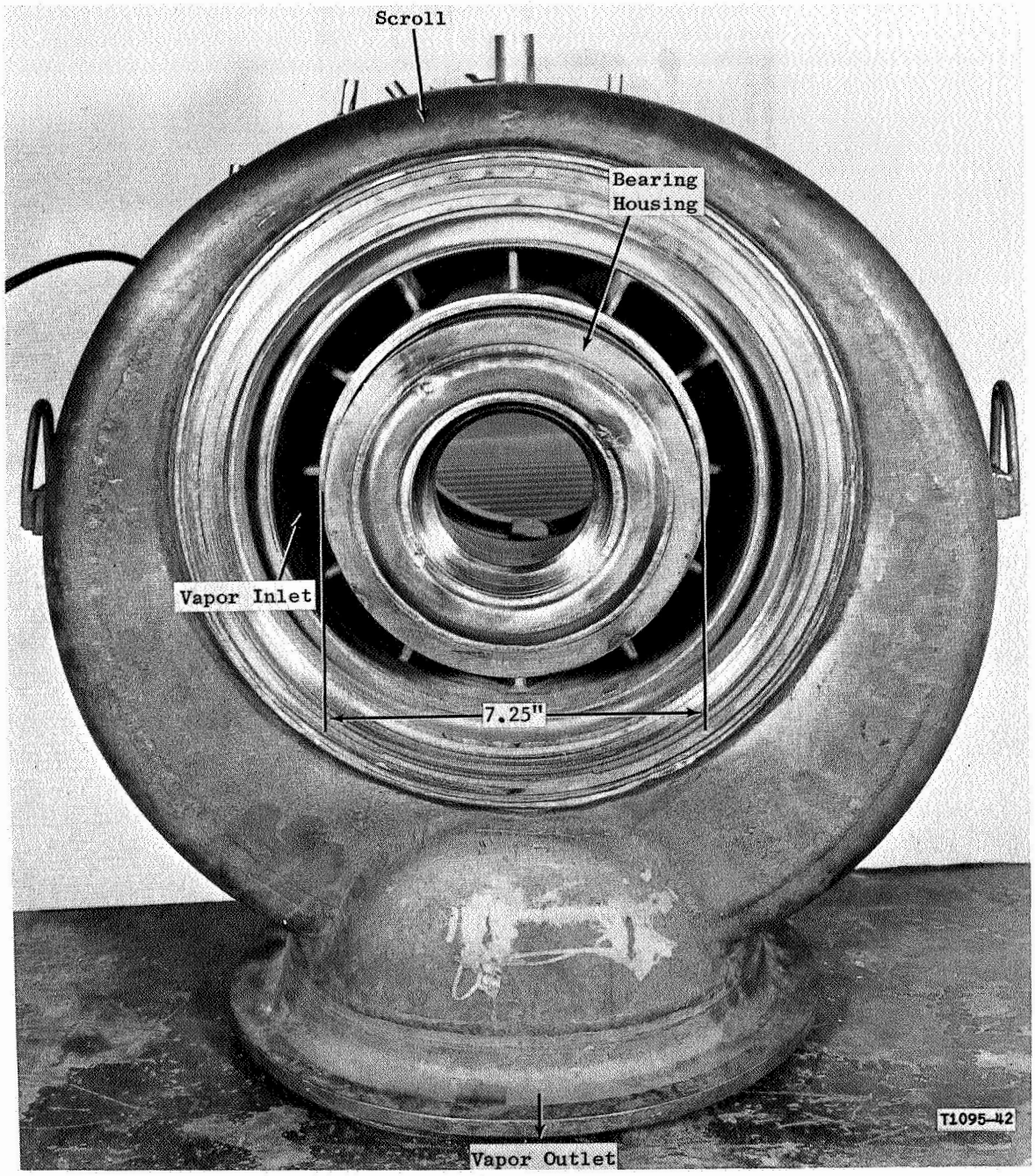


Figure 30. Turbine Exhaust Scroll with Bearing Housing Installed.

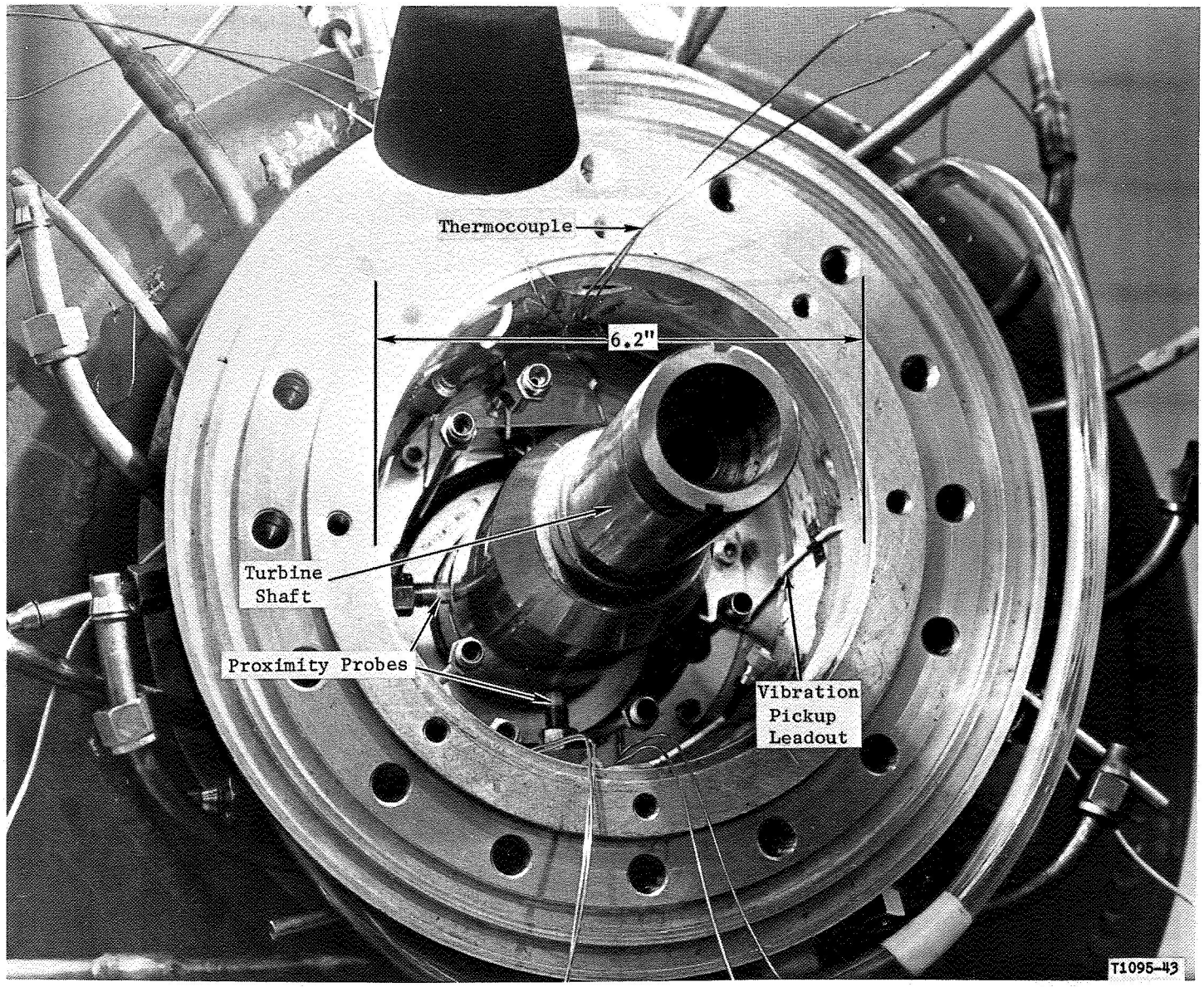


Figure 31. Rear View of Bearing Housing Showing Instrumentation.

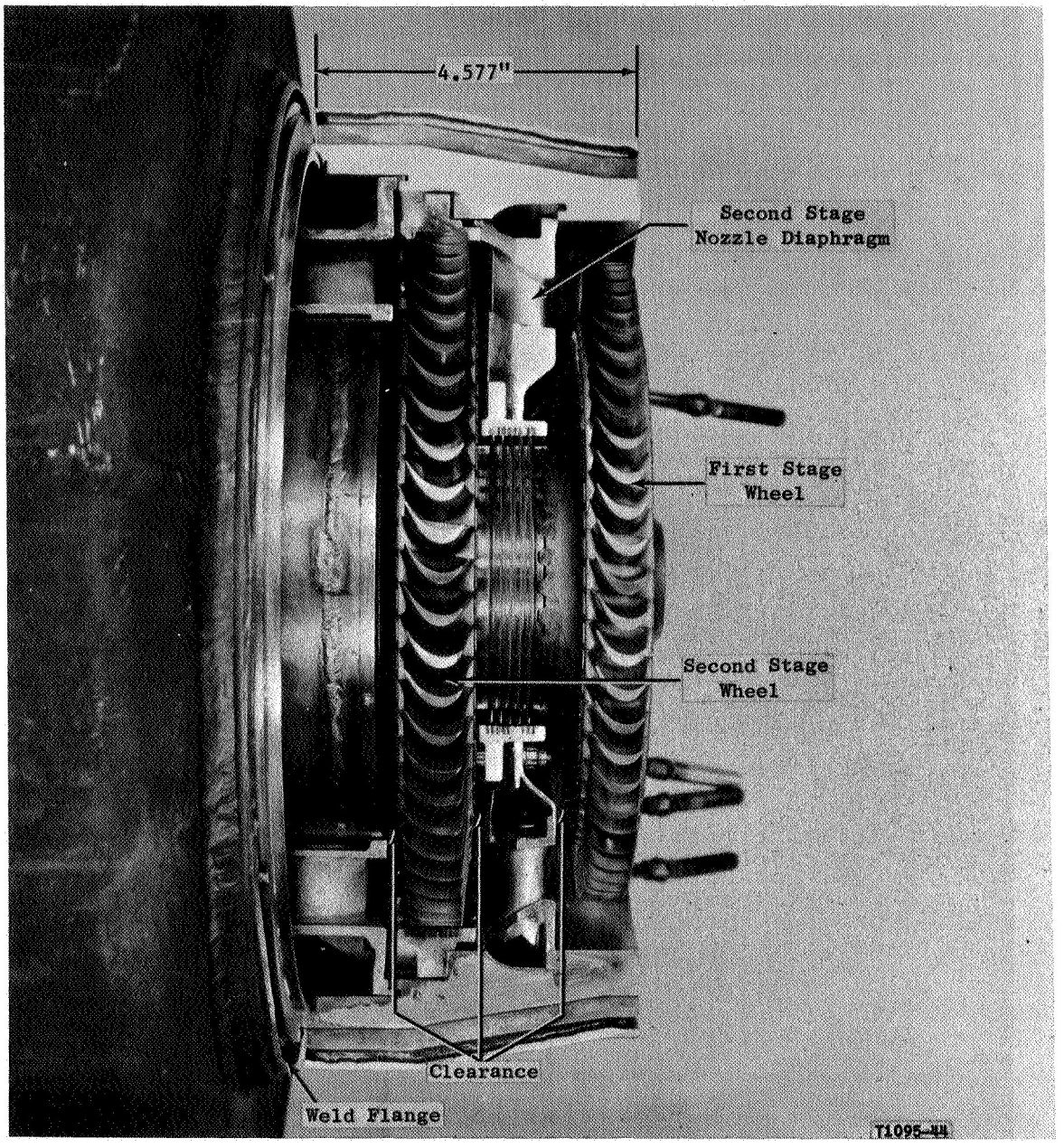
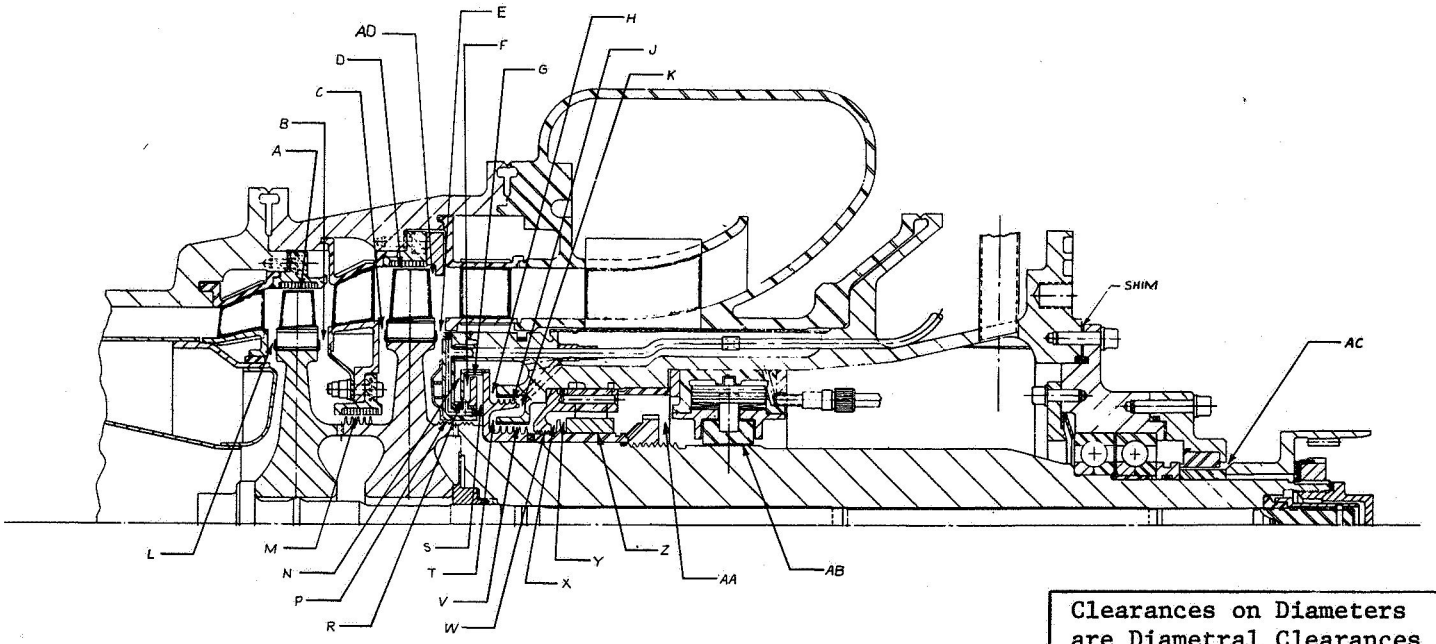


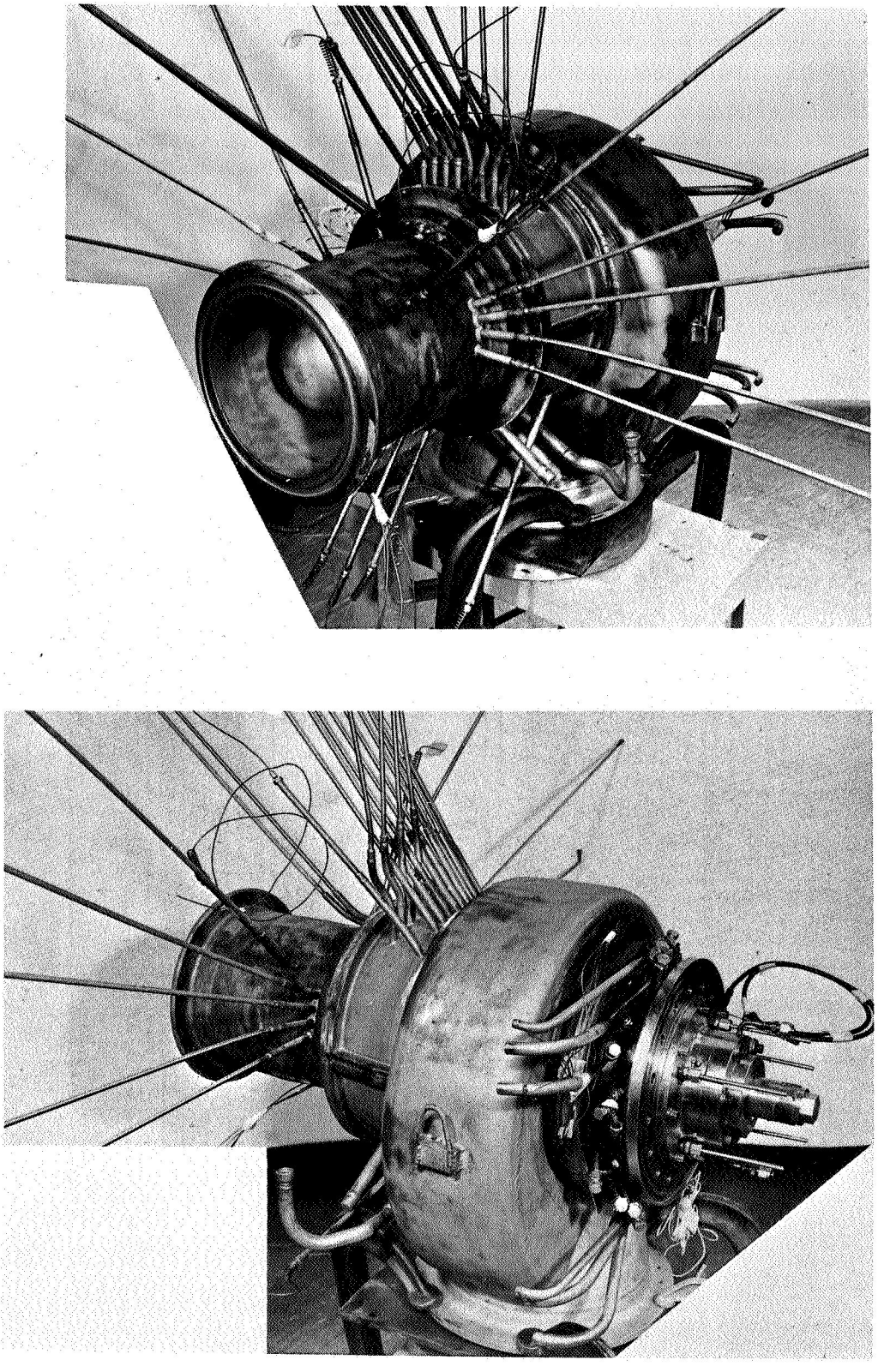
Figure 32. Partial Assembly of Turbine Rotor and Stator Showing Radial and Axial Clearances.



Clearances on Diameters are Diametral Clearances Unless Otherwise Specified (as in A and D)

BUILD-UP NO.	CLEARANCE DIMENSIONS																									
	A RAD	B	C	D RAD	E	F	G	H	J	K	L	M	N	P	R	S	T	V	W	X	Y	Z	AA	AB	AC	SHIM THK	AD
2	.031	.147	.181	.014	.170	.122	.026	.144	.012	.124	.174	.028	.052	.012	.070	.070	.141	.012	.007	.079	.108	.006	.194	—	—	.030	—
3	.031	.144	.182	.014	.166	.124	.026	.139	.017	.116	.175	.028	.045	.026	.070	.074	.139	.019	.014	.090	.098	.005	.146	—	.100	.054	—
4 COLD	.018 MIN	.163	.121	.018 MIN	.158	.186	.077	.155	.014	.132	.048	.017	.061	.024	.069	.075	.155	.016	.011	.077	.100	.0048	.149	.101	.095	.040	—
4 HOT	.034 MIN	.083	.197	.034 MIN	.158	.186	.077	.155	.014	.132	.146	.032	.061	.024	.069	.075	.155	.016	.011	.077	.100	.0048	.149	.101	.095	—	—
5 COLD	.018 MIN	.163	.121	.018 MIN	.158	.201	.077	.155	.014	.132	.068	.017	.049	.024	.069	.060	.155	.016	.011	.077	.100	.0048	—	—	.095	.040	—
5 HOT	.034 MIN	.083	.197	.034 MIN	.158	.201	.077	.155	.014	.132	.146	.032	.049	.024	.069	.060	.155	.016	.011	.077	.100	.0048	—	—	.095	—	—
6 COLD	.023 MIN	.188	.109	.023 MIN	.180	.170	.077	.138	.013	.110	.136	.023	.080	.016	.069	.078	.138	.016	.012	.085	.096	.0051	—	—	.095	.031	.169
6 HOT	.039 MIN	.108	.185	.039 MIN	.180	.170	.077	.138	.013	.110	.214	.038	.080	.016	.069	.078	.138	.016	.012	.085	.096	.0051	—	—	.095	—	.093
7 COLD	.023 MIN	.188	.109	.023 MIN	.180	.170	.077	.138	.013	.110	.136	.023	.080	.016	.069	.078	.138	.016	.012	.085	.096	.0051	—	—	.095	.031	.169
7 HOT	.039 MIN	.108	.189	.039 MIN	.180	.170	.077	.138	.013	.110	.214	.038	.080	.016	.069	.078	.138	.016	.012	.085	.096	.0051	—	—	.095	—	.093

Figure 33. Cross Section of Turbine with Tabulated Clearance Dimensions. T1095-46



T1095-47

Figure 34. Assembled Turbine Ready for Installation into Test Facility.

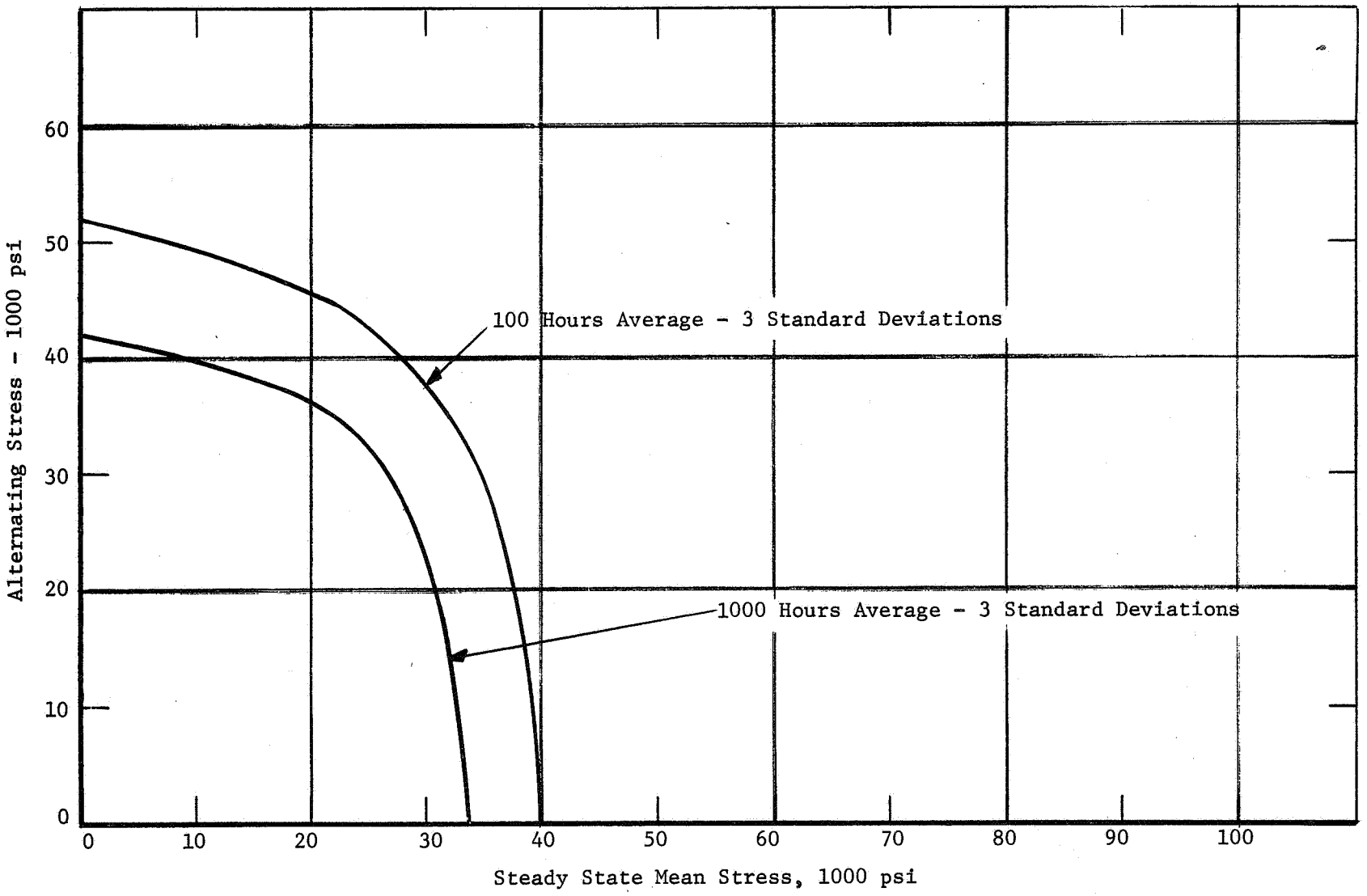


Figure 35a. Goodman Diagram for U-700 at 1500°F.

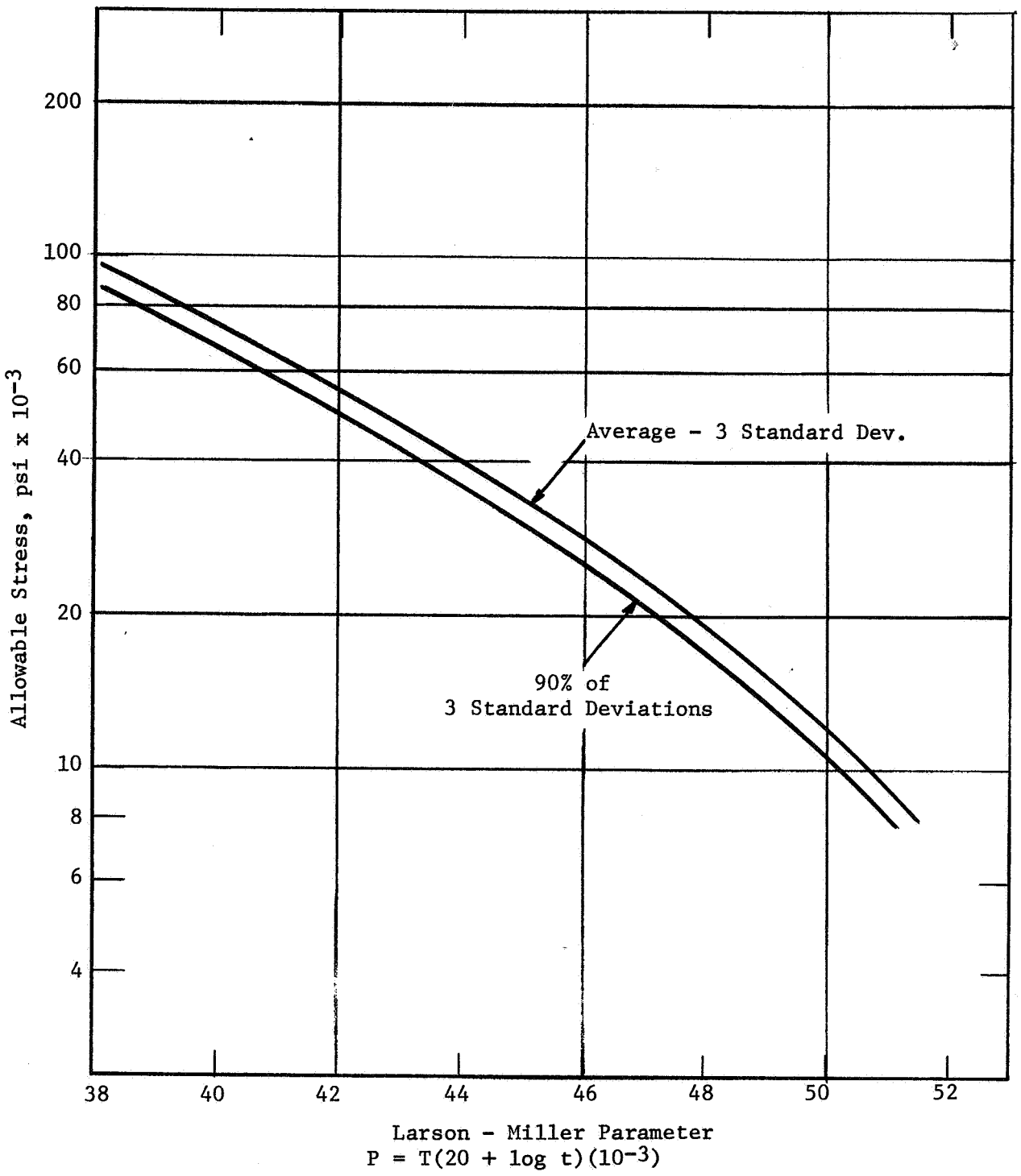
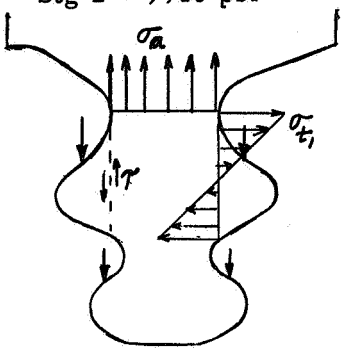


Figure 35b. Master Rupture Strength of U-700 Forging.

DOVETAIL STRESSES

BLADE
Airfoil root Stress
Stg 1 = 6950 psi
Stg 2 = 9940 psi



σ_a = Dovetail neck stress

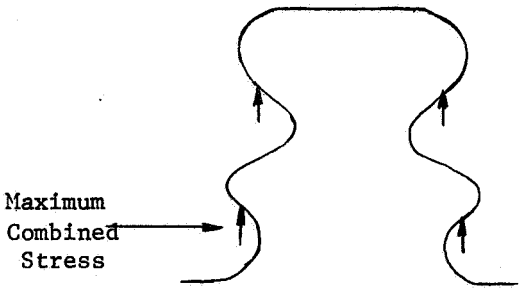
σ_t = Tang bending stress (hook stress)

τ = Tang shear stress

σ_c = Combined stress at dovetail fillet

Stresses may be modified for various speeds by multiplying given values by the factor

$$\frac{(\text{new rpm})^2}{(19{,}200\ \text{rpm})^2}$$



RPM = 19, 200

STAGE I DOVETAIL STRESSES

U-700 Blades				
Stress (psi)	Blade Dovetail		Wheel Dovetail	
	Top Tang	Bottom Tang	Top Tang	Bottom Tang
σ_t	15, 380	12, 150	12, 210	21, 060
σ_a	10, 500	6, 420	15, 260	15, 290
τ	8, 150	5, 870	5, 170	6, 900
σ_c	23, 280	16, 920	24, 160	32, 600

STAGE 2 DOVETAIL STRESSES

Stress (psi)	Blade Dovetail		Wheel Dovetail			
	U-700 Blades		U-700 Blades		Refractory Metal Blades	
	Top Tang	Bottom Tang	Top Tang	Bottom Tang	Top Tang	Bottom Tang
σ_t	19, 500	15, 470	15, 790	27, 090	20, 320	34, 850
σ_a	14, 330	8, 640	14, 380	16, 230	17, 760	20, 630
τ	10, 170	7, 730	6, 550	9, 850	6, 400	9, 100
σ_c	30, 330	21, 900	26, 800	39, 220	33, 880	50, 250

T1095-37

Figure 35c. Turbine Blade and Wheel Dovetail Stresses During 19,200 RPM Operation.

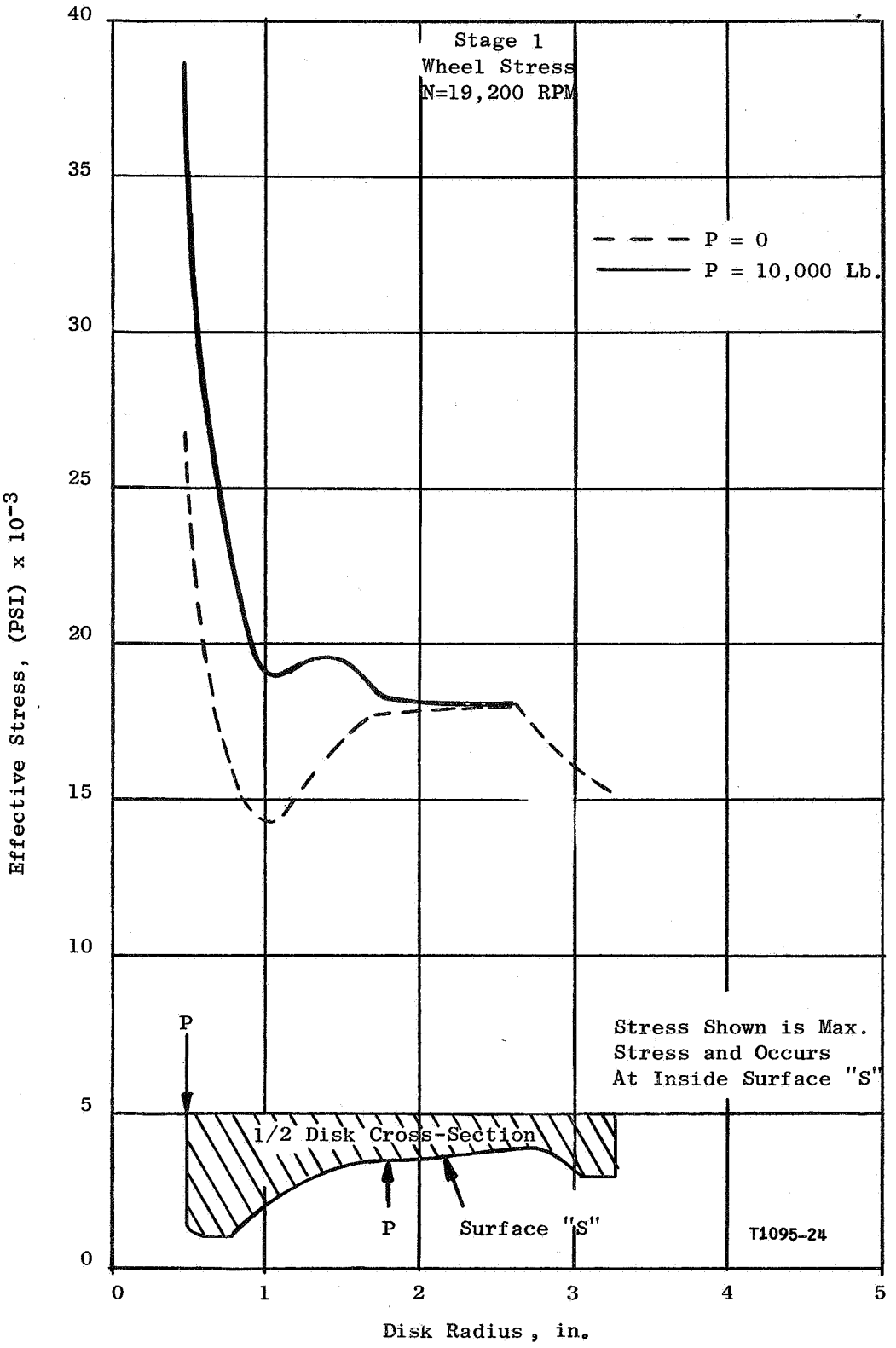


Figure 36. Stage 1 Wheel Stress Distribution During 19,2000 RPM Operation.

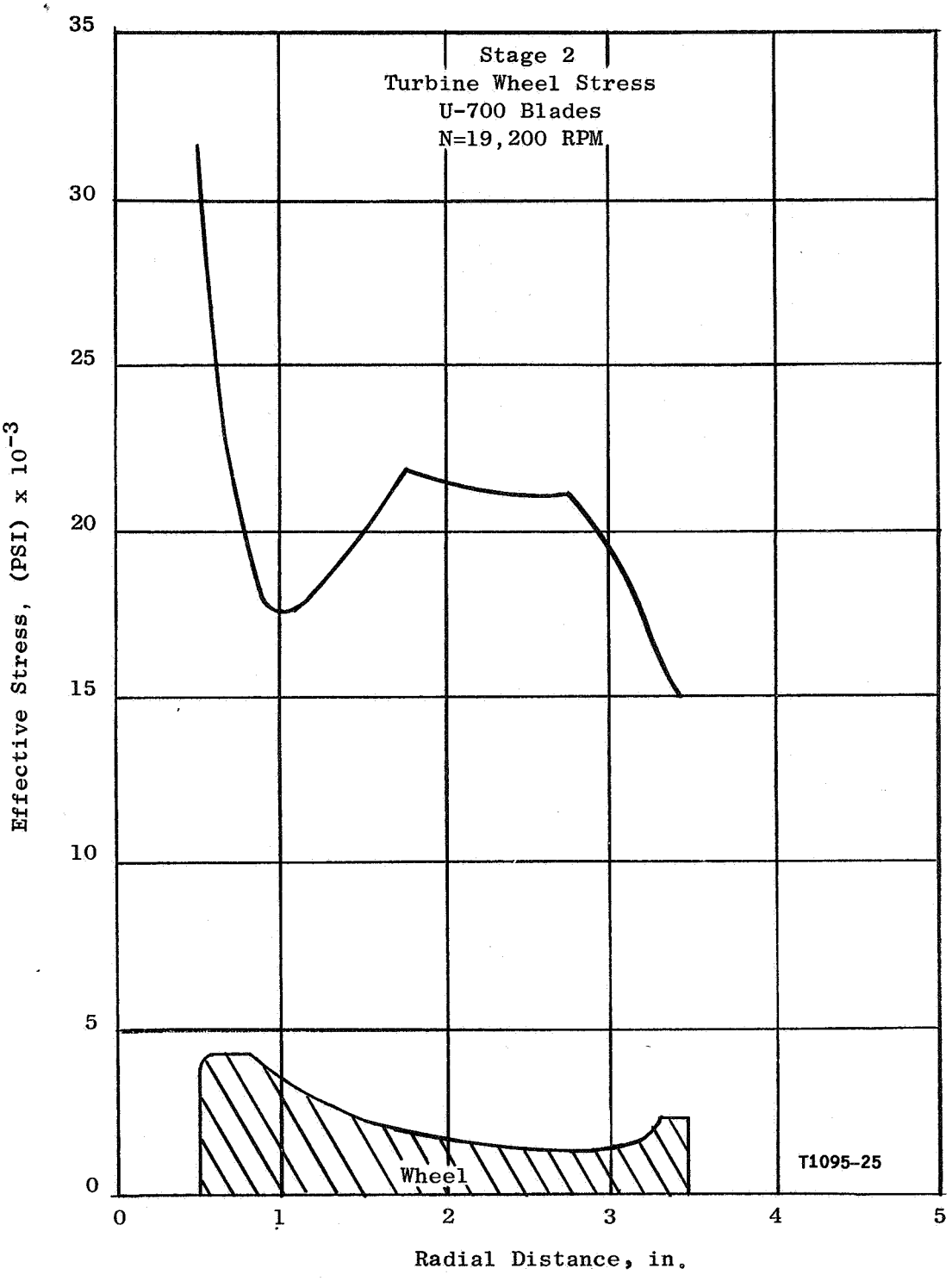


Figure 37. Stage 2 Wheel Stress Distribution During 19,200 RPM Operation.

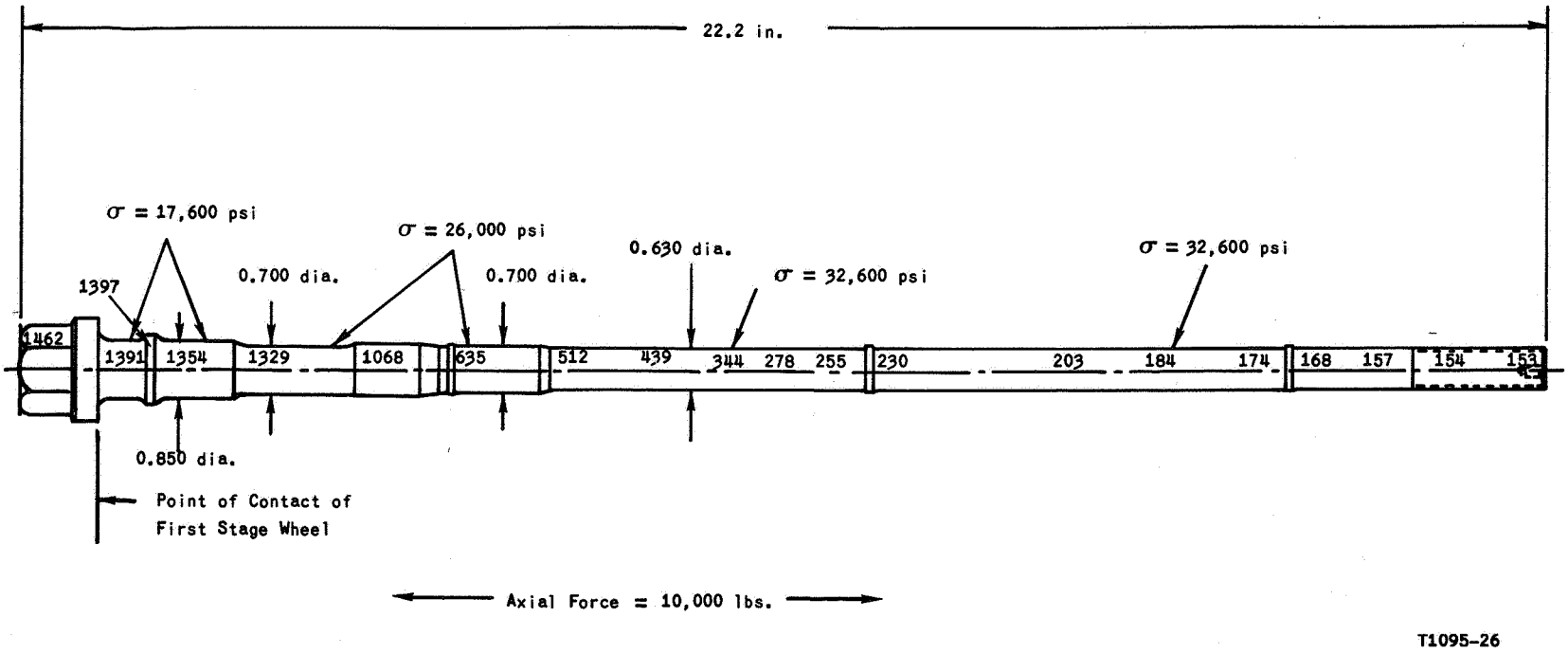
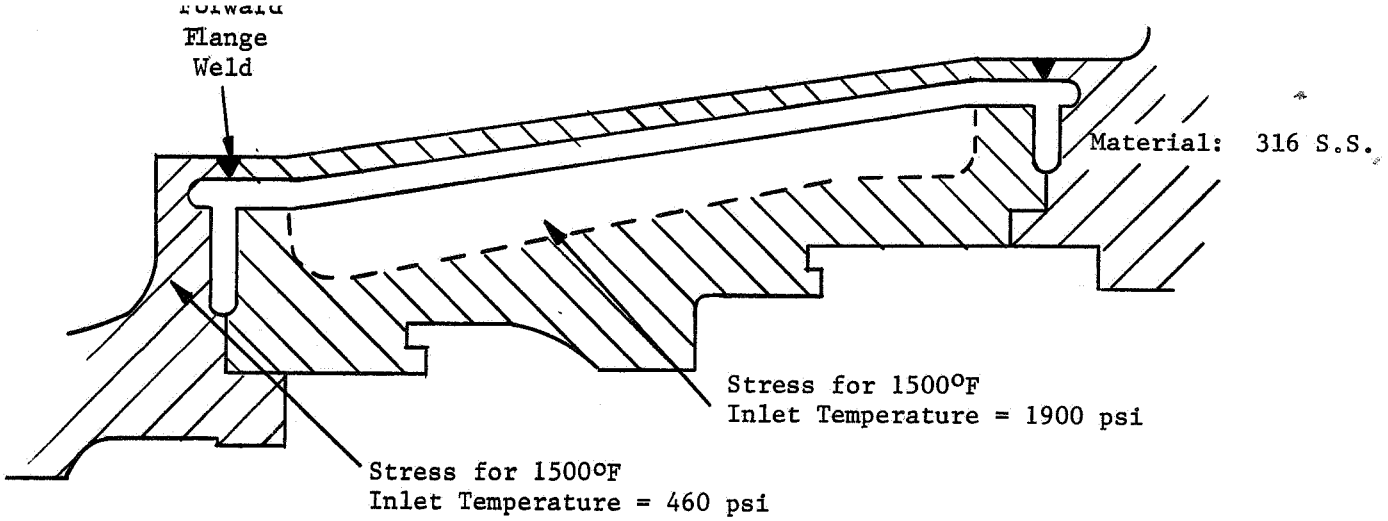


Figure 38. Tie Bolt Showing the Maximum Temperature and Stress Distribution.



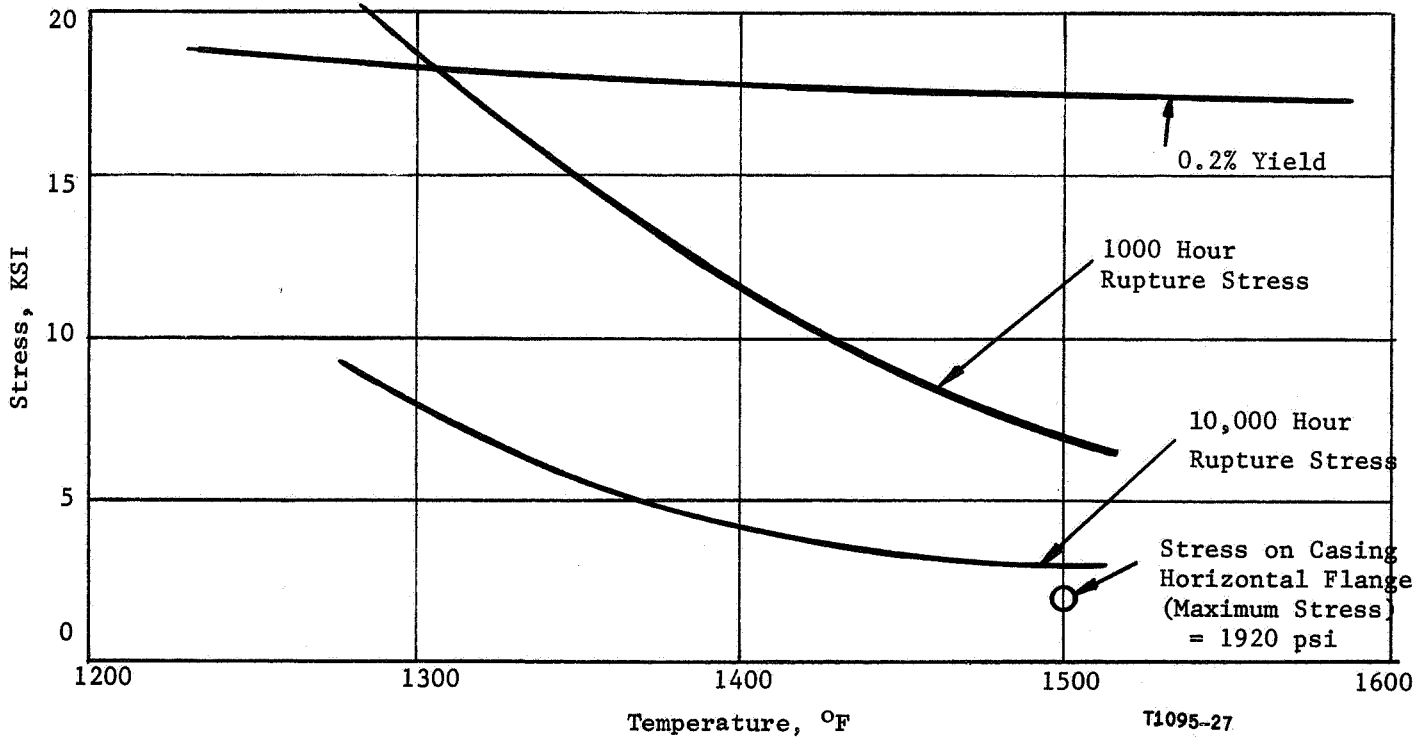


Figure 39. Turbine Casing Stress Distribution.

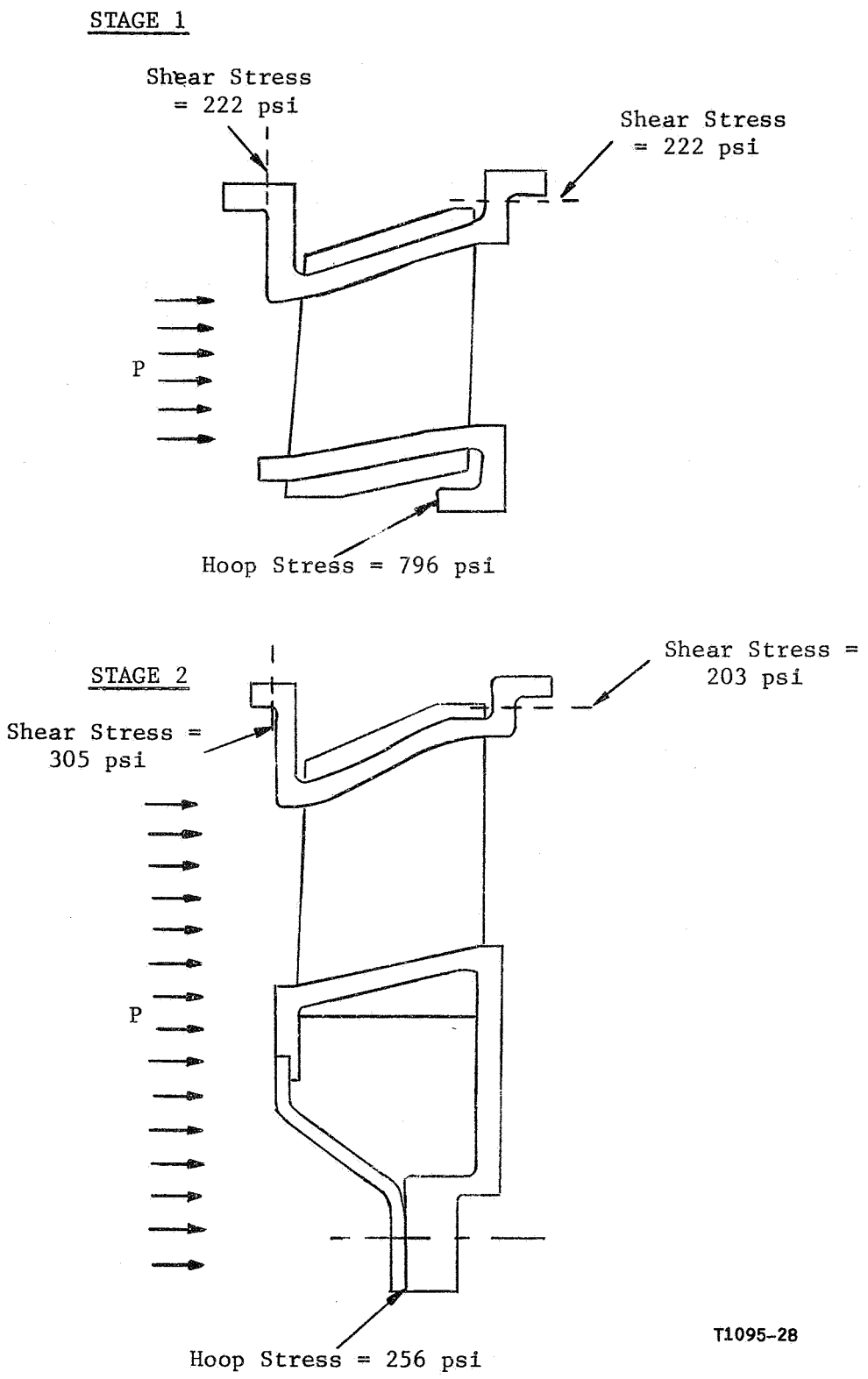


Figure 40. Stresses in Nozzle Diaphragms.

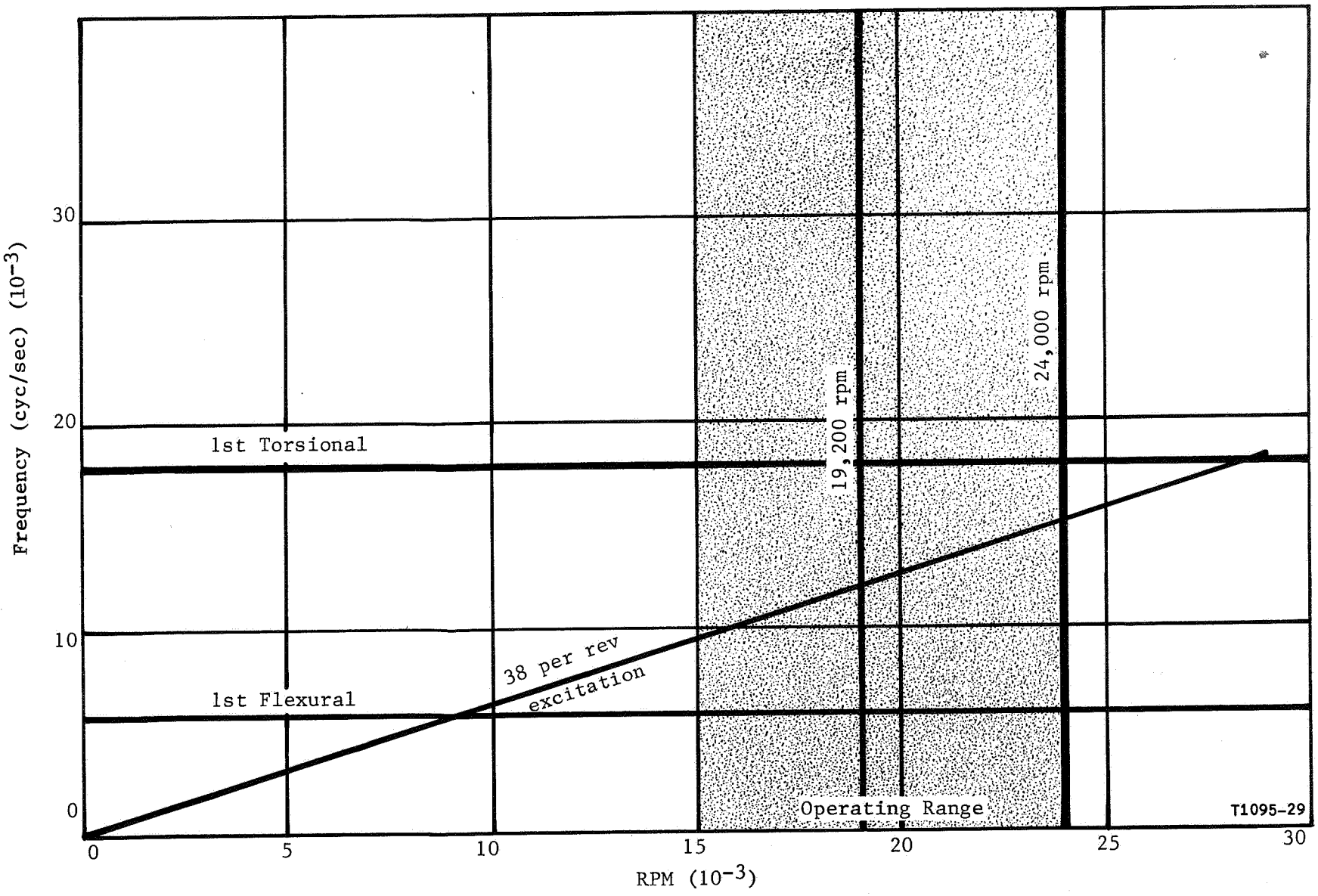


Figure 41. Stage 1 Blade Excitation and Natural Frequency Range.

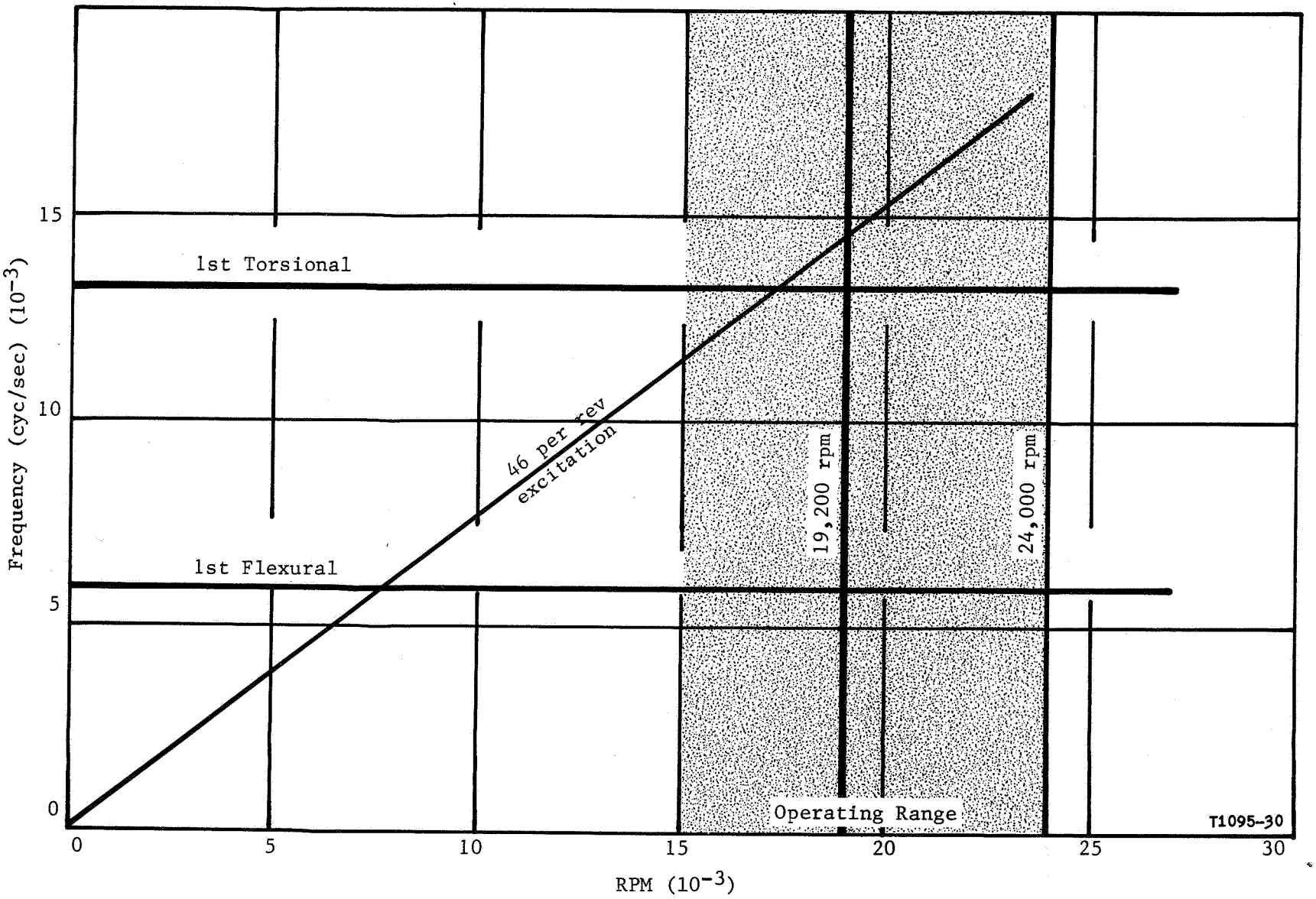
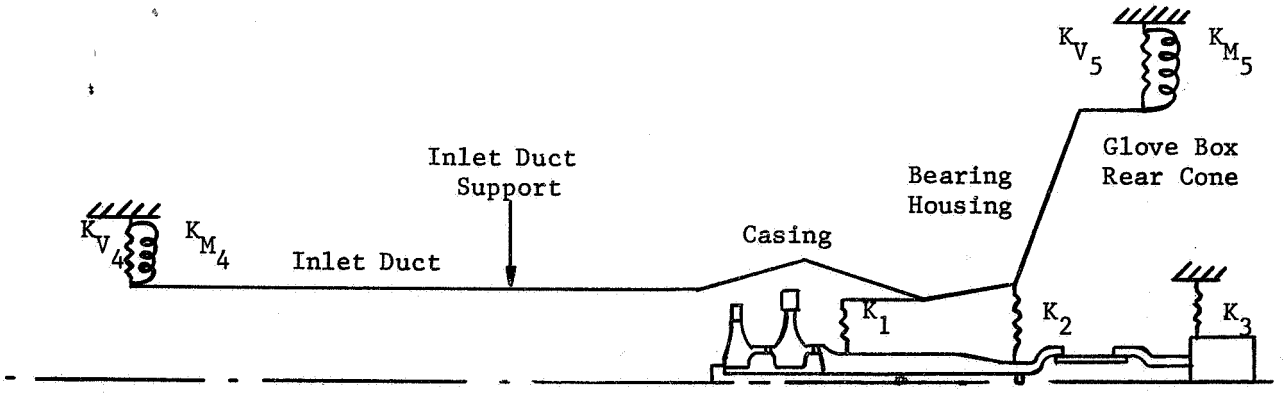
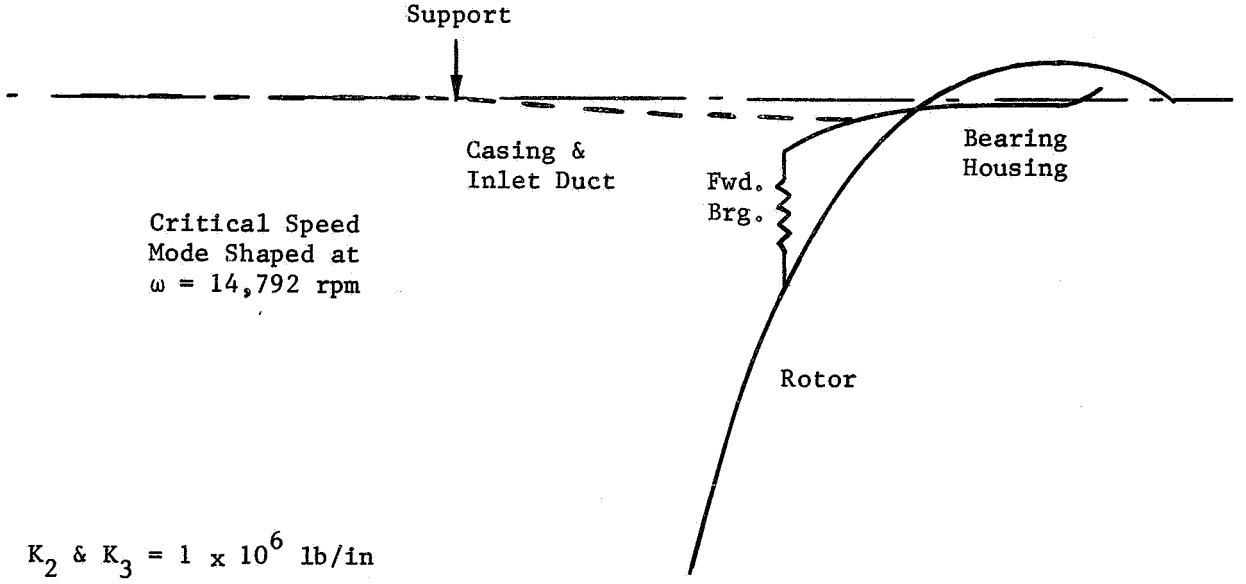


Figure 42. Stage 2 Blade Excitation and Natural Frequency Range.



Physical Model For Critical Speed Analysis



K_2 & K_3 = 1 x 10^6 lb/in

SPRING 1	SPRING 4		SPRING 5		SPRING 6		CRITICAL SPEED (RPM)
K_{V_1}	K_{V_4}	K_{M_4}	K_{V_5}	K_{M_5}	K_{V_6}	K_{V_6}	
0.5 x 10^6	∞	1 x 10^4	∞	∞	∞	∞	1. 14,792 2. 33,830 3. 44,735

T1095-31

Figure 43a. Two Stage Turbine Installed Resonant Frequency Survey.

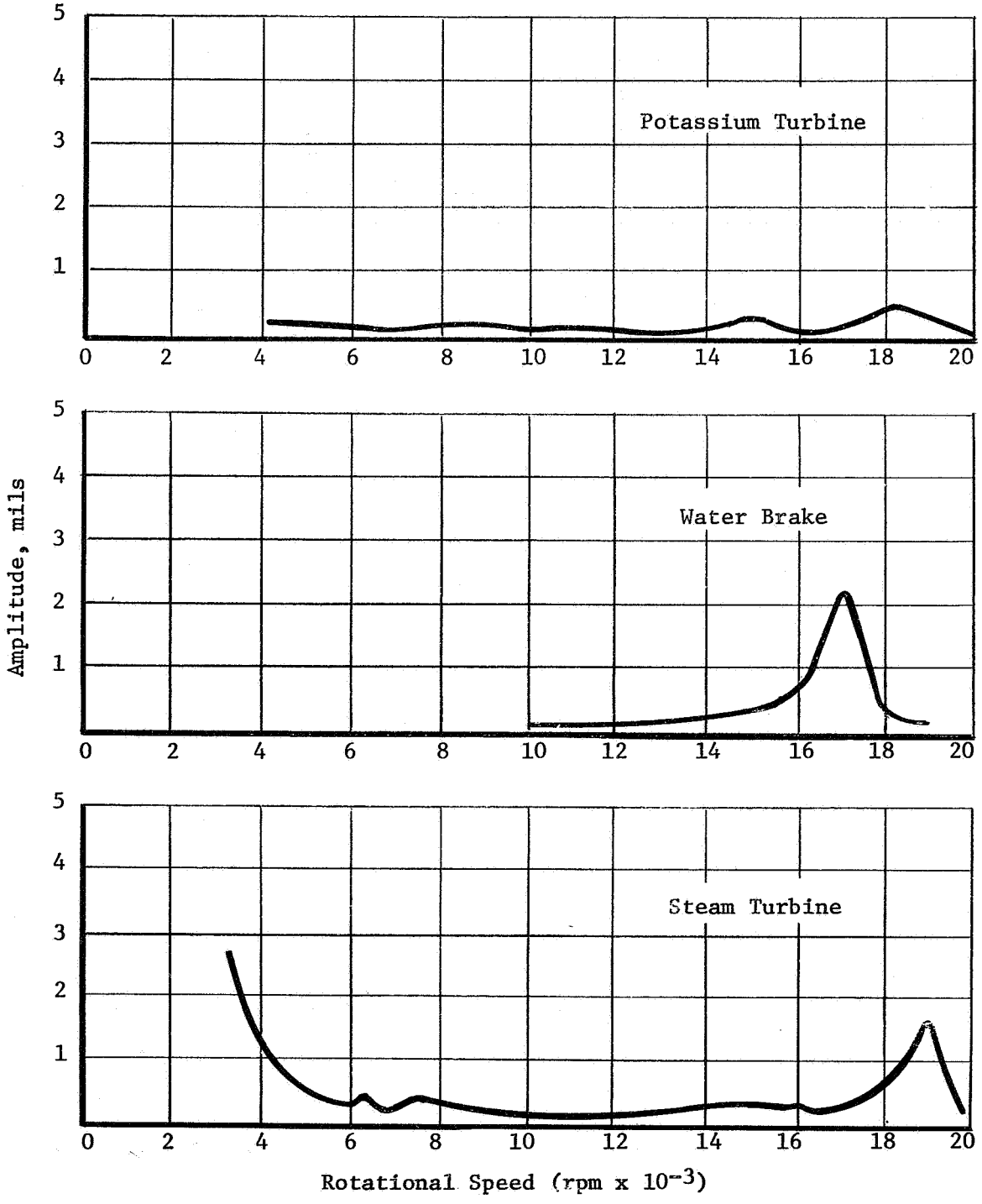


Figure 43b. Measured Vibratory Amplitudes of Major Test Rig Components.

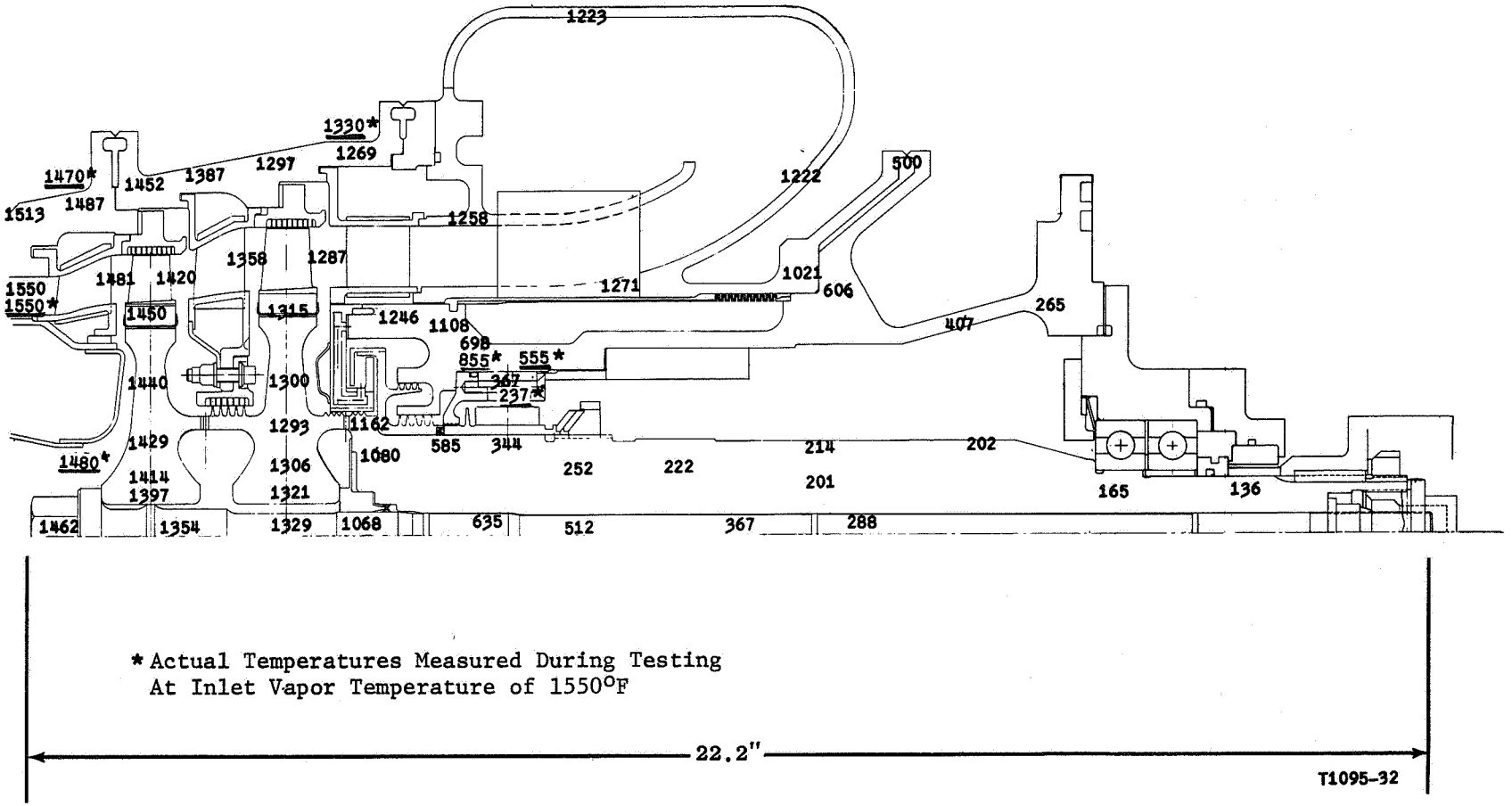
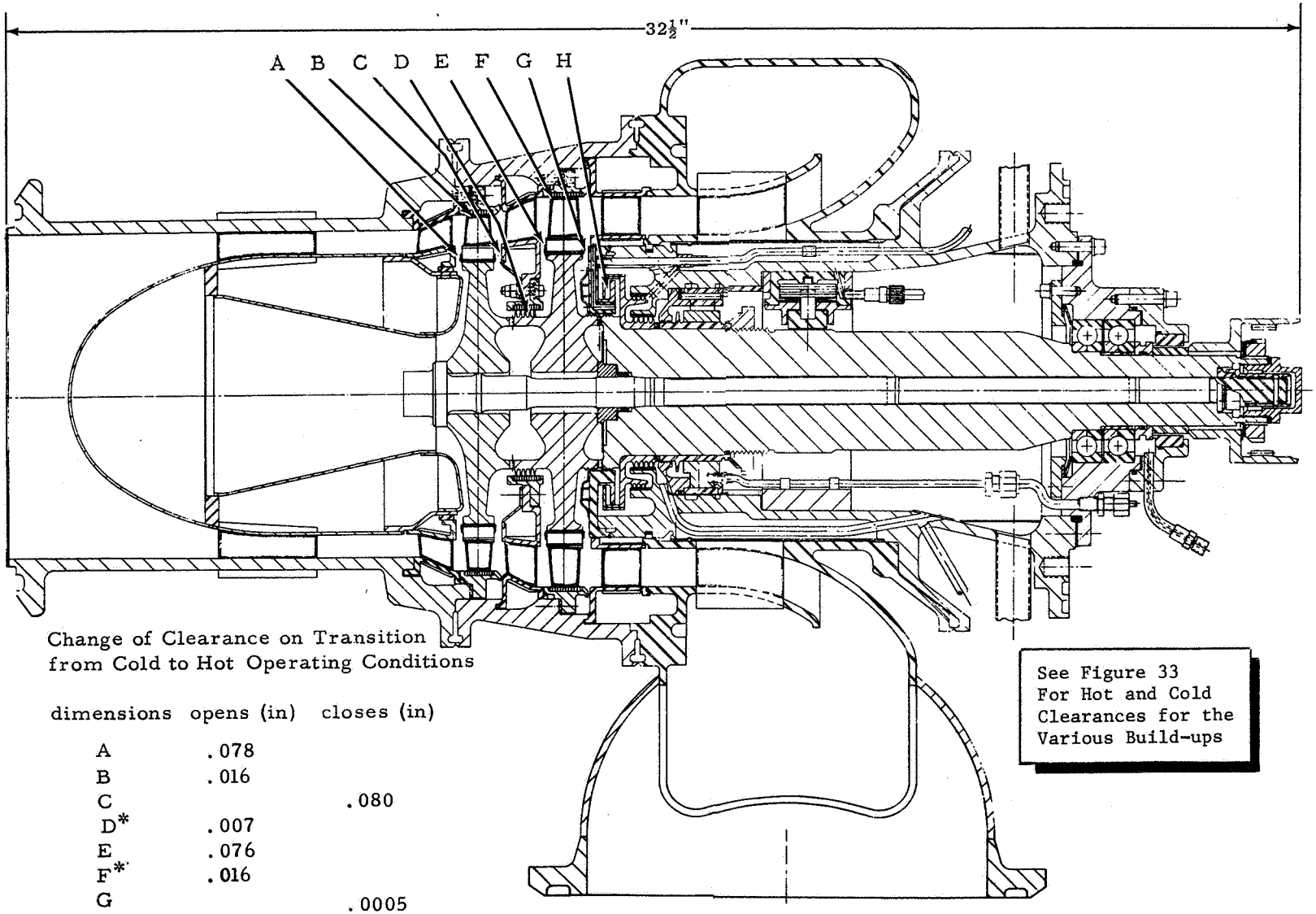


Figure 44. Two Stage Turbine Temperature Distribution.



Change of Clearance on Transition
from Cold to Hot Operating Conditions

dimensions	opens (in)	closes (in)
A	.078	
B	.016	
C		.080
D*	.007	
E	.076	
F*	.016	
G		.0005
H	.0015	

*radially

Figure 45. Two Stage Turbine Thermal Expansion.

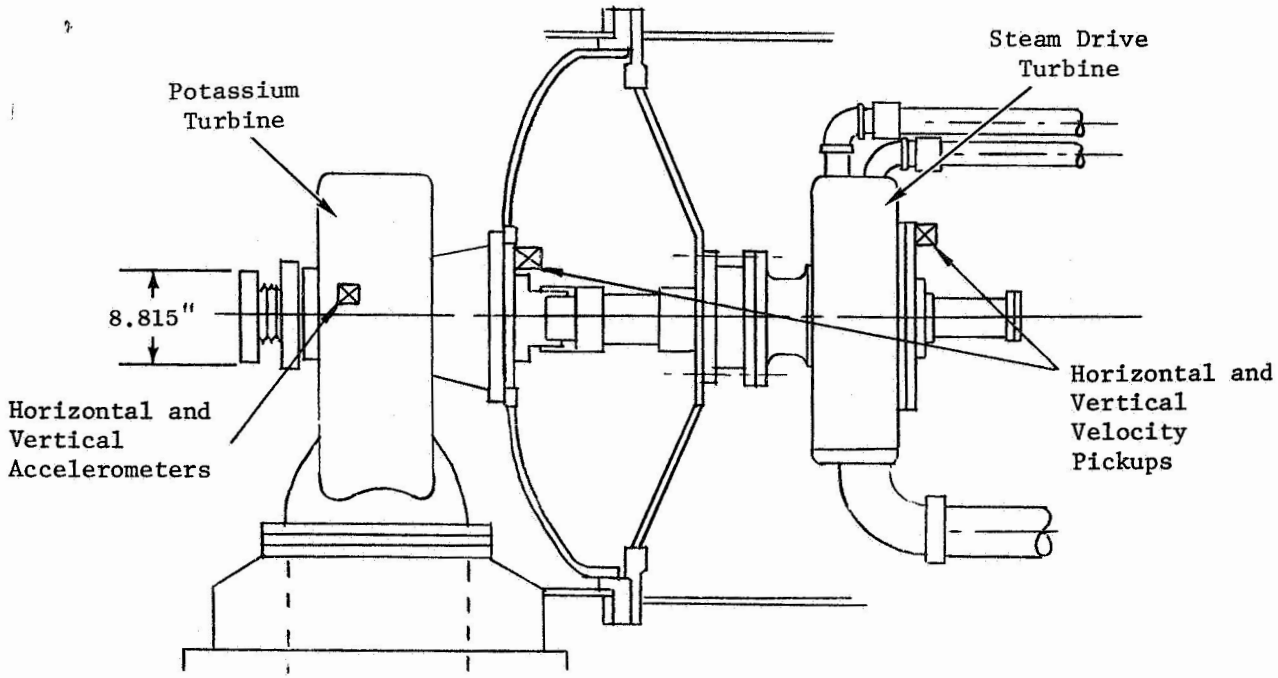


Figure 46a. Schematic Diagram of Turbine Pretest Installation.

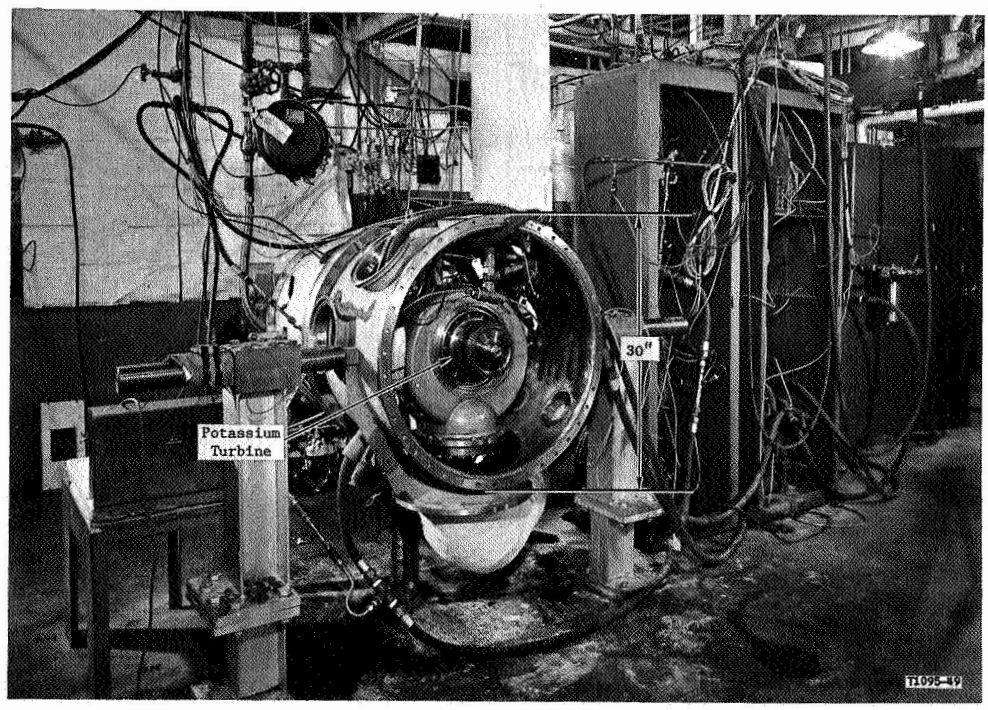


Figure 46b. Turbine Pretest Installation.

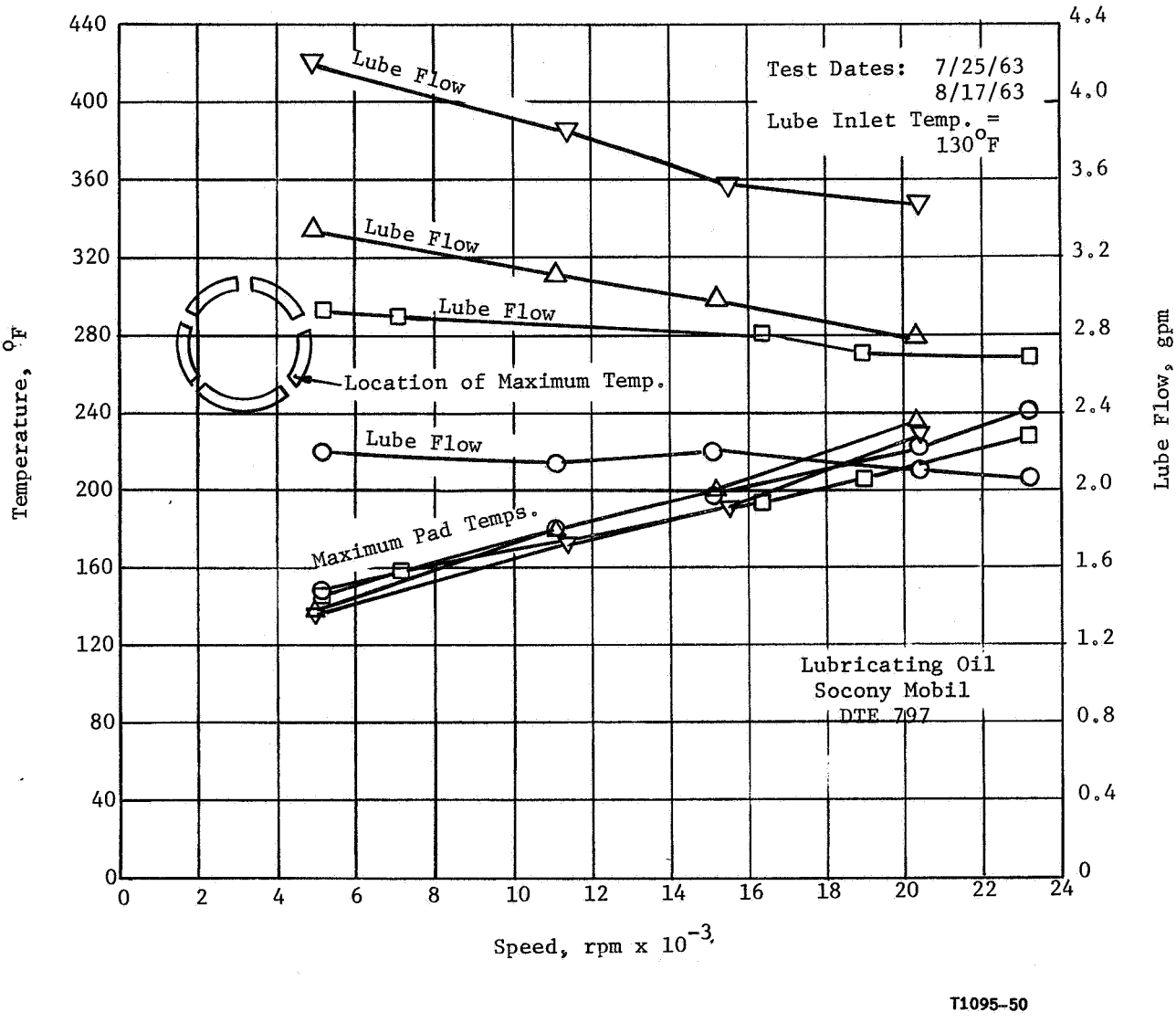


Figure 47. Pad Bearing Temperatures During Pretesting.

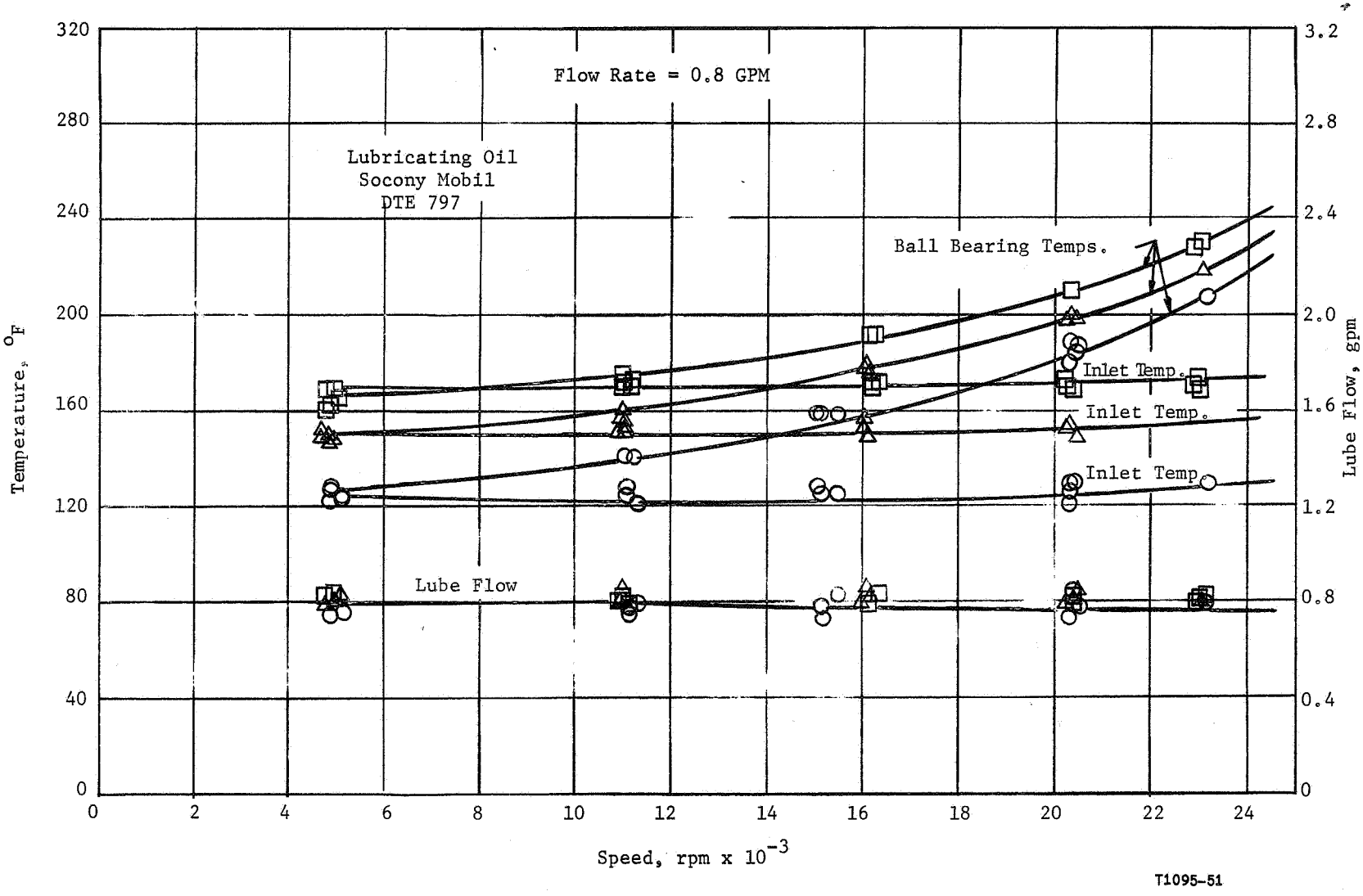
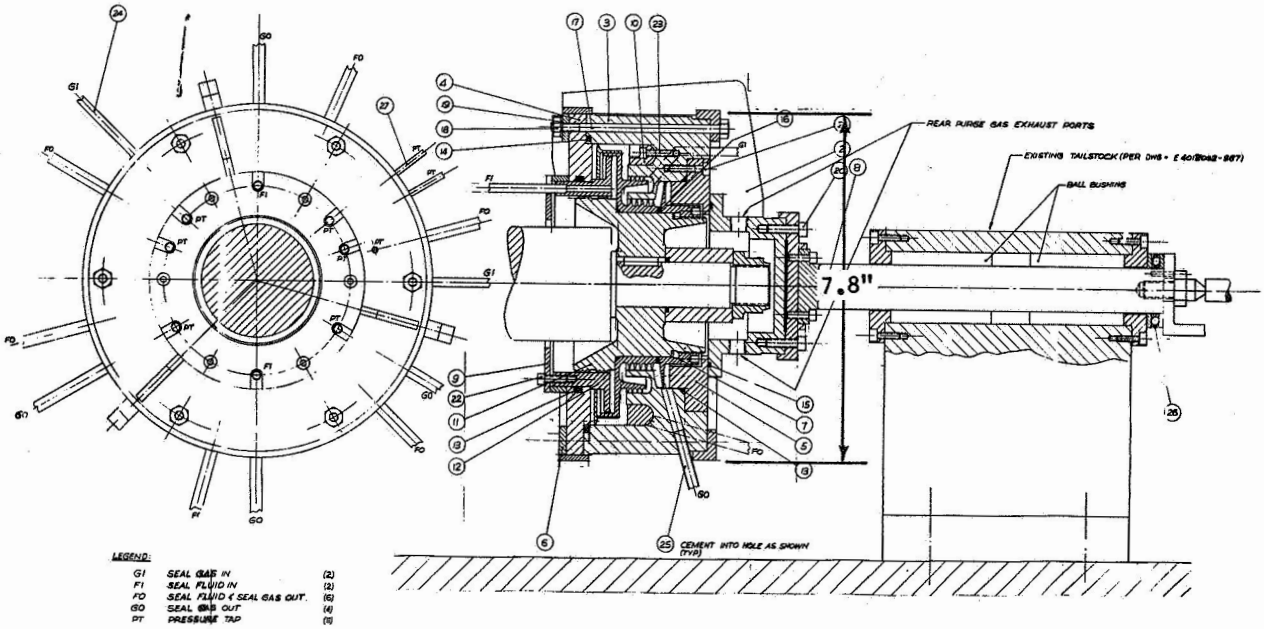


Figure 48. Ball Bearing Temperatures During Pretesting.



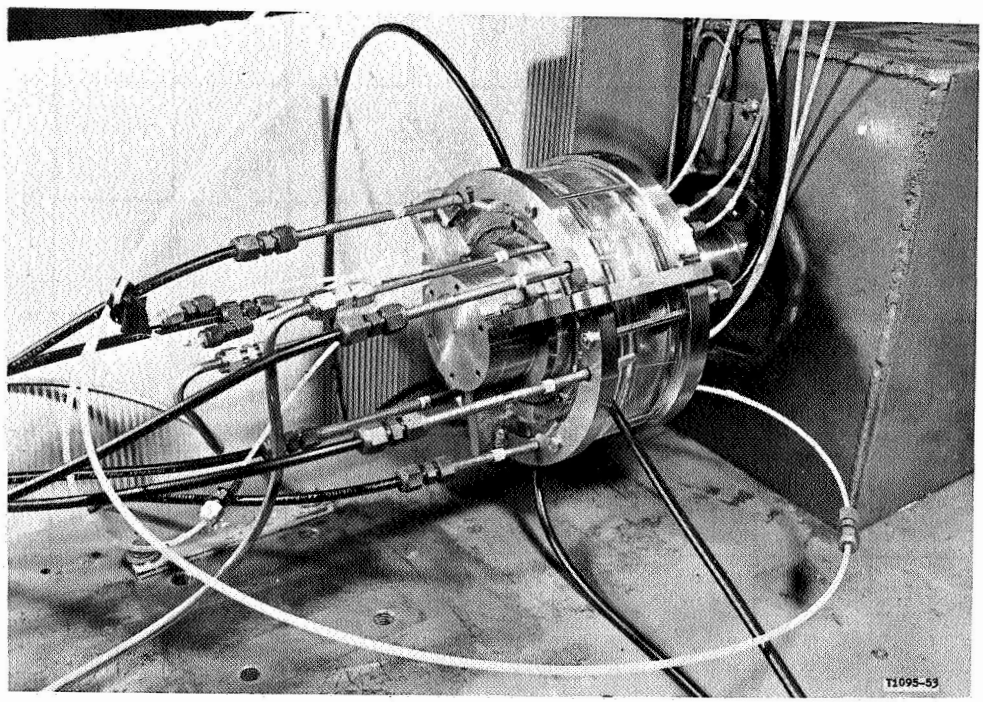


Figure 49. Hydrodynamic Seal Test Rig.

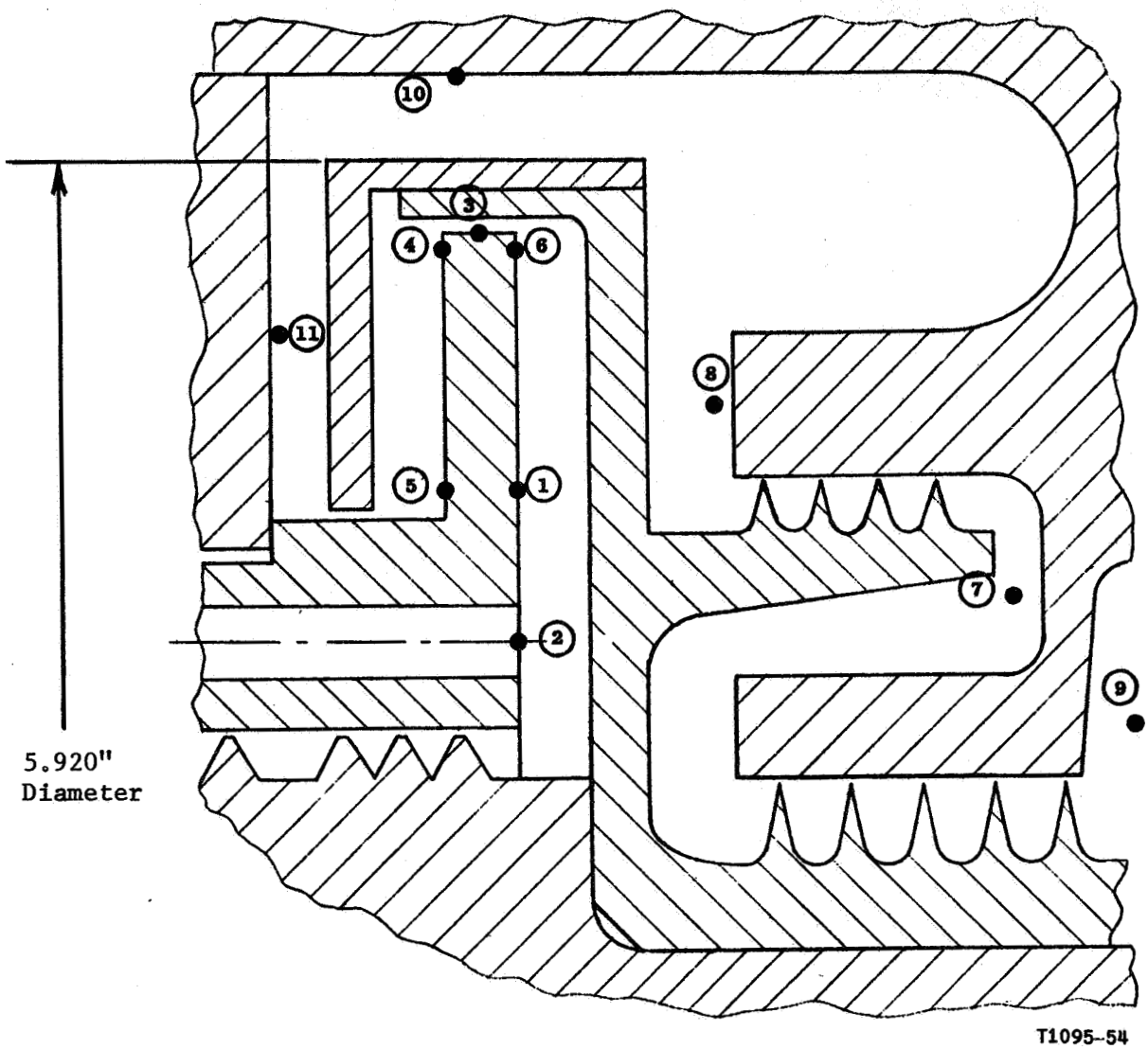


Figure 50. Pressure Instrumentation Locations within Hydrodynamic Seal.

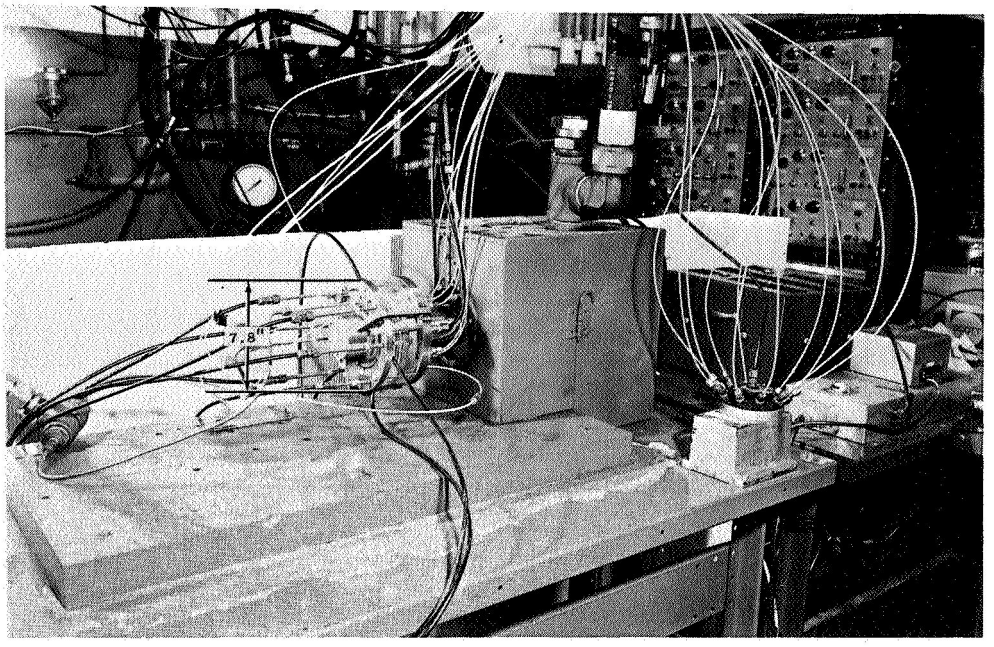


Figure 51a. Overall View.

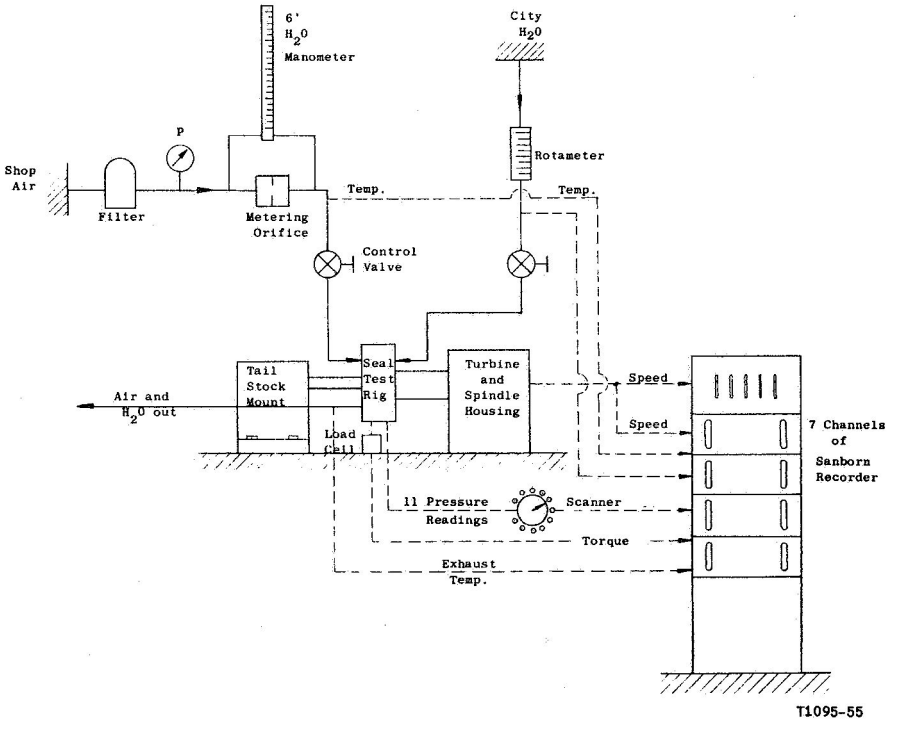


Figure 51b. Schematic of Seal Test Rig.

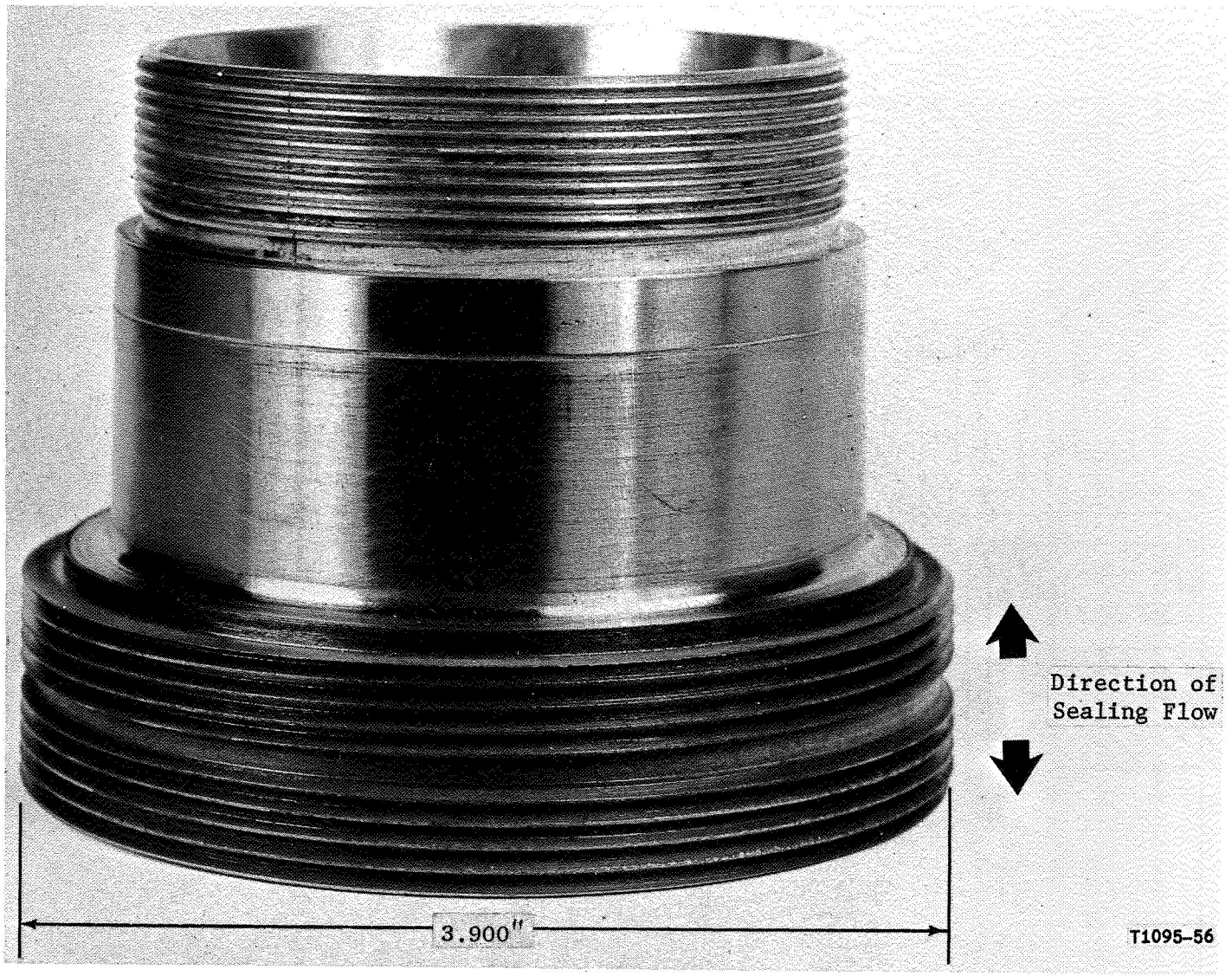


Figure 52. Right and Left Hand Screw Seal.

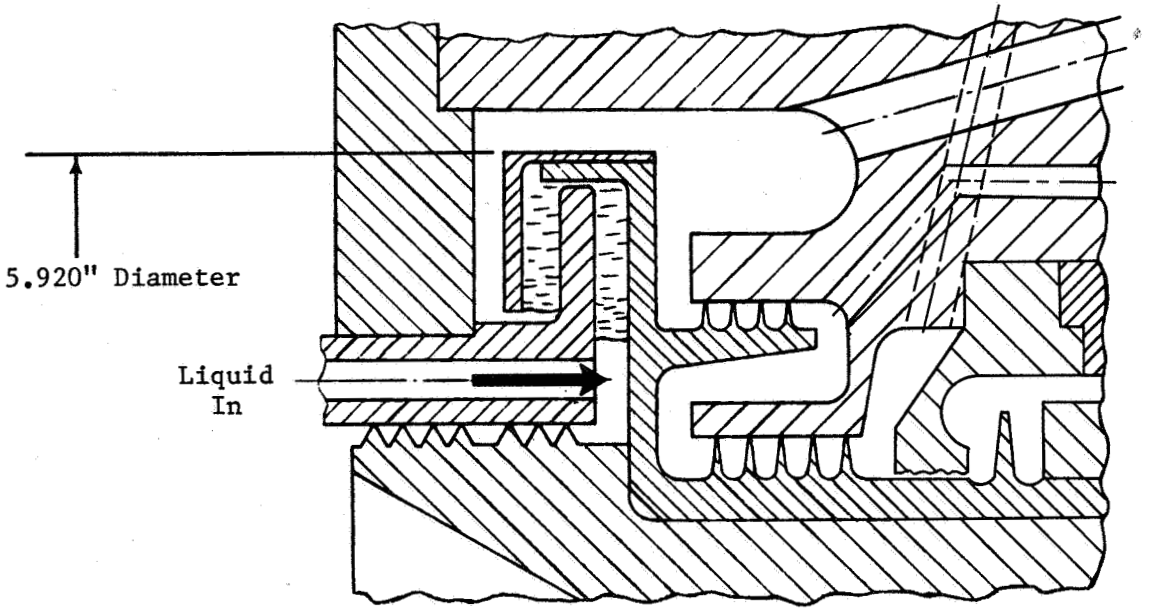


Figure 53a. Hydrodynamic Seal Showing Seal Liquid Injected Into Aft Rotor Cavity.

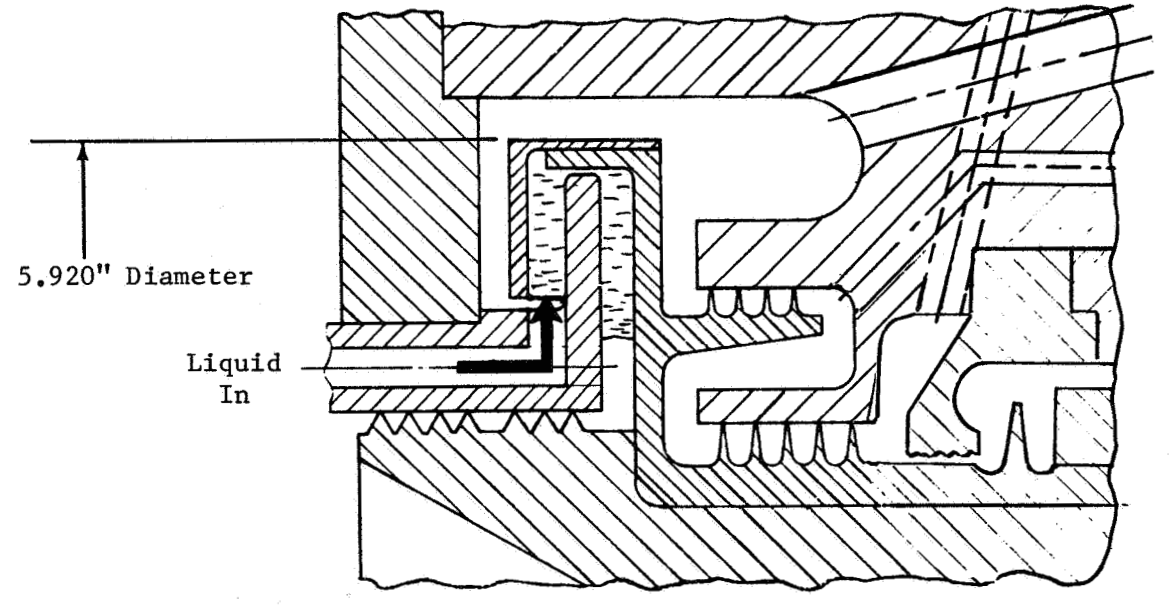


Figure 53b. Hydrodynamic Seal Showing Liquid Injected Into Forward Rotor Cavity.

T1095-58

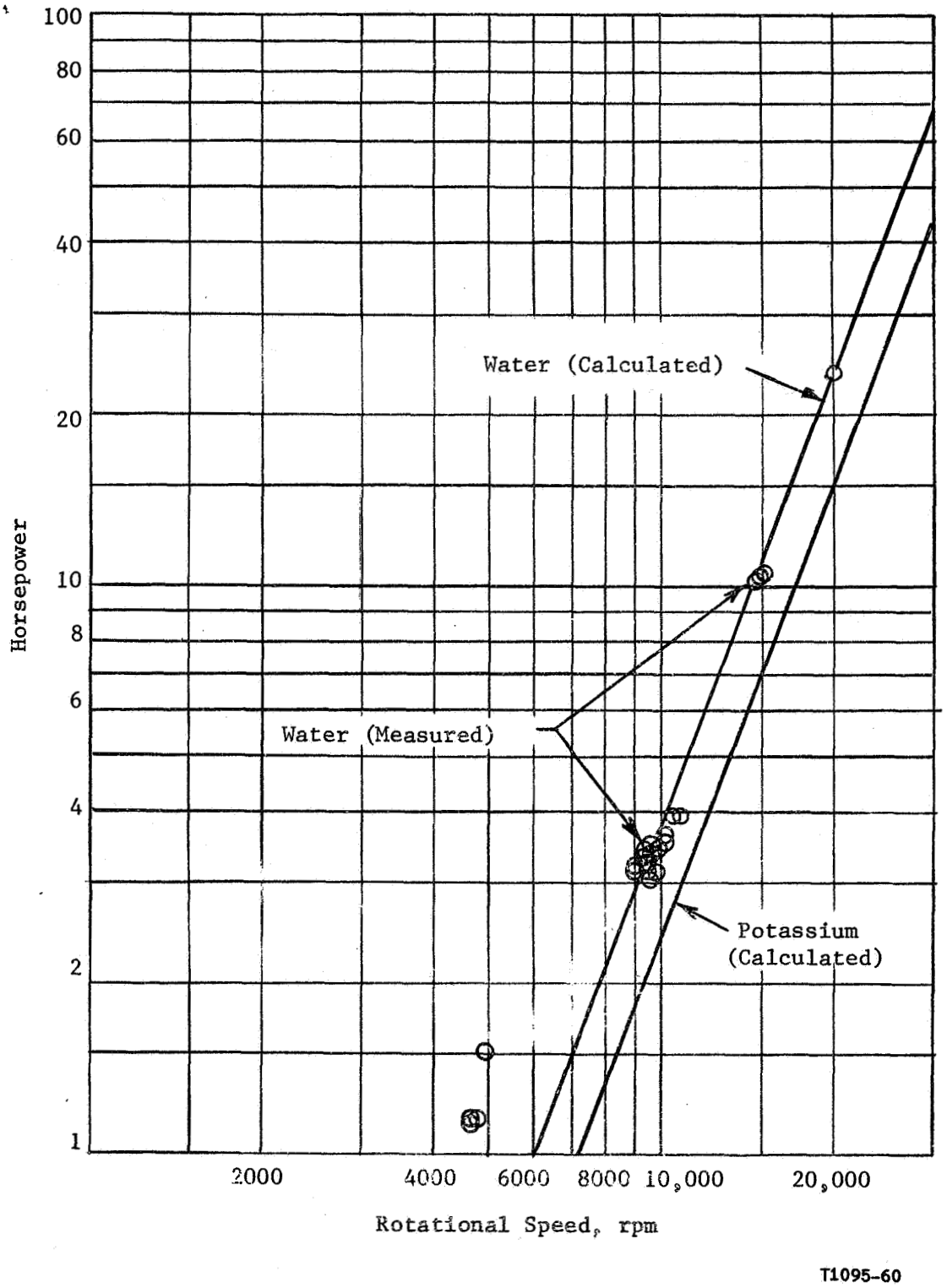


Figure 54. Hydrodynamic Seal Horsepower Consumption.

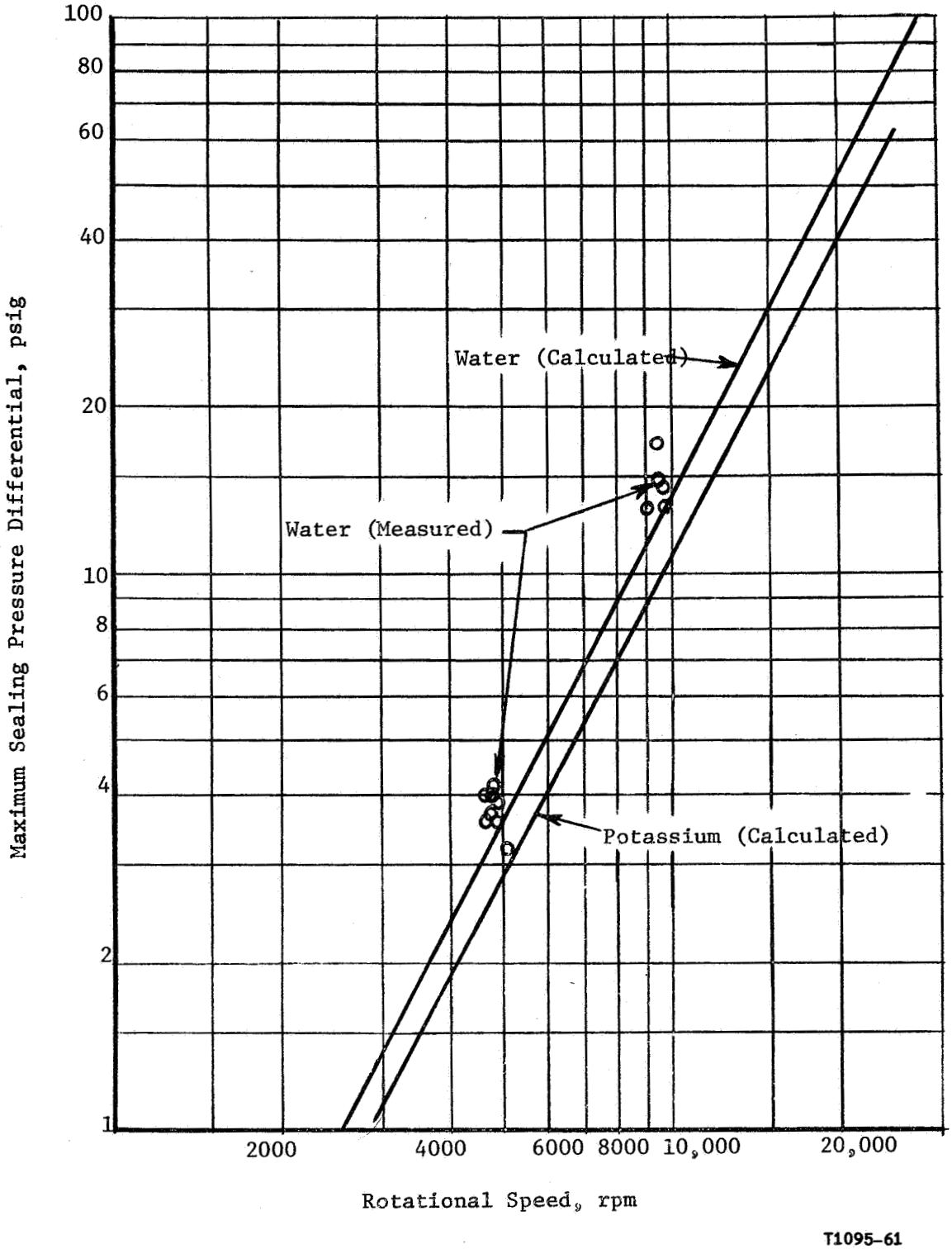


Figure 55. Hydrodynamic Seal Sealing Pressure.

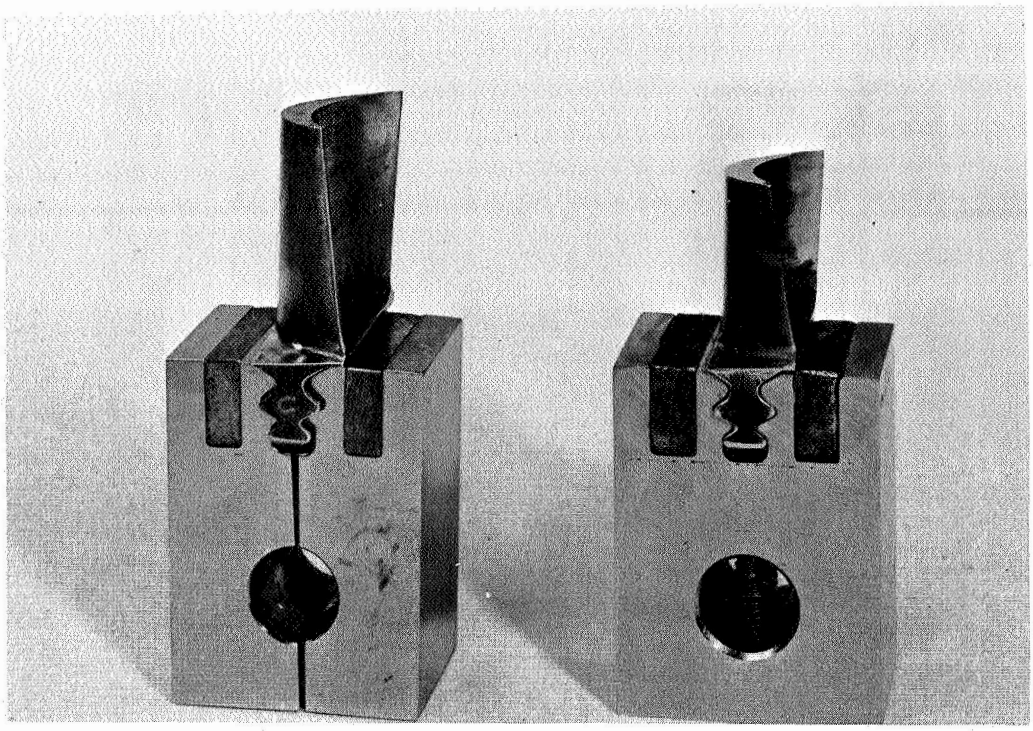


Figure 56a. Bucket Clamping Coupons for Vibration Bench Tests.

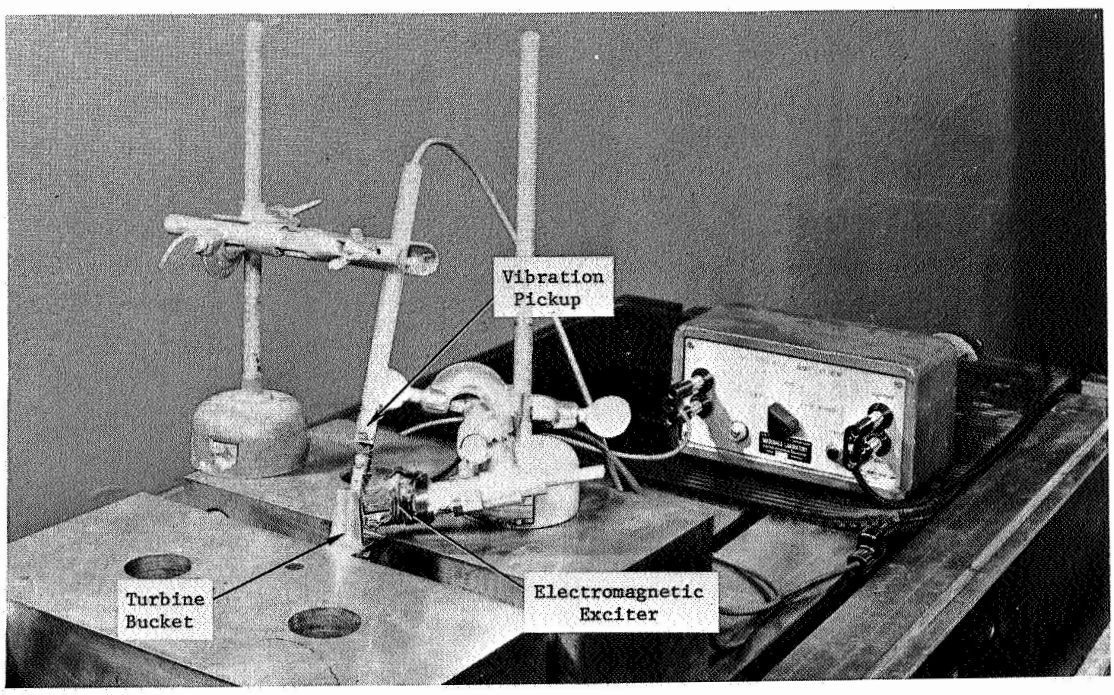
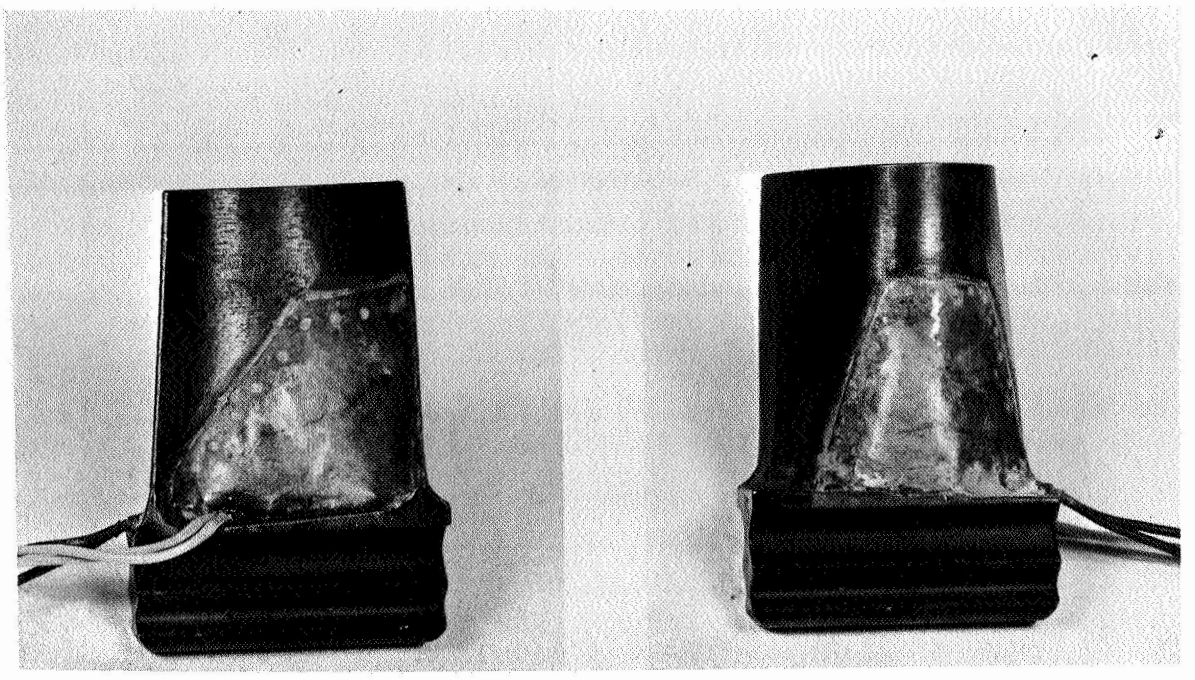


Figure 56b. Blade Vibration Bench Test Setup.



Concave Surface

Convex Surface

Figure 57a. Strain-Gauged Buckets.

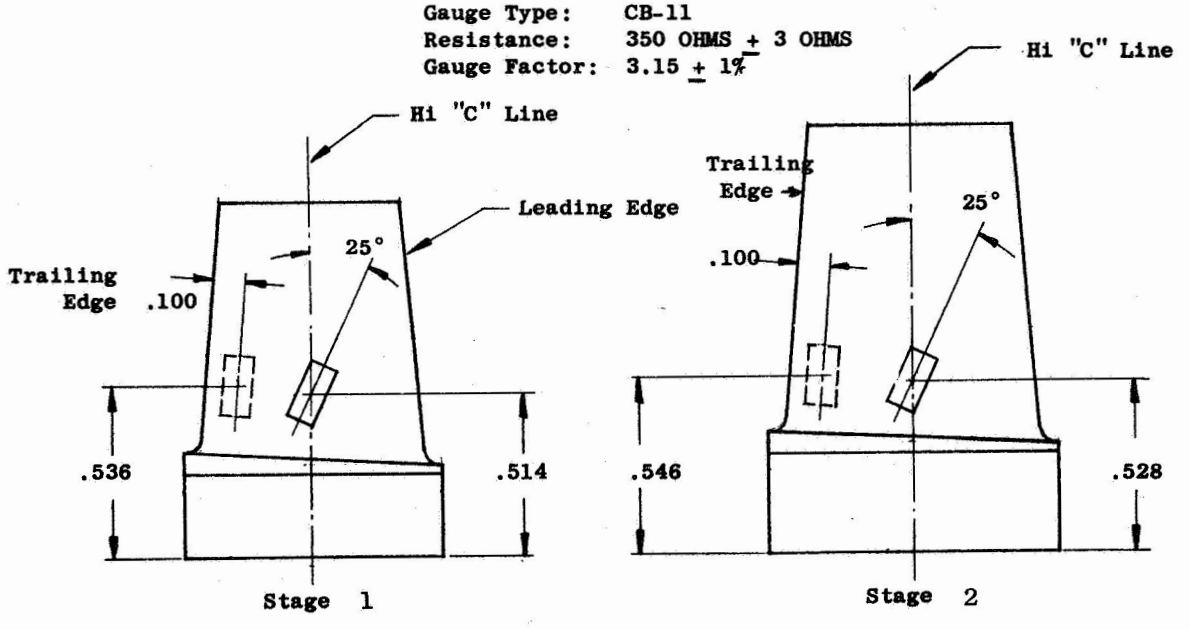
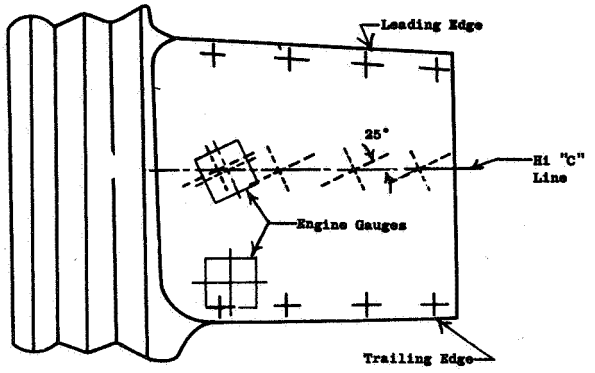
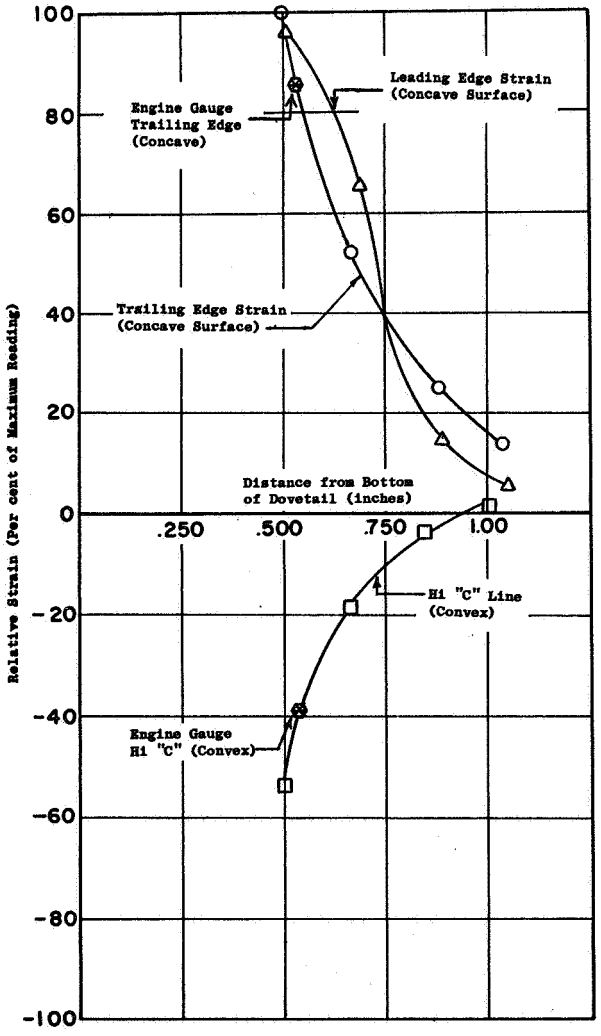


Figure 57b. Placement of Strain-Gauges. T1095-63



1. All strain distribution gauges are Cb-111 Foil with 1/16 inch grid.
2. Hi "C" gauges are at 65°, on convex side.
3. Gauges on leading and trailing edge are parallel to, and close to edge.

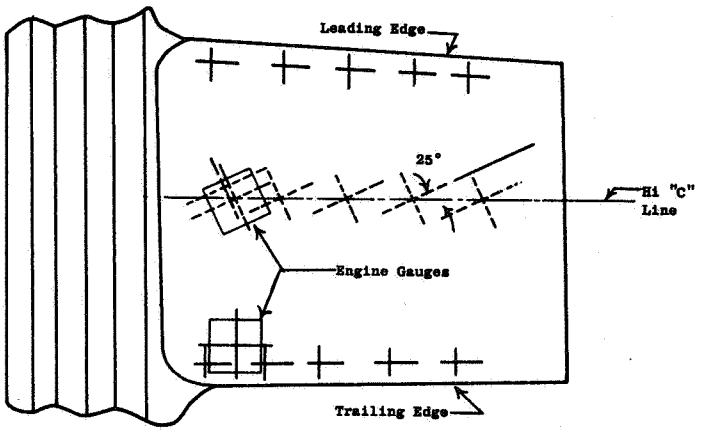


BLADE NUMBER 46

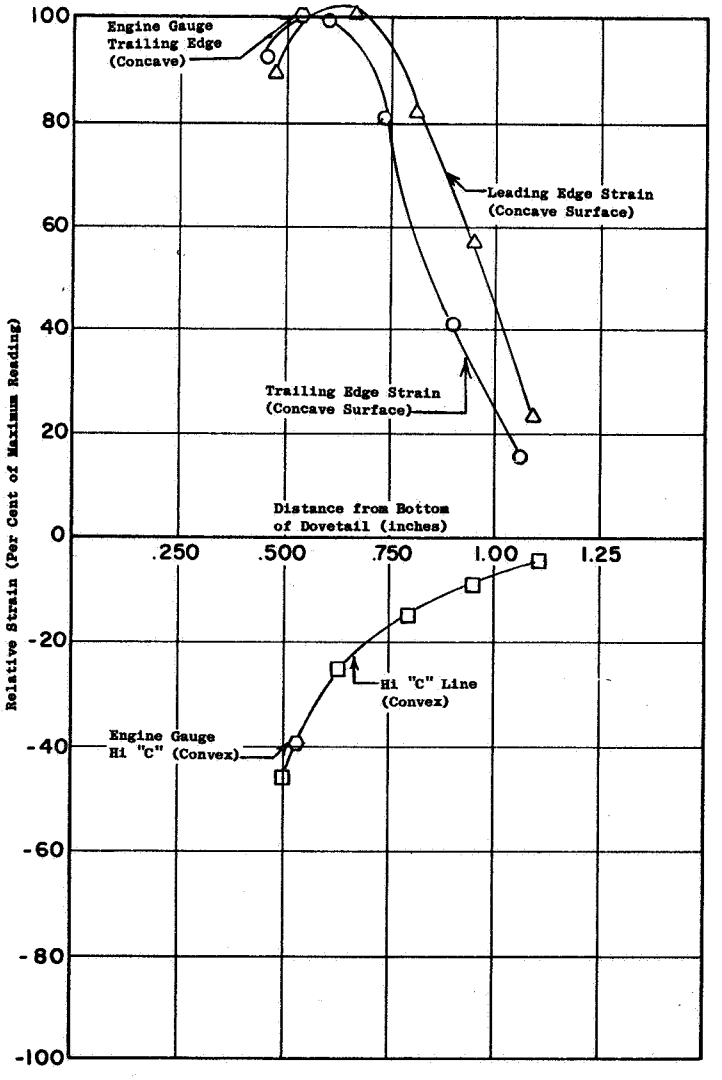
RESONANT FREQUENCY = 7269 cps

T1095-64

Figure 58. Strain Distribution for Potassium Test Turbine Blade - Stage 1 First Flexural Mode.



1. All strain distribution gauges are Cb-111 Foil with 1/16 inch grid.
2. Hi "C" gauges are at 85°, on convex side.
3. Gauges on leading and trailing edge are parallel to, and close to edge.



BLADE NUMBER 28

RESONANT FREQUENCY = 5142 cps

T1095-65

Figure 59. Strain Distribution for Potassium Test Turbine Blade - Stage 2 First Flexural Mode.

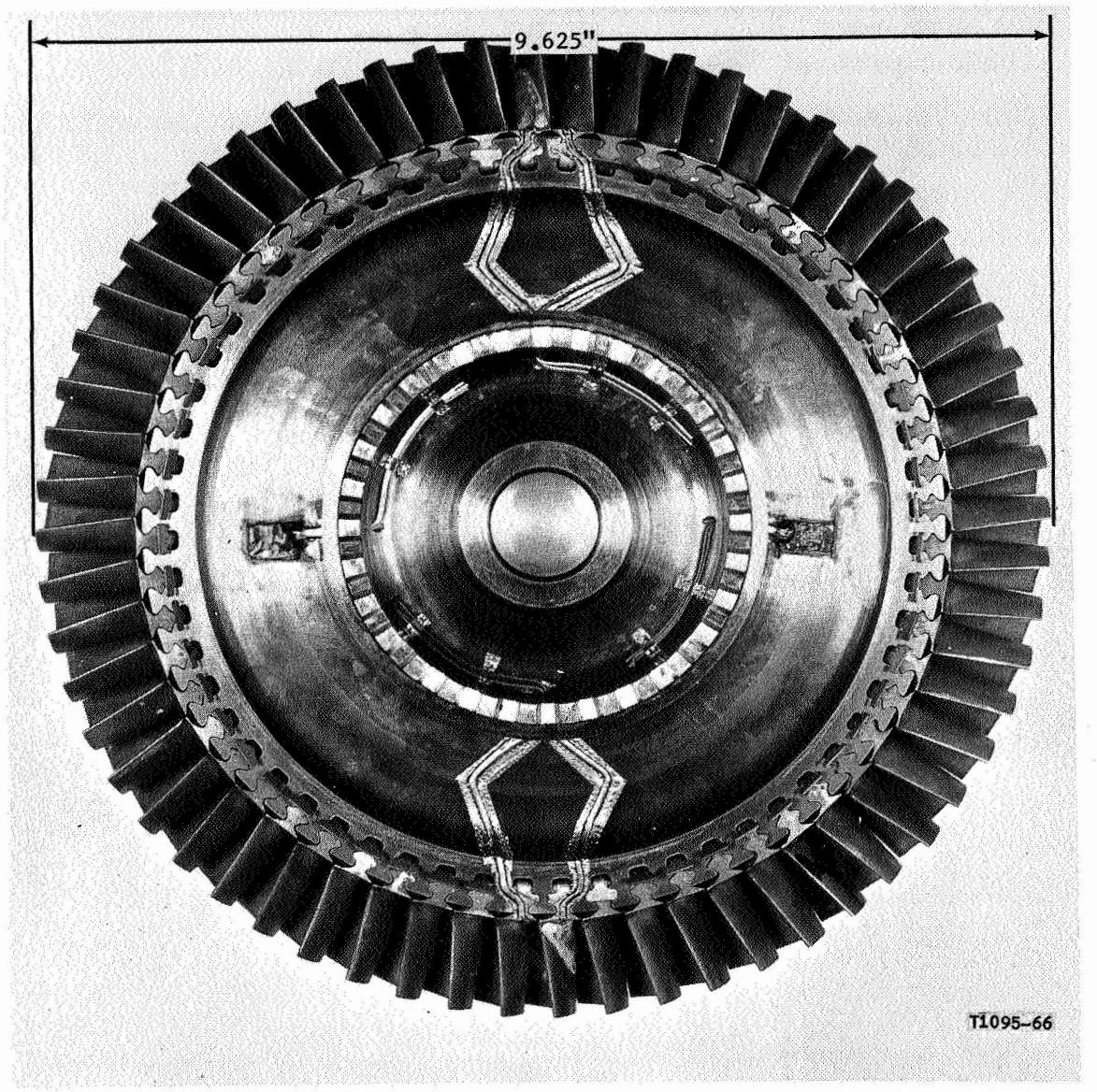


Figure 60. Second Stage Turbine Wheel Blade Strain Gauge Installation.

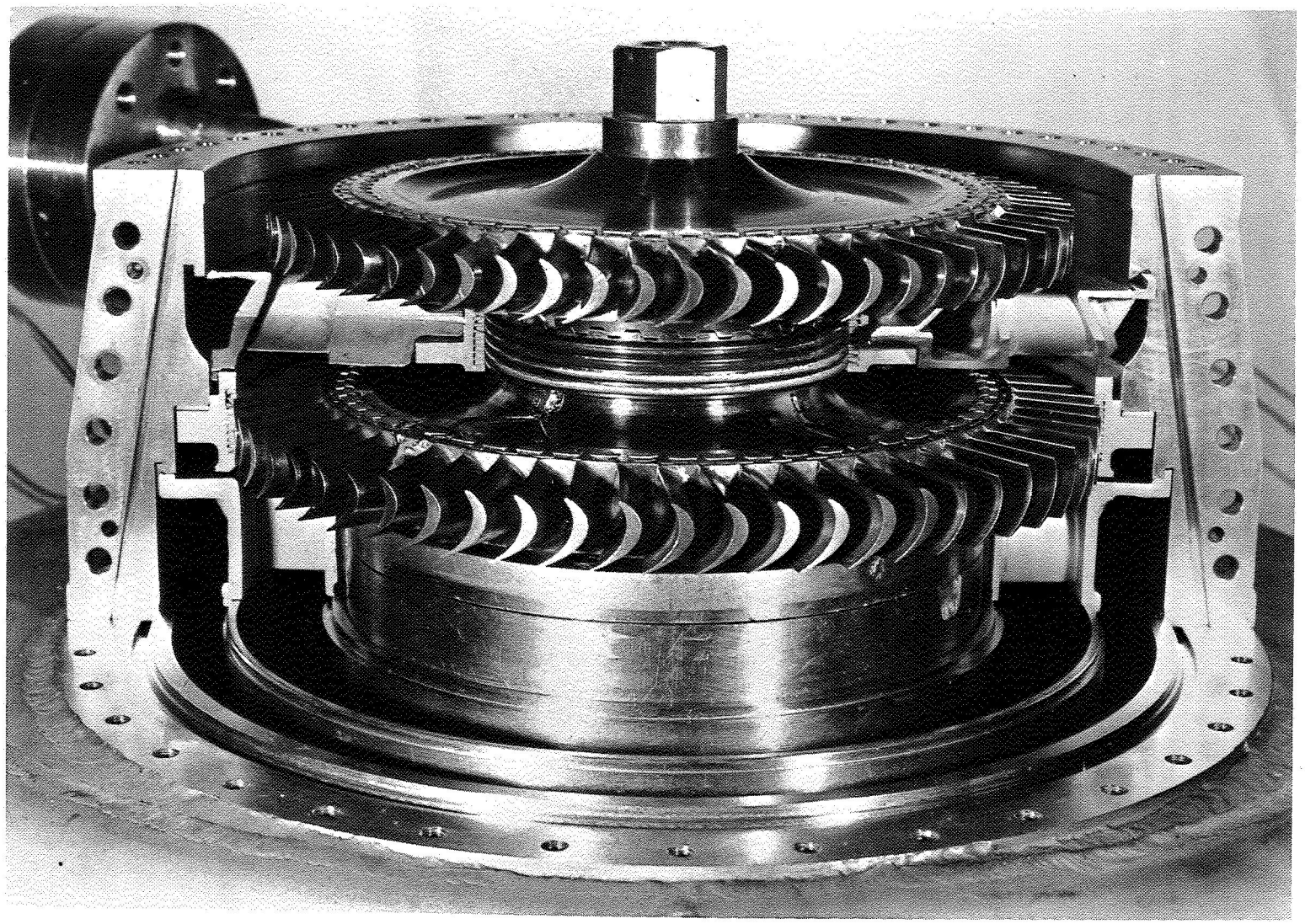


Figure 61. Turbine During Build-Up for Pretesting. T1095-67

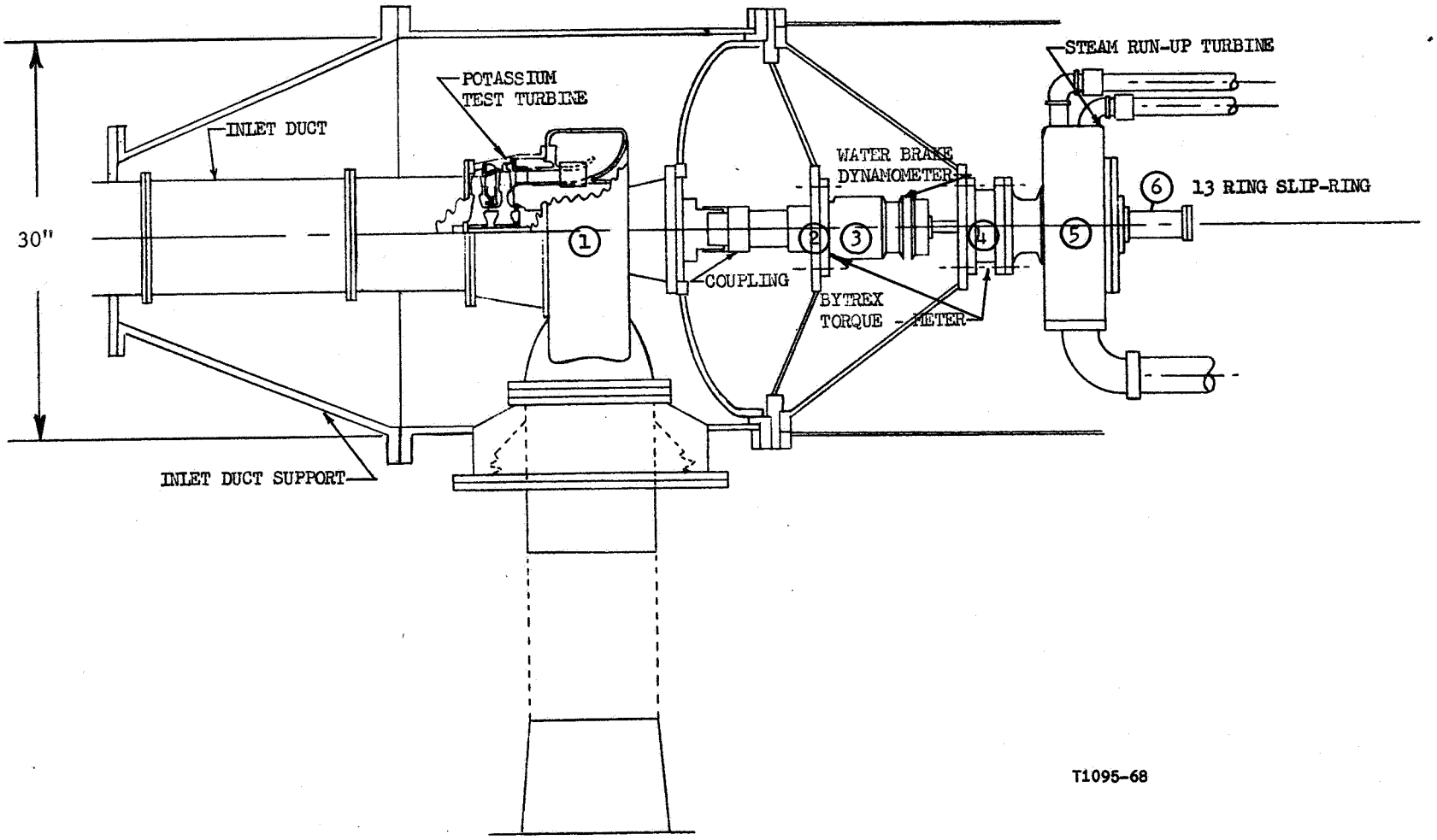


Figure 62. Schematic Diagram of Turbine Pretest Rig Assembly.

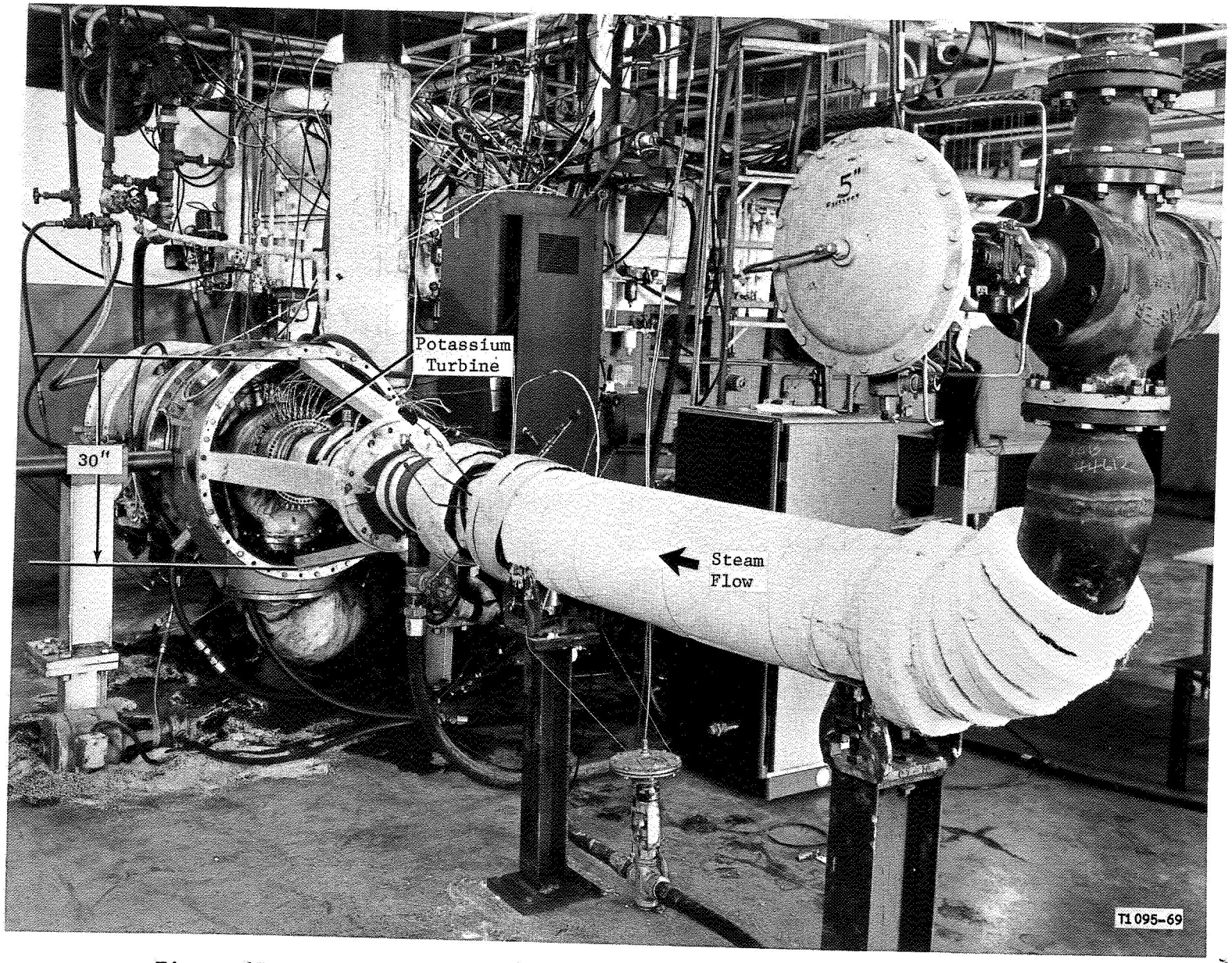


Figure 63. Overall Installation of Potassium Turbine in Steam Pre-Test Facility.

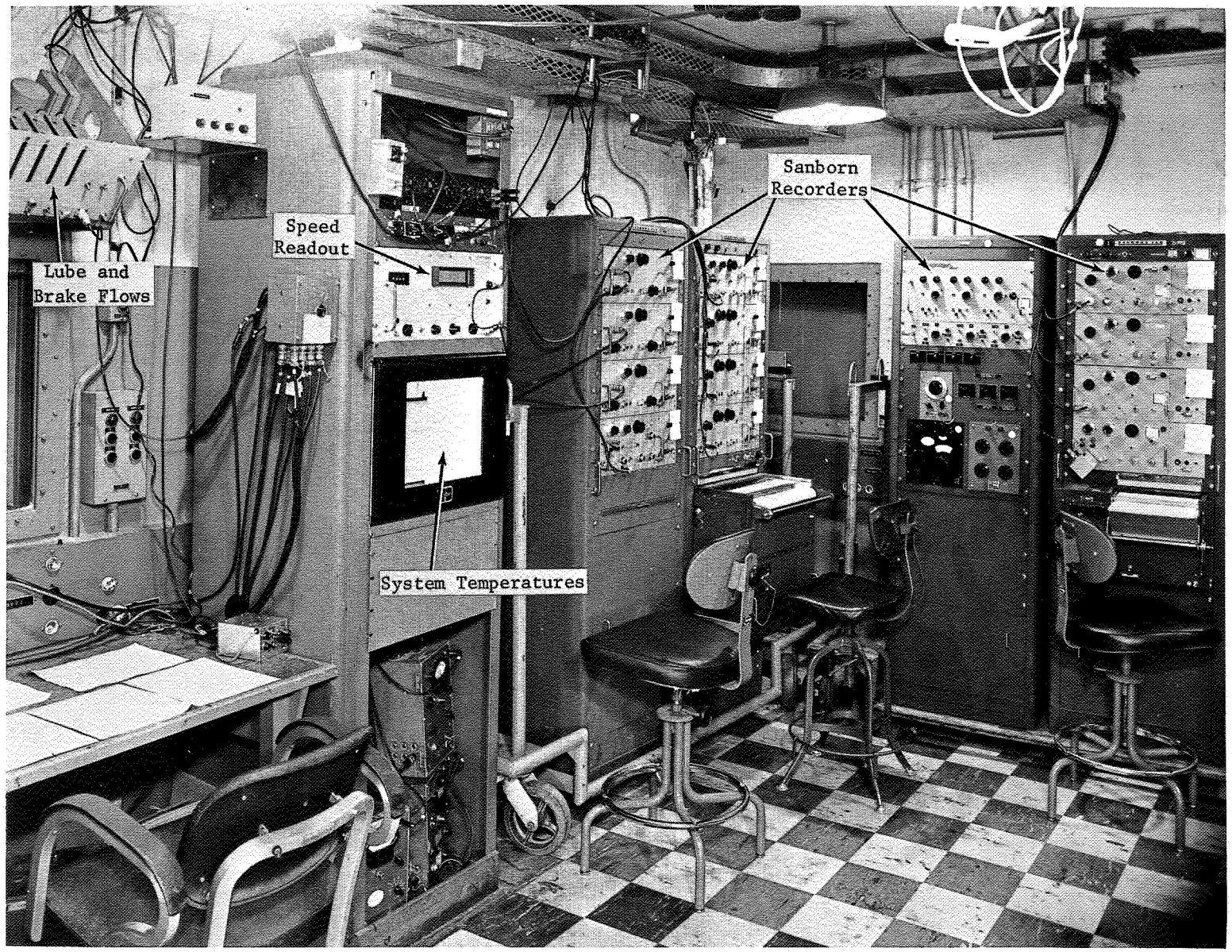


Figure 64a. Pretesting Control Room Looking North West.

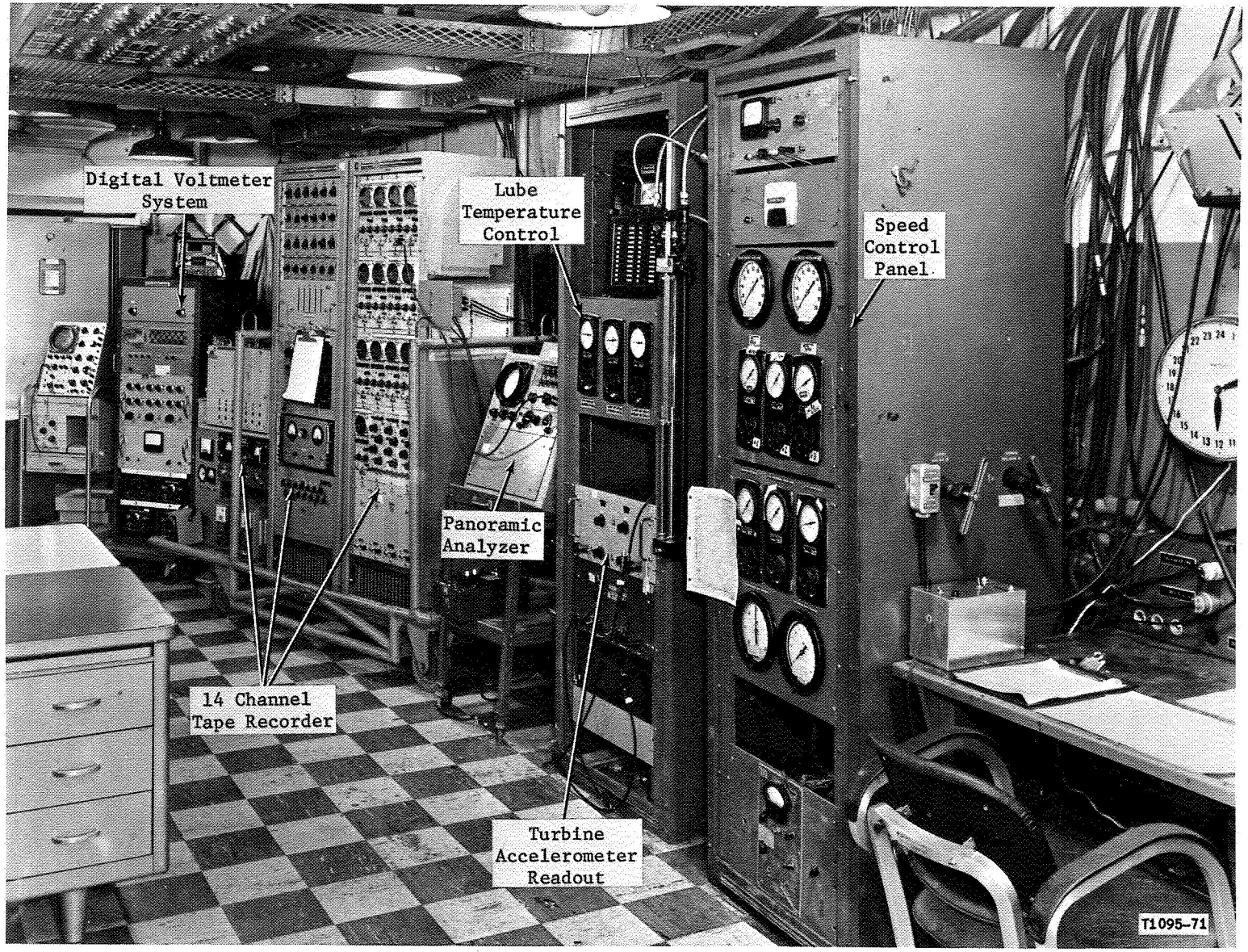


Figure 64b. Pretesting Control Room Looking South West.

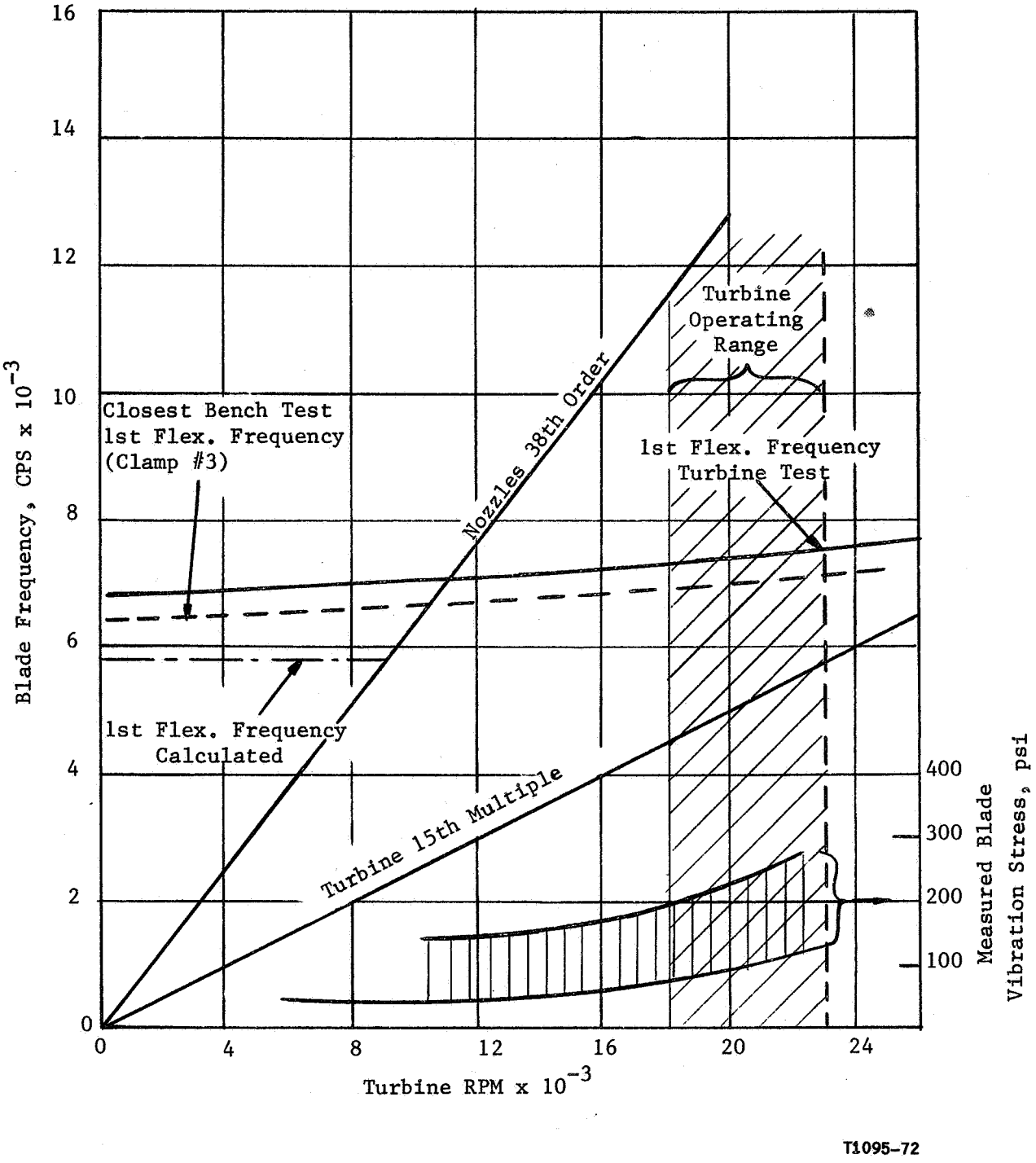


Figure 65. Blade Natural Frequencies and Vibratory Stress - Stage 1.

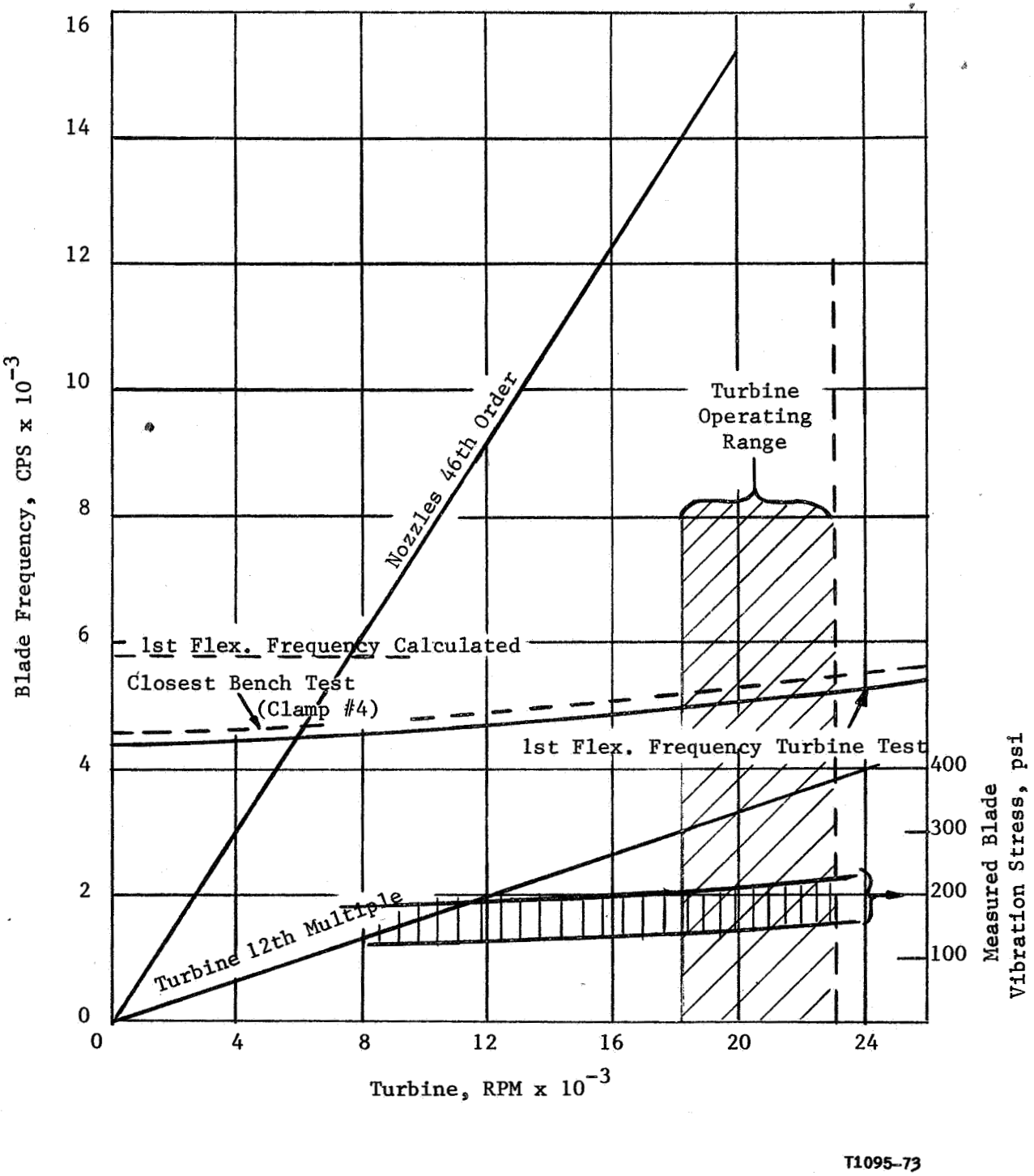


Figure 66. Blade Natural Frequencies and Vibratory Stress - Stage 2.

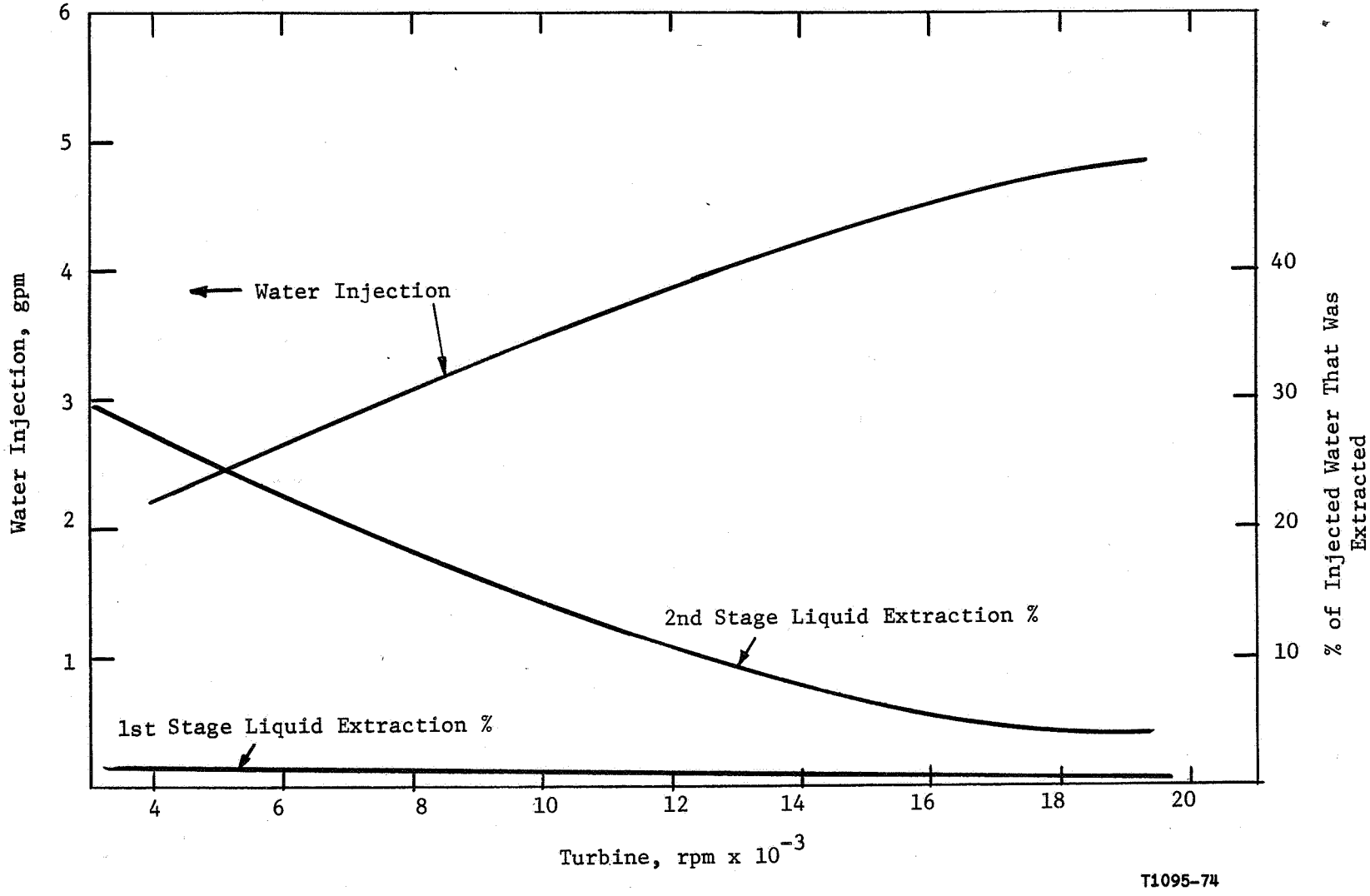


Figure 67. Effectiveness of Moisture Extraction System.

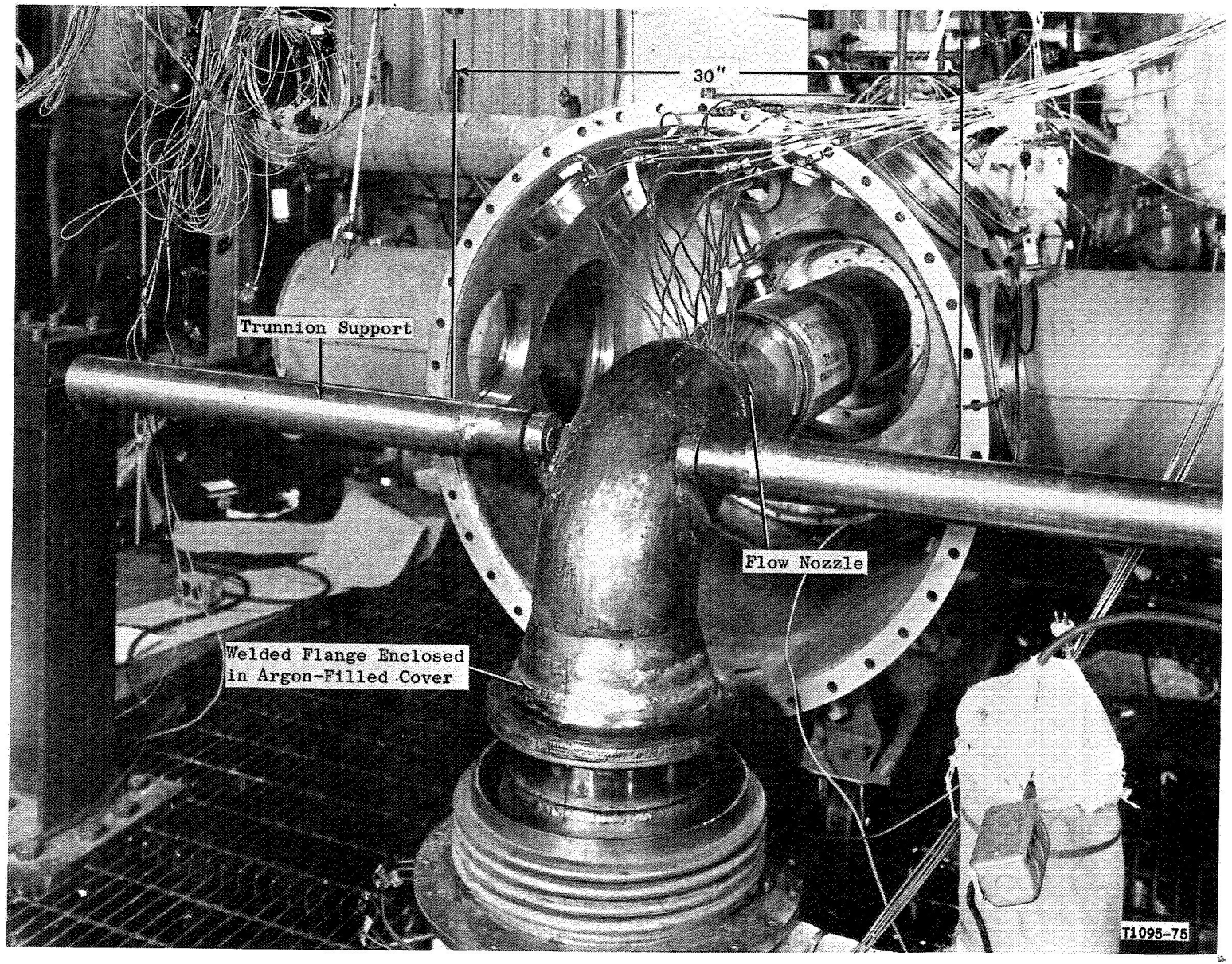


Figure 68. Nozzle Installation Showing Welded Flange Construction.

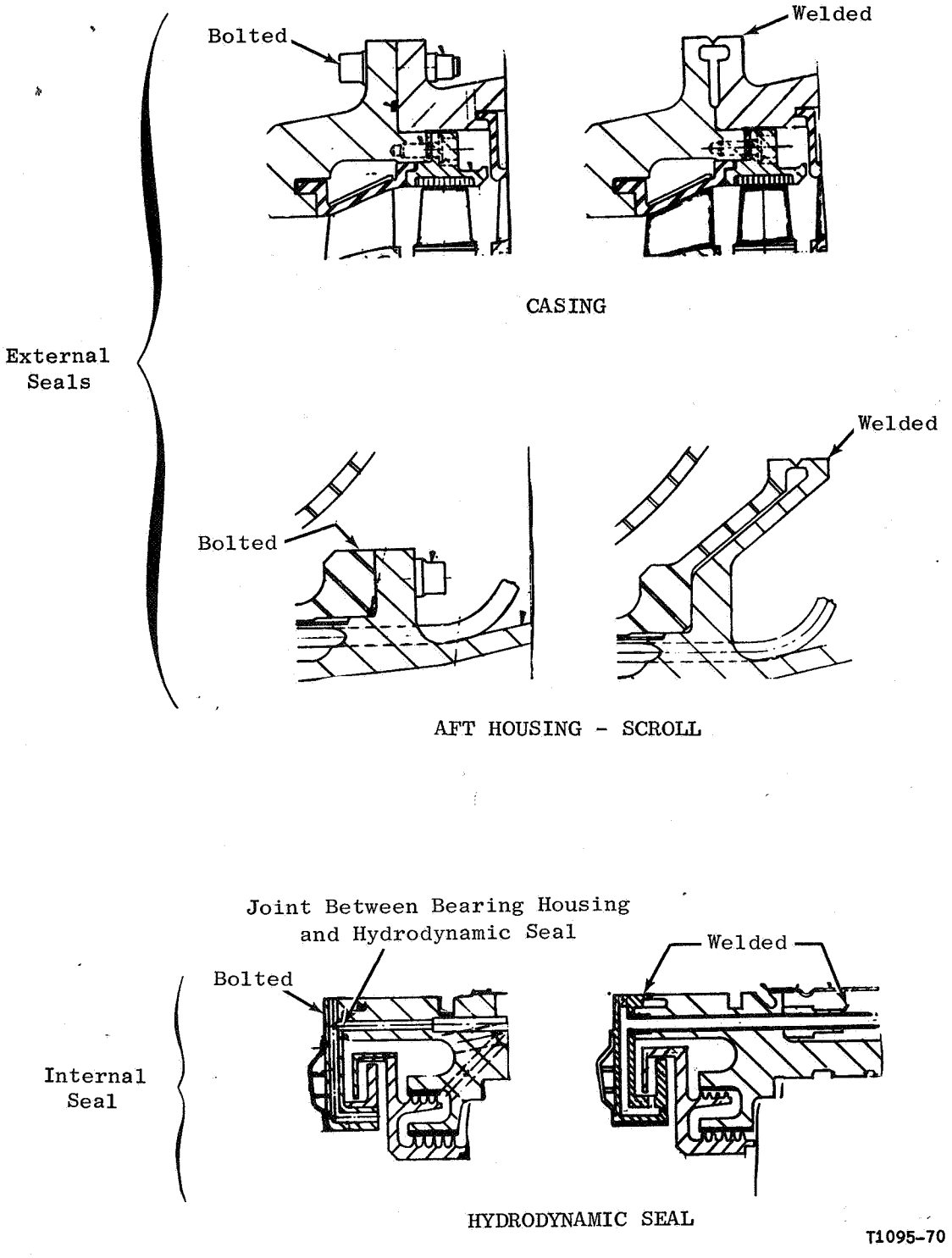


Figure 69. Cross-section Views Showing the Change From a Bolted to Welded Construction.

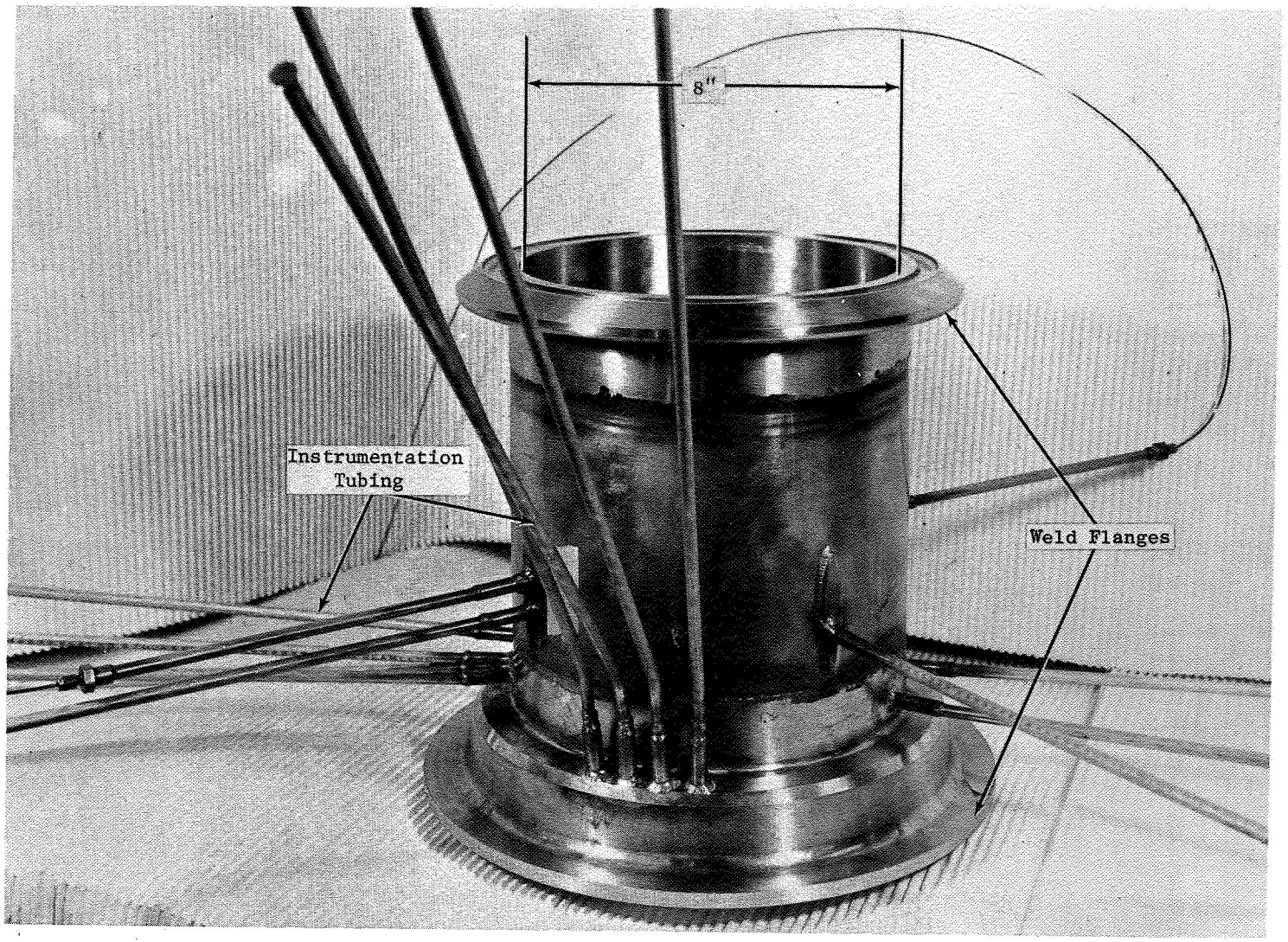


Figure 70. Inlet Duct Weldment Showing Welded Flanges and Instrumentation Lead Outs.

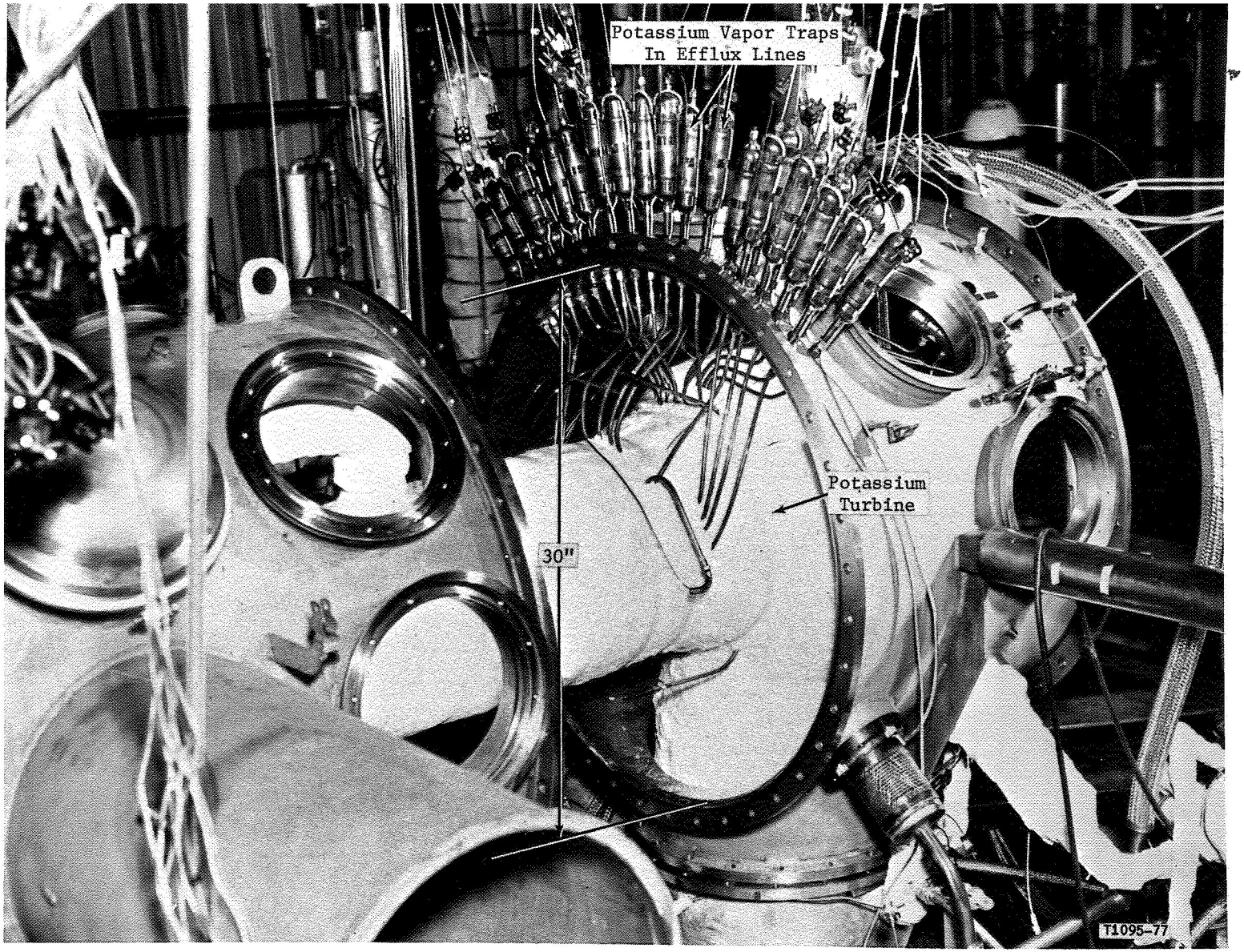


Figure 71. Front Quarter View of Turbine After Being Welded Into the 3000 KW Facility.

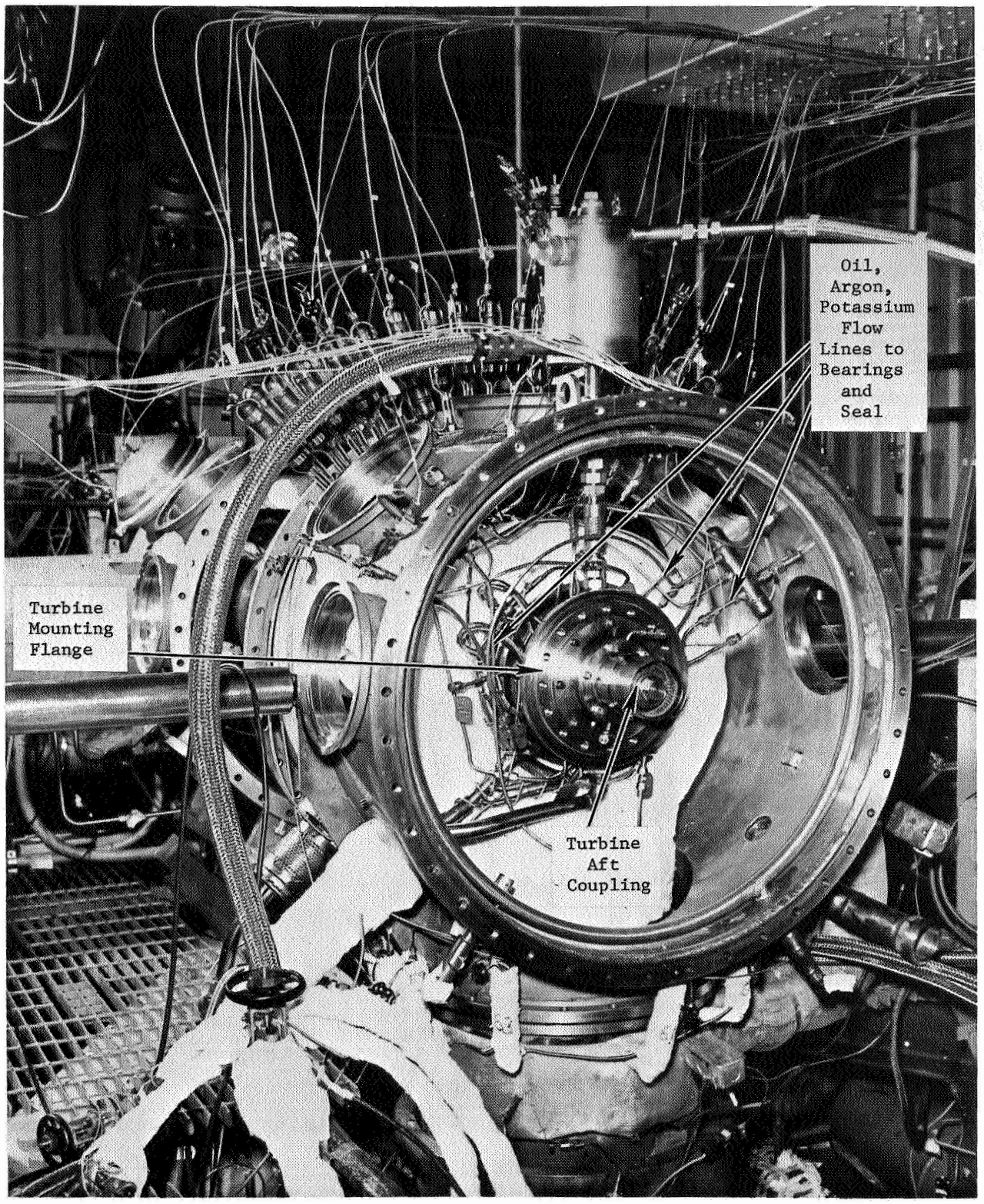


Figure 72. Aft View of Turbine After Being Welded Into the 3000 KW Facility.

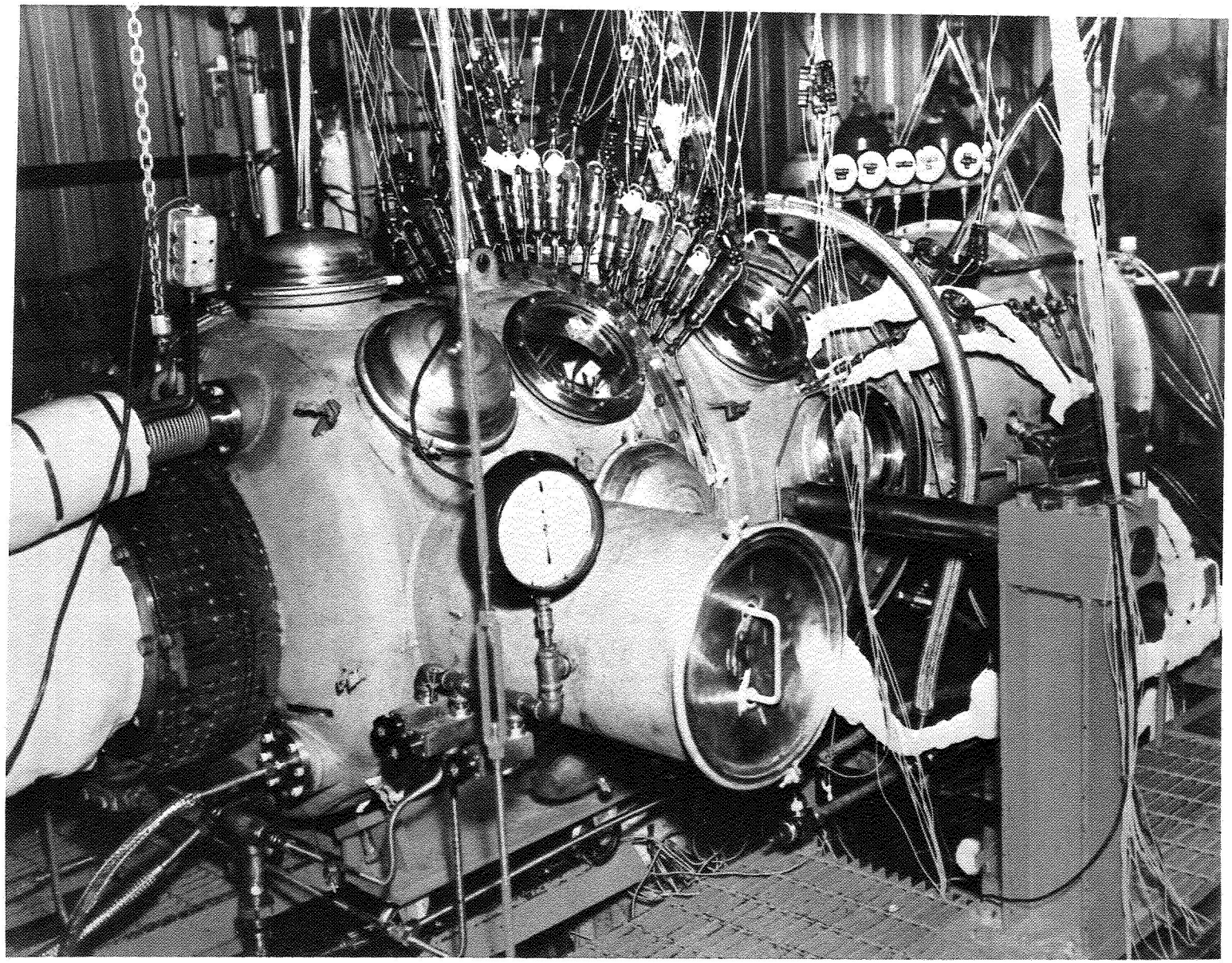


Figure 73. Front Quarter of Completed Turbine Installation. T1095-79

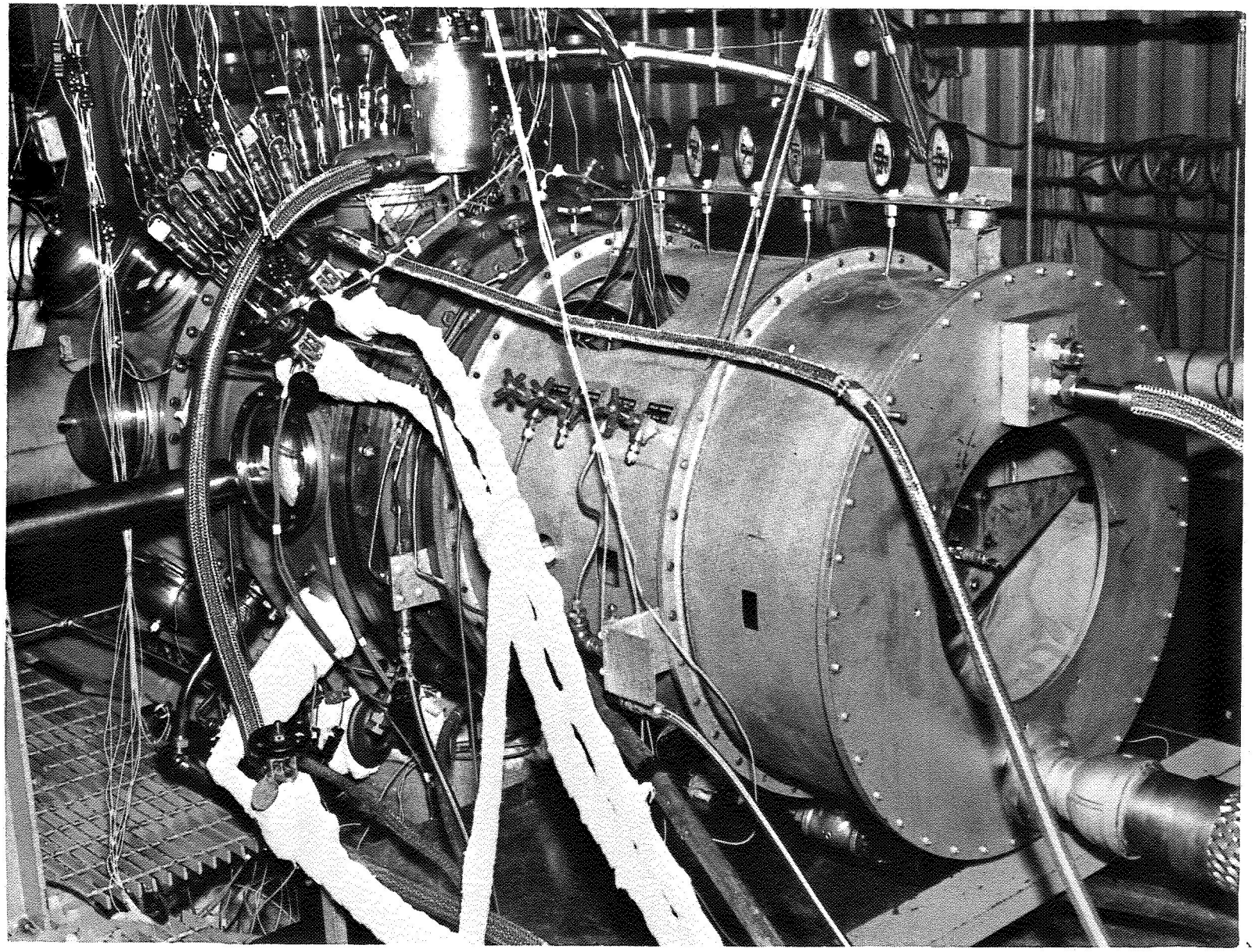
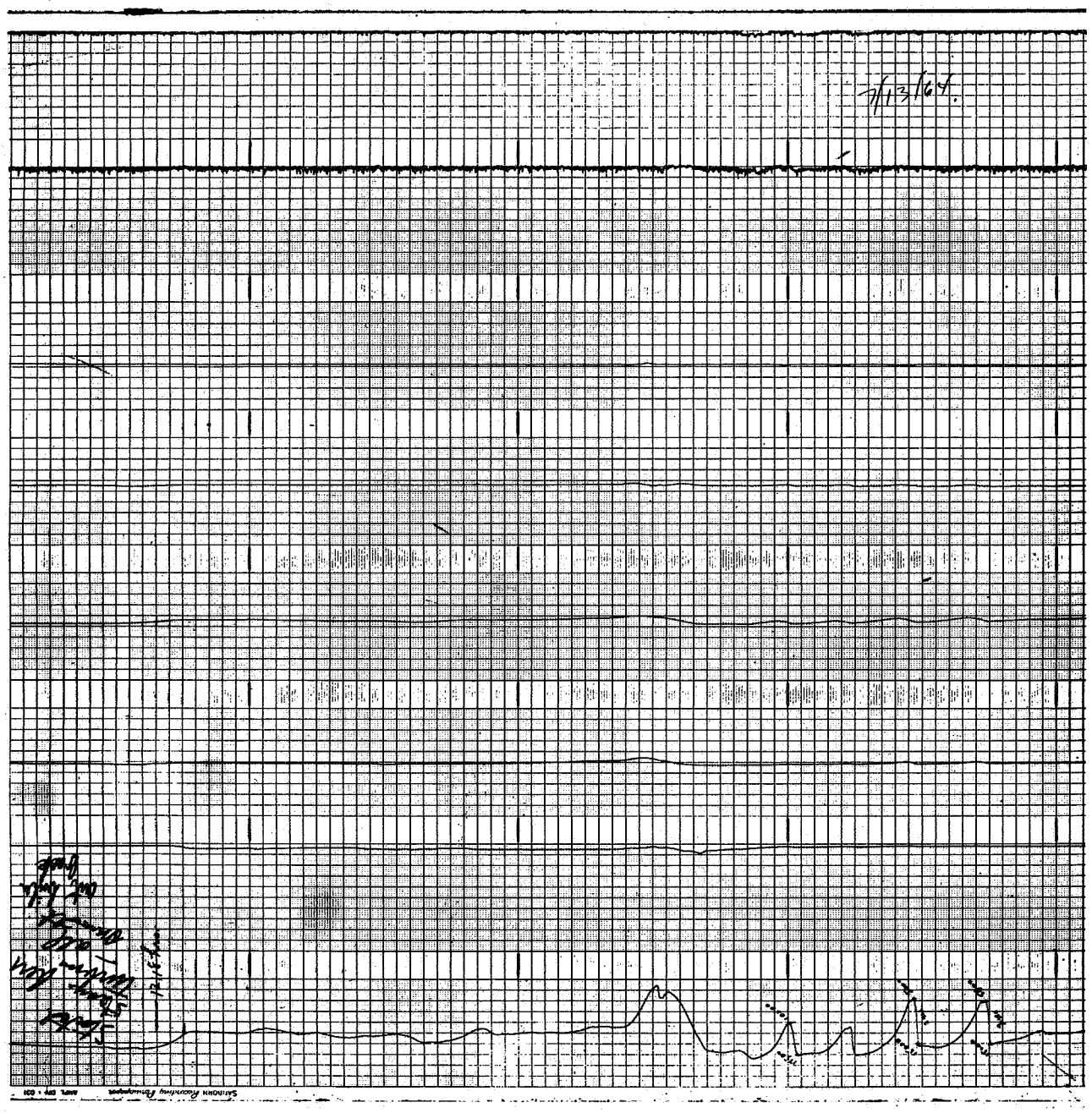


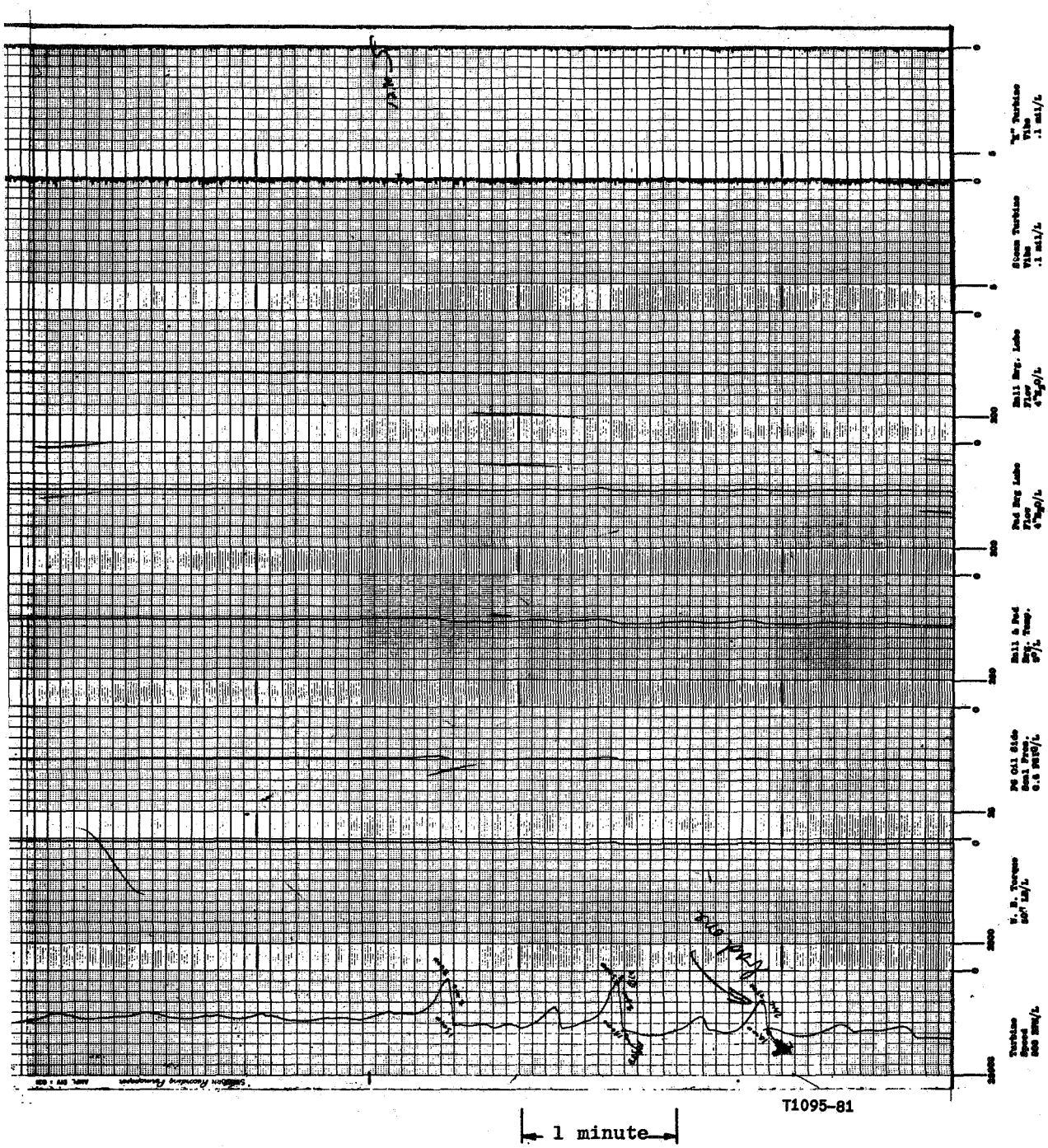
Figure 74. Rear Quarter of Completed Turbine Installation. T1095-80



Direction of
Travel of Recording Stylus

Figure 75. Continuous Chart Recording Speed Excursion.

PRECEDING PAGE BLANK NOT FILMED.



of Turbine Instrumentation During

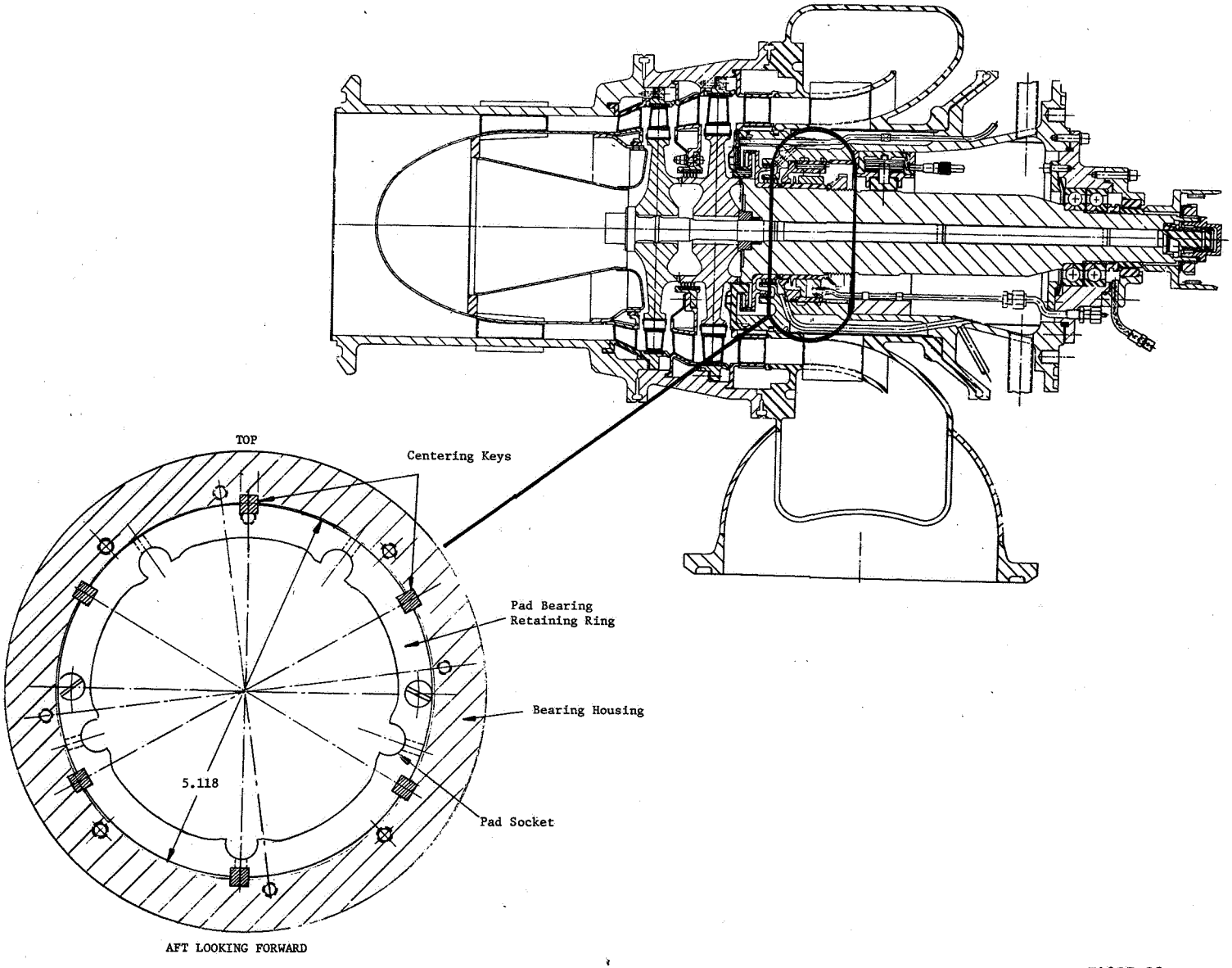


Figure 76. Radial Key Design and Double Ball Thrust Bearing

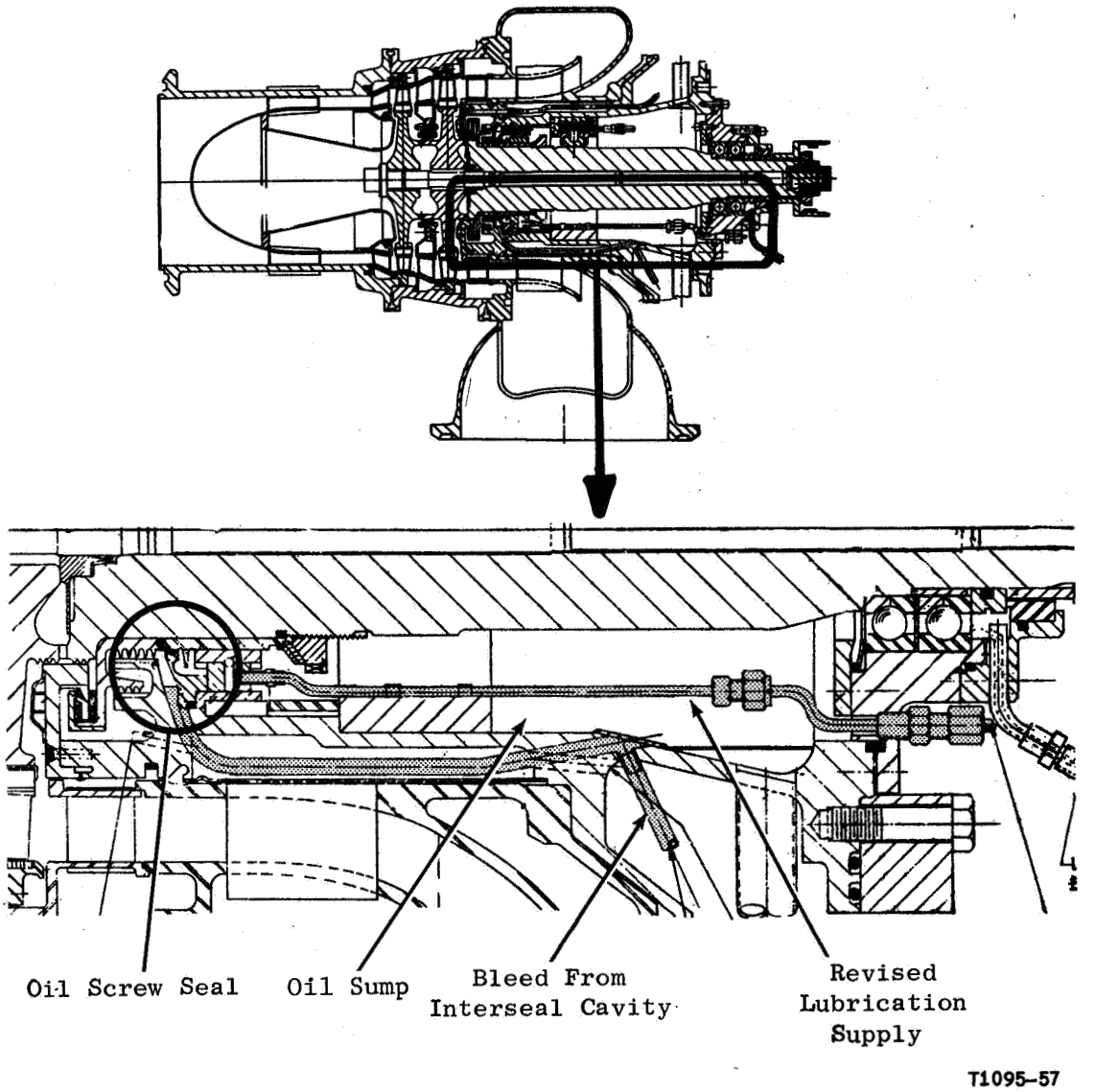


Figure 77. Design of Individually Fed Bearing Pads and Interseal Cavity Bleed Design.

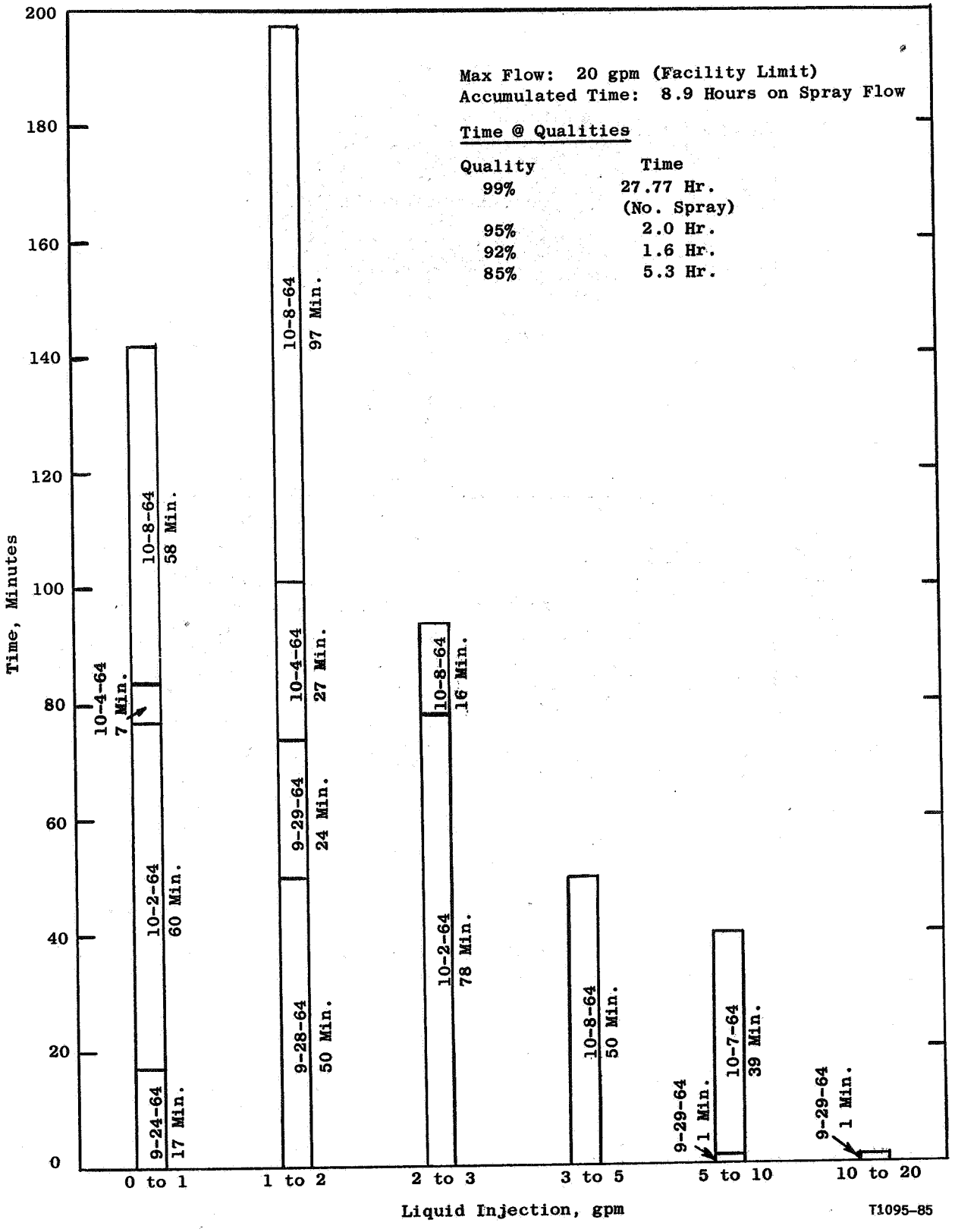


Figure 78. Time History of Potassium Liquid Injection into Turbine.

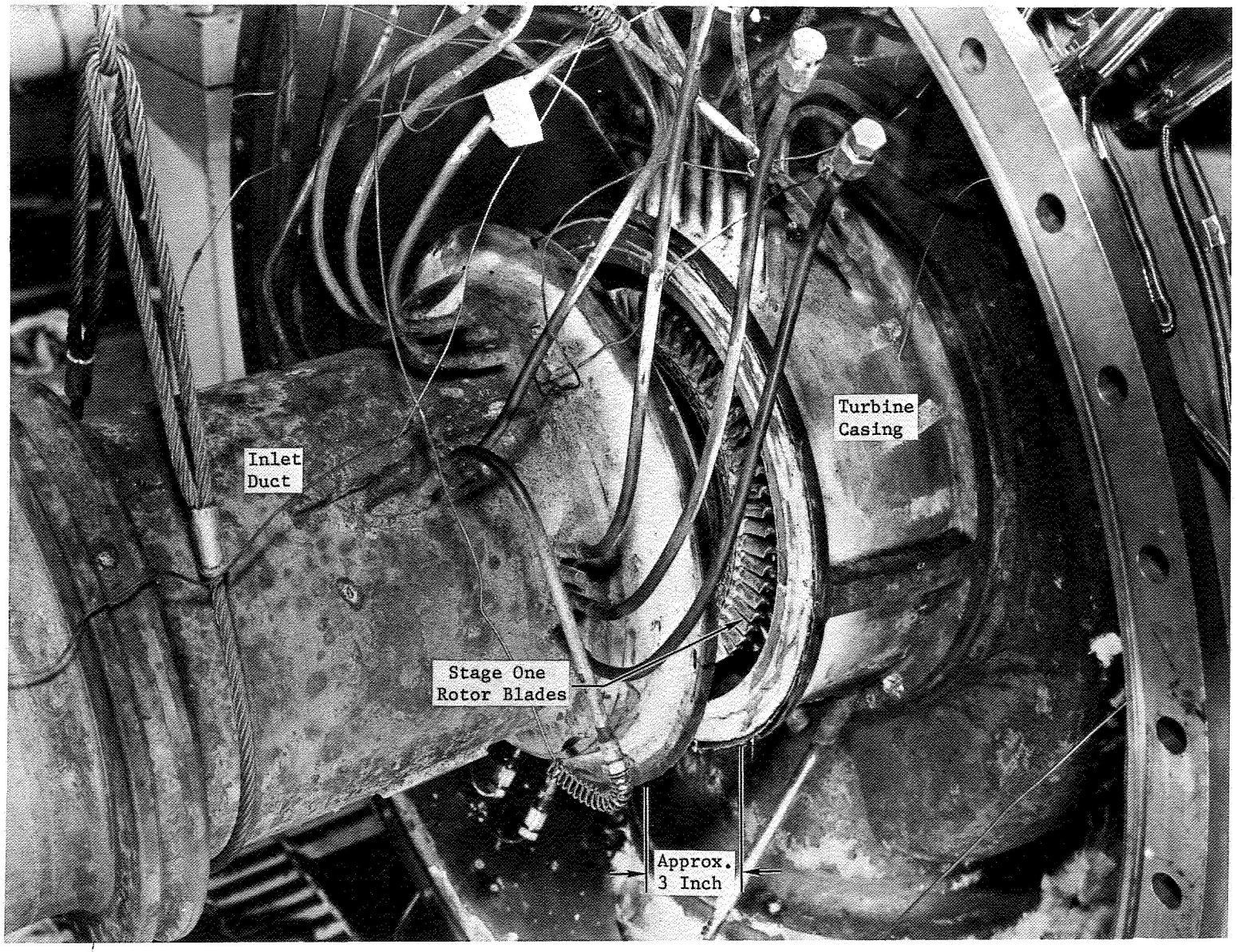


Figure 79. Turbine Following Opening of Forward Flange for Inspection After Initial Potassium Vapor Testing.

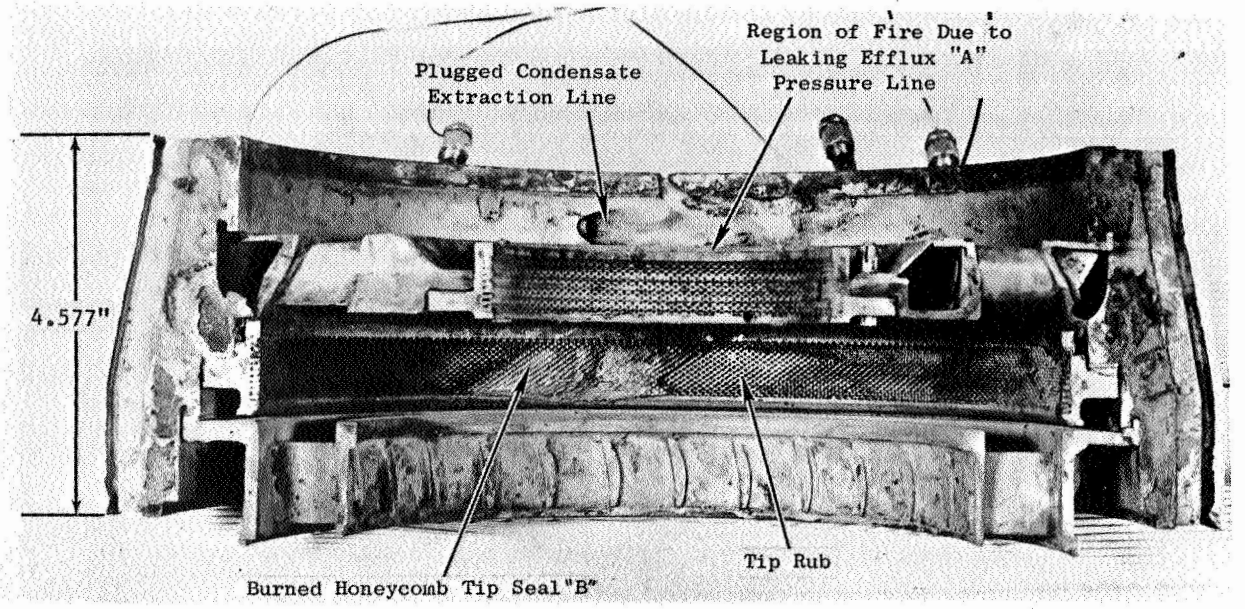


Figure 80a. Assembled Turbine Casing Half Removed From Turbine After Potassium Vapor Testing.

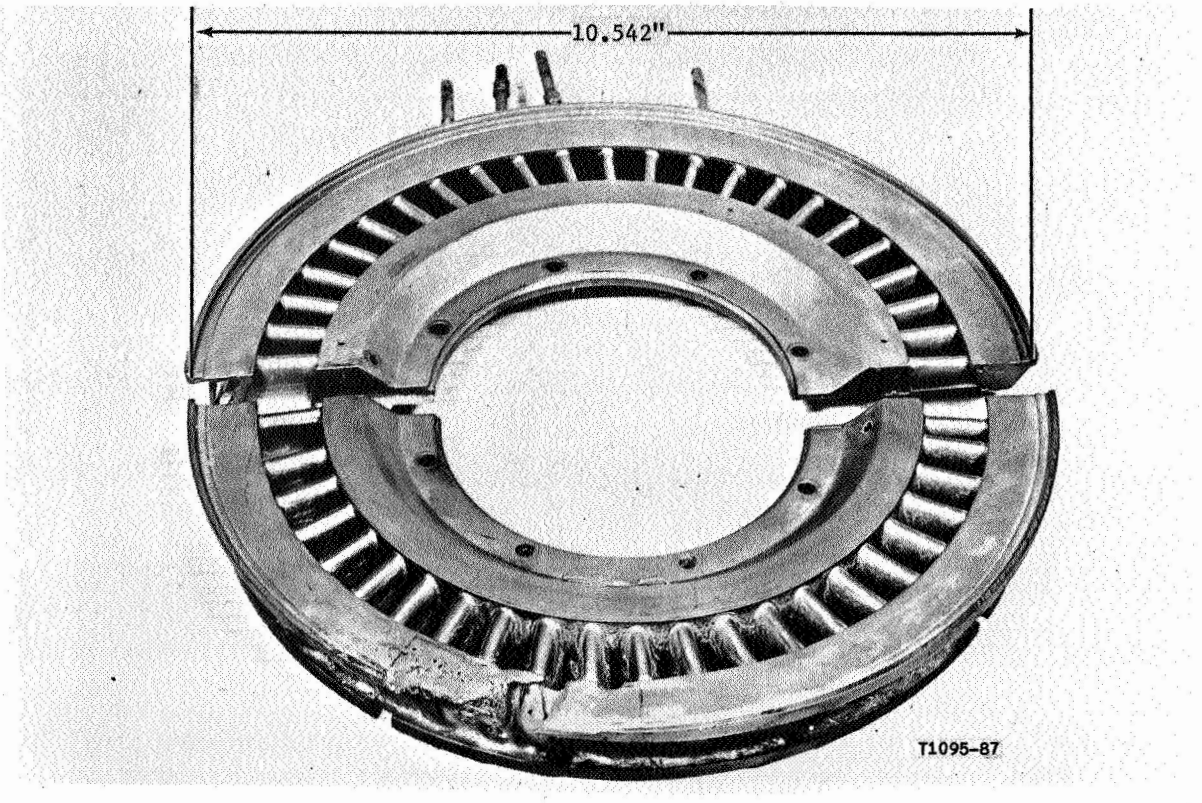


Figure 80b. Stage 2 Nozzle Diaphragm Upon Removal From Casing After Potassium Vapor Testing.

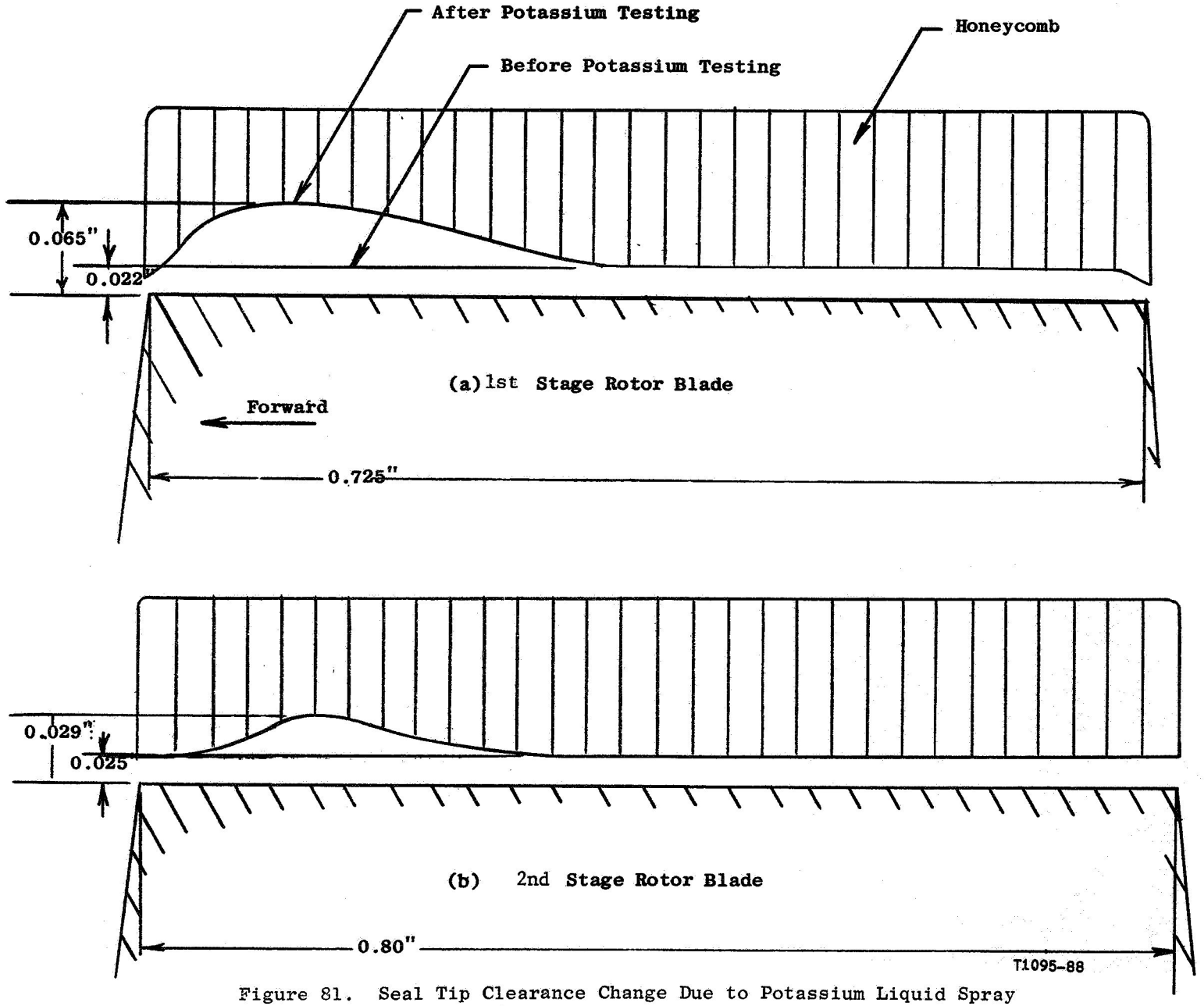


Figure 81. Seal Tip Clearance Change Due to Potassium Liquid Spray Injection Performance Testing.

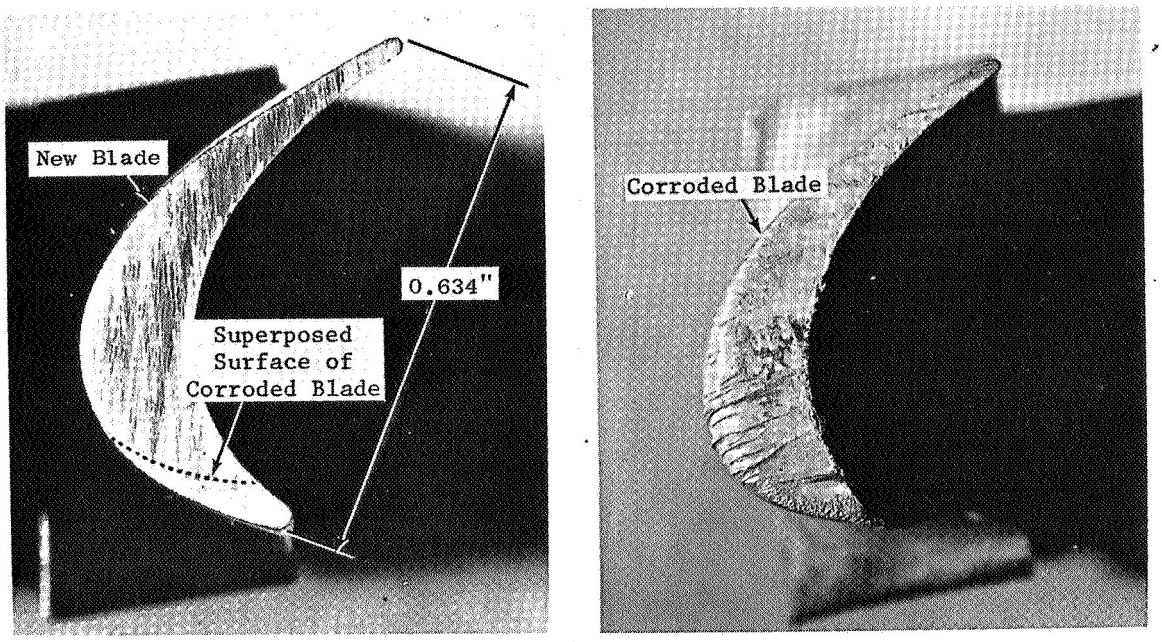


Figure 82a. Comparison of Tip Section of First Stage Blade Before and After 35 Hour Turbine Checkout

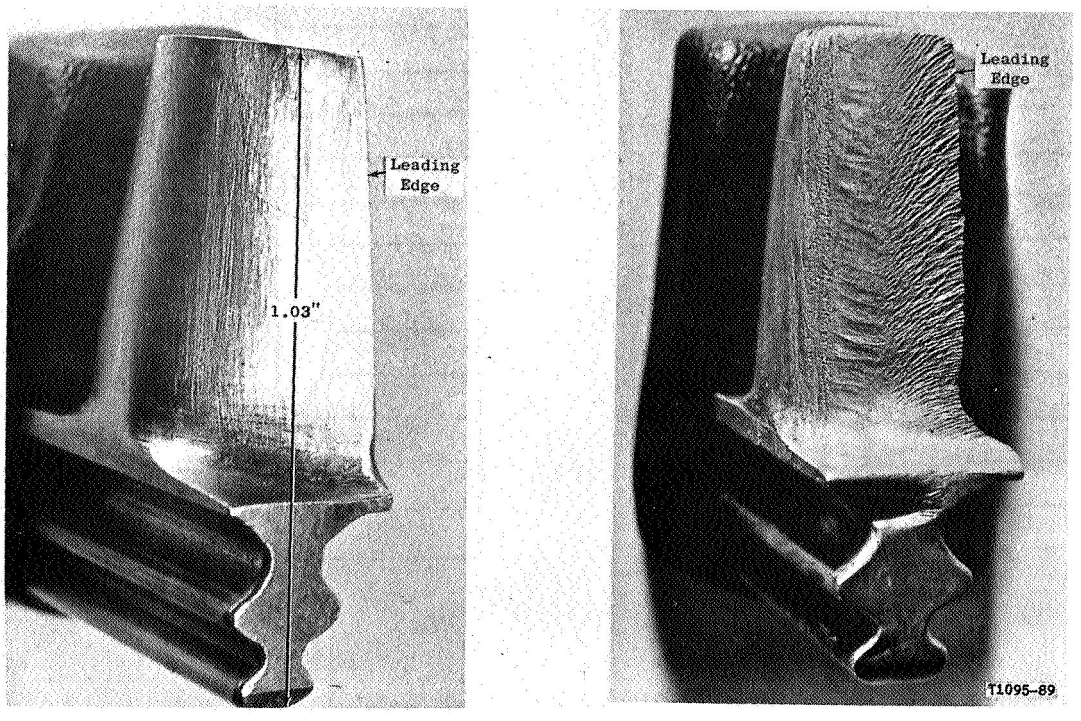


Figure 82b. Comparison of a First Stage Blade Before and After 35 Hour Turbine Checkout.

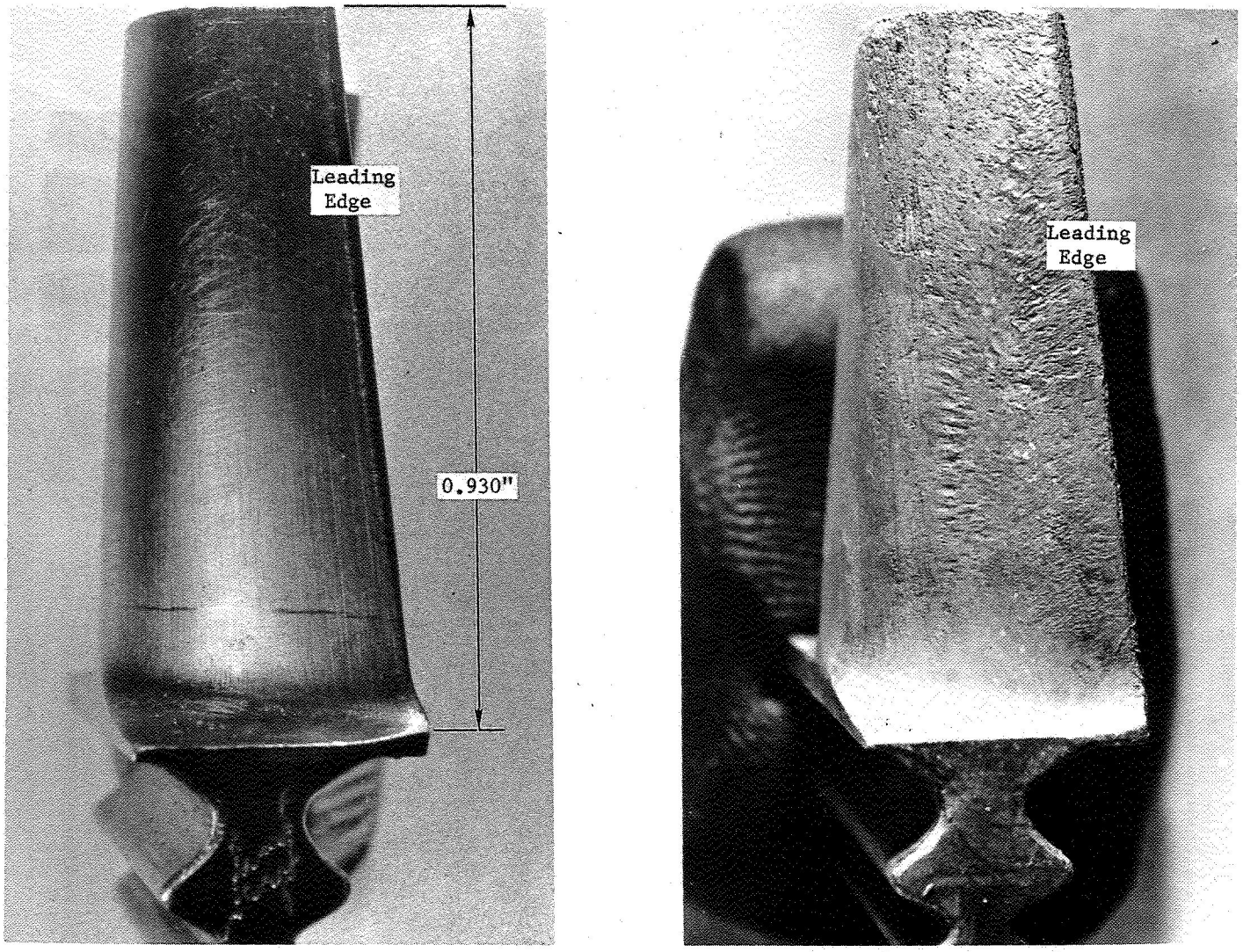


Figure 82c. Comparison of a Second Stage Blade Before and After 35 Hour Turbine Checkout.

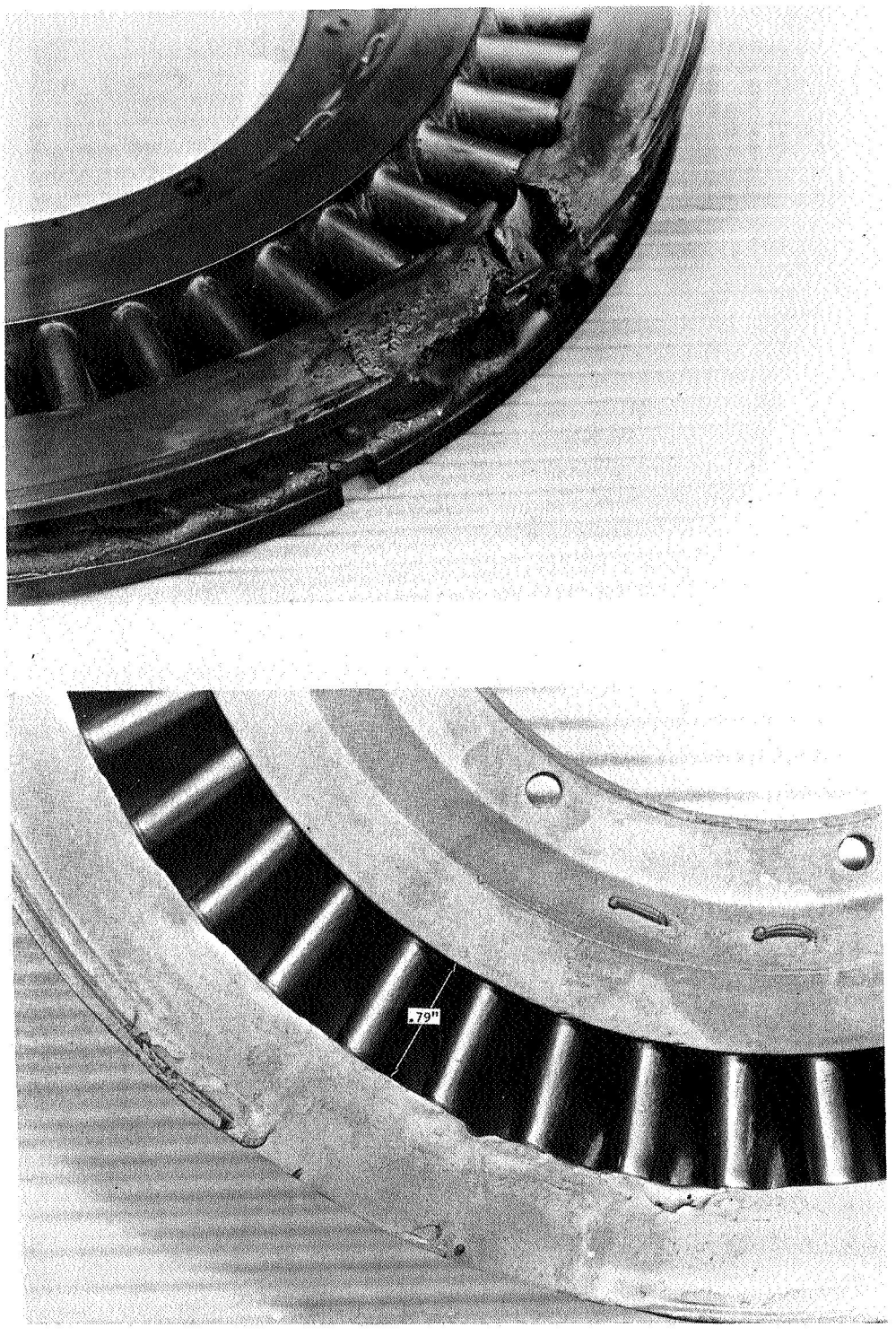


Figure 83. Stage 2 Nozzle Diaphragm Outer Shroud Fire Damage and Subsequent Repair.

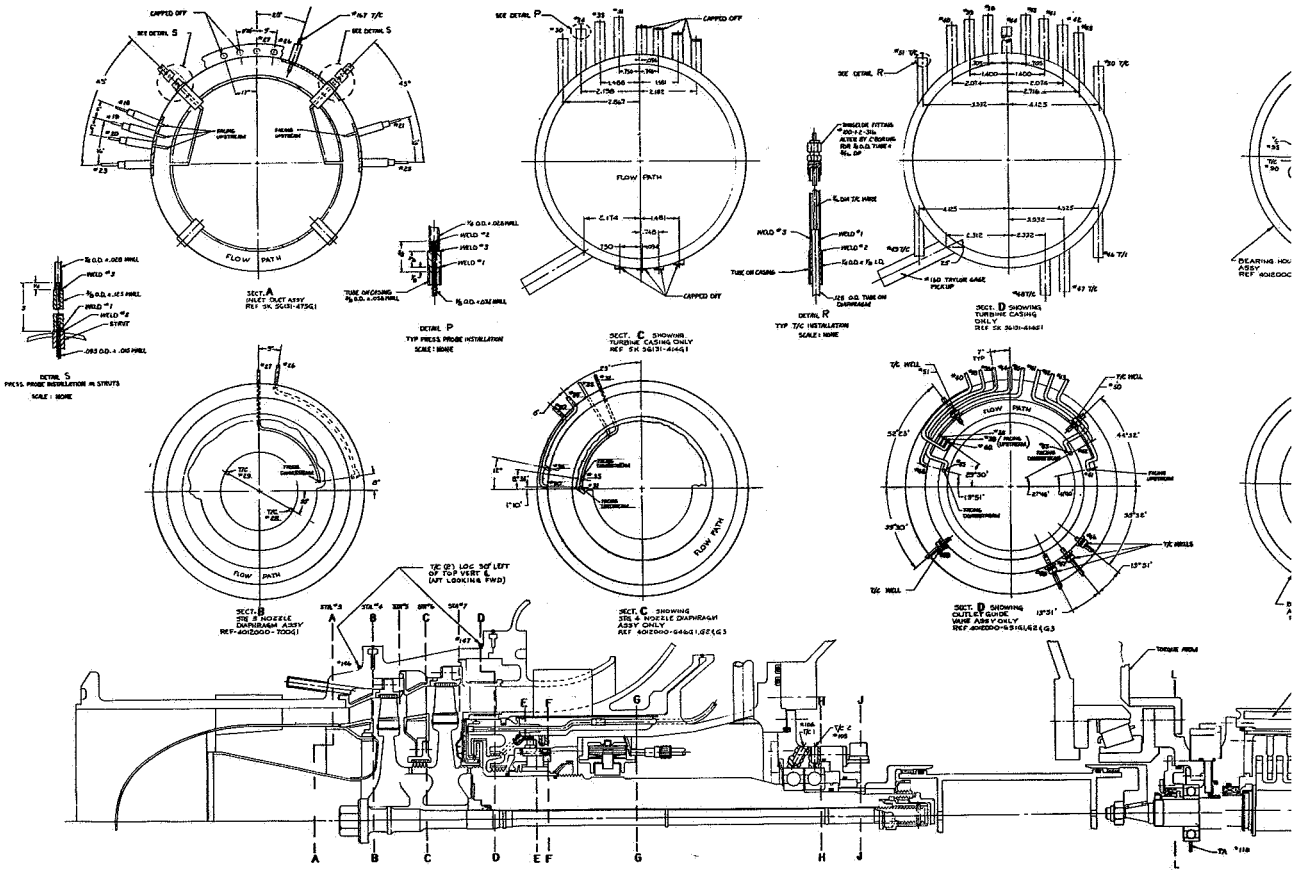
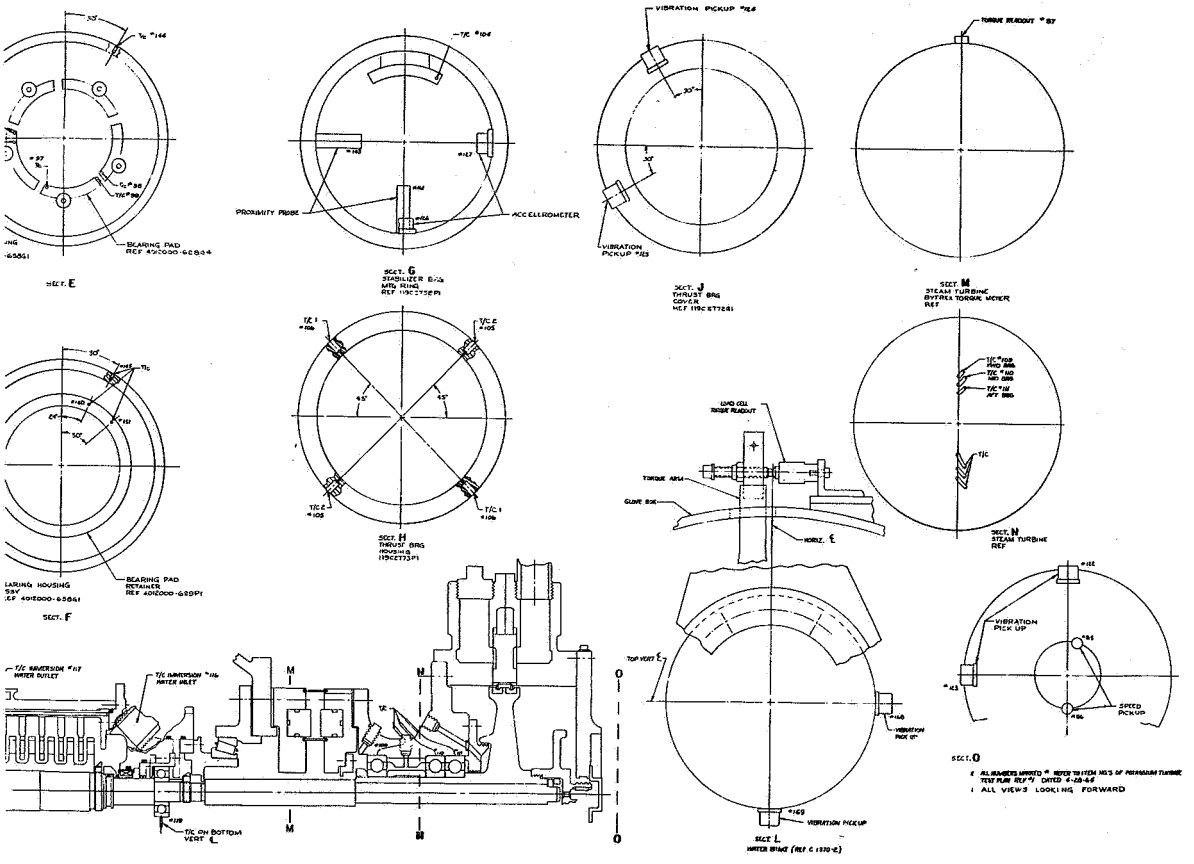


Figure 84. Instrumentation

PRECEDING PAGE BLANK NOT FILMED.



for Performance Testing.

T1095-91

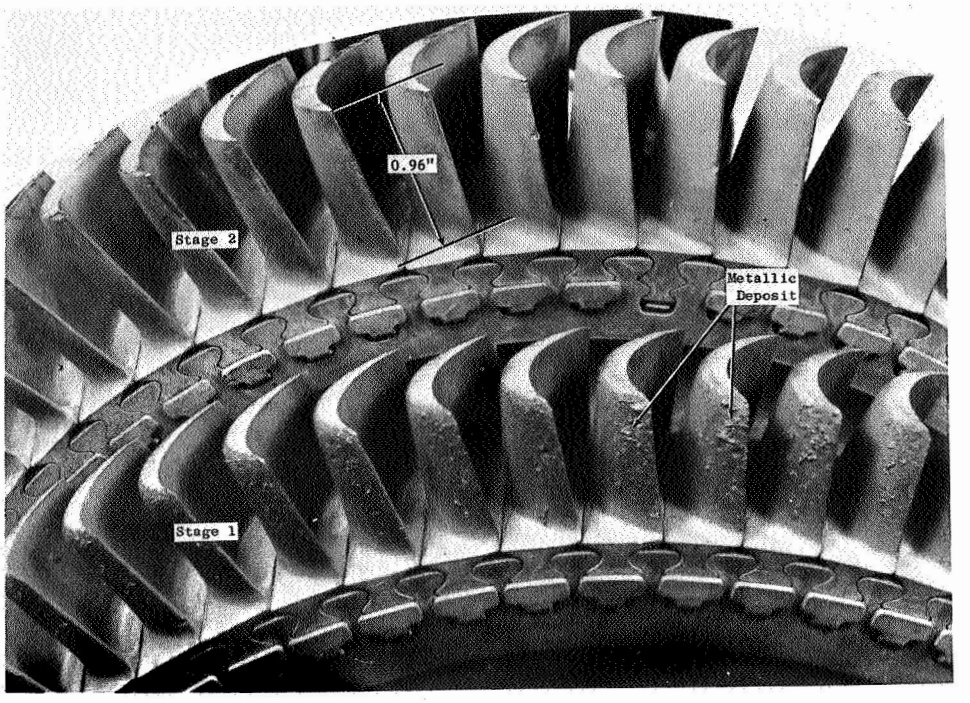


Figure 85a. First and Second Stage Blades Showing Metallic Deposit After Performance Testing of May, 1965.

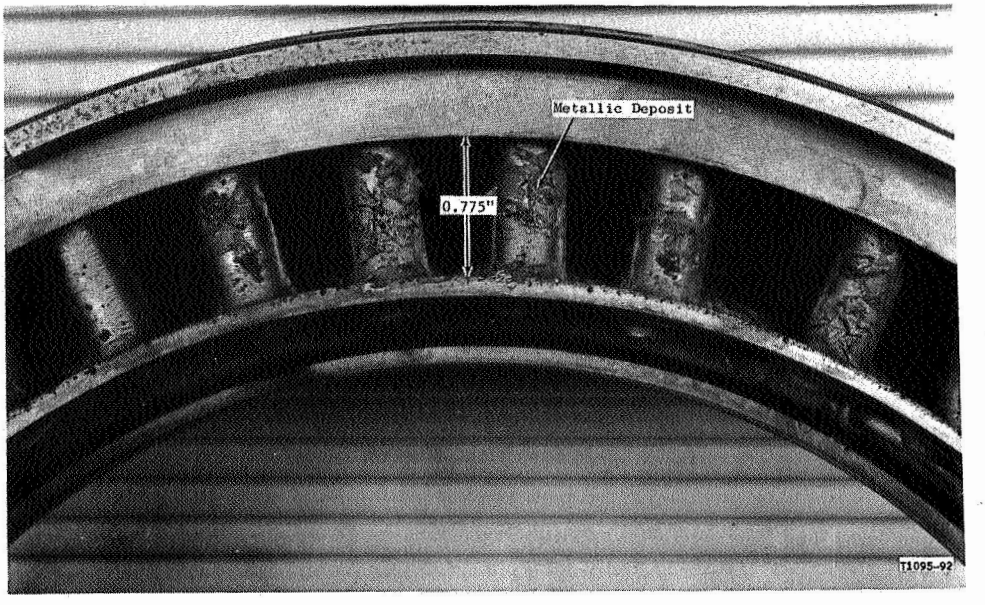


Figure 85b. Leading Edge of Stage 1 Nozzle Blades Showing Metallic Deposit After Performance Testing of May, 1965.

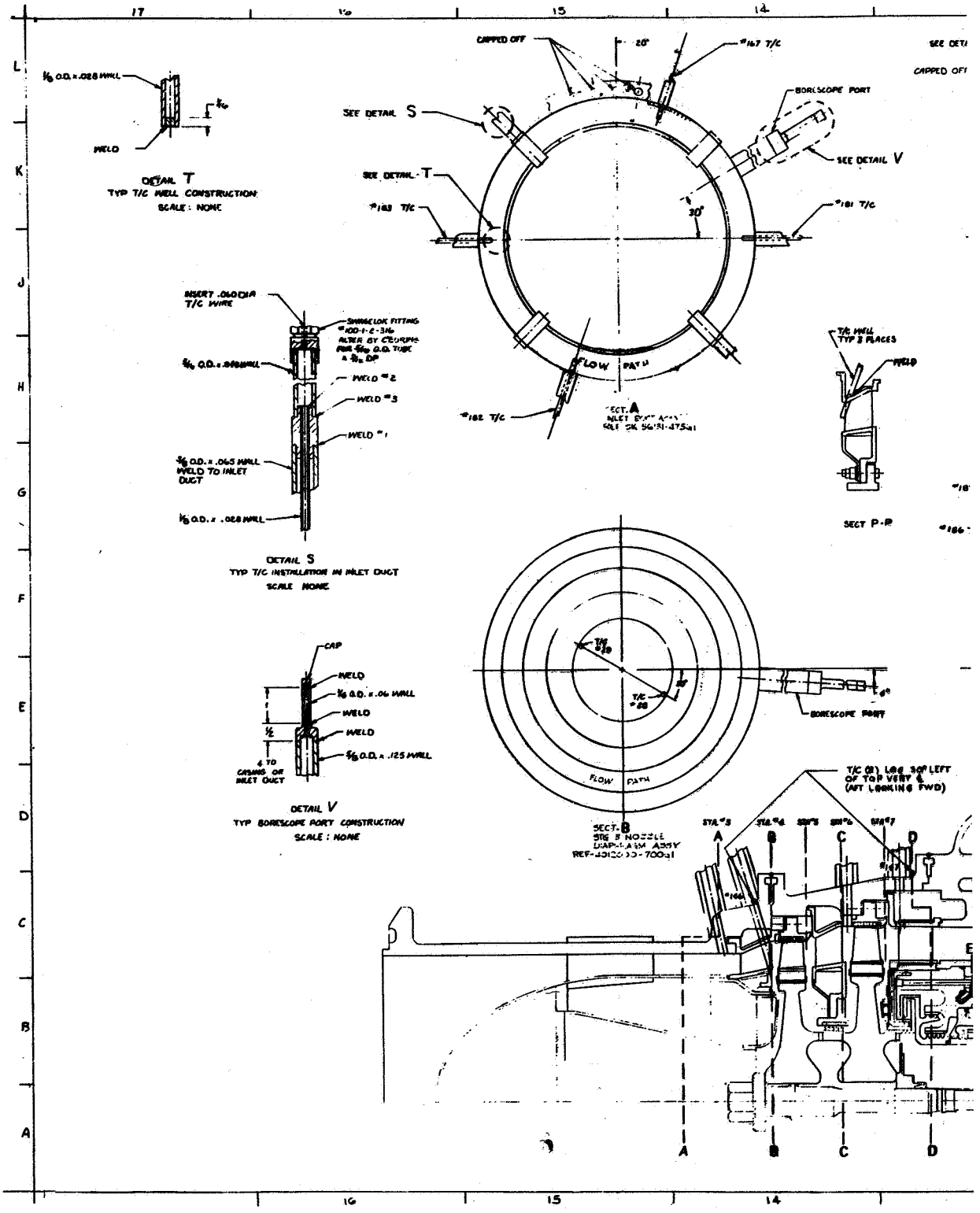
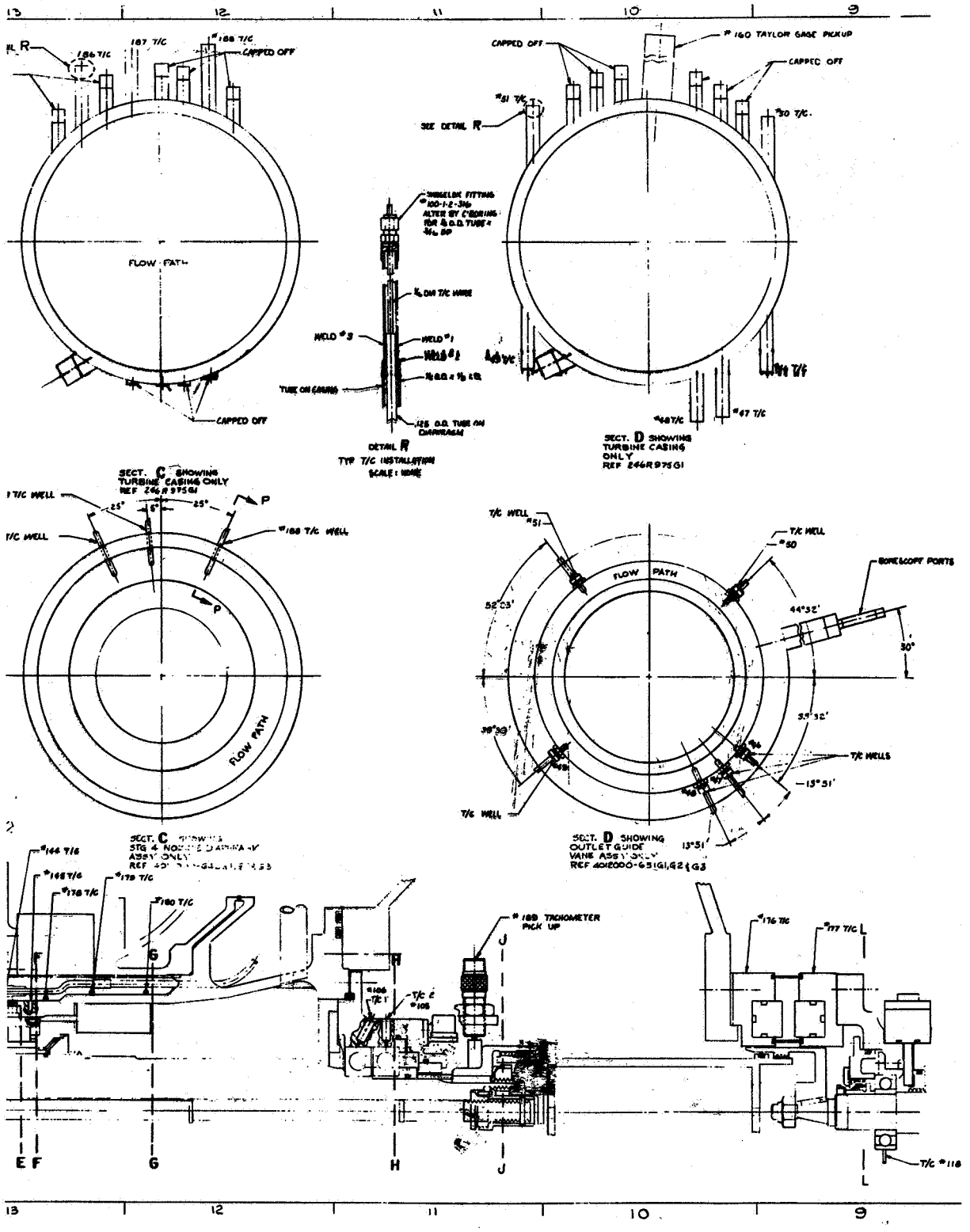


Figure 86. Instrumentation

PRECEDING PAGE BLANK NOT FILMED.



for Endurance Testing.

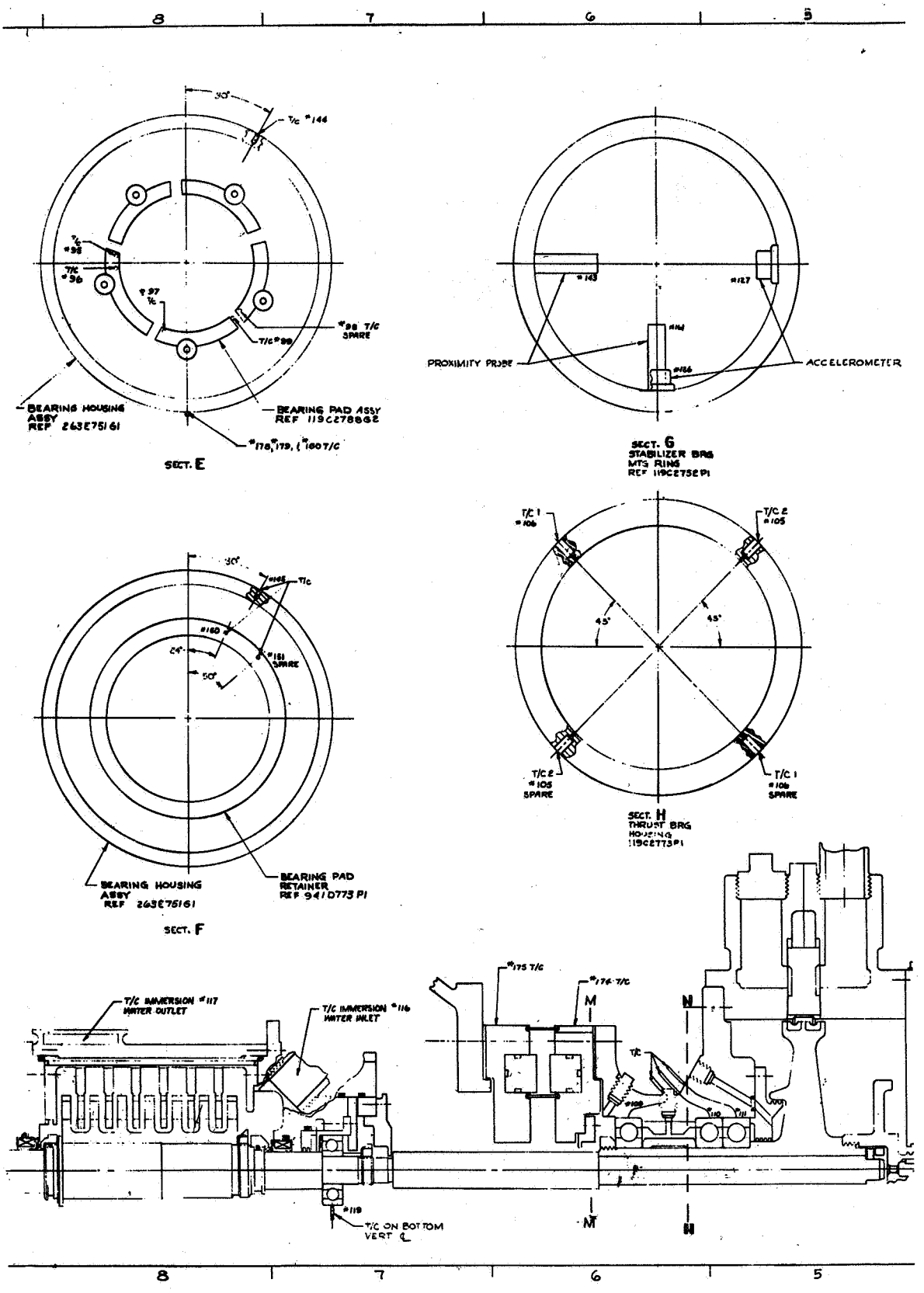
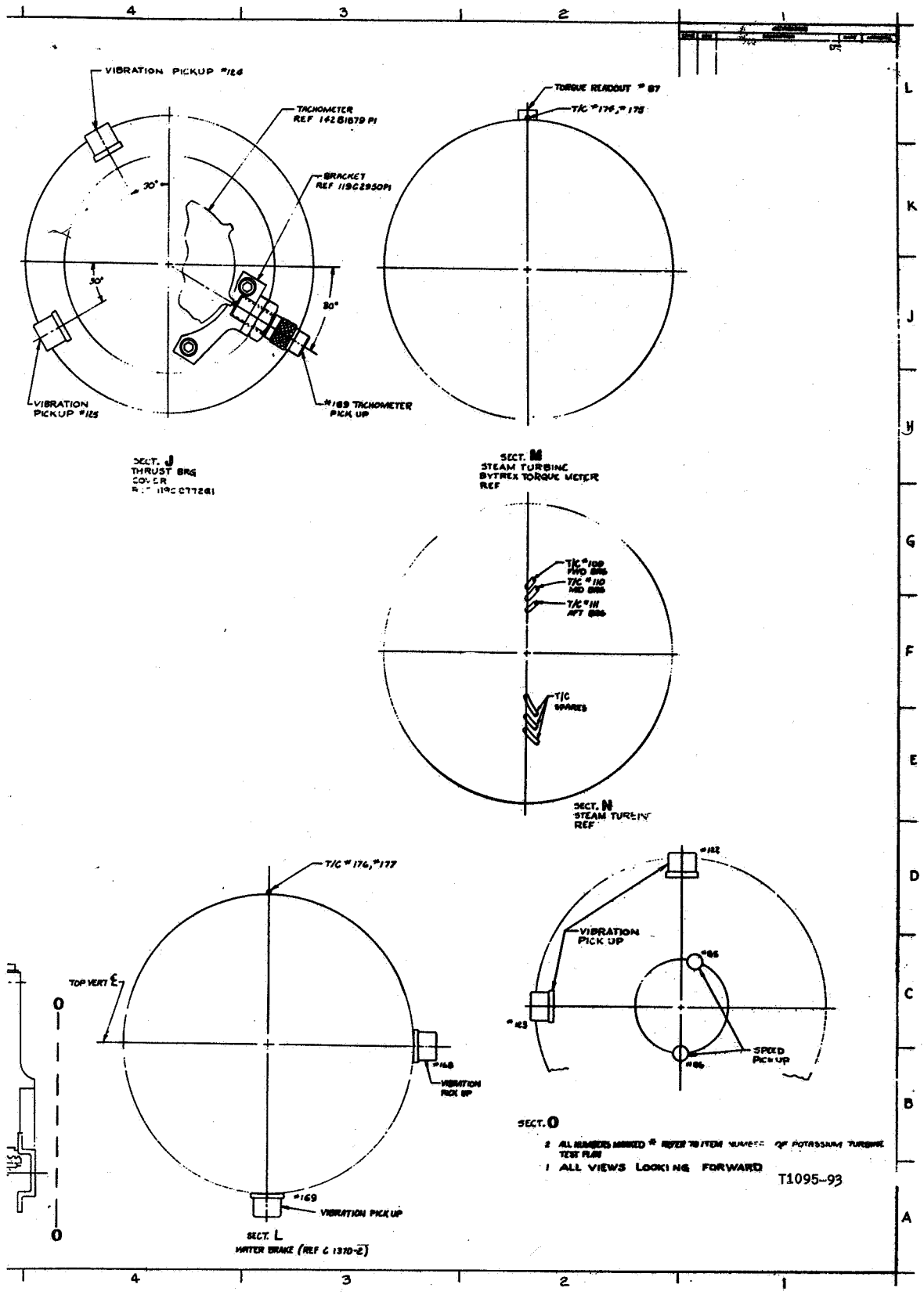


Figure 86. Concluded.



nstrumentation for Endurance Testing.

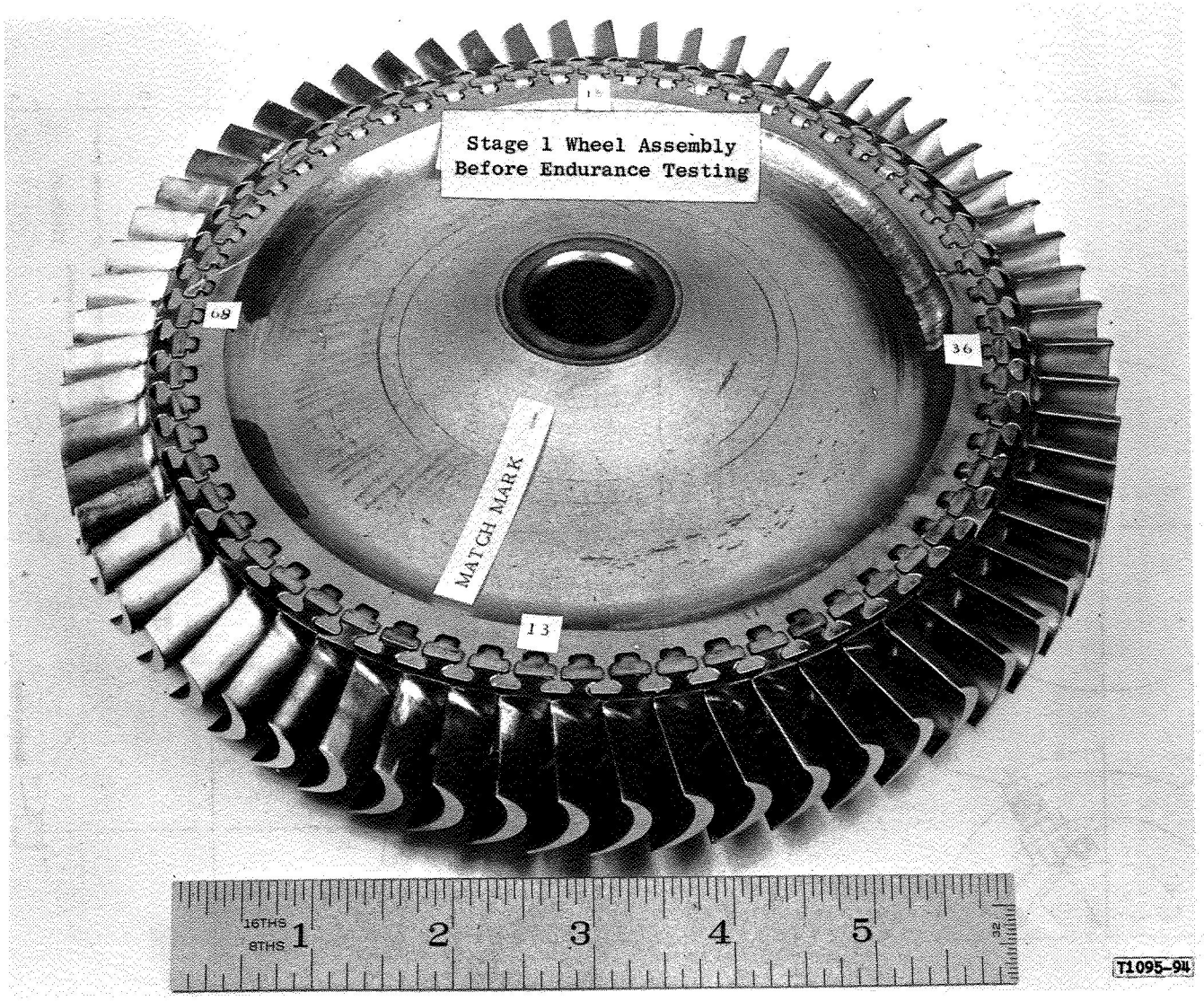


Figure 87. Stage 1 Wheel Assembly Before Endurance Testing.

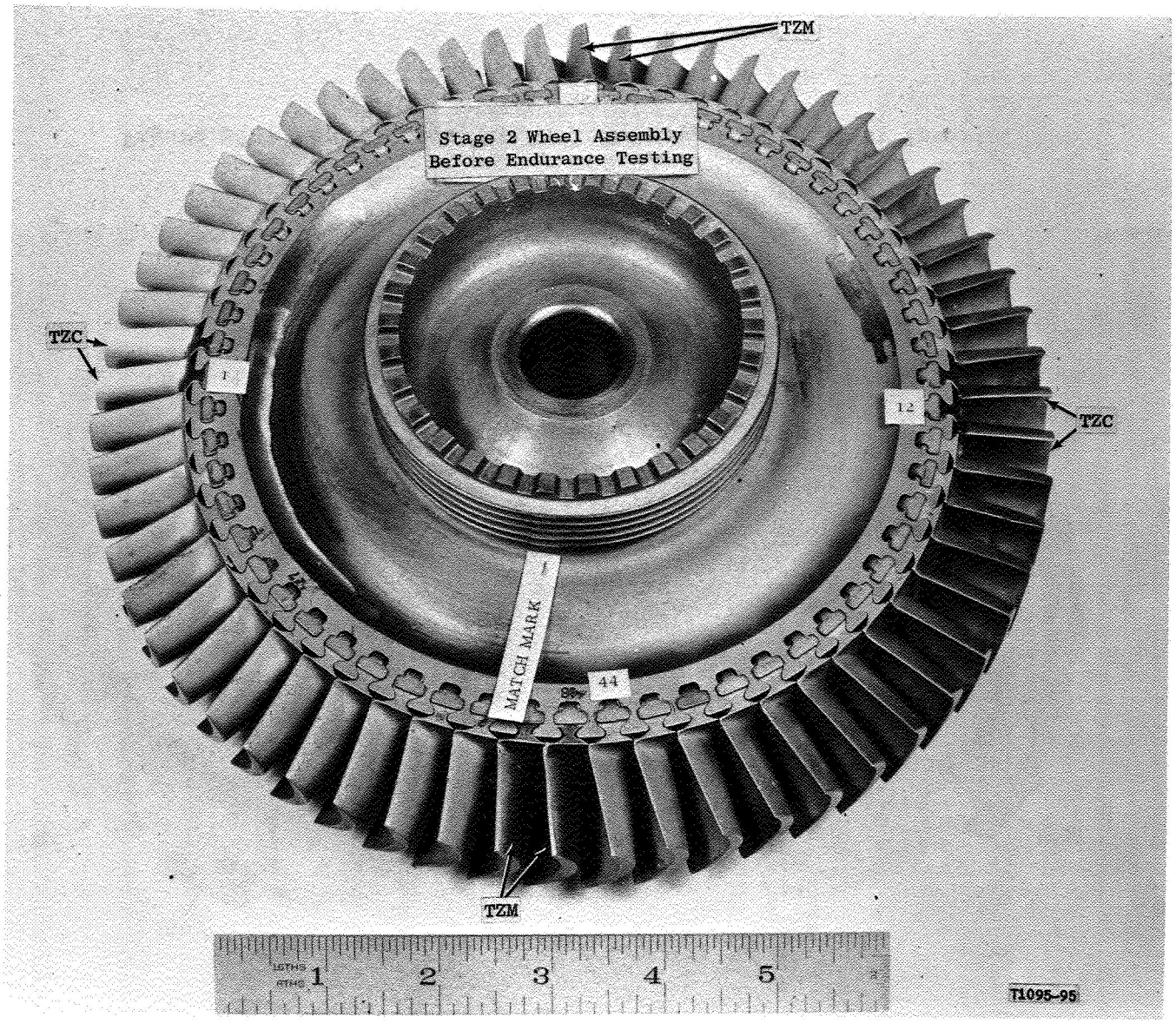


Figure 88. Stage 2 Wheel Assembly Before Endurance Testing.

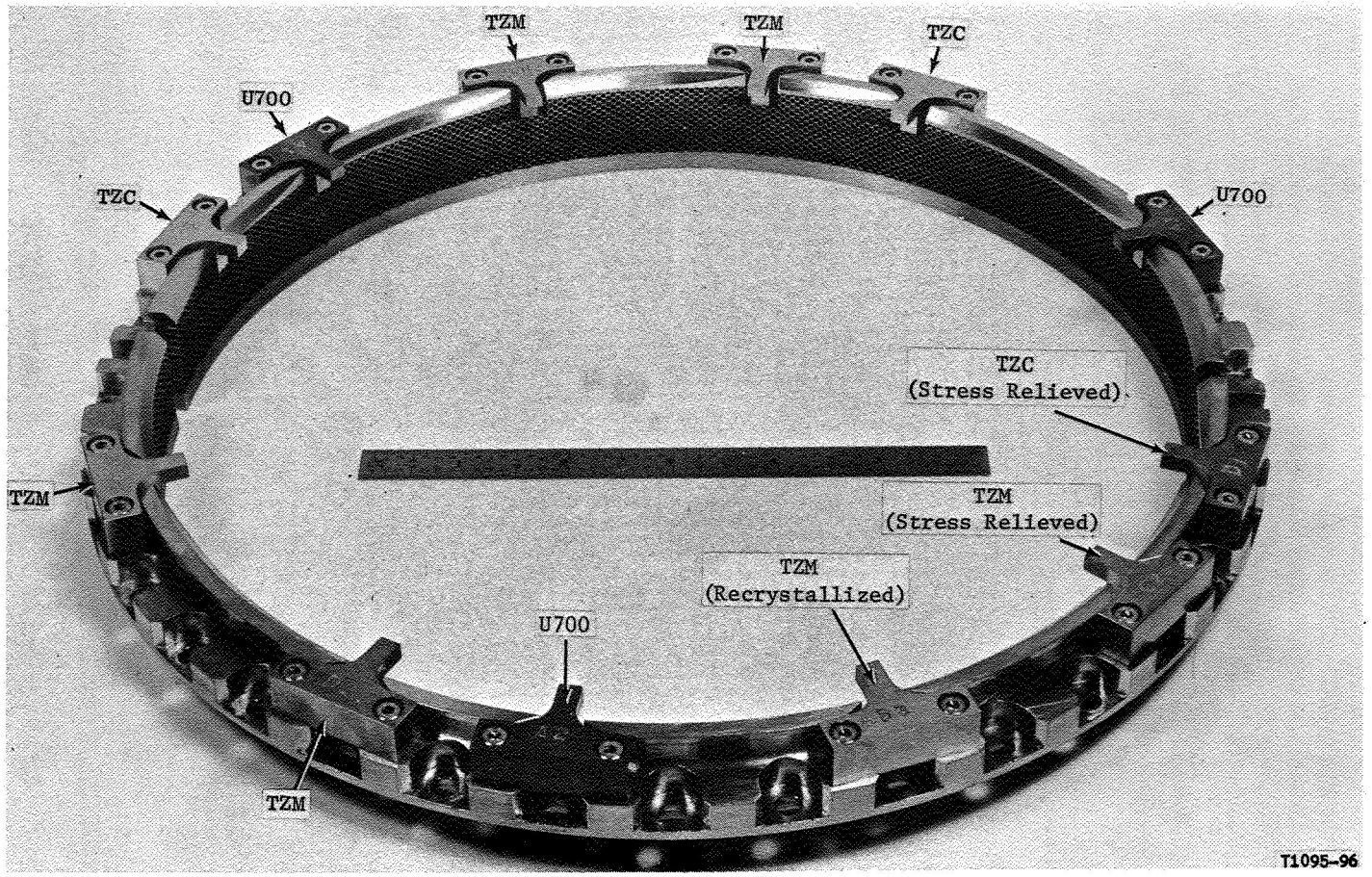


Figure 89. Second Stage Tip Seal Showing Material Test Inserts.

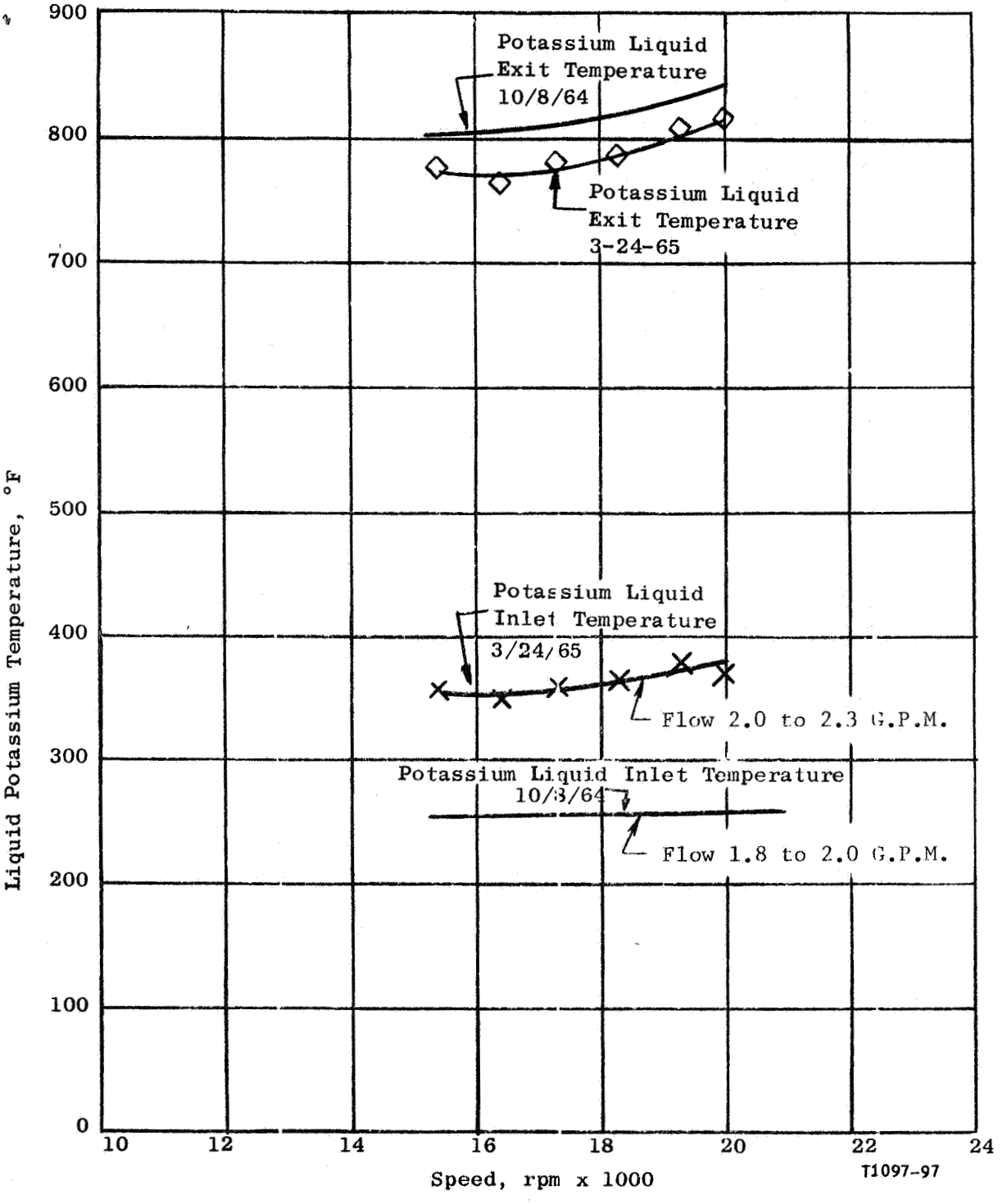


Figure 90. Hydrodynamic Seal Liquid Potassium Temperatures During Performance Test of 3/24/65.

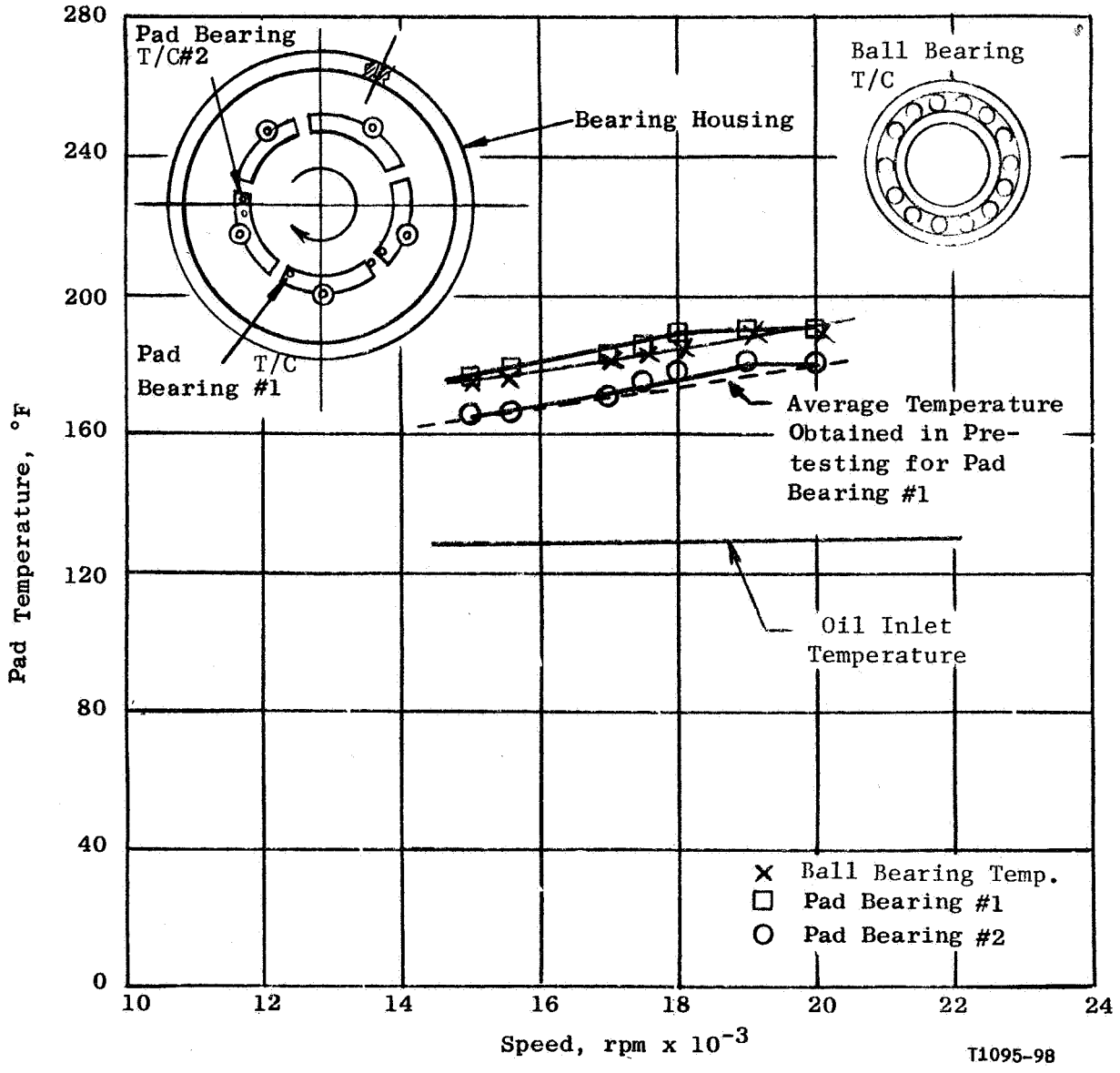


Figure 91. Pad Bearing Temperatures During Performance Test of 3/24/65.

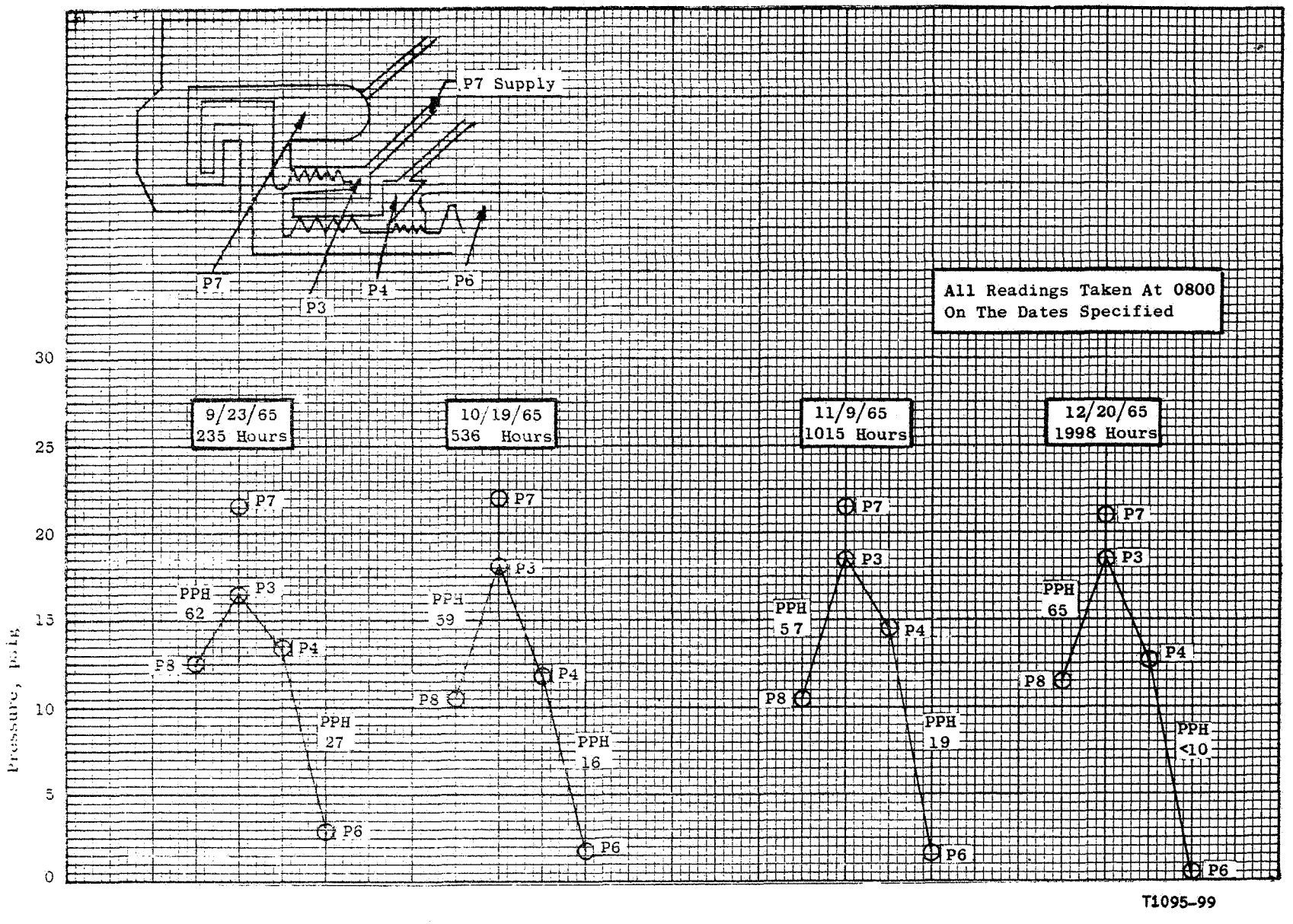
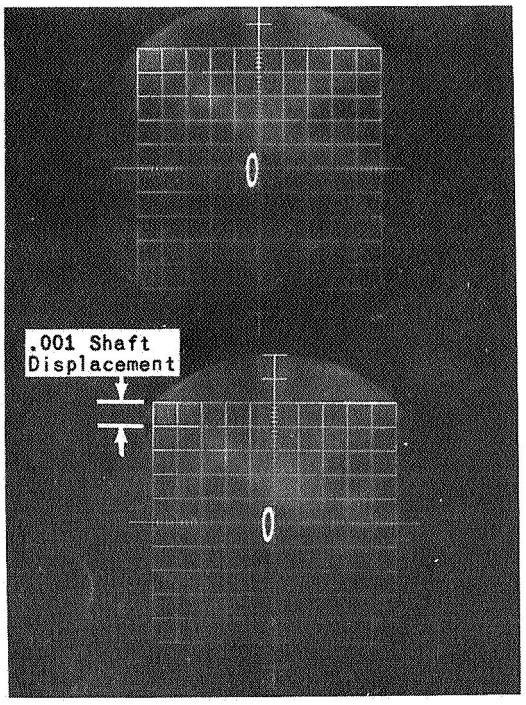
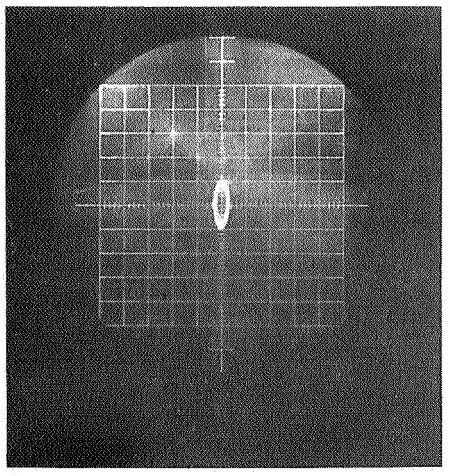


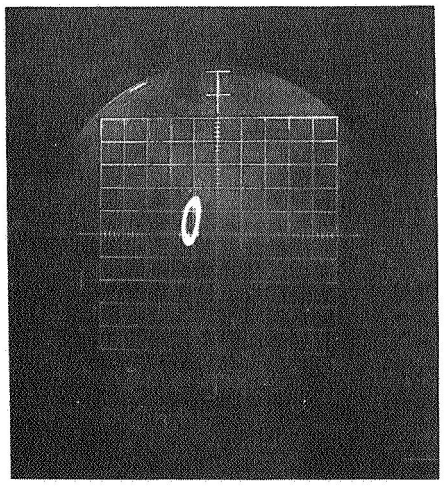
Figure 92. Seal Cavity Pressures During Endurance Testing.



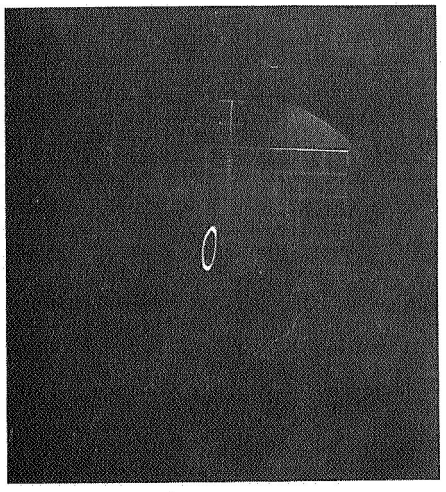
Accumulated Endurance
Test Time 351 Hours



Accumulated Endurance
Test Time 543 Hours



Accumulated Endurance
Test Time 1383 Hours



Accumulated Endurance
Test Time 2000 Hours

T1095-100

Figure 93. Oscilloscope Trace Showing Rotor Shaft Excursion During Endurance Testing in September, October, November and December, 1965.

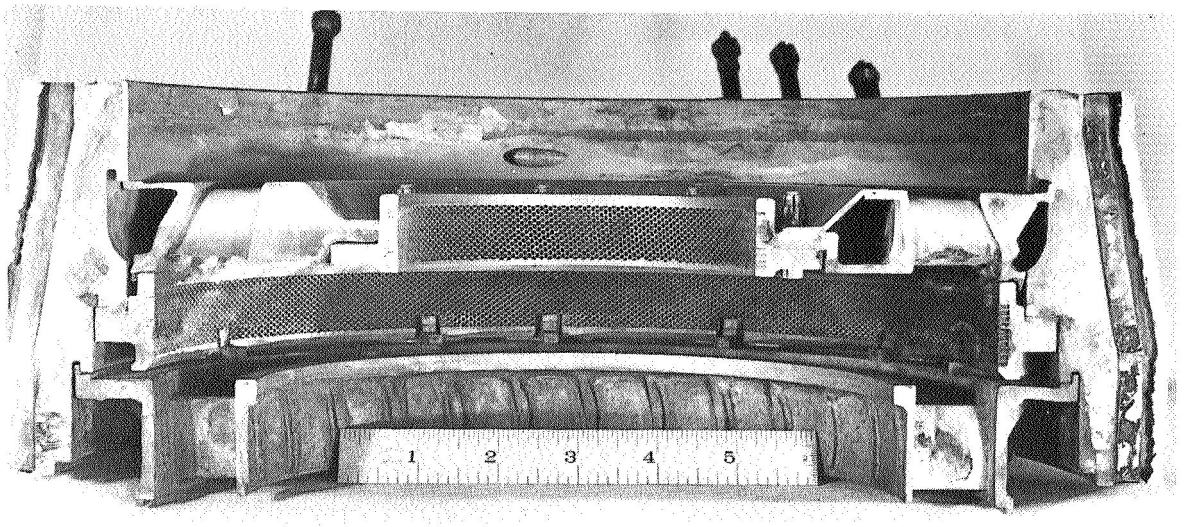


Figure 94a. Top Half of Turbine Casing Assembly After 2000 Hour Endurance Test.

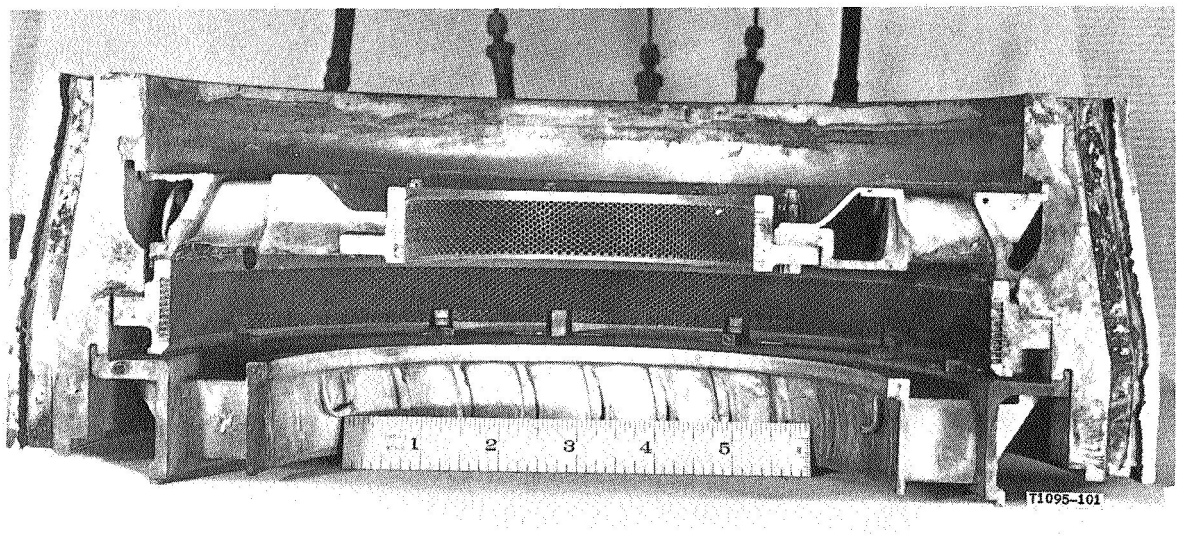


Figure 94b. Bottom Half of Turbine Casing Assembly After 2000 Hour Endurance Test.

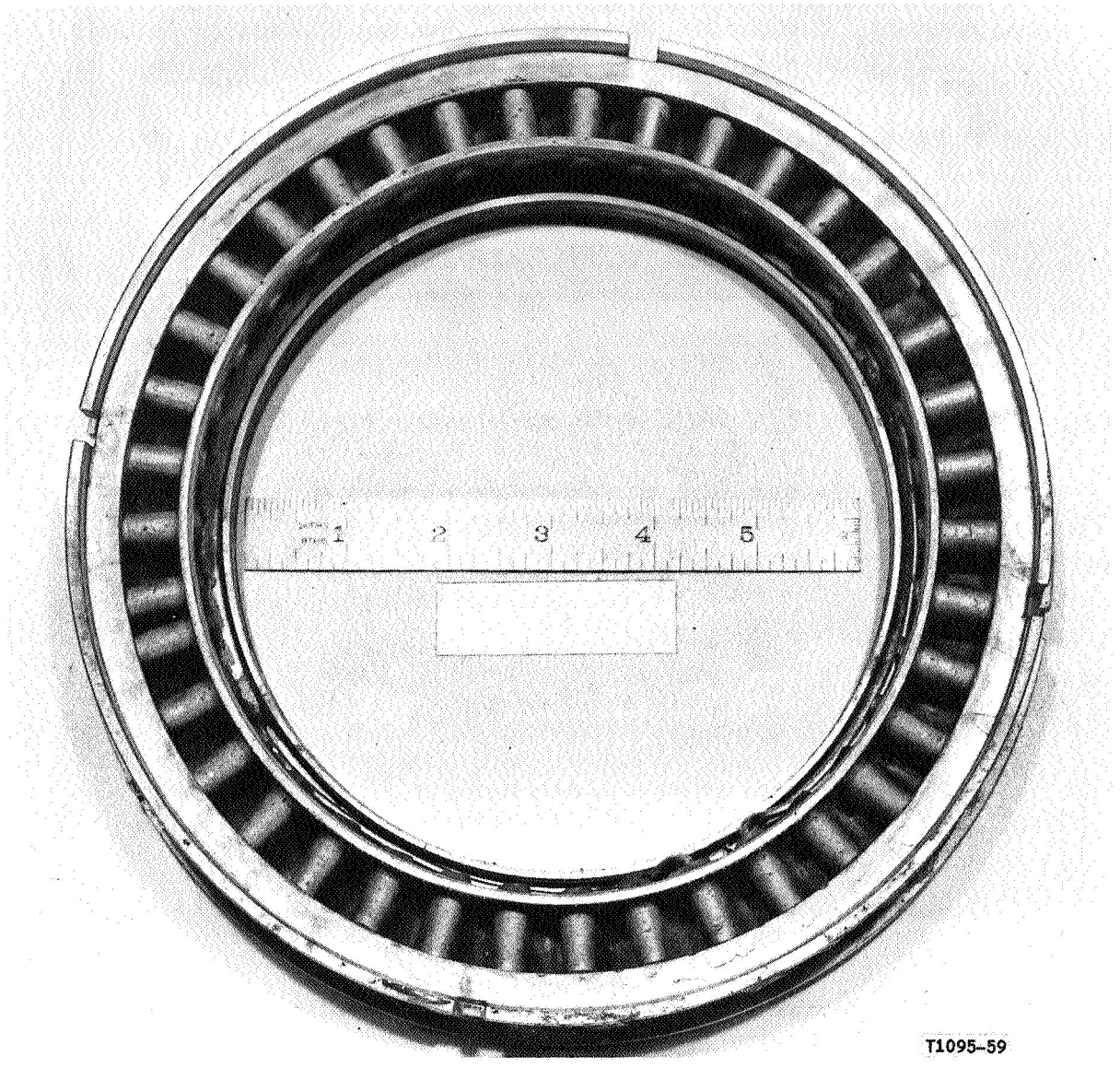


Figure 95. First Stage Nozzle Diaphragm (Inlet Side) After 2000 Endurance Test.

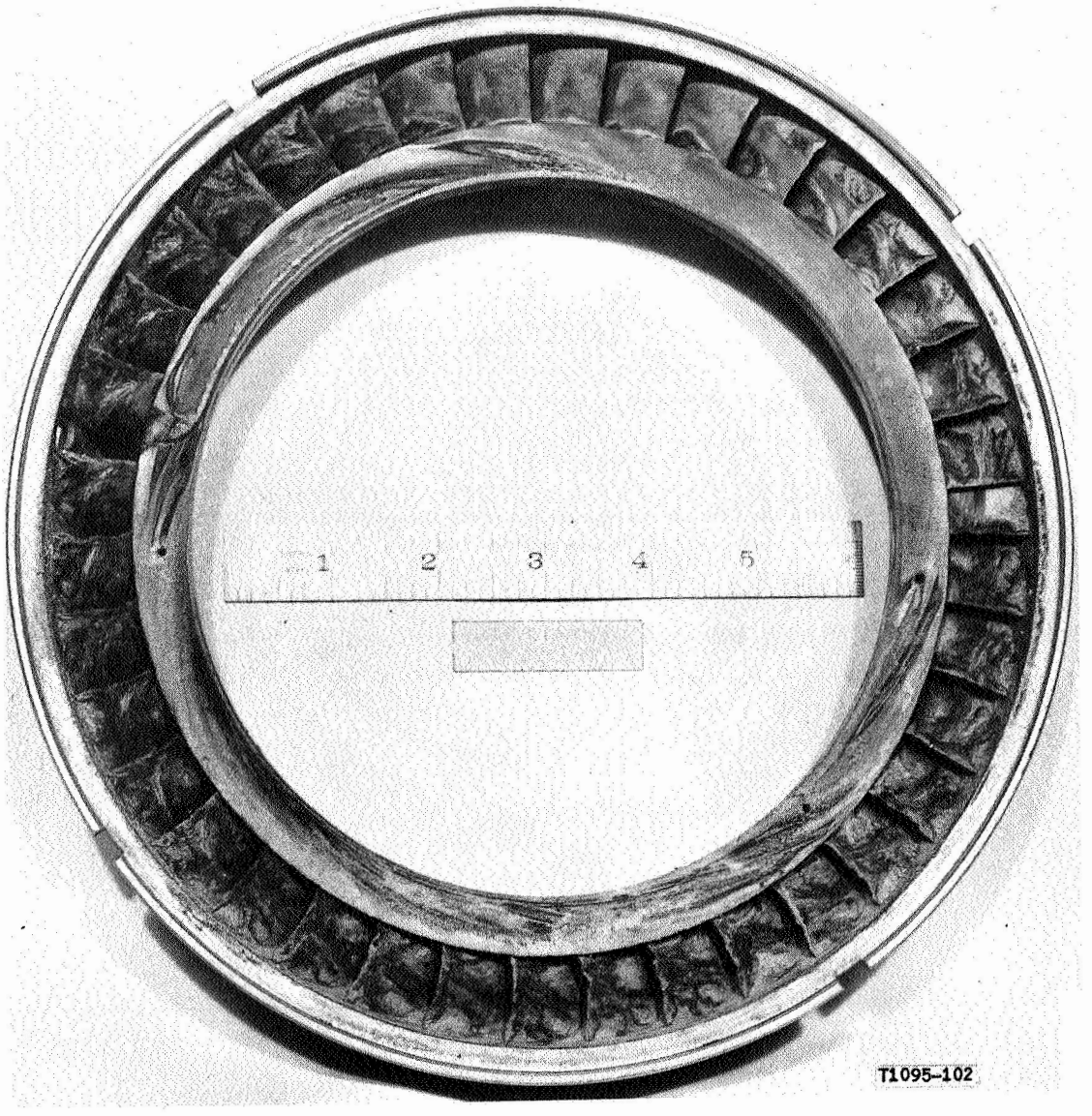


Figure 96. First Stage Nozzle Diaphragm (Outlet Side) After 2000 Hour Endurance Test.

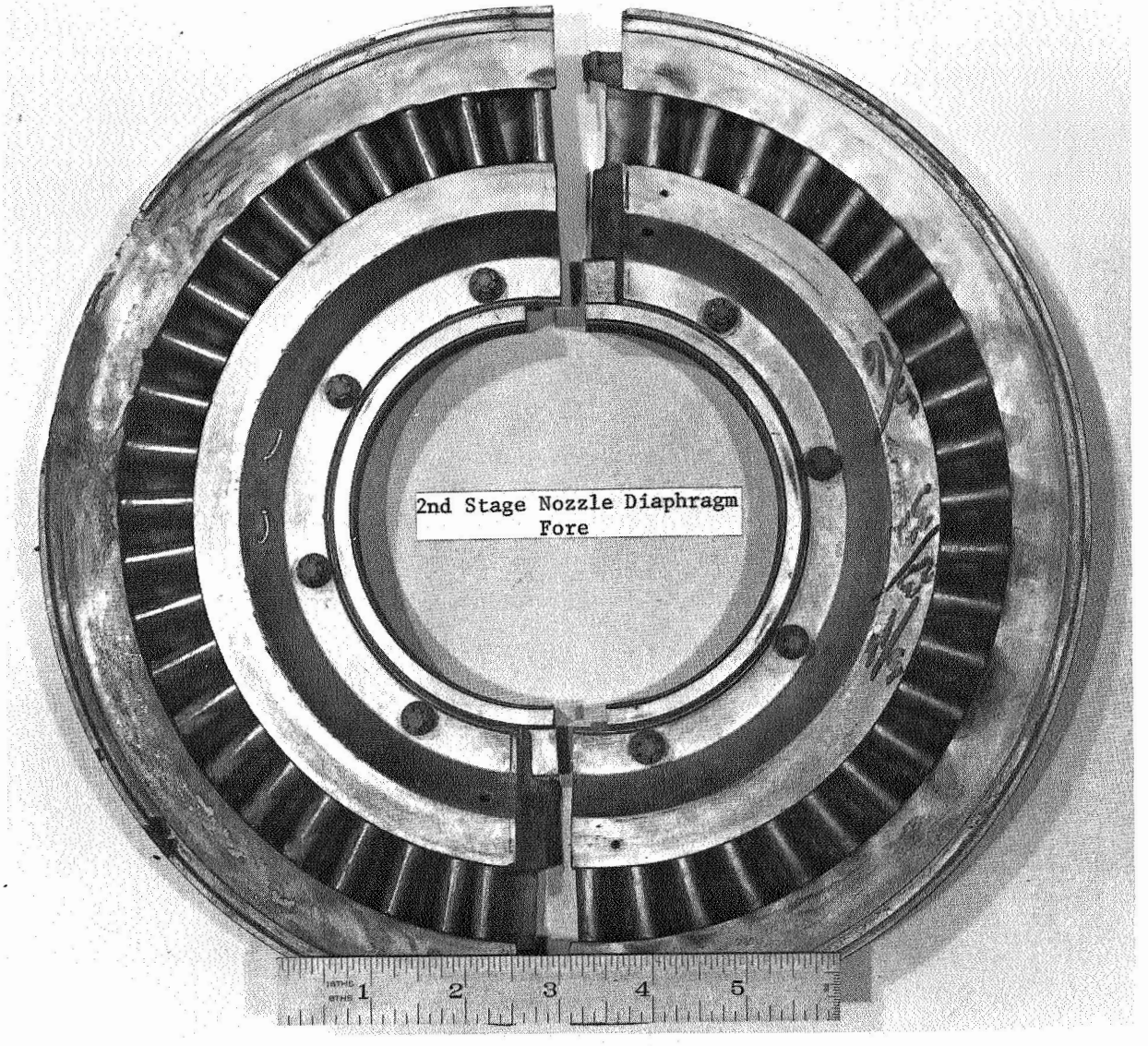


Figure 97a. Second Stage Nozzle Diaphragm (Inlet Side) After 2000 Hour Endurance Test.

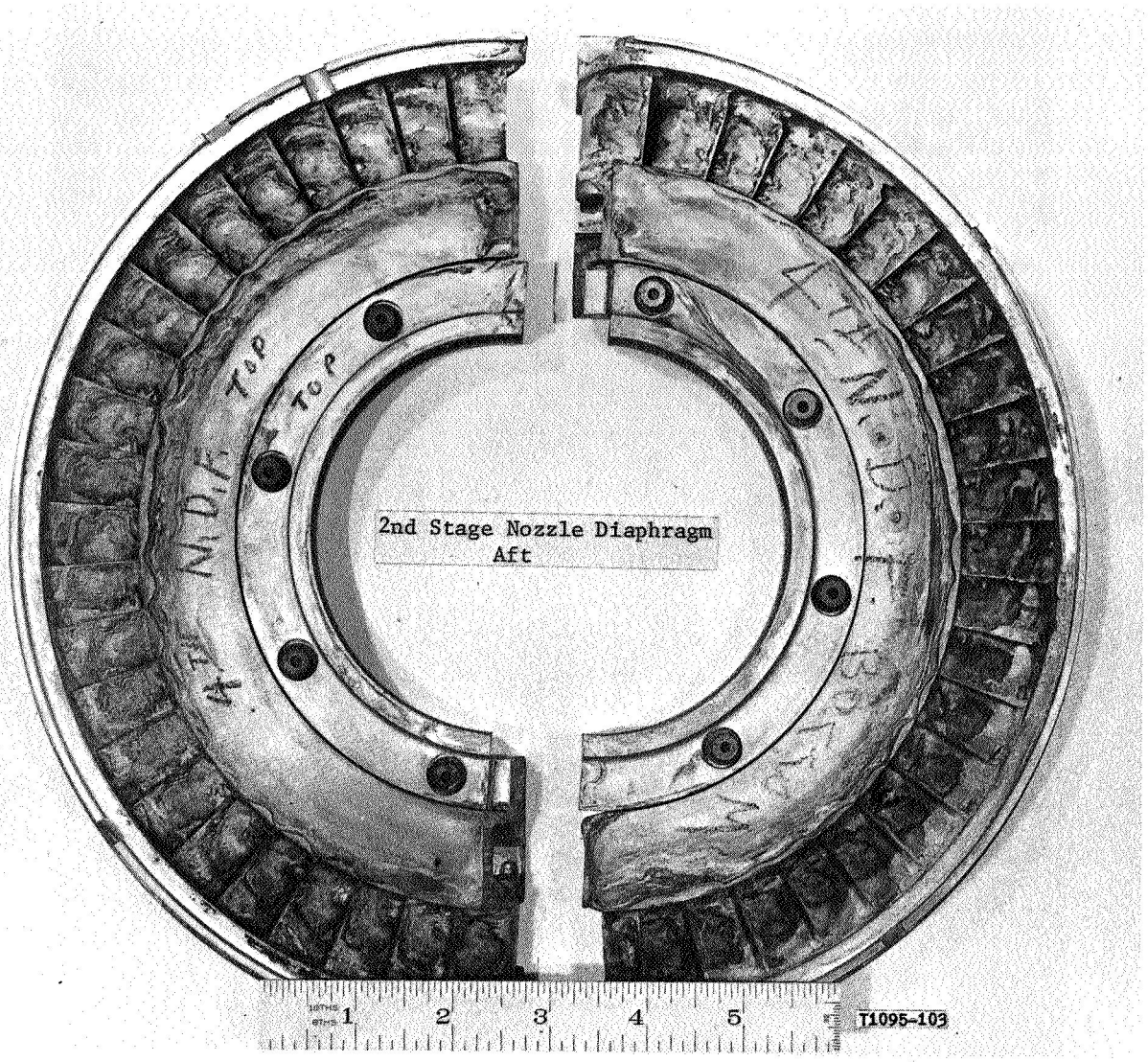


Figure 97b. Second Stage Nozzle Diaphragm (Exit Side) After 2000 Hour Endurance Test.

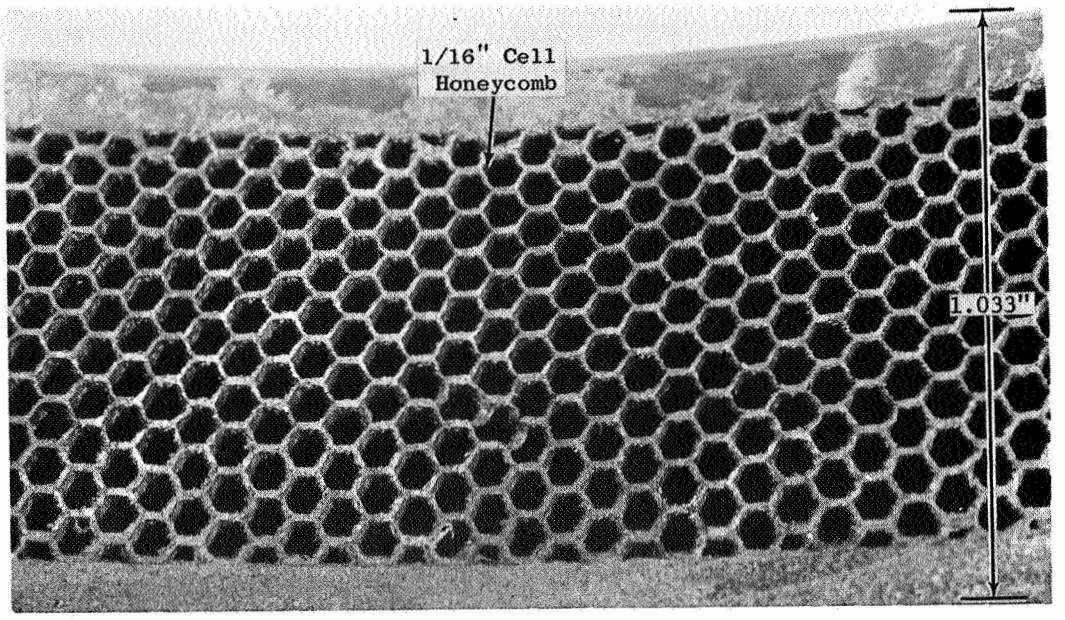


Figure 98a. First Stage Tip Seal After 2000 Hour Endurance Test.

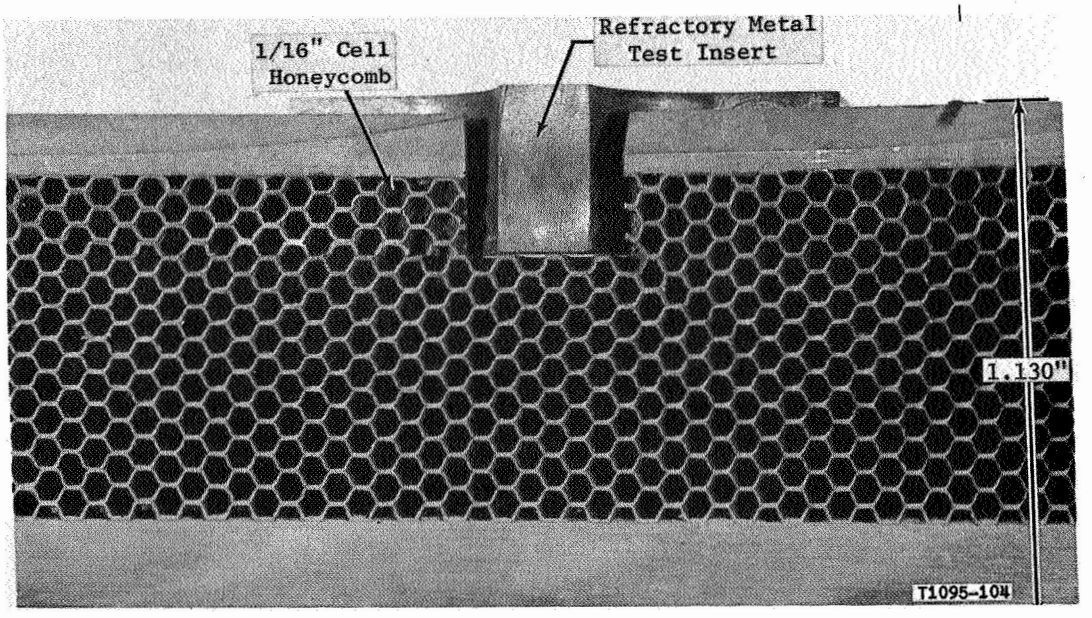


Figure 98b. Second Stage Tip Seal After 2000 Hour Endurance Test.

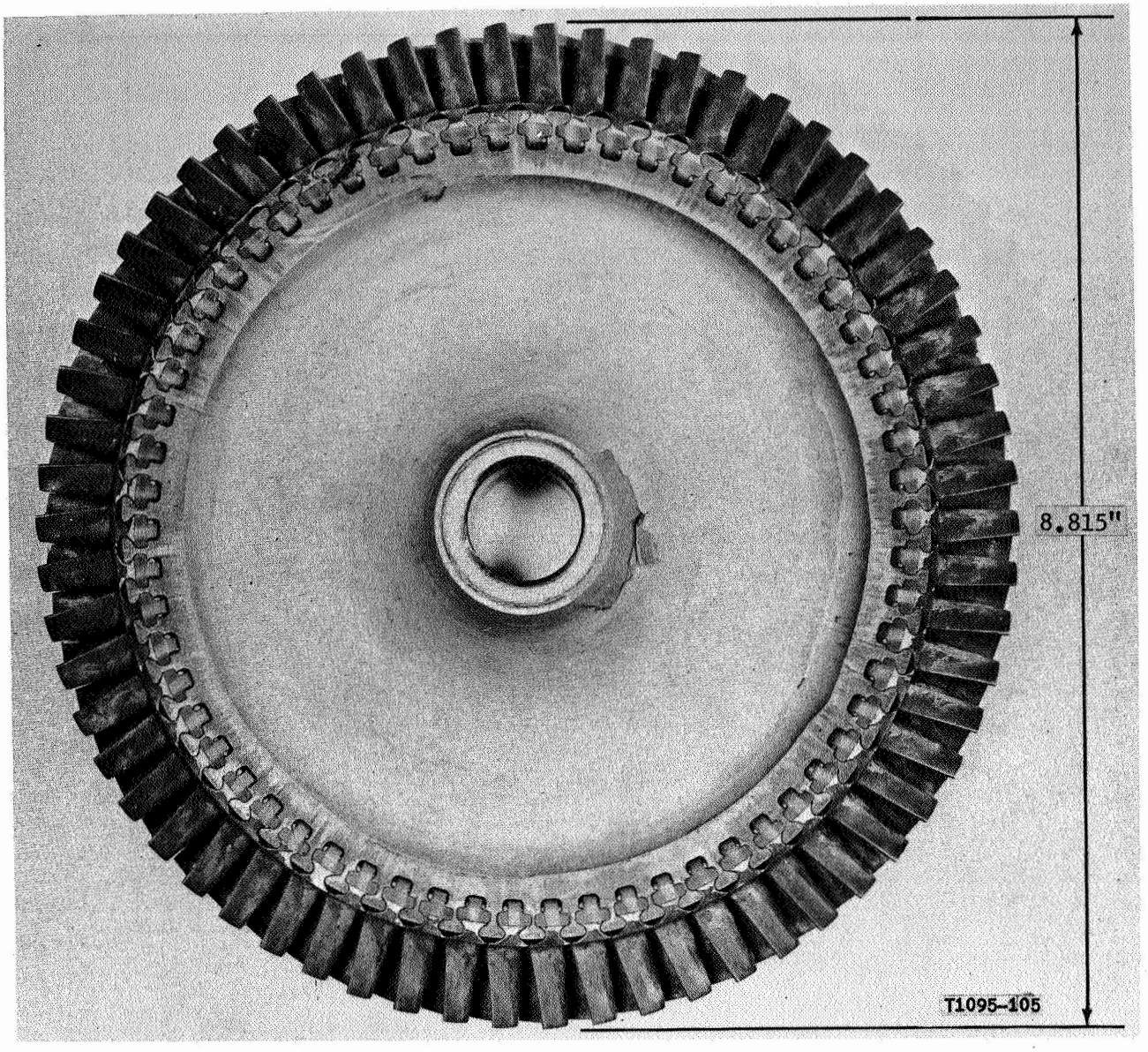


Figure 99. First Stage Turbine Wheel After 2000 Hour Endurance Test.

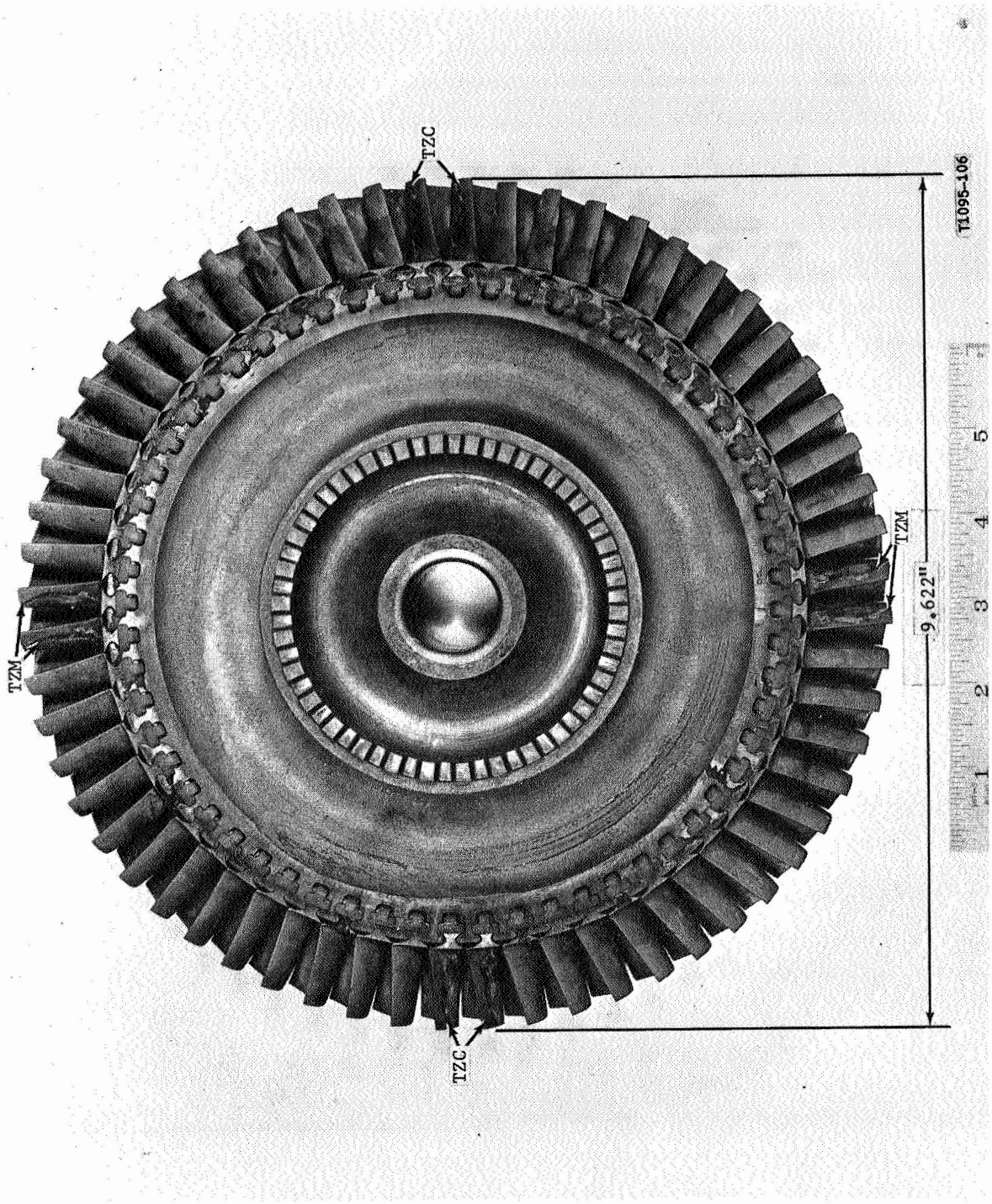


Figure 100. Second Stage Turbine Wheel After 2000 Endurance Test.

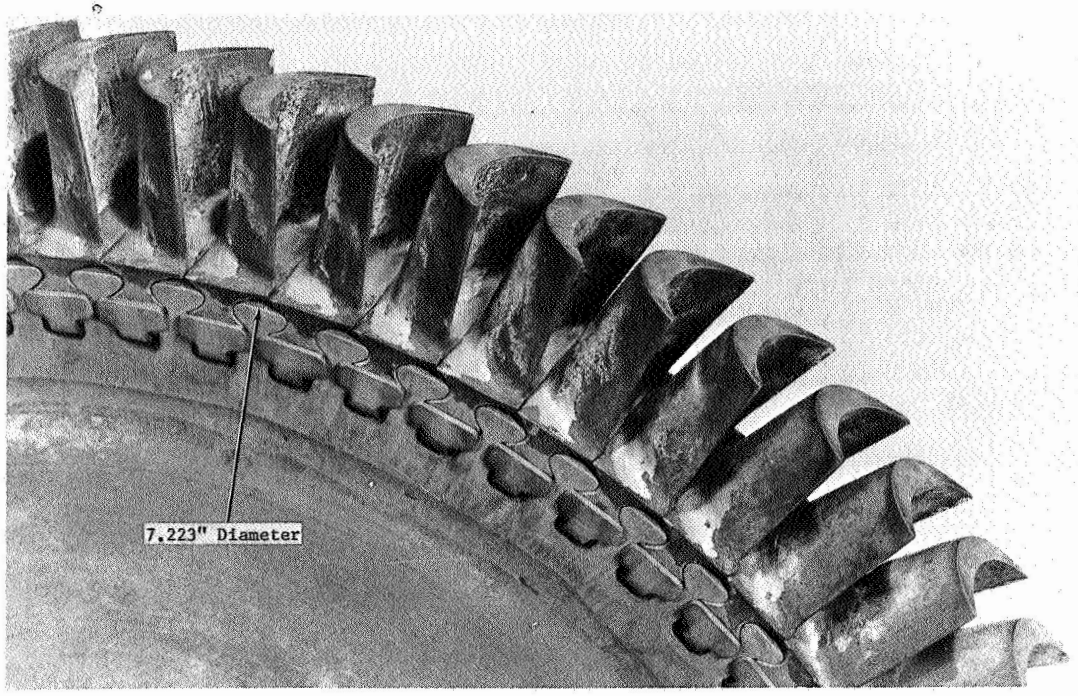


Figure 101a. 2000 Hour Test First Stage Wheel Assembly Showing Leading Edges of Blades Before Wheel Disassembly.

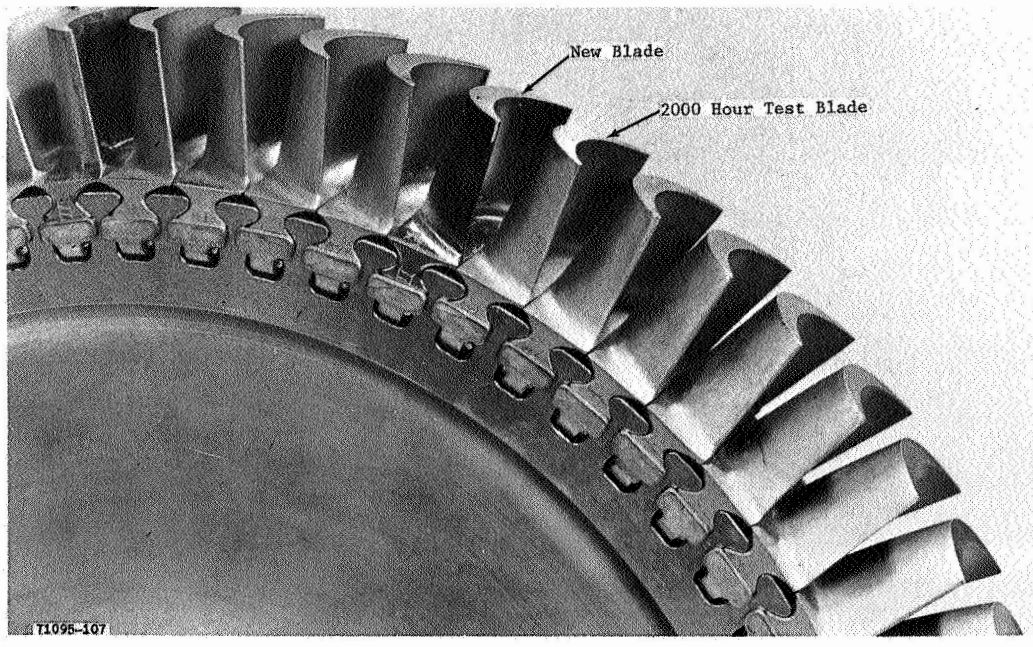


Figure 101b. 2000 Hour First Stage Wheel Assembly Showing Leading Edges of Blades After Vapor Blast Cleaning and Assembled for Subsequent 3000 Hour Endurance Test.

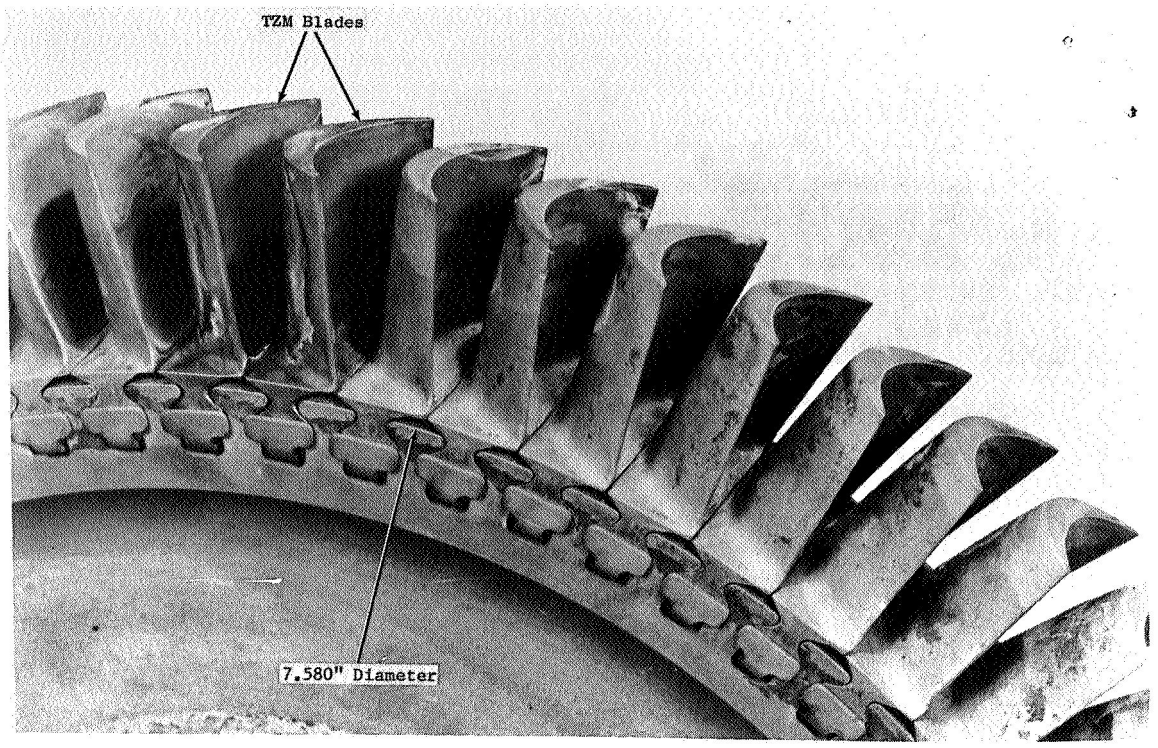


Figure 102a. 2000 Hour Test Second Stage Wheel Assembly Showing Leading Edges of Blades Before Wheel Disassembly.

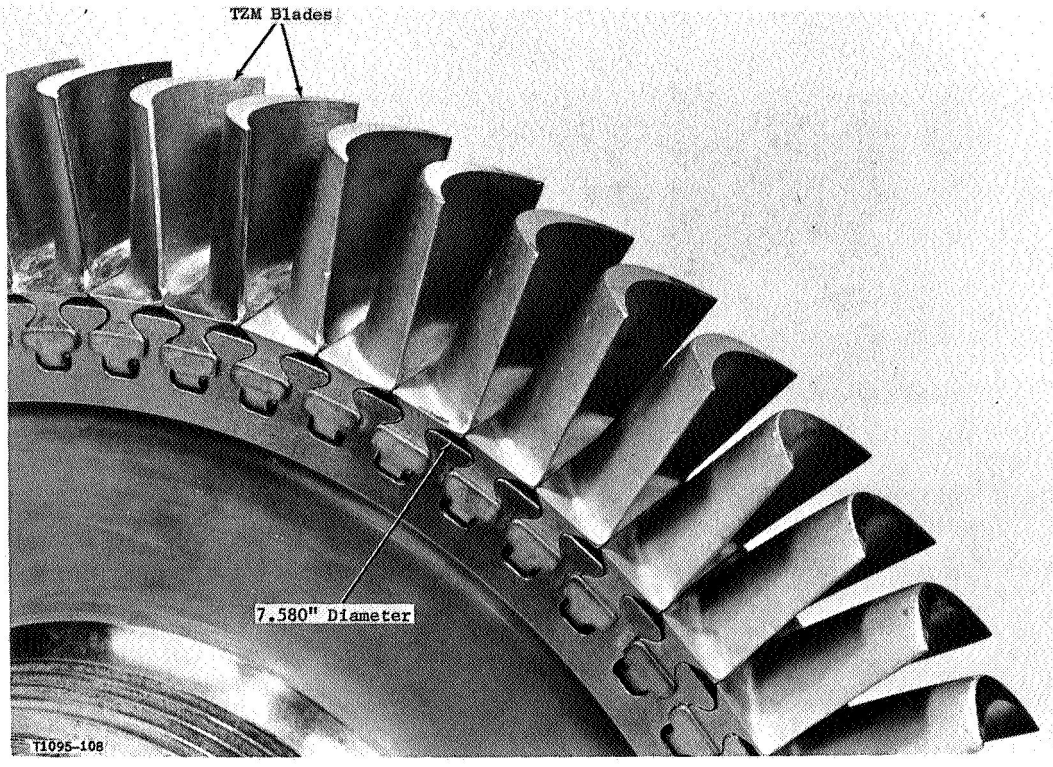


Figure 102b. 2000 Hour Test Second Stage Wheel Assembly Showing Leading Edges of Blades After Vapor Blast Cleaning and Assembled for Subsequent 3000 Hour Endurance Test.

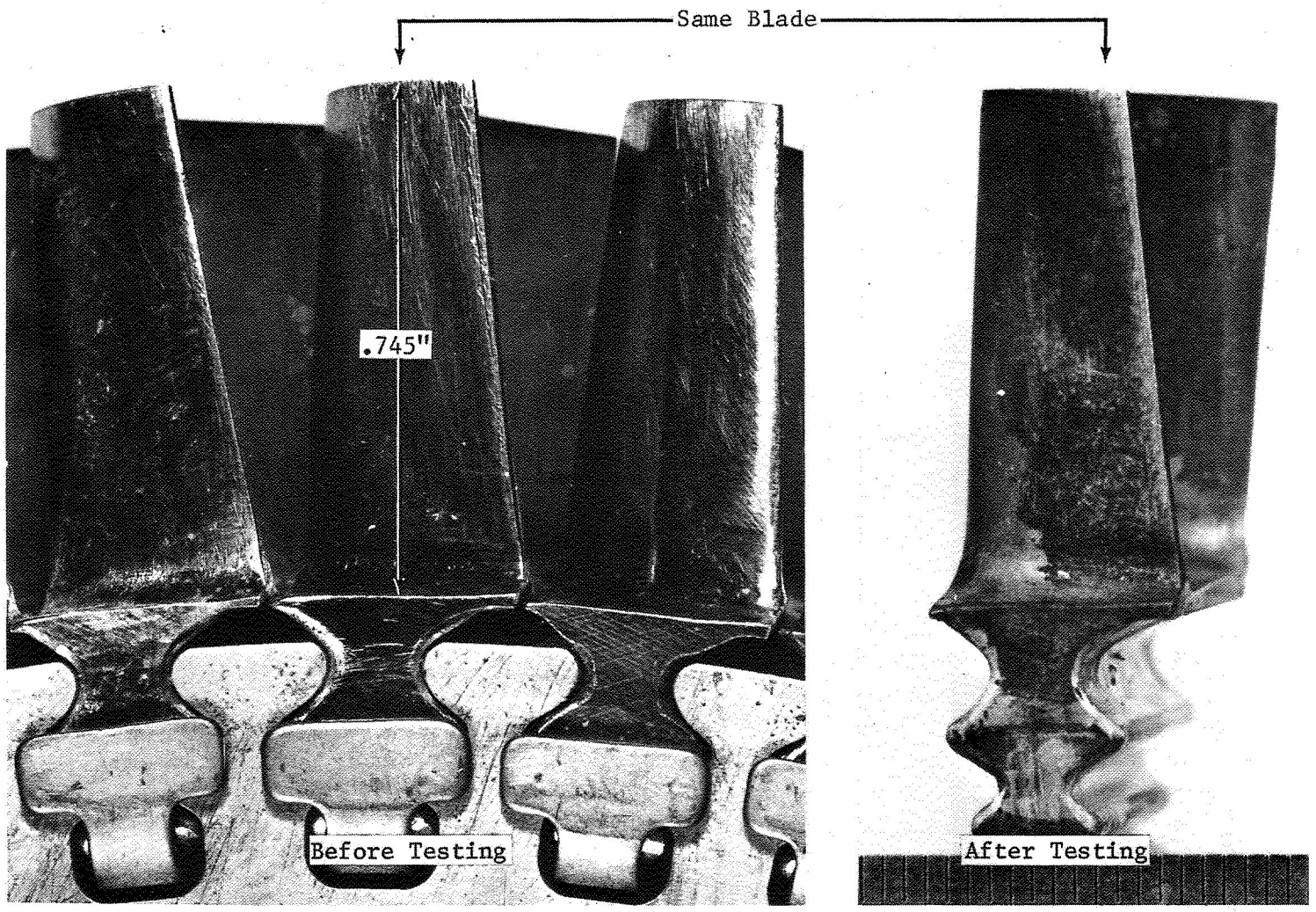


Figure 103a. Comparison of Stage 1 U700 Turbine Blade Before and After 2000 Hour Endurance Testing.

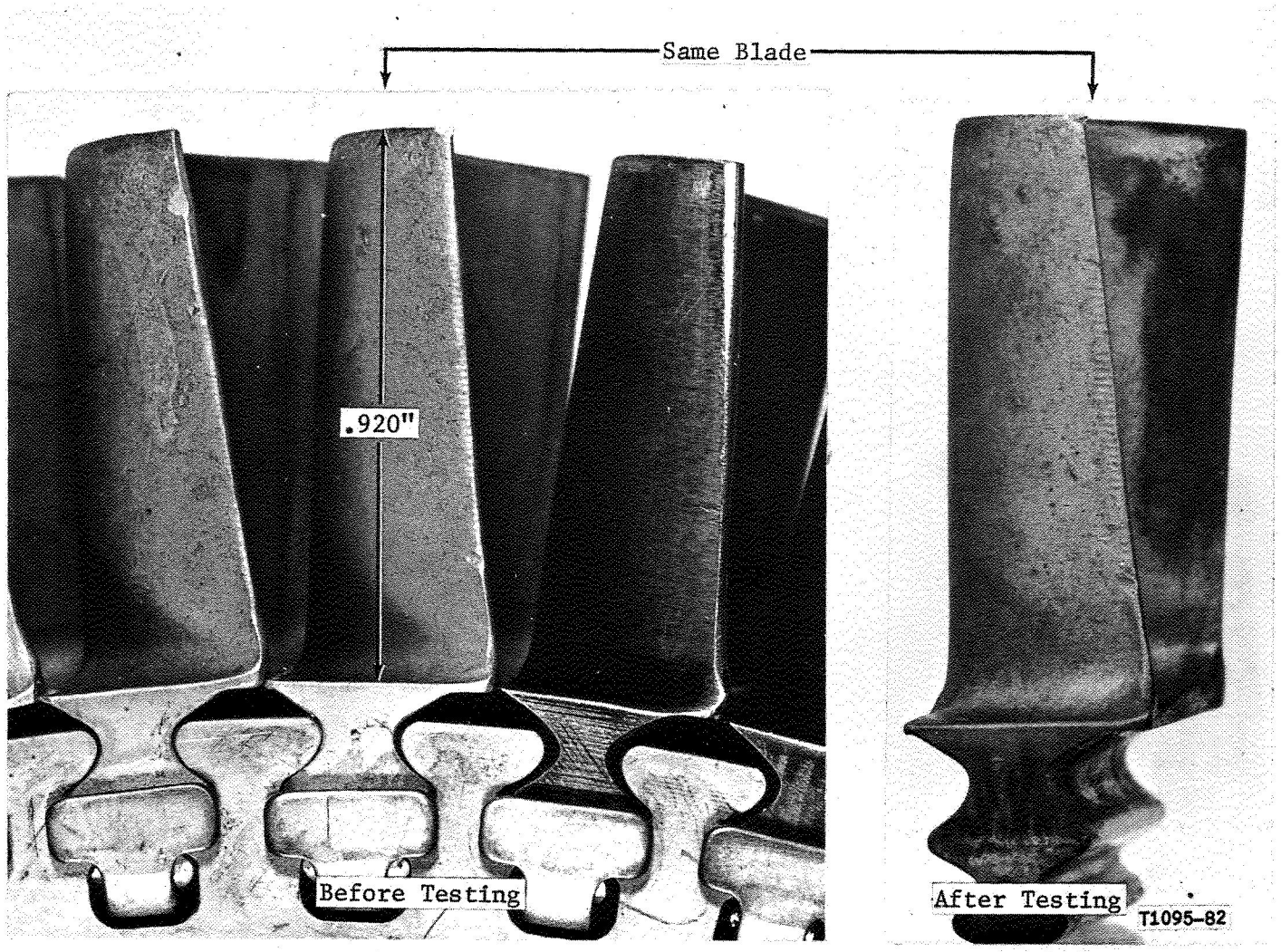


Figure 103b. Comparison of Stage 2 U700 Turbine Blade Before and After 2000 Hour Endurance Testing.

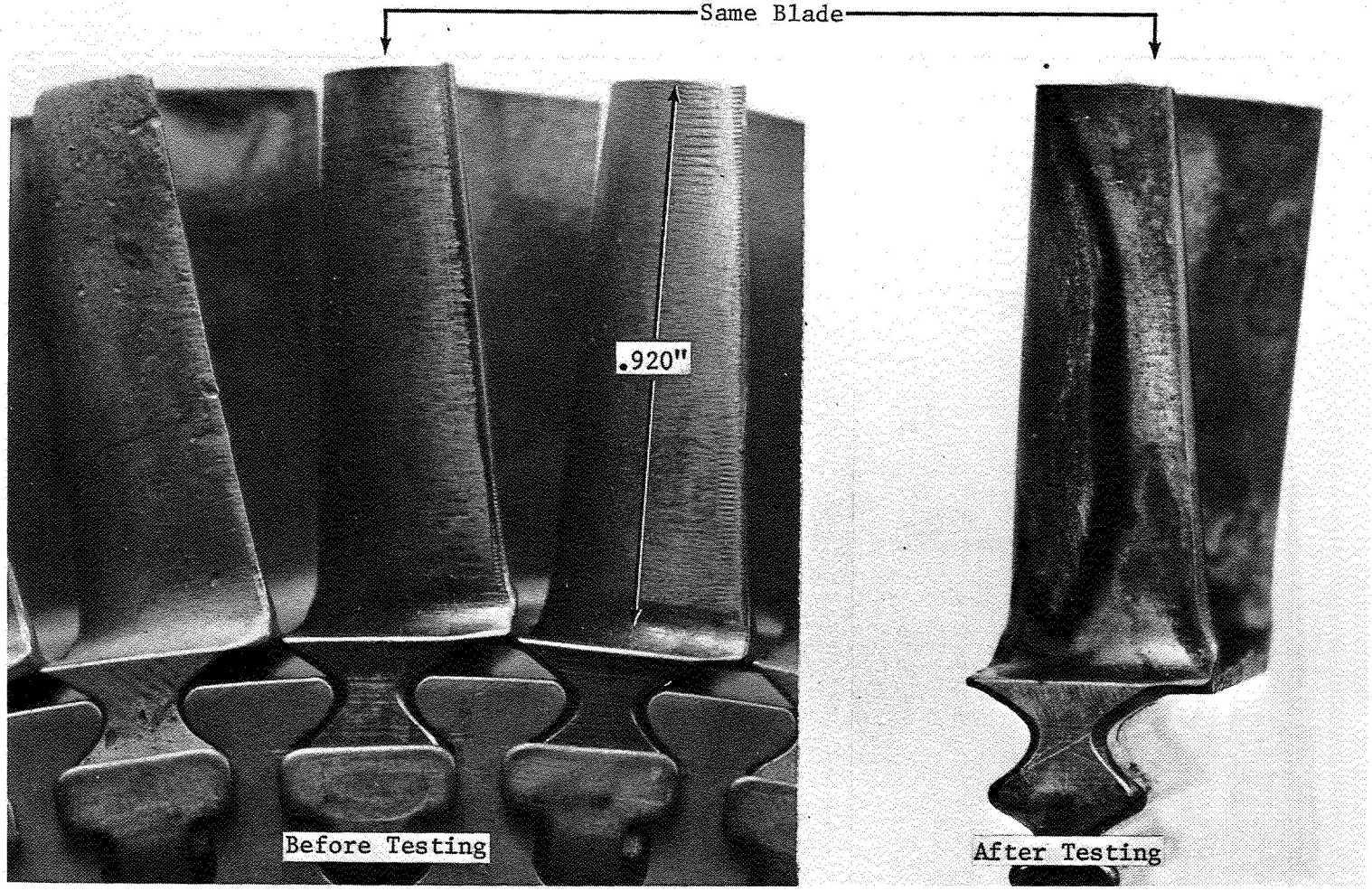


Figure 104a. Comparison of Stage 2 TZM Refractory Metal Turbine Blade Before and After 2000 Hour Endurance Testing.

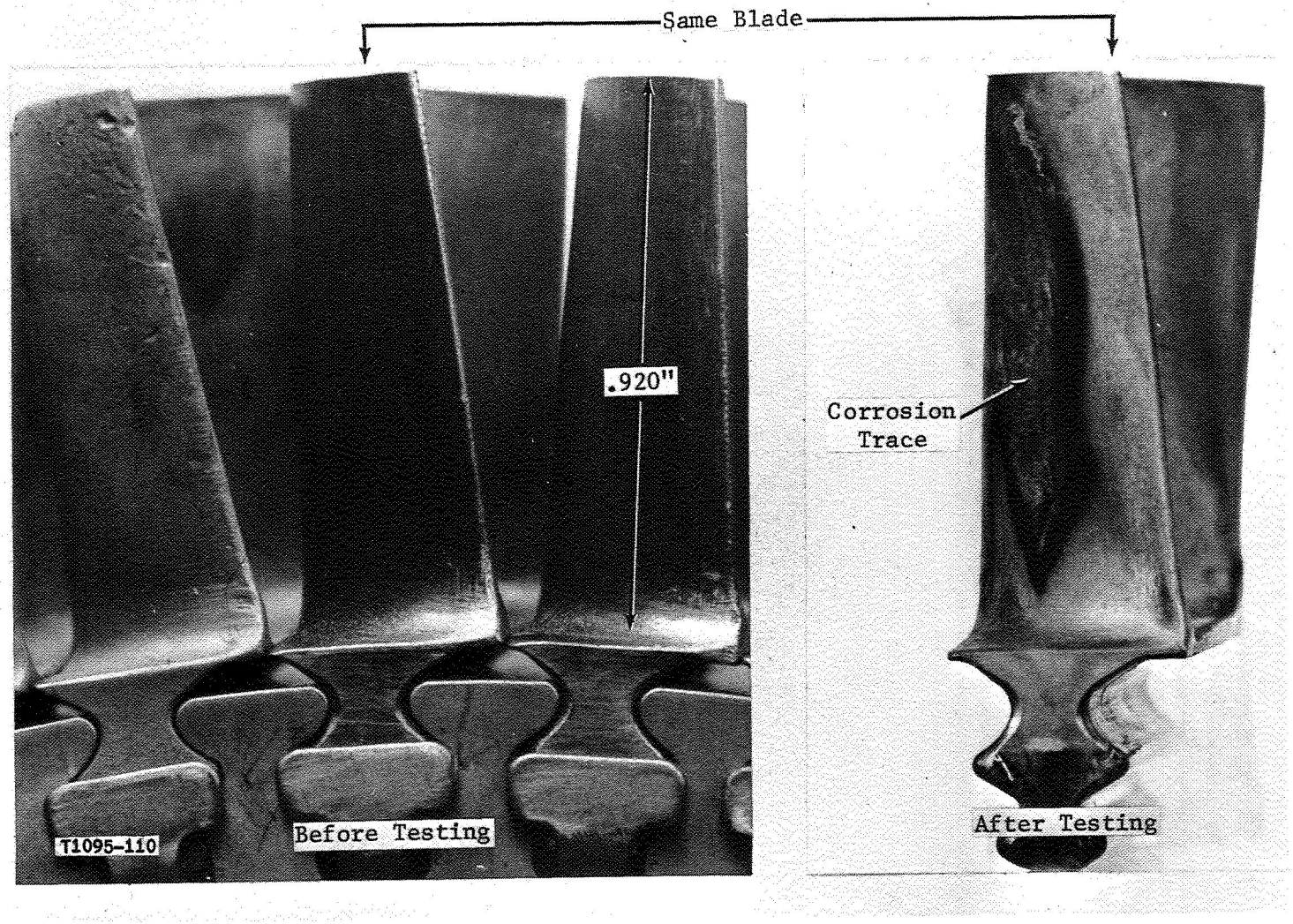


Figure 104b. Comparison of Stage 2 TZC Refractory Metal Turbine Blade Before and After 2000 Hour Endurance Testing.

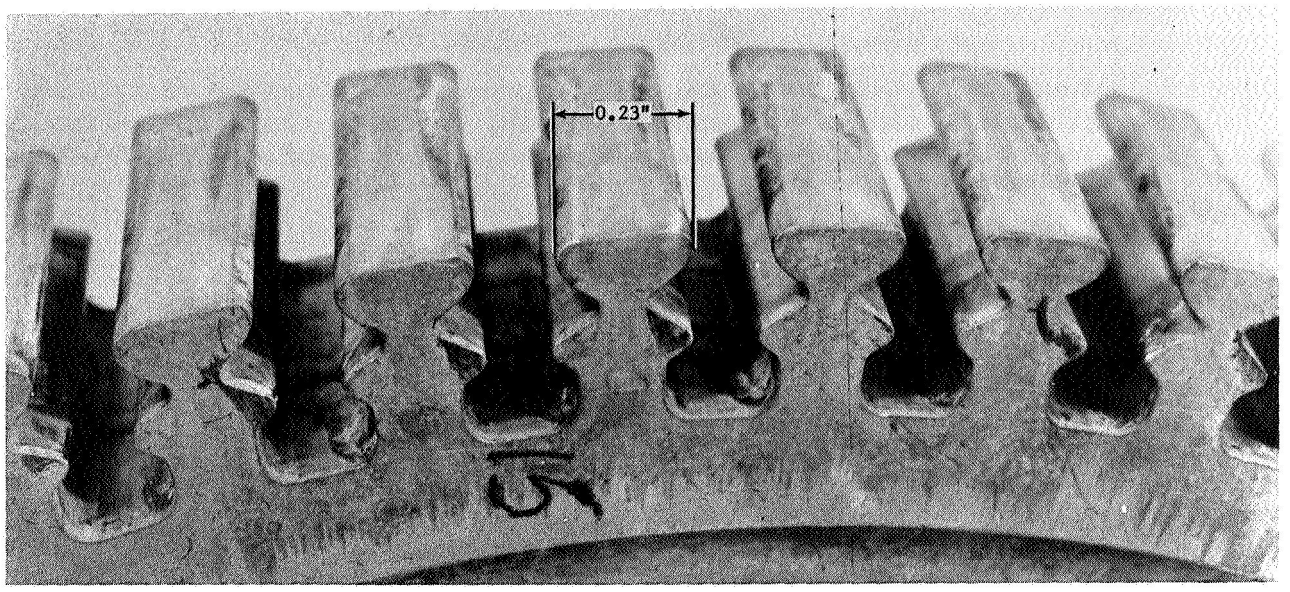


Figure 105a. 2000 Hour Test First Stage Wheel Showing Dovetails After Cleaning.

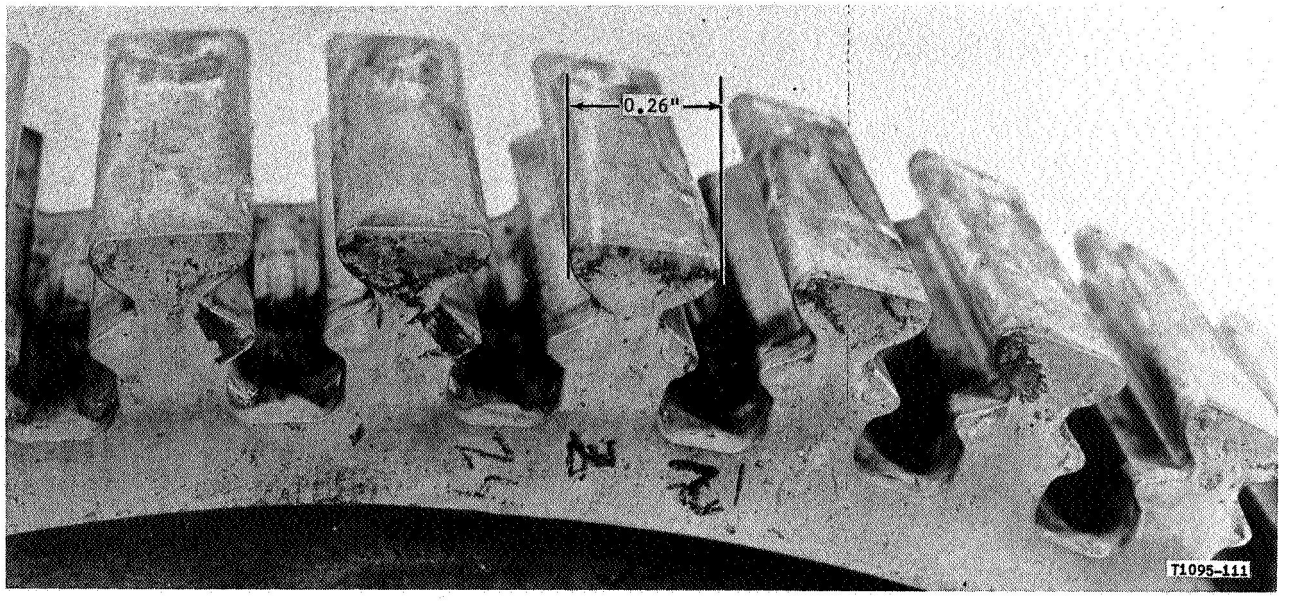


Figure 105b. 2000 Hour Test Second Stage Wheel Showing Dovetails After Steam Cleaning.

NASA-Langley, 1968 —— 3 E-4022